

**Identification of Non-Essential Host Genes Required for
PrP¹⁰⁶⁻¹²⁶ Mediated Neurotoxicity**

By

Michael James Stobart, B.Sc.

A Thesis

Submitted to the Faculty of Graduate Studies of

The University of Manitoba

In Partial Fulfillment of the Requirements of the Degree of

DOCTOR OF PHILOSOPHY

Department of Medical Microbiology and Infectious Diseases

University of Manitoba

Winnipeg, Manitoba, Canada

Copyright © Michael James Stobart, August 2011

Abstract

Prion diseases are invariably fatal proteinaceous neurodegenerative disorders of the central nervous system. The infectious agent is the host encoded prion protein which has undergone a post-translational refolding from a predominantly α -helical to highly β -sheet containing structure. The mechanism of prion-induced neurotoxicity remains elusive in large part due to the absence of a sufficiently neurotoxic cell culture assay. A modern technique for identifying previously unrecognized mediators of a biological pathway is to screen a commercially available library of gene silencing molecules targeting all known open reading frames. Synthetic gene silencing molecules, such as short hairpin RNA (shRNA), employ the endogenous gene silencing pathway to inhibit protein synthesis. To date, no publication has described the implementation of a large-scale library to screen for genetic mediators of prion neurotoxicity.

This project was aimed at developing a cell culture model of acute prion neurotoxicity and screening a library of shRNA molecules in order to identify previously unrecognized gene targets essential to prion-induced neurotoxicity. Using a fragment of the prion protein (PrP¹⁰⁶⁻¹²⁶ peptide) to mimic prion neurotoxicity, human neuroblastoma cells transduced with a retroviral shRNA library were screened for resistance. Involvement of a subset of library identified gene targets in prion disease was assessed *in vivo* by quantitative real-time PCR (qPCR) analysis. Validation of the protection conferred by reducing expression of a gene target of interest was accomplished using individual lentiviral vectors expressing shRNA.

Of the approximately 54,000 shRNA sequences screened, 80 different shRNA sequences recovered from neurotoxic prion peptide-resistant cells were considered to be

of interest. Of these, 49 corresponding gene targets were assessed *in vivo* by qPCR with the majority demonstrating significant differential expression in brains of prion infected mice. Validation of the protection conferred from knockdown of two identified genes, *abcb4* and *ube2cbp*, was completed. Knockdown of either gene imparted significant protection against prion-induced neurotoxicity, with qPCR analysis confirming significantly reduced mRNA transcript levels. Overall, the validity of the novel assay system developed has been demonstrated, and the first comprehensive list of gene candidates involved in mediating acute prion neurotoxicity has been determined.

Acknowledgements

First and foremost, I thank my supervisor, Dr. J. David Knox, and the entire Knox lab for their continuing support, guidance, and ability to find ways of keeping me relaxed throughout my graduate career. The members of the lab included Dr. J. David Knox, Sharon Simon, Lise Lamoureux, and Margot Plews, without whom I could not have found the strength to keep plugging away at this intensive and time consuming project. Whenever I needed anything, you were always there for me. Two outstanding students that worked in the lab and provided indispensable support throughout this project were Simone Brunet and Kamilla Kosciuczyk.

I must also thank the DNA Core Facility at the National Microbiology Laboratory, especially Shari Tyson and Claude Ouellette, for their dedicated work towards preparing the ~73,000 individual retroviral clones. Without their support, the initial screening would have been impossible.

I would also like to profusely thank the members of my graduate committee, Dr. Michael Carpenter, Dr. Heinz Feldmann, and Dr. John Wilkins, all of whom made me work harder than I thought possible. They provided me with invaluable guidance and educated me with new methods and techniques for solving an issue. I extend many thanks to my external committee member Dr. Xavier Roucou who took the time out of his busy schedule to not only read this thesis, but also attend my oral defense in person. Given his notability within the prion research field, it was a great honor to have him accept my invitation.

I extend many thanks to Dr. Reuben Saba, Rhiannon Huzarewich, Anna Majer, Brittany Lagasse and Kyle Caligiuri. Even though we worked in separate labs, you kept

me laughing and helped me relieve stress, even if this meant we ended up at Tim Hortons for a coffee or Carlos & Murphy's for a Friday "lab meeting".

I also thank my entire family, with special thanks to my parents, Sheila and Rick, my brother, John, and my nephew, Hudson. You all encouraged me to keep going even when the going got tough. I extend many thanks to a collaborator and my fiancée, Jill LeMaistre, who acted like a sounding board for all my complaints and with her extensive scientific knowledge, shared ideas and suggestions to overcome hurdles.

Last but not least I would like to thank the Public Health Agency of Canada, the Canadian Institutes of Health Research (CIHR), the Natural Sciences and Engineering Research Council (NSERC), the International Infectious Diseases & Global Health Training Program (IID&GHTP), and the University of Manitoba for monetary support of this project.

Table of Contents

Abstract.....	ii
Acknowledgements	iv
List of Tables	xv
List of Figures.....	xvi
List of Abbreviations	xviii
1. Introduction.....	1
1.1 Prion Diseases	2
1.1.1 Species Susceptibility to Prion Diseases.....	2
1.1.2 Disease Characteristics	8
1.1.2.1 Phenotypic Characteristics of Prion Diseases	9
1.1.2.2 Histological Presentation of Prion Diseases	9
1.1.3 Identification of the Causative Agent of Prion Disease.....	10
1.2 Description of the Human Prion Protein.....	13
1.2.1 Cellular Prion Protein (PrP ^c) Structure	15
1.2.1.1 Variants of the Prion Protein.....	15
1.2.1.2 Predicted Function of PrP ^c	17
1.2.1.3 Antioxidant Function of PrP ^c	18
1.2.1.4 PrP ^c Mediated Signal Transduction	19
1.2.1.5 Anti-Apoptotic Function of PrP ^c	20
1.2.2 Disease Associated Prion Protein (PrP ^{res}).....	20
1.2.2.1 Structure and Physical Properties of PrP ^{res}	21
1.2.2.2 PrP ^{res} Associated Neurotoxicity.....	22

1.2.2.3	PrP ^{res} -Mediated Neurodegeneration.....	24
1.2.2.4	PrP ^{res} Induced Apoptosis.....	24
1.2.2.5	PrP ^{res} Induced Gliosis	26
1.3	Concept of Prion Strains	27
1.4	Conversion Theories	28
1.4.1	Template-Assisted Refolding Theory	28
1.4.2	Seeded Nucleation Theory	28
1.5	Peptide Model of Prion-Mediated Neurotoxicity	30
1.5.1	Description of the PrP ¹⁰⁶⁻¹²⁶ Peptide.....	32
1.5.2	Neurotoxic Properties of the PrP ¹⁰⁶⁻¹²⁶ Peptide	32
1.5.3	Mechanism of PrP ¹⁰⁶⁻¹²⁶ Neurotoxicity.....	33
1.5.3.1	Functional Importance of the 106-126 Region	34
1.5.3.2	PrP ¹⁰⁶⁻¹²⁶ Insertion within Lipid Membranes.....	34
1.5.3.3	PrP ¹⁰⁶⁻¹²⁶ Induced Apoptosis.....	36
1.5.3.4	PrP ¹⁰⁶⁻¹²⁶ Induced Gliosis.....	38
1.5.4	Limitations of Using Brain Homogenate to Mimic Prion Neurotoxicity	38
1.6	Tools for Inhibition of RNA Transcription and Translation.....	39
1.6.1	Innate Catalytic Activity via Hydrolysis (Nucleozymes)	40
1.6.1.1	Ribozymes.....	41
1.6.1.2	DNAzymes.....	42
1.6.2	Recruitment of the RISC Complex for Function (dsRNA)	43

1.6.2.1	Endogenous MicroRNA (miRNA) Processing Pathway	44
1.6.2.2	Short Interfering RNA (siRNA).....	45
1.6.2.3	Short Hairpin RNA (shRNA).....	47
1.7	Short Hairpin RNA (shRNA) Library Evolution.....	48
1.8	Short Hairpin RNA (shRNA) Library Screening Considerations.....	50
1.9	Methods for Validating shRNA Library-Identified Positives.....	51
1.10	Objectives	52
1.11	Hypothesis.....	52
2.	Materials and Methods.....	53
2.1	Cell Culture	54
2.1.1	Maintenance of HEK-293-based Packaging Cells.....	54
2.1.2	Maintenance of Mouse Fibroblast NIH/3T3 Cells.....	55
2.1.3	Maintenance of Human Neuroblastoma SK-N-FI Cells.....	55
2.1.4	Freezing Down Cells.....	55
2.1.5	SK-N-FI Cell Viability Assay Using AlamarBlue.....	56
2.2	PrP ¹⁰⁶⁻¹²⁶ Mediated Neurotoxicity.....	58
2.3	Preparation and Retroviral Packaging of the pSM2+shRNA ^{mir} Library.....	60
2.3.1	Replication and Amplification of the Human shRNA ^{mir} Library.....	60
2.3.2	Human pSM2+shRNA ^{mir} Plasmid Isolation, Quantification and Pooling	62

2.3.3	Removal of Endo Toxins from pSM2+shRNA ^{mir} Pools.....	63
2.3.4	Packaging of pSM2+shRNA ^{mir} Library Pools.....	64
2.3.5	Retroviral Titre Determination	67
2.4	pSM2+shRNA ^{mir} Library Screening.....	68
2.4.1	SK-N-FI Cell Transduction with pSM2 Retrovirus.....	68
2.4.2	PrP ¹⁰⁶⁻¹²⁶ Mediated Neurotoxicity.....	68
2.4.3	Identification of Protective shRNA ^{mir}	69
2.4.3.1	Extraction of Genomic DNA from PrP ¹⁰⁶⁻¹²⁶ Resistant SK-N-FI Cells	69
2.4.3.2	Amplification of shRNA ^{mir} Conferring Resistance	71
2.4.3.3	Cloning of shRNA ^{mir} Conferring Resistance.....	72
2.4.3.4	Sequencing of shRNA ^{mir} Conferring Resistance	73
2.5	Preliminary Validation of the First 30 shRNA ^{mir} Identified.....	74
2.5.1	Purification of Endotoxin Free Plasmid from Individual Bacterial Clones.....	75
2.5.2	Retroviral Packaging, Titration, and Transduction.....	75
2.5.3	Confirming pSM2+shRNA ^{mir} Confer Resistance Against PrP ¹⁰⁶⁻¹²⁶ Peptide.....	76
2.5.4	Individual pSM2+shRNA ^{mir} Conferred Cellular Resistance	76
2.6	Confirming Protection of 2 Identified shRNA ^{mir} Using Lentiviral Vectors	77
2.6.1	Replication and Isolation of Lentiviral Vectors.....	77

2.6.2	Replication and Purification of the Lentiviral Packaging	
	Vectors	77
2.6.3	Packaging of Lentiviral Vectors	81
2.6.4	Lentiviral Titre Determination.....	82
2.6.5	SK-N-FI Cell Transduction with Lentivirus	82
	2.6.5.1 Confirmation of Identified shRNA ^{mir} for Conferring	
	PrP ¹⁰⁶⁻¹²⁶ Resistance.....	83
	2.6.5.2 Collection of RNA and protein from SK-N-FI Cells.....	84
	2.6.5.3 Generation of cDNA from SK-N-FI RNA.....	85
	2.6.5.4 Quantification of <i>abcb4</i> , <i>ube2cbp</i> , and <i>prnp</i> from	
	SK-N-FI cDNA	86
	2.6.5.5 Quantification of Ube2cbp Protein from SK-N-FI	
	Cells	88
2.7	Validating Identified shRNA ^{mir} in a Mouse Model of Prion Disease.....	89
	2.7.1 Collection of RNA from Mouse Brains	89
	2.7.2 Generation of cDNA from RNA Collected from Mice	91
	2.7.3 Quantification of Library Identified Gene Targets from	
	Mouse Brain cDNA	91
3.	Results	100
	3.1 Assay Development	101
	3.1.1 Culture Conditions to Minimize Background.....	102
	3.1.1.1 Influence of Peptide Concentration and Exposures	102

3.1.1.2	Influence of Cell Plating Density and Serum Concentration.....	104
3.1.2	Optimized Prion Neurotoxicity Assay Conditions	104
3.1.2.1	Validation of Optimized Prion Neurotoxicity Assay....	108
3.1.3	Visualization of PrP ¹⁰⁶⁻¹²⁶ Aggregation	110
3.2	Library Screen.....	110
3.2.1	Transfection Efficiency of GP2-293 and Retroviral Titre	110
3.2.2	Overview of Identifying Protective pSM2+shRNA ^{mir} Sequences.....	113
3.2.3	Stably Integrated shRNA ^{mir} Sequences from PrP ¹⁰⁶⁻¹²⁶ Resistant SK-N-FI.....	116
3.2.4	Predicted Association of pSM2+shRNA ^{mir} Library Identified Positives	126
3.2.4.1	Analysis of Direct and Indirect Associations between Library Identified Proteins of Interest	126
3.2.4.2	Analysis of Direct Associations between Library Identified Proteins of Interest.....	127
3.2.5	Verification of Pooled Library Identified Gene Targets <i>in</i> <i>vivo</i>	127
3.3	Verifying Pooled pSM2+shRNA ^{mir} Library Identified Gene Targets <i>in vitro</i>	141
3.3.1	Analyzing Resistance Conferred by Identified pSM2- shRNA ^{mir}	142

3.3.2 Validation of <i>abcb4</i> and <i>ube2cbp</i> Knockdown Conferring Protection <i>in vitro</i>	145
3.3.3 Protection Conferred by pGIPZ+shRNA ^{mir} Mediated Gene Knockdown	147
3.3.4 Confirming <i>abcb4</i> , <i>ube2cbp</i> , and <i>prnp</i> Targeted shRNA Functionality	149
3.3.4.1 Analysis of <i>abcb4</i> , <i>ube2cbp</i> , and <i>prnp</i> mRNA Knockdown Efficiency	149
3.3.4.2 Analysis of <i>abcb4</i> , <i>ube2cbp</i> , and <i>prnp</i> Protein Knockdown Efficiency	150
4. Discussion.....	156
4.1 Genes Known to Mediate Prion Disease	157
4.2 Development of the Novel Prion Neurotoxicity Assay Utilized to Screen an shRNA ^{mir} Library	158
4.2.1 Manipulation of Culture Conditions to Optimize SK-N-FI Susceptibility to PrP ¹⁰⁶⁻¹²⁶ -Induced Neurotoxicity	161
4.2.2 Gene Targets Identified from Screening the pSM2+shRNA ^{mir} Human Library Utilizing the Novel Prion Neurotoxicity Assay	163
4.2.3 Predicted Network Association of Candidate Genes Identified	163
4.2.3.1 Predicted Indirect Network Association of Library Identified Positives.....	168

4.2.3.2	Predicted Direct Network Association of Library Identified Positives.....	168
4.2.3.3	Association of Library Identified Gene Targets with Htt-Interacting Proteins.....	170
4.2.3.4	MicroRNAs Involved in the Identified Network Association.....	171
4.3	Gene Expression of Identified Gene Targets in Mouse Brain	171
4.4	Validation Studies of Library Identified Gene Targets of Interest <i>in vitro</i>	174
4.4.1	Confirming Protection against PrP ¹⁰⁶⁻¹²⁶ Induced Neurotoxicity Using a Subset of Library Identified pSM2+shRNA ^{mir} Sequences	175
4.4.2	Limiting the Analysis to <i>abcb4</i> and <i>ube2cbp</i>	175
4.5	The ABC Transporter System.....	176
4.5.1	Correlation of <i>abcb4</i> Analysis and Molecular Expectations	177
4.6	The Ubiquitin-Proteasome System (UPS)	178
4.6.1	Involvement of the UPS in Prion Disease.....	180
4.6.2	Function of Ube2cbp.....	182
4.6.2.1	Predicting Ube2cbp Protein Interactions	183
4.6.2.2	Correlation of <i>ube2cbp</i> Analysis and Molecular Expectations.....	184
4.7	Summary of Library Screening.....	187
5.	Conclusions.....	189

6. References.....192

List of Tables

Table 1.1: TSE Diseases of Various Mammalian Species.....	3
Table 2.1: Primer Pairs for qPCR Analysis of SK-N-FI <i>abcb4</i> , <i>ube2cbp</i> , and <i>prnp</i>	87
Table 2.2: Primer Pairs for qPCR Analysis of pSM2+shRNA ^{mir} Library Identified Gene Targets	93
Table 3.1: Peptide Concentration and Number of Applications Compared	103
Table 3.2: Cell Number and Serum Concentrations Compared to Cell Viability	106
Table 3.3: Identification of shRNA ^{mir} gene targets from surviving SK-N-FI cells	118
Table 3.4: Biological Disorders Associated with Identified Gene Targets	131
Table 3.5: Gene Targets, Vectors Backbones, and shRNA Tested for Protection	146
Table 3.6: pGIPZ+shRNA ^{mir} 93067 (<i>abcb4</i>) and 139486 (<i>ube2cbp</i>) Summary	155

List of Figures

Figure 1.1: Number of BSE and vCJD Cases in the United Kingdom	5
Figure 1.2: Diagrammatic representation of the human PrP protein.	6
Figure 1.3: Scrapie-Induced Neuronal Vacuolation	11
Figure 1.4: Tertiary Structure of PrP ^c and PrP ^{res}	23
Figure 1.5: Proposed Models for PrP ^c to PrP ^{res} Re-folding	29
Figure 1.6: Proposed Models of PrP Mutant and PrP ¹⁰⁶⁻¹²⁶ Toxicity	35
Figure 1.7: RNAi Molecule Expression and Processing	46
Figure 2.1: SK-N-FI Challenge Schedule with the PrP ¹⁰⁶⁻¹²⁶ Peptide	59
Figure 2.2: Features of the pSM2 shRNA ^{mir} Retrovector.	61
Figure 2.3: Retro- or Lentiviral production by co-transfection of HEK-based cells	65
Figure 2.4: Features of the pVSV-G Expression Vector	66
Figure 2.5: Overview of Identifying Protective shRNA ^{mir} Sequences	70
Figure 2.6: Features of the pGIPZ+shRNA ^{mir} Expression Vector.....	78
Figure 2.7: Features of the psPAX2 Lentiviral Packaging Vector	79
Figure 2.8: Features of the pMD2.G VSV-G Expression Vector	80
Figure 3.1: Effect of FBS Concentration on SK-N-FI Susceptibility to Peptide.....	105
Figure 3.2: Fine Tuning of Peptide Application Conditions.....	107
Figure 3.3: SK-N-FI Neurotoxicity Associated with 50µM PrP ¹⁰⁶⁻¹²⁶ Challenge	109
Figure 3.4: Visualization of PrP ¹⁰⁶⁻¹²⁶ Peptide Aggregation.....	111
Figure 3.5: Monitoring efficiency of GP2-293 transduction	112
Figure 3.6: Strategy for Selecting PrP ¹⁰⁶⁻¹²⁶ Resistant Clones.....	114
Figure 3.7: Flow Chart of Library Screening Steps and <i>in vitro</i> Validation.....	115

Figure 3.8: Representative gel image of shRNA ^{mir} amplicons	117
Figure 3.9: Associated Function of Library Identified Gene Targets	125
Figure 3.10: Legend of Associated Protein Function for IPA Generated Networks	128
Figure 3.11: Direct and Indirect Network Associations between Library Positives.....	129
Figure 3.12: Direct Network Association Analysis of Library Positives	130
Figure 3.13: qPCR Analysis of Library Identified Gene Targets in Mouse Brain	140
Figure 3.14: Percent Protection Conferred by Individual pSM2-based shRNA ^{mir}	143
Figure 3.15: Criteria for Selecting <i>abcb4</i> and <i>ube2cbp</i> for Further Analysis.....	144
Figure 3.16: Relative Protection Conferred upon SK-N-FI Cells Expressing pGIPZ-based shRNA ^{mir}	148
Figure 3.17: qPCR Analysis of <i>abcb4</i> , <i>ube2cbp</i> , and <i>prnp</i> Expression Levels	151
Figure 3.18: Western Blot Detection of SK-N-FI Ube2cbp Protein.....	153
Figure 3.19: Ube2cbp Protein Knockdown Efficiency in Human SK-N-FI Cells	154
Figure 4.1: Analysis of all shRNA ^{mir} Gene Targets Identified, Network 1	164
Figure 4.2: Analysis of all shRNA ^{mir} Gene Targets Identified, Network 2	165
Figure 4.3: Analysis of all shRNA ^{mir} Gene Targets Identified, Network 3	166
Figure 4.4: Analysis of all shRNA ^{mir} Gene Targets Identified, Network 4	167
Figure 4.5: Human <i>abcb4</i> Targeting and Detection.....	179
Figure 4.6: Overview of the Ubiquitination Pathway	181
Figure 4.7: Human <i>ube2cbp</i> Targeting and Detection.....	186
Figure 4.8: Subcellular Localization of Ube2cbp in Mouse Brain	188

List of Abbreviations

Abcb4 = ATP-binding cassette, subfamily B, member 4

BSE = Bovine spongiform encephalopathy

cDNA = complementary deoxyribonucleic acid

CJD = Creutzfeldt-Jakob disease; human prion disease

dpi = days post inoculation

FFI = fatal familial insomnia; human genetic prion disease

FS-DMEM2 = DMEM + 2% FS-FBS + 1% Ab/Am, used for transduction experiments

FS-DMEM10 = DMEM + 10% FS-FBS + 1% Ab/Am

gDNA = genomic DNA

GPI = glycosyl-phosphatidyl-inositol anchor

GSS = Gerstmann-Sträussler-Scheinker syndrome; human genetic prion disease

kDa = kilodalton

Kuru = human prion disease resulting from ritualistic cannibalism; Papua, New Guinea

LB^{cb} = Lauria-Bertani media + 200µg/mL Carbenicillin

LB^{Chlor} = Lauria-Bertani media + 25µg/mL Chloramphenicol

mRNA = messenger ribonucleic acid

miRNA = microRNA

PCR = polymerase chain reaction

PrP^c = cellular isoform of the prion protein

PrP^{res} = infectious or protease resistant isoform of the prion protein.

PrP¹⁰⁶⁻¹²⁶ = cytotoxic peptide consisting of amino acids 106-126 of human prion protein

PrP^{Scram} = amino acids 106-126 of human PrP in a scrambled order; control peptide

pGIPZ = lentiviral plasmid GIPZ from OpenBiosystems encoding shRNA^{mir}

pMD2.G = plasmid encoding Vesicular stomatitis virus glycoprotein from Addgene

pSM2 = retroviral plasmid Shag-Magic 2 from OpenBiosystems encoding shRNA^{mir}

psPAX2 = plasmid encoding lentiviral packaging accessory proteins from Addgene

pVSV-G = plasmid encoding Vesicular stomatitis virus glycoprotein

qPCR = Quantitative real-time PCR

RISC = RNA-induced silencing complex

RNAi = RNA interference

sCJD = sporadic CJD; human prion disease with no known underlying cause

shRNA = short hairpin RNA

shRNA^{mir} = short hairpin RNA encompassed by microRNA recognition sequences

SK-HI-DMEM1 = DMEM + 1% HI-FBS + 1X NEAA

SK-HI-DMEM5 = DMEM + 5% HI-FBS + 1X NEAA + 1% Ab/Am

SK-FS-DMEM10 = DMEM + 10% FS-FBS + 1X NEAA + 1% Ab/Am

siRNA = short-interfering RNA

TSEs = transmissible spongiform encephalopathies

Ube2cbp = Ubiquitin-conjugating enzyme E2C binding protein

vCJD = variant CJD disease; human prion disease acquired from BSE-tainted meat

For amounts, sizes, times or other physical definitions, the SI (International Unit System) or legal units were chosen.

1. Introduction

1.1 Prion Diseases

Prion diseases are defined as a group of invariably fatal, neurodegenerative disorders characterized by deterioration of coordinated muscle movement, widespread neuronal vacuolation (spongiosis), gliosis, and are often accompanied by the presence of amyloid aggregate deposition within the brain. The phenotypic and histological presentation is dependent upon host genetics and prion strain (Korth, Kaneko, and Prusiner 2000; Klamt et al. 2001; Knaus et al. 2001; Maiti and Surewicz 2001; Belay and Schonberger 2005). There is no definitive ante-mortem test for prion diseases.

Prion diseases may arise sporadically with no known underlying cause or be familial in nature due to genetic susceptibility. Prion diseases may also be acquired from an exogenous source, and are termed transmissible spongiform encephalopathies (TSEs). TSE diseases are transmissible horizontally from one host to another of the same species, with certain strains capable of inter-species transmissibility. Unlike familial prion diseases, TSE diseases can be acquired iatrogenically or through dietary exposure to the infectious agent. Blood products represent a potential transmission vector (Hunter et al. 2002; Bird 2004; Llewelyn et al. 2004), and though still controversial, evidence exists for a causal link between a subset of sporadic disease cases (no known underlying cause) and surgical procedures (Pedro-Cuesta et al. 2011).

1.1.1 Species Susceptibility to Prion Diseases

Species afflicted by TSE diseases include sheep and goats, cervids (elk and deer), mink, cats, cattle, and humans (Table 1.1). The phenotypic and histological disease

Table 1.1: TSE Diseases of Various Mammalian Species

Below is a list of some of the known prion diseases. The name of disease and the species affected are listed.

Prion Disease	Affected Species
Creutzfeldt-Jakob Disease (CJD)	Human
Variant Creutzfeldt-Jakob Disease (vCJD)	Human
Kuru	Human
Fatal Familial Insomnia (FFI)	Human
Gerstmann-Sträussler-Scheinker Disease (GSS)	Human
Chronic Wasting Disease (CWD)	Cervids
Bovine Spongiform Encephalopathy (BSE)	Cattle
Scrapie	Sheep, Goats
Transmissible Mink Encephalopathy (TME)	Mink
Exotic Ungulate Encephalopathy (EUE)	Greater Kudu, Oryx, Bison
Feline Spongiform Encephalopathy (FSE)	Domestic and Large Cats

*Compiled from (Sigurdson and Miller 2003; Aguzzi and Calella 2009).

manifestation is influenced by the host species and the prion strain (Williams and Young 1993).

In sheep and goats, TSE disease is referred to as scrapie due to the tendency of affected animals to rub against trees and fence posts, scraping off their coat. Scrapie was the first TSE recognized and has been reported in sheep populations in Western Europe since at least the mid-eighteenth century (Parry 1960).

In cervids, such as deer and elk, TSE disease is termed chronic wasting disease (CWD) and was first reported in the mid-to-late 1960s among wildlife research facilities in Colorado and was further recognized in Wyoming a decade later (Williams and Young 1980; Williams and Young 1982).

TSE disease is probably most notably known in cattle, and is termed bovine spongiform encephalopathy (BSE or “mad cow”) disease. The first reported case was in 1985 in the United Kingdom (U.K.), which is classified as the epicentre of the BSE outbreak (Anderson et al. 1996) (Figure 1.1). The major public health concern regarding BSE is evidence suggesting zoonotic transmissibility to humans through consumption of BSE contaminated meat products (Beghi et al. 2004).

In humans, there are at least five variants of the disease:

(i) Creutzfeldt-Jakob disease (CJD). Sporadic CJD (sCJD) is the most common of the human prion diseases, with an incident rate of 1-2 cases/1 million people/year worldwide. Disease onset is generally reserved to the elderly population (55-65 years of age) (Will et al. 1998; Head et al. 2004). The underlying causes of sCJD are unknown. CJD can also occur as the result of familial mutations (fCJD, Figure 1.2), or exposure to the infectious CJD agent (iatrogenic, iCJD). Exposure to the infectious CJD agent has

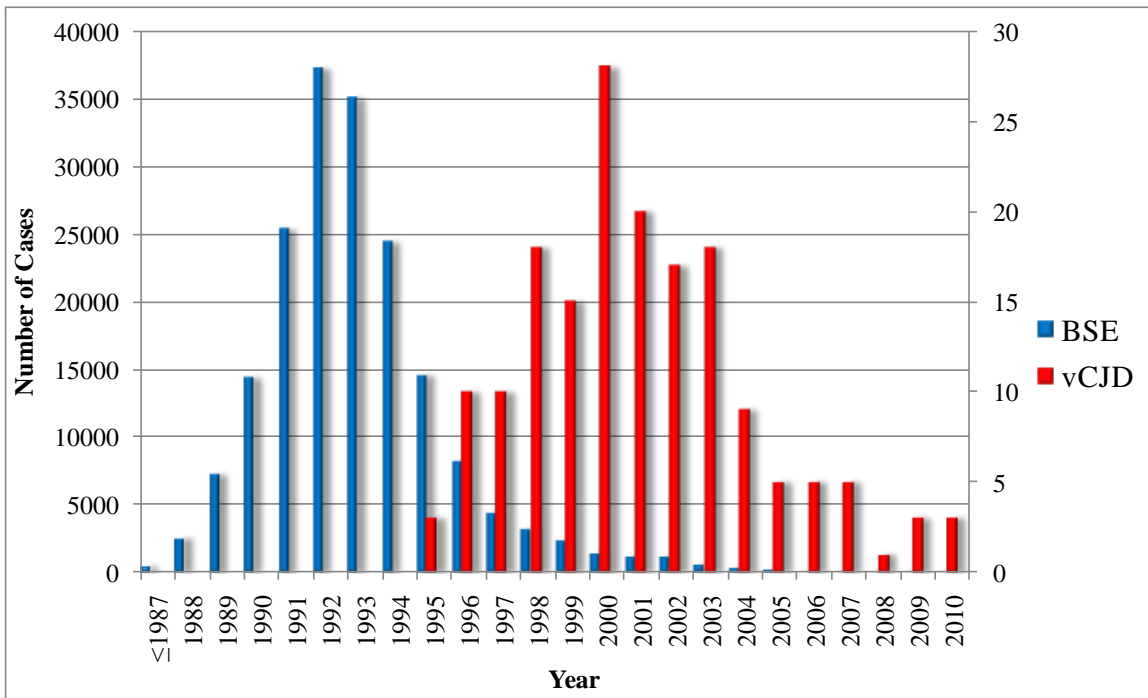


Figure 1.1: Number of BSE and vCJD Cases in the United Kingdom

This graph shows that the number of BSE cases peaked in the early 1990s, with a maximum of 37,280 cases reported for the year 1992. The number of vCJD cases peaked 8 years later with 28 confirmed human cases in 2000. BSE cases are shown using the left axis, and the vCJD cases use the right axis. These data were recent as of September 30th, 2010 and were found on the World Organization for Animal Health website (OIE, <http://www.oie.int/animal-health-in-the-world/bse-specific-data/>) and the National Creutzfeldt-Jakob Disease Surveillance Unit website (NCJDSU, <http://www.cjd.ed.ac.uk/figures.htm>) for BSE and vCJD statistics respectively.

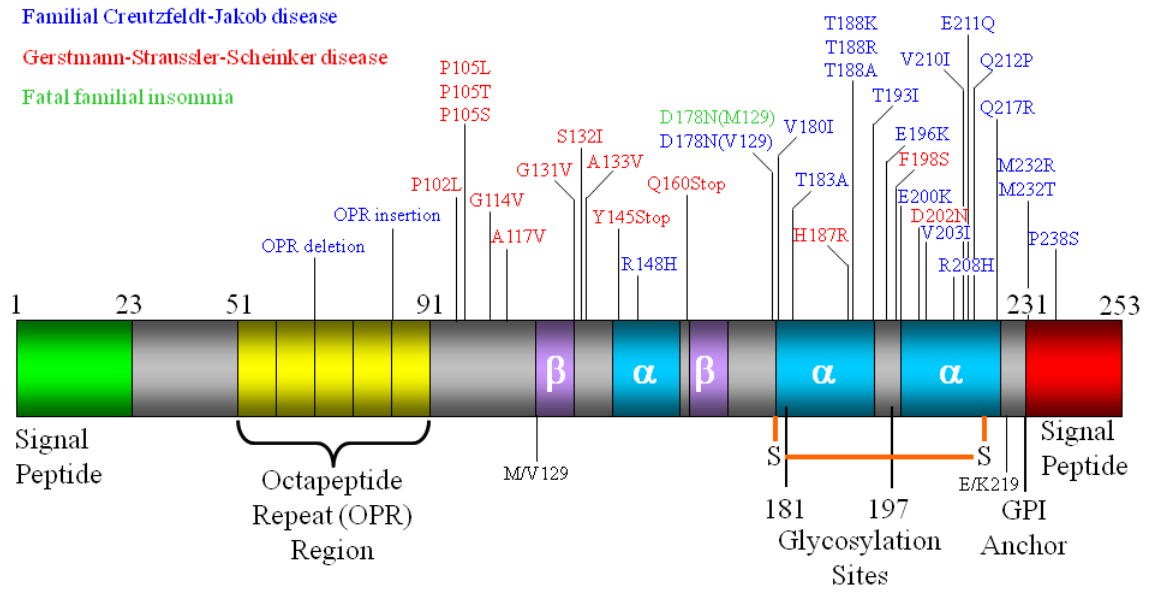


Figure 1.2: Diagrammatic representation of the human PrP protein.

Disease-associated mutations and key structural regions are depicted. Disease-associated mutations are color-coded to the associated prion disease. The vast majority of amino acid mutations are associated with familial Creutzfeldt-Jakob's disease and Gerstmann-Sträussler-Scheinker disease, with only 1 so far identified to predict fatal familial insomnia (D178N). Key structural features include a N-terminus signal peptide which targets PrP to the endoplasmic reticulum lumen, and a C-terminus signal peptide which directs addition of a GPI membrane anchor. A disulfide bond between asparagine residues 179 and 214 stabilizes α -helix 2 and 3, and variable glycosylation sites at amino acids 181 and 197 give rise to three distinct glycoforms. Amino acids 129 and 219 both encode common polymorphisms which may influence disease onset and disease phenotype. GPI = glycosylphosphatidylinositol membrane anchor; α = helical region; β = beta pleated sheet region. Adapted from (Feraudet et al. 2005; van der Kamp and Daggett 2009).

been correlated with injection of cadaver-derived human growth hormone and dura mater grafts, as well as a few instances of contaminated surgical instruments and corneal grafts (Hoshi et al. 2000; Croes et al. 2002; Lumley 2008; Maddox et al. 2008). CJD manifests as neurological and cerebellar deterioration, is rarely associated with detectable protein aggregates, and the affected individual usually succumbs within 1 year of symptom onset (Weihl and Roos 1999).

(ii) Variant CJD (vCJD, infectious form). This variant of CJD is unique from classical CJD in that it predominantly affects young individuals (19-39 years of age) (Collinge et al. 1996; Will et al. 1996; Will et al. 2000; Ironside et al. 2000). vCJD is proposed to be transmitted through human consumption of BSE tainted beef products, with an approximate 8 year incubation period. Disease duration is approximately 14 months from onset of symptoms to death (Zeidler et al. 1997; Beghi et al. 2004; Glatzel et al. 2005). As of September 30th, 2010, 170 cases of vCJD had been reported in the United Kingdom (Figure 1.1), with a total of 224 cases reported worldwide (as of March 2011, <http://www.cjd.ed.ac.uk/vcjdworld.htm>). Evidence suggests that asymptomatic carriers may support replication of the infectious agent, which raises the potential that a population of BSE exposed individuals harbour the infectious agent and could act as carriers of the vCJD agent (Hill et al. 2000).

(iii) Kuru (infectious). Kuru arose due to mortuary ritualistic cannibalism among the Fore people of Papua, New Guinea with reports of the disease as early as 1951 (Gajdusek and Zigas 1959). This strain of human TSE is only known to have endemically spread through the Fore tribespeople of Papua, New Guinea. Death of the affected person typically occurs within 6-9 months of disease onset, with few patients

surviving more than 1 year. Although Kuru has been observed in young individuals, the incubation period can be as long as 45 years, with mid-life adults most often affected (Gajdusek and Zigas 1959).

There are two dominant forms of familial non-CJD prion diseases in humans.

(iv) Fatal Familial Insomnia (FFI) is a rare autosomal dominant and highly penetrant hereditary disorder due to a unique point mutation (Figure 1.2). As the name suggests, those affected with FFI experience disruptions in their normal sleep cycle, with insomnia as the major symptom (Padovani et al. 1998; Montagna et al. 1998). The age of onset ranges from 36-62 years old, with a disease duration of 8-72 months from the time of insomnia onset (Montagna et al. 1998). Death may be sudden while the patient is fully conscious, or they may lapse into a vegetative state and succumb to infection (Montagna et al. 1998; Montagna et al. 2003).

(v) Gerstmann-Sträusler-Scheinker syndrome (GSS) is also a rare hereditary disorder associated with a number of point mutations within the prion protein (Figure 1.2), with an incidence rate of approximately 1 case per 10 million people annually. GSS is always associated with a genetic mutation, and is inherited in an autosomal dominant pattern (Pocchiari 1994; Ghetti et al. 1995). Disease onset of GSS typically starts when the carrier is 50-70 years old, with disease duration ranging from 1-10 years (Ghetti et al. 1995; Young et al. 1997).

1.1.2 Disease Characteristics

Although all proteinaceous neurodegenerative diseases share some similarities such as aggregation of misfolded proteins and neuronal vacuolation, important

differences exist. The major difference between TSEs and other protein-misfolding disorders such as Huntington's, Alzheimer's and Parkinson's disease is that, as the name implies, TSEs are capable of disease transmission both within and between species from one host to another (Nunziante, Gilch, and Schatzl 2003; Muchowski and Wacker 2005).

1.1.2.1 Phenotypic Characteristics of Prion Diseases

Independent of the host species, general commonalities exist among all known prion diseases. Early symptoms include behavioural disturbances, loss of concentration and memory, as well as mild twitching (myoclonus). These symptoms progress to difficulty swallowing (dysphagia), loss of verbal articulation in the case of humans (dysarthria), ataxia, and inevitably death. The age at which phenotypic onset occurs varies significantly from youth to senior, with most sporadic or familial forms of the disease being characterized by their long incubation periods (it can be more than 30 years in humans). In contrast, the length of time from disease onset of vCJD to death is measured in months (Goldfarb and Brown 1995; Montagna et al. 2003).

1.1.2.2 Histological Presentation of Prion Diseases

Although prion diseases manifest differently and present varying histological observations, including amyloid plaque size and distribution, there are some general features associated with disease pathology. Histological examination of brain sections from late stage prion-affected hosts stained with hematoxylin and eosin (H&E) demonstrate a generalized neuronal vacuolation, gliosis, and astrocytosis. In most instances, the presence of amyloid plaques are observed when viewed under high

magnification coupled with immunohistochemical techniques (Chandler 1961; Williams and Young 1993; Vital et al. 1998; Montagna et al. 2003; Budka 2003) (Figure 1.3).

1.1.3 Identification of the Causative Agent of Prion Disease

Early studies of the scrapie agent in sheep flocks led researchers to hypothesize that transmission of prion disease was purely hereditary, with an unusual inheritance pattern (Parry 1960; Draper and Parry 1962). It was subsequently shown that scrapie arises from an infectious agent, but that susceptibility is influenced by host genetics. Although studies performed in sheep provided early research of the infectious scrapie agent, experiments were very long-term, expensive, and required huge areas of land.

It was not until the scrapie agent was transmitted to laboratory strains of mice that research into the underlying mechanisms of disease could be studied by typical laboratories. Dr. R. L. Chandler was the first researcher to successfully confirm transmission of the scrapie agent from infected sheep brain to mice, simultaneously providing the first detailed description of phenotypic behaviour and the histological lesion profile (Chandler 1961). Results of these initial transmission studies also demonstrated that successful transmission was dependent upon the inoculated “strain” of scrapie and the genetic background of the recipient mouse. Together, these transmission studies implied an infectious agent was responsible for TSEs, with host susceptibility influenced by a genetic determinant (Chandler 1961). Further supportive evidence for a genetic determinant came from realization that the incubation period of scrapie in mice was regulated by a gene, which was termed *sinc* for scrapie *incubation* period (Dickinson, Meikle, and Fraser 1968). Almost 10 years after the first reported successful

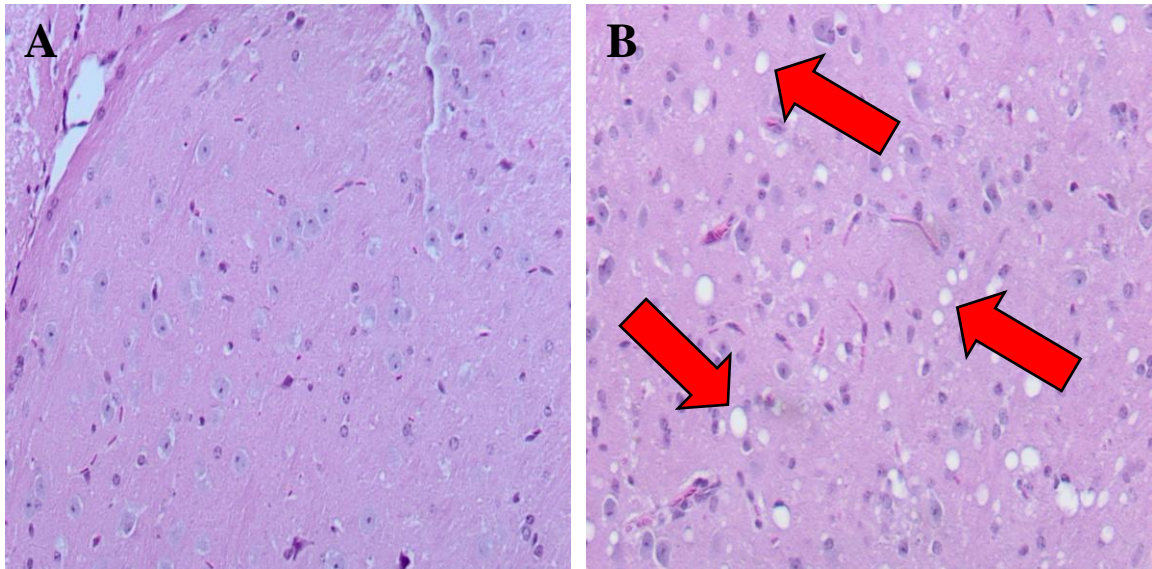


Figure 1.3: Scrapie-Induced Neuronal Vacuolation

One classic histological presentation of prion infection is widespread neuronal vacuolation. The above panels represent coronal sections of mouse brains at ~day 145 post intracranial inoculation, stained with hematoxylin and eosin (H&E). Dark purple staining highlights nuclei, while pink denotes cell cytoplasm. Images were taken at 40X magnification. Panel A represents a typical staining pattern for mice inoculated with control brain homogenate. Panel B represents a typical staining pattern for mice inoculated with scrapie ME7 brain homogenate. Note the abundance of vacuoles in panel B compared to panel A, which appear as white circular shapes where neurons have undergone apoptosis, leaving cell-free spaces. This appearance gave rise to the term “spongiform” in transmissible spongiform encephalopathies (TSEs). Red arrows point to examples of vacuoles. Slides were prepared by our collaborators Catherine Graham and Stephanie Czub in Lethbridge, Alberta. Microscopic images were taken by Michael Stobart.

transmission of scrapie to mice, it was demonstrated that hamsters exhibited even greater susceptibility to the scrapie agent, with disease progressing almost twice as fast (Marsh and Kimberlin 1975).

The generation of a mouse model of scrapie launched a new era of prion research. The primary focus was identifying the nature of the infectious agent which confounded researchers at the time due to the extremely small predicted size of the agent and its resistance to excessively high doses of ionizing radiation (IR), which argued against a nucleic acid-based pathogen. Early estimates deduced that the infectious agent, if nucleic acid based, would possess approximately 800 bases, nearly ten times smaller than the smallest viral particles known at the time (Alper, Haig, and Clarke 1966). Further studies utilizing IR to inactivate the scrapie agent demonstrated the infectious material to be extremely resistant to doses which inactivate even the most radiation resilient microorganisms known. The potential of a protein as being the scrapie agent was alluded to at an early stage due to a slight decrease in infectivity when ultraviolet light, at a wavelength absorbed maximally by proteins, was used (Alper et al. 1967).

The infectious agent was proposed to be protein-based in 1982 by Dr. Stanley Prusiner. Through a series of biological and biochemical assays, chemical and enzymatic treatments, as well as UV irradiation, the infectious agent responsible for TSEs was confirmed to be a low molecular weight species resistant to nucleases, irradiation, hydrolysis, and resistant to denaturation by heating to 90°C for 30 minutes. Combining these results led Dr. Prusiner to suggest that the infectious agent is protein in nature, and proposed the acronym “prion”, derived from the words *proteinaceous infectious particle* (Prusiner 1982). Using a variety of assays and purification steps, a protease-resistant

peptide was isolated from brains of scrapie-infected hamsters with an approximate molecular weight of 27-30 kDa, and the N-terminus was sequenced. Synthesis of oligonucleotides coding for all possible combinations of open reading frames (ORFs) encoding the sequenced peptide initially identified partial cDNA clones for both the hamster and mouse genes (Oesch et al. 1985; Chesebro et al. 1985). These initial cDNA clones paved the way for determination of the hamster and mouse gene sequences through library probing experiments. Mapping of cDNA sequences to the genome localized the corresponding allele to human chromosome 20p12 and mouse chromosome 2p13 (Sparkes et al. 1986). The allele was named *prnp* and the encoded protein, the prion protein or PrP (Oesch et al. 1985; Basler et al. 1986; Sparkes et al. 1986; Lochter et al. 1986).

1.2 Description of the Human Prion Protein

The 253 amino acid human prion protein (PrP) is expressed in a wide range of tissues and cell types (such as placenta, heart, liver, spleen, and brain tissues, as well as endothelial cells, astrocytes, and oligodendrocytes), but is predominantly found in neurons (up to 50 mRNA copies per neuron) (Kretzschmar et al. 1986; Brown et al. 1990; Tanji et al. 1995; Moser et al. 1995; McLennan et al. 2001; Simák et al. 2002; Aguzzi and Polymenidou 2004; Ning et al. 2005b) (Figure 1.2). It is translated as a pro-protein from a single exon, with N- and C-terminus signal peptides of 22 and 23 amino acids respectively. The N-terminal localization signal targets PrP to the cell membrane. Mature PrP is anchored to the membrane by a glycosylphosphatidylinositol (GPI) anchor, which is added upon cleavage of the C-terminus signal peptide, with specific localization

to cholesterol-rich lipid rafts (Shyng, Heuser, and Harris 1994; Gorodinsky and Harris 1995; Taraboulos et al. 1995). The normal PrP typically contains 5 octapeptide repeats spanning amino acids 51-91, with insertions and deletions in this region associated with disease (Glatzel et al. 2005). These octapeptide repeats are predicted to bind copper ions (Brown et al. 1999; Brown 2001; Glatzel et al. 2005). A short hydrophobic domain, also referred to as the transmembrane domain, spans amino acid residues 112-135 (including the AGAAAAGA palindromic sequence), which influences PrP membrane topology (Hegde et al. 1998; Gu et al. 2006). Amino acid codon 129 of human PrP is polymorphic, encoding either methionine or valine, which influences disease susceptibility and histological presentation (Palmer et al. 1991; Collinge, Palmer, and Dryden 1991; Parchi et al. 1999; Alperovitch et al. 1999). A disulfide bond between cysteine residues 179 and 214 stabilizes the tertiary structure (Riek et al. 1996; Riek et al. 1997; Zahn et al. 2000). Two potential glycosylation sites exist, asparagine residues 181 and 197, such that the protein may be un-, mono-, or diglycosylated (Collinge et al. 1996; Parchi et al. 1999; Will et al. 2000; Ironside et al. 2000; Glatzel et al. 2005) (Figure 1.2). The prion protein exists in 2 alternate tertiary configurations. Cellular PrP (PrP^c) consists predominantly of α -helices and the disease related isoform PrP^{res} (for its increased resistance to proteases, or PrP^{Sc} for its association with scrapie), predominantly of β -sheet. It is currently not known whether disease pathogenesis is the result of a loss of normal PrP^c functioning, or a gain of function of the PrP^{res} protein.

1.2.1 Cellular Prion Protein (PrP^c) Structure

The normal form of the human cellular prion protein (PrP^c) consists of ~40% α -helical and ~3% β -sheet secondary structure (Pan et al. 1993; Stahl et al. 1993; Riek et al. 1996; Hornemann et al. 1997; Knaus et al. 2001). PrP^c has a molecular weight ranging from 30-35 kDa depending upon glycosylation, and is very sensitive to cellular proteases (Pan et al. 1993). The 3 α -helices span amino acids 144-154, 173-194, and 200-228, while the 2 short anti-parallel β -sheets span 128-131, and 161-164 (Riek et al. 1996; Riek et al. 1997; Zahn et al. 2000) (Figure 1.2).

1.2.1.1 Variants of the Prion Protein

The majority of PrP^c is secreted to the plasma membrane from the endoplasmic reticulum (ER). However, a portion (~10%) is retained in the ER membrane as a transmembrane form, with 35% of the retained PrP proteins oriented with the C-terminus in the ER lumen (^{Ctm}PrP), 15% with the N-terminus in the ER lumen (^{Ntm}PrP), and the remaining 50% spanning the membrane. Beyond these alternate PrP topologies, there are N-terminal truncated, cytoplasmic (CyPrP), and nuclear forms (Chen et al. 1995; Hegde et al. 1998; Hegde et al. 1999; Kim and Hegde 2002; Ma, Wollmann, and Lindquist 2002; Harris 2003). The role of these minor forms of PrP^c is unknown, but neurotoxicity is associated with some variants. Site directed mutagenesis of the transmembrane domain and the N-terminus signal sequence of PrP results in the preferential expression of ^{Ctm}PrP. The overexpression of ^{Ctm}PrP induces neurotoxicity (Chen et al. 1995; Hegde et al. 1998; Hegde et al. 1999; Kim and Hegde 2002; Ma, Wollmann, and Lindquist

2002; Harris 2003). Expression of CyPrP, accomplished by cloning of the *prnp* transcript without the N- and C-terminal signal sequences, leads to aggregation of CyPrP and neuronal apoptosis (Grenier et al. 2006; Wang et al. 2006; Wang et al. 2009). Expression of N-terminally truncated forms of PrP (PrP Δ 32-121 or PrP Δ 32-134, collectively termed PrP Δ N) in a *prnp*^{0/0} mouse background leads to ataxia, extensive neurodegeneration, and fatality, with rescue of the normal phenotype by co-expression of *prnp* (Shmerling et al. 1998; Flechsig et al. 2003).

A short 179 amino acid protein termed Doppel shows sequence and structure similarity to the C-terminus of the prion protein, and is encoded by a genomic locus (*prnd*) downstream of *prnp*. Over expression of Doppel in *prnp*^{0/0} mice leads to ataxia with prominent degeneration of cerebellar Purkinje neurons. The normal phenotype can be rescued by over expression of PrP^c (Moore et al. 1999; Anderson et al. 2004). These observations led the authors to posit that altered expression of Doppel in a prion-infected host could exacerbate neurodegeneration (Moore et al. 1999). Doppel-mediated neurodegeneration in *prnp*^{0/0} mice is abolished by also knocking out *prnd*, further supporting a potential role of Doppel in prion disease-associated neurodegeneration (Genoud et al. 2004). However, altered expression of Doppel is not the sole cause of prion-induced neurodegeneration as ablation of the *prnd* locus confers no protection against prion-mediated neurodegeneration (Behrens et al. 2001). This suggests that disruption of normal PrP^c functioning and signaling could be responsible for the observed pathology in brains of prion-infected hosts.

1.2.1.2 Predicted Function of PrP^c

The exact function of PrP^c is unknown, with knockout animals showing various symptoms. Of the numerous theories that have been proposed, three are discussed below (Glatzel et al. 2005). It should be noted that the proposed functions of PrP^c could require the involvement of associated proteins, such as laminin, Hsp60 (chaperone protein), Nrf2 (transcription factor), or Bcl-2 (regulator of apoptosis) (Kurschner and Morgan 1995; Edenhofer et al. 1996; Yehiely et al. 1997; Graner et al. 2000a; Graner et al. 2000b; Stockel and Hartl 2001).

Susceptibility to prion pathogenesis is PrP dependent as mice devoid of PrP^c are resistant to development of disease when challenged with infectious tissue. Susceptibility is restored through expression of a prion transgene (Sailer et al. 1994; Fischer et al. 1996; Katamine et al. 1998). The ablation of PrP^c expression leads to varying phenotypic manifestations including no visible characteristics, disturbances of sleep patterns, enhanced susceptibility to induced seizures, or ataxia depending upon the background mouse strain (Tobler et al. 1996; Katamine et al. 1998; Rangel et al. 2007; Gadotti, Bonfield, and Zamponi 2011). Most *prnp*^{0/0} mice display no obvious symptoms, complicating the determination of the normal function of PrP^c (Bueler et al. 1992; Manson et al. 1994).

Using the mouse strain C57BL/6J, a group in Japan described PrP^c null mice (*prnp*^{0/0}) with severe symptoms. Embryonic and post-natal development was unperturbed, but by 70 weeks of age all *prnp*^{0/0} mice displayed abnormal gait, and hindlimb trembling. Symptoms progressed to an inability to stand up, and severe loss of coordinated muscle movement. Pathologically, *prnp*^{0/0} mice had an overall smaller brain,

severe cerebellar atrophy, and extensive loss of Purkinje cells (Sakaguchi et al. 1996; Katamine et al. 1998).

Due to inconsistencies of phenotypes observed in *prnp*^{0/0} rodent models, the normal function of PrP^c remains elusive (Roucou, Gains, and LeBlanc 2004). It has been proposed to play a role in response to oxidative stress, act as a signal transducer to mediate intracellular response mechanisms, and mediate apoptosis.

1.2.1.3 Antioxidant Function of PrP^c

The octapeptide repeat region is capable of binding copper ions, which led to the hypothesis that PrP^c may play a role in protecting the cell against oxidative damage (Brown et al. 1997a; Brown et al. 1999; Glatzel et al. 2005). The PrP^c copper ion binding may modulate the activities of copper (Cu²⁺)/zinc (Zn²⁺) superoxide dismutase (SOD) and the glutathione reductase pathway (Brown and Besinger 1998; Rachidi et al. 2003). PrP^c expression and Cu/Zn-SOD activity show a direct correlation, with correspondingly increased levels of intracellular hydrogen peroxide (H₂O₂) due to increased Cu/Zn-SOD activity with increasing PrP^c expression (Brown and Besinger 1998). Excess H₂O₂ is normally detoxified via the glutathione pathway to H₂O and O₂. Accumulation of H₂O₂ leads to genomic DNA mutations and induces apoptosis. Neurons devoid of PrP (*prnp*^{0/0}) show increased susceptibility to H₂O₂-induced oxidative stress, which could be explained by the significantly reduced glutathione reductase activity measured both *in vitro* and *in vivo* (Brown et al. 1997b; White et al. 1999).

Through exposure of PrP^c-inducible cells to physiological levels of radioactive copper, PrP^c has been confirmed to bind copper directly, but this does not result in the

internalization of copper under physiological conditions. The authors propose that PrP^c is acting as a copper sensor, activating intracellular anti-oxidant response mechanisms via a signal transduction pathway (Rachidi et al. 2003).

1.2.1.4 PrP^c Mediated Signal Transduction

PrP^c has been proposed to mediate the transduction of a neuroprotective signal (Chiarini et al. 2002). Studies demonstrate cell membranous PrP^c to be a mediator of signal transduction through interaction with a number of cellular receptors including Fyn and laminin that are associated with neuronal proliferation and survival, and/or neurite outgrowth, respectively (Graner et al. 2000a; Chen et al. 2003; Bizat et al. 2010). Along this same line, PrP^c has been proposed to play a role in synaptic transmission through synapsin 1b and Grb2, but evidence for PrP^c involvement in synaptic transmission is debated due to conflicting results obtained from PrP^c knockout mice (Collinge et al. 1994; Lledo et al. 1996; Spielhauer and Schatzl 2001). Further evidence for PrP^c possessing a signal transduction capability, either directly or through as yet unidentified binding partners, includes the observation that dimerization of PrP^c molecules by divalent antibodies leads to apoptotic neurotoxicity *in vivo*, whereas monovalent antibodies do not cause toxicity. The authors propose that PrP^c may function as an anti-apoptotic signaling molecule, and that dimerization of PrP^c extinguishes this ability, leading to pro-apoptotic signaling (Solforosi et al. 2004).

1.2.1.5 Anti-Apoptotic Function of PrP^c

PrP^c has been demonstrated to interact with the anti-apoptotic protein, Bcl-2 (Kurschner and Morgan 1995). Strong evidence for PrP^c playing a protective, anti-apoptotic role came from a study in which the potent pro-apoptotic inducer Bax, was overexpressed in human primary neurons alone, with Bcl-2, or PrP^c. Bax overexpression led to prominent apoptosis, while co-expression with either Bcl-2 or PrP^c provided significant protection. Corroborating this result, deletion of 4 of the 5 octapeptide repeats completely abolished the protection against Bax-mediated apoptosis, while PrP^c lacking a GPI-anchor showed no difference in the protection conferred (Bounhar et al. 2001). Nonetheless, the hypothesis that Bax and Bcl-2 play a role in prion pathogenesis is not supported *in vivo*. Mice null for Bax or overexpressing Bcl-2 did not alleviate the clinical severity of prion infection (Steele et al. 2007). These results imply that PrP^c confers protection against Bax-mediated apoptosis, but that prion-disease associated apoptosis is independent of Bax.

The anti-apoptotic effect of PrP is also abolished when amino acid residue 178 is mutated from an aspartate to an asparagine residue (D178N), as is seen with FFI. This suggests that other mutations underlying familial forms of TSE disease could manifest due to the loss of protection against apoptosis (Roucou, Gains, and LeBlanc 2004).

1.2.2 Disease Associated Prion Protein (PrP^{res})

The infectious form of the PrP^c protein is termed PrP^{res} for its partial resistance to protease degradation (McKinley, Bolton, and Prusiner 1983). Upon proteinase K digestion, an approximate 6kDa shift in molecular weight is visualized by immunoblot,

with this protease resistant core fragment referred to as PrP²⁷⁻³⁰ (Oesch et al. 1985). Through passaging of prions from different hosts to different models expressing *prnp* genes of varying species, strains based upon the PrP²⁷⁻³⁰ banding patterns have been identified that possess distinct phenotypic and chemical characteristics (Prusiner 1998).

The primary amino acid sequence, as well as glycosylation and GPI anchor, of both PrP^c and PrP^{res} are the same, but PrP^{res} (and the aforementioned PrP²⁷⁻³⁰) isoforms are capable of aggregating into fibrils that exhibit significantly enhanced resistance to IR, heat, and chemical sterilization (Stahl et al. 1993). PrP^{res} also possesses the ability to direct re-folding of PrP^c molecules to match that of the initial PrP^{res} tertiary structure, leading to an accumulation of infectious particles (Jarrett and Lansbury, Jr. 1993; Telling et al. 1995; Prusiner 1998; Aguzzi and Polymenidou 2004).

1.2.2.1 Structure and Physical Properties of PrP^{res}

The primary amino acid sequence of PrP^{res} is identical to that of the normal PrP^c. The distinguishing features of PrP^{res} are based on the secondary structure, which is predominantly rigid β -sheet whereas PrP^c is principally α -helix. PrP^{res} is predicted to be comprised of ~40% β -sheet and ~30% α -helical secondary structure (Pan et al. 1993; Safar et al. 1993b), but no successful detailed analysis of individual PrP^{res} molecules has been accomplished to date. However, analysis of amyloid rods resulting from polymerization of protease treated PrP^{res} (PrP²⁷⁻³⁰) suggested a ~50% β -sheet and 20% α -helix content (Prusiner et al. 1983; Caughey et al. 1991; Pan et al. 1993; Gasset et al. 1993; Safar et al. 1993a). Due to this abundance of β -sheet, the tertiary structure of PrP^{res} is also unique from PrP^c. α -helix 2 and 3 are predicted to remain intact, possibly due to

stabilization by the disulfide bond, but the N-terminus, α -helix 1, and both β -sheet stretches are predicted to re-fold into a triangular stack. Trimeric aggregates of PrP^{res} molecules are theorized to result in a flat, disc-like unit, with fibrils consisting of stacks of these individual units (Govaerts et al. 2004) (Figure 1.4).

Anchorage of PrP^{res} to the membrane via its GPI anchor may represent an underlying neurotoxic mechanism, as anchorless (lacking a GPI anchor) PrP^{res} accumulate as amyloid plaques in the brain, but leads to minimal clinical disease manifestation. When anchorless and normal PrP are co-expressed, disease manifestation proceeds at an accelerated rate (Chesebro et al. 2005).

PrP^{res} exhibits increased resistance to proteases, heat, UV, and chemical treatments. It is insoluble in mild detergents, and, as mentioned above, PrP^{res} is capable of forming aggregates and directing re-folding of PrP^c molecules (Meyer et al. 1986). The short pre-fibrillary PrP^{res} oligomers composed of 14-28 PrP^{res} molecules constitute the most infectious particles (Jarrett and Lansbury, Jr. 1993; Lansbury 1994; Silveira et al. 2005; Simoneau et al. 2007).

1.2.2.2 PrP^{res} Associated Neurotoxicity

The neurotoxicity of short oligomeric species of β -sheet rich PrP relative to that of long fibrils has been compared. By applying β -sheet rich PrP preparations onto a primary cortical neuronal cell line and by injecting β -sheet rich PrP preparations or control solution into either the right or left brain hemisphere of both normal and *prnp*^{0/0} mice, it was demonstrated that the β -sheet rich PrP oligomers were much more

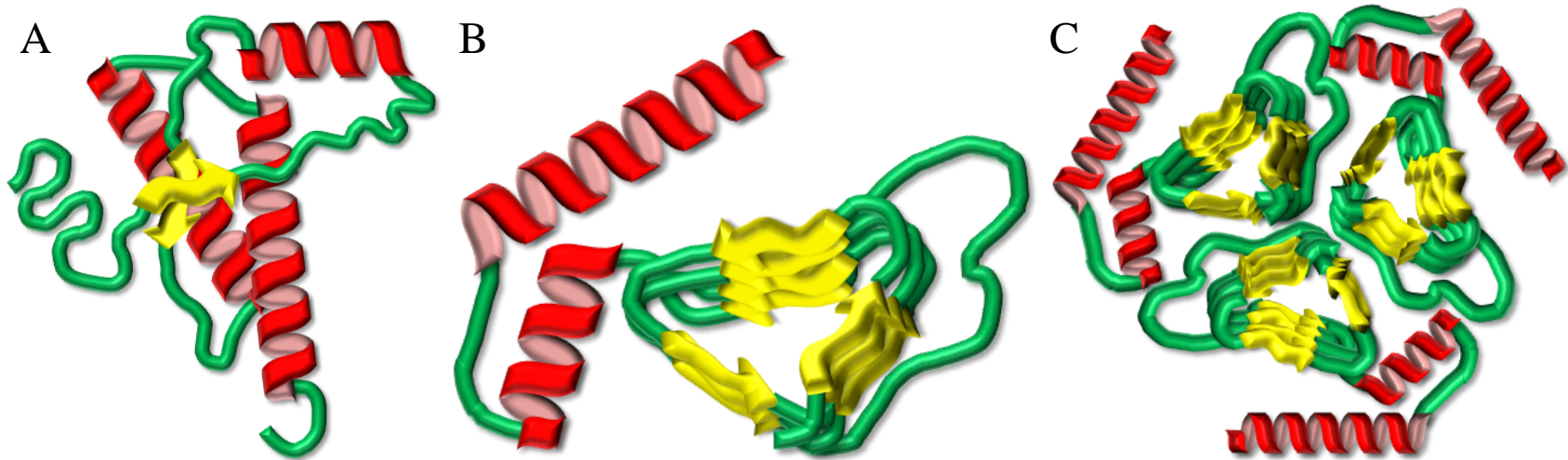


Figure 1.4: Tertiary Structure of PrP^c and PrP^{res}

The crystal structure for PrP^c has been determined, but that of PrP^{res} and the aggregated forms are predicted. Unstructured regions are denoted by green lines, α -helix regions by red corkscrew shapes, and β -sheet stretches by yellow arrows. (A) PrP^c tertiary structure with the N-terminus on the left, and the C-terminus as the bottom. (B) The predicted structure of PrP^{res}, with helix 2 and 3 on the left. The N-terminus, the 2 β -sheet stretches, and α -helix 1 are re-folded into the β -sheet triangle. (C) Three PrP^{res} molecules associated into a trimeric aggregate (some authors suggest a hexameric aggregate), which can stack like discs into fibrils. The GPI anchor is not shown in any of the structures. Adapted from (Riesner 2003; Govaerts et al. 2004).

neurotoxic than β -sheet rich PrP fibrils. Controls showed no neurotoxicity (Simoneau et al. 2007). This study highlights two points: (i) oligomeric β -sheet rich PrP is much more toxic than β -sheet rich PrP fibrils, which has been confirmed by others (Kristiansen et al. 2007); and (ii) PrP^c expression may not be required for β -sheet rich PrP-induced neurotoxicity, but is essential for disease propagation (Simoneau et al. 2007). Chronic exposure to degradation products of β -sheet rich PrP, such as PrP²⁷⁻³⁰, or β -sheet rich PrP oligomers, may be the underlying cause of neurodegeneration observed in brains of affected individuals (Forloni et al. 1993).

1.2.2.3 PrP^{res}-Mediated Neurodegeneration

Neuronal loss and spongiosis are prominent features of prion disease, but neuronal vacuolation occurs prior to, and does not correlate with, intensity of PrP^{res} deposition. Neuronal degeneration is prominent and wide spread throughout the brain as observed upon histological examination of brains from symptomatic rodent models of disease (Baringer, Bowman, and Prusiner 1983; Muhleisen, Gehrman, and Meyermann 1995; Lasmezas et al. 1996; Theil et al. 1999; Jamieson et al. 2001). The mechanism of neurodegeneration appears to be mediated by the endogenous apoptotic pathway, as evidenced from the close proximity of apoptotic neurons to existing vacuolated brain regions, and detectable markers of apoptosis (Gray et al. 1999).

1.2.2.4 PrP^{res} Induced Apoptosis

Apoptosis is a regulated mechanism by which cells undergo coordinated cell death. It is a tightly regulated cell response pathway that involves numerous check points

to prevent unnecessary cell death. Neuronal apoptosis may be induced by a number of insults including oxidative damage, microglial activation, and accumulation of misfolded proteins (Okouchi et al. 2007).

Genomic DNA extracted from brain cells of scrapie-infected sheep demonstrates a laddering banding pattern upon electrophoresis, a result of apoptosis-induced endonuclease-mediated fragmentation of nuclear DNA (Arends, Morris, and Wyllie 1990; Fairbairn et al. 1994). Brains examined from humans that had succumbed to CJD or FFI showed apoptotic neurons, typically in the vicinity of vacuolation (Dorandeu et al. 1998; Gray et al. 1999). The apoptotic neurons of BSE infected cattle brains were typically associated with prominent spongiform change, astrocyte and microglia recruitment, but association with PrP^{res} deposition was variable (Theil et al. 1999). A similar divergence between apoptotic neurons and PrP^{res} deposition is observed in prion diseases such as FFI, where PrP^{res} aggregates are minimal (Giese et al. 1995; Dorandeu et al. 1998; Theil et al. 1999; Jamieson et al. 2001). This may be explained by aggregates too small to detect by immunohistochemical (IHC) methodologies, or deposits of PrP^{res} aggregates not being directly responsible for observed neurodegeneration, but rather a result of disease.

Mouse models of prion disease have identified a significant induction of active caspase 3, a mediator of apoptosis, prior to detection of PrP^{res} aggregates and consistent throughout disease course (Jamieson et al. 2001). Inhibition of the protein degradation complex (proteasome) increases PrP^c expression, and a concomitant activation of caspase 3, suggesting overexpression of the prion protein, potentially either PrP^c or PrP^{res}, may be responsible for the induced caspase 3 activation observed. These studies also revealed

that prolonged activation of caspase 3 is not sufficient for induction of apoptosis, but may sensitize cells to further insult (Paitel et al. 2002; Kristiansen et al. 2005; Bourteele et al. 2007). Supporting evidence for caspase-mediated apoptosis comes from detectable increases in the endoplasmic reticulum (ER) caspase 12, which is activated in the presence of altered calcium homeostasis or following accrual of improperly folded protein (Nakagawa et al. 2000; Hetz et al. 2003). Application of highly purified PrP^{res} from scrapie-infected mouse brains onto mouse neuroblastoma cells induced the activation of caspase 3, but not caspase 1 or 8, and led to the release of ER Ca²⁺. Activation of caspase 12, but not caspase 8, has been confirmed in brains of mouse models infected with scrapie and human patients affected by either sCJD or vCJD, strongly supporting perturbations of the ER are a result of prion infection (Hetz et al. 2003). Together, these experiments demonstrate that PrP^{res} induces apoptosis through activation of caspases 3 and 12, with activation of both caspases sufficient to commit the cell to apoptosis. Others argue that stimulated microglial cells induce neuronal apoptosis.

1.2.2.5 PrP^{res} Induced Gliosis

Microglial and astrocyte activation and migration has been observed prominently around areas of neuronal vacuolation and apoptotic neurons in CJD, FFI, scrapie, and BSE (Williams et al. 1994; Muhleisen, Gehrman, and Meyermann 1995; Lasmezas et al. 1996; Dorandeu et al. 1998; Theil et al. 1999; Gray et al. 1999; Gray et al. 2006). Using a microglial cell line, it has been demonstrated that neurons or astrocytes exposed to PrP^{res} induce recruitment of microglial cells via soluble factors (Marella and Chabry 2004). The role of gliosis (migration and activation of astrocytes and microglia) in prion

disease remains elusive. It may be that glial cells are responding to neuronal apoptosis, with recruited microglia engulfing and breaking down apoptotic neurons. Alternatively, activation and recruitment of glial cells may induce apoptosis of damaged or PrP^{res}-expressing neurons and therefore represent an underlying explanation of observed neurodegeneration (Williams et al. 1994; Dorandeu et al. 1998; Theil et al. 1999; Gray et al. 1999). Evidence supports the first view, in which gliosis occurs as a result of neurodegeneration, as evidenced by markers of neuronal apoptosis in the absence of microglial activation (Theil et al. 1999).

1.3 Concept of Prion Strains

Unlike nucleic acid-based pathogens, prion proteins encipher strain specific characteristics within their structure (Prusiner 1998). These characteristics may include phenotypic manifestation, incubation time, pattern of aggregate deposition throughout the brain, neuronal lesion profile, susceptible host range, and tertiary conformation. Generally, these traits are transmitted true from one host to another and mimic the characteristics of the initial infectious agent, but “strain mutations” can arise when transmitted across species or when the host encodes a specific mutation of the prion gene (Bruce et al. 2002; Wadsworth et al. 2004).

Strains are classified based upon their proteinase K resistant banding pattern by immunoblotting, which permits visualization of the size of bands and relative abundance of glycosylation moieties (Collinge et al. 1996; Parchi et al. 1999). This distinction provides a means of diagnosing and surveying prion diseases, including cross-species

transmission. This strain typing provided strong evidence for BSE as the infectious agent in human vCJD (Collinge et al. 1996; Hill et al. 1997).

1.4 Conversion Theories

Conversion of PrP^c to PrP^{res} occurs post-translationally by an as yet unidentified mechanism. There are 2 predominant theories: (i) “template-assisted” protein refolding, and (ii) “seed nucleation”. Both theories revolve around the hypothesis that infectious PrP^{res} is capable of acting as a scaffold for PrP^c to undergo a conformational reconfiguration, which is required for propagation of the infectious form (Figure 1.5).

1.4.1 Template-Assisted Refolding Theory

This theory assumes that conversion of PrP^c to PrP^{res} is thermodynamically unfavorable, and that an endogenous protein or protein complex termed “protein X” destabilizes PrP^c to a transitory state termed PrP*. The protein X/PrP* complex interacts with exogenous or endogenous PrP^{res}, which acts as a template for reconfiguring the tertiary structure of PrP* to mimic that of PrP^{res}. Newly formed PrP^{res} molecules are then capable of associating with nearby protein X/PrP* complexes, amplifying the number of PrP^{res} molecules, which spontaneously aggregate into fibrils (Telling et al. 1995; Prusiner 1998) (Figure 1.5A).

1.4.2 Seeded Nucleation Theory

The seeded nucleation theory is the more commonly accepted of the two hypotheses. It assumes that PrP^c and PrP^{res} are in constant equilibrium, with PrP^c being

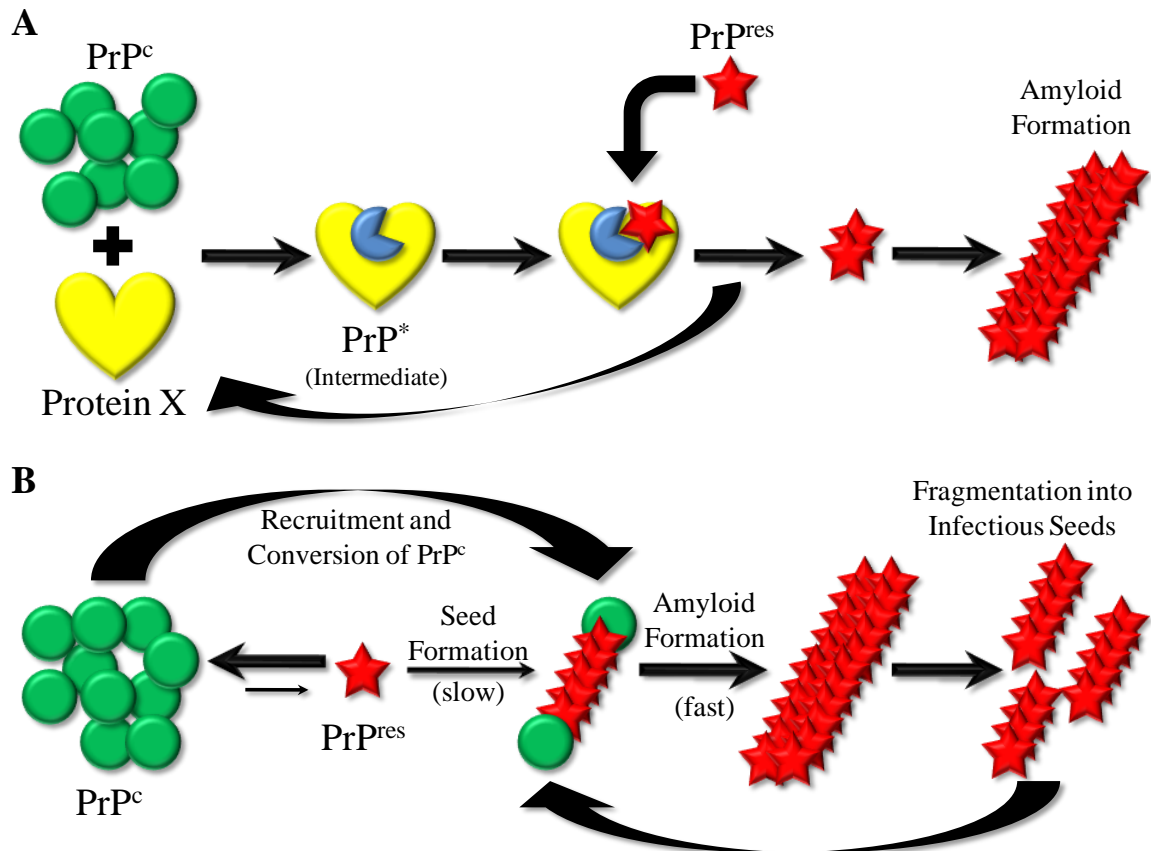


Figure 1.5: Proposed Models for PrP^c to PrP^{res} Re-folding

There are 2 models describing PrP^c to PrP^{res} conversion. (A) The template-assisted model assumes an unidentified chaperone “protein X” partially denatures PrP^c to PrP*. Protein X/PrP* complex binds exogenous or spontaneous/familial PrP^{res} molecules, which act as a template for re-folding of PrP* to PrP^{res}. PrP^{res} molecules spontaneously aggregate into fibrils. (B) The seeded nucleation model states that PrP^c and PrP^{res} are in equilibrium, strongly favoring PrP^c. Rarely, spontaneous PrP^{res} molecules associate, stabilizing the tertiary structure, and form infectious seed oligomers, which direct PrP^c re-folding. Oligomer seeds readily associate to form long fibrils, which fragment into short oligomers, propagating PrP^{res} accumulation and aggregation. Adapted from (Serio et al. 2000; Aguzzi and Calella 2009).

the favored state. Monomeric PrP^{res} molecules exist in minute amounts and individually are harmless, but interaction of small numbers of monomeric PrP^{res} to form aggregates stabilizes the infectious state. These aggregate seeds then form highly ordered and stable amyloid fibrils which direct refolding of PrP^c into PrP^{res}, extending the amyloids into fibrils. These fibrils fragment forming further seeds and conversion propagates at an ever accelerating rate (Jarrett and Lansbury, Jr. 1993; Aguzzi and Polymenidou 2004) (Figure 1.5B).

1.5 Peptide Model of Prion-Mediated Neurotoxicity

The incubation period of prion diseases in laboratory animal models inoculated via intracranial (I.C.) injection of infectious brain homogenate is typically measured in months, with other routes of inoculation requiring longer incubation times. The shortest disease course in a rodent model of prion disease is approximately 2 months before mice succumb to the disease. This rapid model requires extensive preparation of a mouse adapted scrapie “fast strain” inoculum, and a transgenic mouse model that expresses a sheep prion protein variant known to enhance susceptibility (Tixador et al. 2010). When turning to non-human primates as disease models, the incubation time span increases to years, with a Rhesus monkey model requiring 3 years for development of clinical symptoms when inoculated intraperitoneally (I.P.) (Krasemann et al. 2010). Complexities with generating transgenic animals and the long time spans associated with laboratory animal models have prevented the undertaking of large scale, genome-wide “shot-gun” approaches to identify genes or drug targets fundamental to disease toxicity (Solassol, Crozet, and Lehmann 2003). The development of a cell culture-based model

of disease neurotoxicity is needed in order to perform large-scale gene or drug therapy screens. Advancing to animal models only those treatments that showed promise in the cell culture model would save time, money, and animals.

As with any model system, a mimic of disease toxicity which shows similar characteristics to the natural infectious agent must be identified. Analysis of an 11kDa amyloid deposit within brains from a family affected by GSS led to the identification of a common peptide sequence, spanning human prion amino acids 90-150. Focusing on this region led to the identification of the minimal amino acid sequence capable of forming spontaneous amyloid aggregates *in vitro* (Tagliavini et al. 1991). Using synthetic peptides of varying length spanning amino acid residues 90-150, amino acids 106-126 (human prion protein numbering) were determined to represent the minimal peptide sequence resulting in recapitulation of PrP^{res} chemico-physical characteristics observed in prion-diseased brains. These include the propensity to form β -sheet rich fibrils which are insoluble in mild detergents, partial resistance to proteases, induction of astrocyte proliferation, *in vivo* cytotoxicity, and induction of caspase-3 mediated apoptosis (Forloni et al. 1993; Ettaiche et al. 2000; White et al. 2001; Tagliavini et al. 2001; Stewart et al. 2001; O'Donovan, Tobin, and Cotter 2001; Corsaro et al. 2003; Ning et al. 2005a; Fioriti et al. 2005b; Simoneau et al. 2007). It has also been observed that exposure of neuronal cultures to PrP¹⁰⁶⁻¹²⁶ significantly reduces glutathione reductase activity, and sensitizes the neurons to H₂O₂ toxicity which is similar to results observed *in vivo* in response to prion infection (White et al. 1999).

Since its identification, the PrP¹⁰⁶⁻¹²⁶ peptide has become the major disease mimic utilized by prion researchers studying both immortalized neuronal cell lines and primary

neuronal cultures (Forloni et al. 1993; Thellung et al. 2000; White et al. 2001; Della-Bianca et al. 2001; Thellung et al. 2002; Drisaldi et al. 2003; Corsaro et al. 2003).

1.5.1 Description of the PrP¹⁰⁶⁻¹²⁶ Peptide

Although homogenized brain tissue from infected rodent models can be used to mimic disease pathogenesis and induce cell death *in vitro*, use of a defined amino acid sequence in the absence of extraneous substances has numerous advantages. It is readily available from numerous peptide synthesis companies in very pure form. It is considered non-infectious and therefore is a biological safety level 2 (BSL2) agent. It can be applied at known concentrations and under controlled conditions thereby permitting more accurate studies as to the neurotoxic potential of this peptide fragment. In humans, the amino acid residues 106-126 encode KTNMKHMAGAAAAGAVVGGLG (PrP¹⁰⁶⁻¹²⁶), with the mouse equivalent being amino acids 105-125. For experimental control, a peptide that contains the same amino acids, but does not form aggregates or induce neurotoxicity is necessary. In this case, the control peptide contains the same amino acids as PrP¹⁰⁶⁻¹²⁶, but in a scrambled order (PrP^{Scram}, NGAKALMGGHGATKVMVGAAA) (McHattie, Brown, and Bird 1999; White et al. 2001; Fioriti et al. 2005b).

1.5.2 Neurotoxic Properties of the PrP¹⁰⁶⁻¹²⁶ Peptide

The neurotoxicity and fibrillogenic nature of the PrP¹⁰⁶⁻¹²⁶ peptide has been predicted to be the result of the amyloidogenic palindrome AGAAAAGA (Tagliavini et al. 1993; Forloni et al. 1993; Norstrom and Mastrianni 2005). Mutants in which the

palindromic sequence has been deleted from the wild type PrP (wtPrP) protein are processed and localized like the wtPrP, and associate with infectious PrP^{res} proteins, but fail to undergo conversion to PrP^{res} (Norstrom and Mastrianni 2005). Point mutations within the palindromic sequence of the PrP¹⁰⁶⁻¹²⁶ peptide significantly influence the caspase-3 activation profile and neurotoxicity as compared to normal PrP¹⁰⁶⁻¹²⁶, providing evidence for the importance of the palindromic region in neurotoxicity (Jobling et al. 1999; Ettaiche et al. 2000; White et al. 2001; Corsaro et al. 2003; Bergstrom et al. 2007). Knowledge gained from studying the PrP¹⁰⁶⁻¹²⁶ peptide suggests that it is not necessarily the secondary structure of PrP^{res} which encodes its neurotoxic nature, but altered presentation of a portion of its primary amino acid sequence (Forloni et al. 1993; Ettaiche et al. 2000; Corsaro et al. 2003; Bergstrom et al. 2007).

1.5.3 Mechanism of PrP¹⁰⁶⁻¹²⁶ Neurotoxicity

The exact mechanism by which PrP¹⁰⁶⁻¹²⁶ elicits its neurotoxic effects remains unknown although numerous theories have been proposed, 4 of which are described below. These mechanisms discuss the importance of the 106-126 critical region, disruption of membrane integrity, PrP¹⁰⁶⁻¹²⁶ induced apoptosis, and microglia recruitment. The actual mechanism of neurotoxicity may be a combination of these theories, in which case no single hypothesis accurately describes the underlying cause of prion peptide-mediated neurotoxicity.

1.5.3.1 Functional Importance of the 106-126 Region

The 106-126 peptide sequence has been experimentally demonstrated to be essential for the overall function of the prion protein, and is therefore sometimes referred to as the critical region (CR). In *prnp* null mice (*prnp*^{0/0}) hemizygous for the prion protein with the CR region deleted (PrP Δ CR, *prnp*^{0/0}/*prnp* ^{Δ CR}) neurodegenerative symptoms which include immobility, myoclonus, and tremors ensue within 4 days of birth, succumbing within 1 week of birth. On a heterozygous background (*prnp*⁺⁰/*prnp* ^{Δ CR}), symptom onset occurs within 2 weeks of birth and the animals succumb within 1 month. Normal phenotype is rescued with expression of wtPrP in a dose-dependent manner (Li et al. 2007). Mouse PrP Δ CR transgenic animals display neurotoxic effects similar to excitotoxicity (Christensen et al. 2010). Two postulated functions of PrP^c have been used to explain the phenotype of PrP Δ CR transgenic mouse models. The hypothesis is that the CR region is essential for the proper interaction of PrP with its theoretical transmembrane ligand (Tr): (i) when the CR region is present, the interaction of PrP with Tr promotes transmission of a protective signal; or conversely (ii) in the absence of the CR region, the binding of PrP to Tr results in the transmission of a neurotoxic signal (Li et al. 2007; Christensen et al. 2010) (Figure 1.6).

1.5.3.2 PrP¹⁰⁶⁻¹²⁶ Insertion within Lipid Membranes

Synthetic liposomes incubated with varying concentrations of PrP¹⁰⁶⁻¹²⁶ exhibit a direct correlation in increasing membrane leakage, as measured by lactate dehydrogenase (LDH) release (Dupiereux et al. 2005). The theory being that the PrP¹⁰⁶⁻¹²⁶ interacts with a membrane due to electrostatic charge, inserts, at least partially, horizontally within

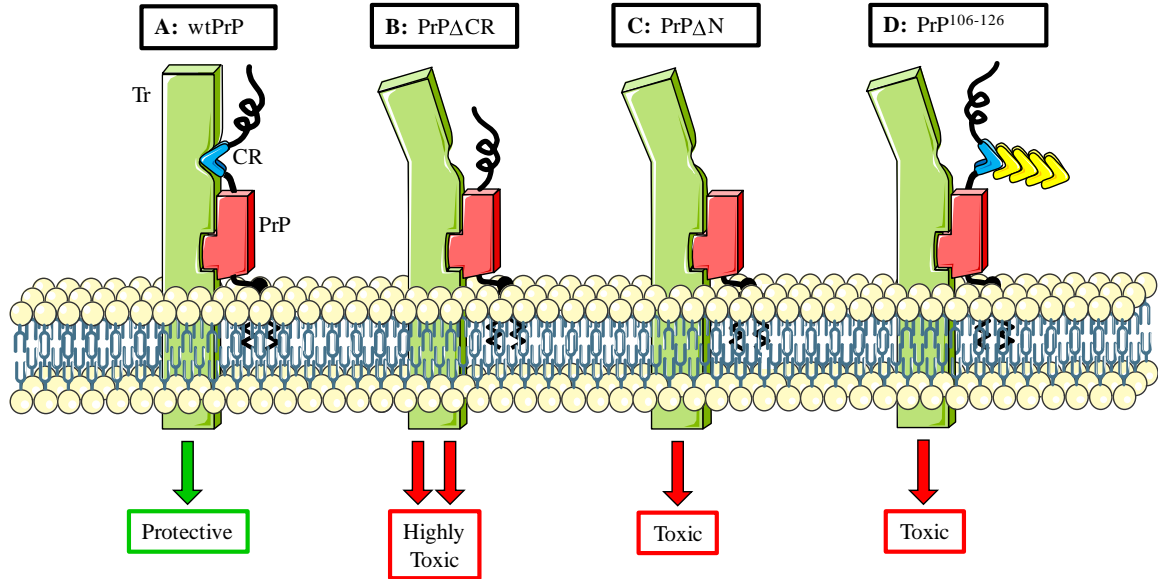


Figure 1.6: Proposed Models of PrP Mutant and PrP¹⁰⁶⁻¹²⁶ Toxicity

The flexible N-terminus is depicted as a squiggly black line, the CR region as a blue V-shape, and the structured C-terminus as a red box. The hypothetical PrP-interacting signal-transducing membrane protein (Tr) is depicted in light green. The GPI anchor is shown as a black line from the bottom of the red box with 2 zig-zag lines buried within the membrane (depicted as beige circles with a pale blue forked line). The hypothetical Tr protein is proposed to contain 2 PrP interacting sites, 1 which interacts with the C-terminus and 1 which interacts with the CR region. (A) When both sites of Tr are occupied, a neuroprotective signal is transduced. (B, C, D) When only 1 binding site of Tr is occupied (i.e. the CR region is absent (PrP Δ CR)), a highly toxic signal is transduced by the Tr protein. Depicted in (D) is the subversion of the CR region binding to Tr due to competition of the PrP¹⁰⁶⁻¹²⁶ peptide, which leads to a neurotoxic signal similar to PrP Δ CR and PrP Δ N. Adapted from (Li et al. 2007).

the lipid membrane, undergoes conversion to a predominantly β -sheet configuration, and aggregates to minimize interaction with the surrounding water, consequently destabilizing the membrane (Dupiereux et al. 2005; Miura et al. 2007; Zheng et al. 2009). Deletion of this hydrophobic domain from recombinant mouse prion protein leads to a significantly reduced ability of this deletion mutant to interact with lipid membranes, and an increased sensitivity to proteinase K digestion (Wang et al. 2010). Further evidence suggests that phospholipid content, cholesterol concentration, ganglioside composition, and overall charge of the membrane significantly influence the ability of PrP¹⁰⁶⁻¹²⁶ to interact with a membrane (Dupiereux et al. 2006; Miura et al. 2007).

Application of PrP¹⁰⁶⁻¹²⁶ leads to rapid destabilization of the mitochondrial membrane, as determined via cytosolic cytochrome *c* concentration and caspase-3 activity, suggesting that perturbation of calcium homeostasis could be the underlying neurotoxic mechanism, but also implicates membrane disruption in neurotoxicity (O'Donovan, Tobin, and Cotter 2001; Ferreira et al. 2006). Chronic exposure of cells to PrP¹⁰⁶⁻¹²⁶ leads to accumulation of a 20kDa fragment derived from a truncated form of the prion protein (carboxy-terminal transmembrane PrP or C_{tm}PrP) on the cytosolic side of the ER membrane that is shuttled to the plasma membrane (Gu et al. 2002). Accumulation of this fragment could explain the loss of ER membrane integrity and the increase in intracellular calcium observed, which could then induce apoptosis.

1.5.3.3 PrP¹⁰⁶⁻¹²⁶ Induced Apoptosis

Challenge of neuronal cells with PrP¹⁰⁶⁻¹²⁶ leads to DNA fragmentation (laddering) in a concentration-dependent manner, and cell death ensues via apoptosis

(White et al. 2001; O'Donovan, Tobin, and Cotter 2001; Thellung et al. 2002; Corsaro et al. 2003; Bai et al. 2008). Intravitreal injections of PrP¹⁰⁶⁻¹²⁶ peptide induces TUNEL-positive cells (dying/dead cells), and fragmentation kinetic studies confirm that apoptosis is the mechanism of cell death (Ettaiche et al. 2000).

Exposure of embryonic cortical neurons from mice to 80µM PrP¹⁰⁶⁻¹²⁶ leads to prominent chromatin condensation, detectable DNA fragmentation, and activation of caspase-3 within 24 hours of exposure, strongly suggesting apoptosis was the mechanism of cell death (Carimalo et al. 2005). Mouse primary cortical neurons exposed to a single application of 80µM or greater of PrP¹⁰⁶⁻¹²⁶ activated caspase-3 mediated apoptosis within 1 hour, and significantly reduced neuronal viability by 50% after 5 days. Activation of caspase-6 and 8 pathways were detected after 2 days exposure, but to a lesser extent than caspase-3 (White et al. 2001). Human SH-SY5Y neuroblastoma cells exposed to 100µM PrP¹⁰⁶⁻¹²⁶ for 3 days showed prominent DNA fragmentation, with exposure of the same cells to 50µM peptide over a 5 day period showing a corresponding increase in apoptotic protein markers including activated caspase-3 (Corsaro et al. 2003).

Mouse N2A neuroblastoma cells exposed to PrP¹⁰⁶⁻¹²⁶ show an increase in cytoplasmic cytochrome *c*, an indicator of mitochondrial membrane disruption, and activation of caspases-3, 6, and 9, with a corresponding increase in p75NTR, a member of the tumor necrosis factor family (Bai et al. 2008). Pre-treatment of cells with inhibitors of ER calcium release (dantrolene or xestospongin C) reduces PrP¹⁰⁶⁻¹²⁶ induced cytochrome *c* release, implicating increased intracellular calcium concentration as the initiator of apoptosis (Ferreiro et al. 2006).

1.5.3.4 PrP¹⁰⁶⁻¹²⁶ Induced Gliosis

Some researchers have reported PrP¹⁰⁶⁻¹²⁶ peptide-mediated recruitment of microglia via chemotaxis in a concentration-dependent manner and enhanced neurotoxicity when mouse CGN are co-cultured with microglia (Brown, Schmidt, and Kretzschmar 1996a; Brown, Schmidt, and Kretzschmar 1996b; Silei et al. 1999; Garcao, Oliveira, and Agostinho 2006; Yang et al. 2008; Zhou et al. 2009). This mechanism is plausible when considering the events that take place in the brain of an infected individual, as protein fragments encompassing the PrP¹⁰⁶⁻¹²⁶ sequence were enriched in brains from GSS affected humans (Forloni et al. 1993), but fails to address the neurotoxicity reported using cell lines. Application of the PrP¹⁰⁶⁻¹²⁶ peptide to the human neuroblastoma cell line SH-SY5Y leads to the activation of transcripts resembling a profile induced by microglia, as well as a pattern similar to that shown for Alzheimer's disease and mitochondrial dysfunction (Martinez and Pascual 2007). However, the SH-SY5Y is a neuroblastoma cell line which is presumed to be free of contaminating microglial cells, strongly suggesting that the PrP¹⁰⁶⁻¹²⁶ peptide is capable of inducing alterations in the expression profile through a direct mechanism (Ning et al. 2005a; Martinez and Pascual 2007).

1.5.4 Limitations of Using Brain Homogenate to Mimic Prion Neurotoxicity

Cell culture techniques and cell lines are extensively used in research as a means to model disease pathogenesis, and provide a rapid alternative to study the underlying mechanisms associated with the disease of interest. In the case of prion disease, various cell lines expressing endogenous or overexpressed levels of PrP have been exposed to

infectious brain homogenate. However, as opposed to neurotoxicity, most studies utilize cell culture systems to study prion strain conversion and propagation of the infectious agent. The use of infectious brain homogenate is also limited due to the difficulty in obtaining reproducible results. Sources of introduced variability include significantly different titres of infectious agent in different homogenate preparations, as well as alternate susceptibilities of cell lines to different prion strains (Rubenstein, Carp, and Callahan 1984; Race, Fadness, and Chesebro 1987; Butler et al. 1988; Schatzl et al. 1997; Nishida et al. 2000; Bosque and Prusiner 2000; Birkett et al. 2001; Vilette et al. 2001; Beranger et al. 2001; Enari, Flechsig, and Weissmann 2001; Klohn et al. 2003).

Use of the PrP¹⁰⁶⁻¹²⁶ neurotoxic peptide recapitulates many of the physicochemical characteristics of PrP^{res} while additionally offering a safe and effective alternative to application of infectious brain homogenate. In particular the ability to apply a chemically defined agent at known concentrations allows precise regulation of the neurotoxicity exhibited. This is an essential quality when using a cell culture model to screen for gene targets essential to prion neurotoxicity.

1.6 Tools for Inhibition of RNA Transcription and Translation

The recent development of innovative gene silencing methods including ribozymes, DNAzymes, microRNA (miRNA), short interfering RNA (siRNA), and short hairpin RNA (shRNA) has made the inhibition of a large number of genes economical (Sioud 2004). These methods all rely upon nucleic acid molecules that complement and bind to specific mRNA sequences, leading to degradation of the transcript or inhibition of translation. The process of regulating protein expression at the mRNA level is referred to

as RNA interference (RNAi). RNAi overcomes the necessity of site-directed mutagenesis of all genomic allelic copies, with some genes possessing greater than 22 allelic copies per diploid chromosome set (for example histone deacetylase). It becomes exponentially more difficult to ensure all copies of a gene are knocked out as the number of allelic copies increases.

RNAi relies upon the introduction of biologically active nucleic acid molecules into cells via microinjection, transfection, or transduction (Fire et al. 1998). The method by which RNAi is accomplished involves one of two methods:

1. Nucleozymes possessing innate hydrolytic activity; or
2. Recruitment of the RNA induced silencing complex (RISC).

1.6.1 Innate Catalytic Activity via Hydrolysis (Nucleozymes)

Nucleozymes are molecules made up solely of nucleic acid which possess the innate enzymatic ability to cleave complementary mRNA via hydrolysis, without stimulating the endogenous antiviral interferon response pathway. Nucleozymes hydrolytically cleave mRNA at specific nucleotide sequences, with a catalytic efficiency similar to that of protein enzymes, leading to degradation of the mRNA from both the 3' and 5' ends by cellular ribonucleases. Nucleozymes may be modified to recruit cellular helicases to unwind mRNA species. This allows for more efficient association between the nucleozyme and mRNA, increasing accessibility to complementary sequences, as well as unwinding of the nucleozyme/mRNA duplex following scanning and degradation (Haseloff and Gerlach 1988; Herschlag and Cech 1990; Breaker and Joyce 1994; Santoro and Joyce 1998; Kawasaki and Taira 2002b; Breaker 2004). Nucleozymes can also be

modified such that they are only active in the presence (or absence) of a particular substrate such as a drug of interest, a cell-type specific protein, or an infectious form of a cellular protein. These “aptamers” extend the specificity of nucleozymes (and recently siRNA and miRNA species) by providing a mechanism of control over their functional activity, acting like a switch to specifically regulate when and where a particular nucleozyme is active (Bock et al. 1992; Ellington and Szostak 1992; Joshi and Prasad 2002; de Soultrait et al. 2002; Minunni et al. 2004; Savran et al. 2004; Dassie et al. 2009).

1.6.1.1 Ribozymes

Ribozymes are small catalytic molecules consisting of ribonucleotides (RNA). Synthesis of a known active ribozyme with DNA nucleotides leads to an inactive nucleozyme species, although certain replacements are tolerated (Haseloff and Gerlach 1988; Perreault et al. 1990; Yang et al. 1992). The most common ribozymes are termed hammerhead ribozymes (HamRzs) and were originally identified in studies of plant viroids (Kawasaki et al. 2002a). Hammerhead ribozymes consist of two recognition arms of varying sequence length (specificity increases with increasing recognition arm length), encompassing a conserved sequence (the hammerhead portion) of ~22nts, which takes on a stem-loop secondary structure (Uhlenbeck 1987; Haseloff and Gerlach 1988). The triplet NUX (N = any ribonucleotide, X = A, U, or C) within the target mRNA species is required as this base sequence represents the actual site of cleavage by the ribozyme via hydrolysis, with GUC being the most actively cleaved motif (Haseloff and Gerlach 1988; Kawasaki et al. 2002a). Hammerhead ribozymes have been modified to incorporate a 5' tRNA^{Val} promoter sequence, and a 3' polyadenylate (polyA) tail, which are termed

hybrid hammerhead ribozymes (HyHamRzs). The tRNA^{Val} promoter sequence directs efficient export from the nucleus to the cytoplasm. The polyA tail promotes helicase recruitment, enhancing mRNA structure relaxation, and therefore target accessibility, as well as unwinding of the ribozyme-mRNA duplex for rapid recycling of the HyHamRz. Together, these modifications significantly enhance knockdown efficiency (Kawasaki and Taira 2001; Kawasaki et al. 2002a; Kawasaki and Taira 2002a; Kawasaki and Taira 2002b; Kawasaki et al. 2002b; Kawasaki et al. 2003; Suyama et al. 2003; Wadhwa et al. 2003; Kato et al. 2004; Kawasaki et al. 2004; Wadhwa et al. 2004; Stobart et al. 2009).

1.6.1.2 DNAzymes

DNAzymes consist of short (~30mers) deoxyribonucleotide (DNA) sequences that possess two variable length mRNA recognition arms encompassing a loop region of typically 13-15 DNA bases. They are purely synthetic as no naturally occurring DNAzyme has been identified. Active DNAzymes are identified through screening large populations of random DNA oligonucleotide sequences, with the actively hydrolyzed sequence and efficiency varying depending upon the structure and loop sequence. DNAzymes are capable of binding complementary mRNA with high specificity and affinity, and are innately stable molecules which can be chemically modified to increase stability (Breaker and Joyce 1994; Santoro and Joyce 1997; Santoro and Joyce 1998). The rate limiting step of DNAzyme activity appears to be access to the complementary sequence and binding (Santoro and Joyce 1997; Santoro and Joyce 1998). Transcribed mRNA sequences take on a complicated secondary structure which can inhibit access to specific sequences. Modifications to the DNAzyme sequence may allow a mechanism of

relaxing mRNA secondary structure, but could reduce or completely abolish its functional activity.

1.6.2 Recruitment of the RISC Complex for Function (dsRNA)

In contrast to utilizing molecules with innate catalytic activity, this method relies upon recruitment of endogenous RNA-activated enzymes which recognize double stranded RNA (dsRNA) species. The potency of using dsRNA molecules, one of which is complementary to a specific mRNA, for altering protein expression was first noted in the nematode *C. elegans* (Fire et al. 1998). It was recognized that long dsRNA molecules stimulated the endogenous antiviral interferon response pathway which shuts down global protein production, but short dsRNA of ~21-23 nucleotides (siRNA) evaded this pathway. These siRNA molecules retained the ability to reduce post-transcriptional mRNA and protein expression levels of specific targets (Kennerdell and Carthew 1998; Zamore et al. 2000; Elbashir et al. 2001; Bernstein et al. 2001; Donzé and Picard 2002). Identification of endogenous RNAi came from plant studies in which overexpression of an introduced transgene innately repressed its own protein expression. The researchers isolated a short RNA of ~25 nucleotides found only in the line of plants overexpressing the transgene, which repressed its own translation (Hamilton and Baulcombe 1999). Since this original finding, short RNA regulatory molecules have been identified in every mammalian species studied. These endogenous regulators are termed microRNAs (miRNAs) due to their length and hundreds have been subsequently identified (Lagos-Quintana et al. 2001; Lau et al. 2001; Lee and Ambros 2001).

1.6.2.1 Endogenous MicroRNA (miRNA) Processing Pathway

MicroRNA (miRNA) are a relatively new species of short RNA molecules that are key regulators of the cell. They are transcribed by RNA polymerase II as kilobase-length polyadenylated primary miRNA (pri-miRNA) with complex secondary structure. The pri-miRNA are processed in the nucleus by the Drosha/Pasha microprocessor complex to pre-miRNA, consisting of ~70-100 ribonucleotides arranged in a stem-loop structure (Lee et al. 2003; Lee et al. 2004; Cai, Hagedorn, and Cullen 2004; Yeom et al. 2006) (Figure 1.7). The pre-miRNA are exported to the cytoplasm via exportin-5, and are recognized by the cytoplasmic RNase III enzyme, Dicer (Yi et al. 2003; Lund et al. 2004; Bohnsack, Czapinski, and Gorlich 2004). Dicer is evolutionarily conserved across many species from fungi to humans, and processes long dsRNAs to siRNAs of a length characteristic to a species (Bernstein et al. 2001; Ketting et al. 2001). Dicer processes the pre-miRNA to miRNA duplexes (short interfering RNA, siRNA), which consist of two complementary ~21nt ribonucleotide strands with a two nucleotide 3' overhang and a 5' phosphate (Zamore et al. 2000; Elbashir et al. 2001; Ketting et al. 2001; Nykanen, Haley, and Zamore 2001; Grishok et al. 2001; Hutvagner et al. 2001). These Dicer-complexed miRNA (siRNA-like) are bound by a cytoplasmic protein complex termed the RNA-induced silencing complex (RISC) (Hammond et al. 2000).

The RISC complex includes the Dicer enzyme, the short dsRNA molecule, the cytoplasmic Argonaute proteins 1-4, a trans-activation response RNA-binding protein (TRBP), the protein kinase, interferon-inducible double stranded RNA-dependent activator (PRKRA or PACT), and a theoretical helicase (Chendrimada et al. 2005; Haase et al. 2005; Lee et al. 2006). Once the proteins associate to form the mature RISC

complex, it becomes activated and pries one strand away, typically the sense strand, using the remaining strand (the antisense strand, single stranded RNA, ssRNA) as a guide (Hammond et al. 2001; Carmell et al. 2002). The ssRNA/RISC complex scans transcribed mRNA for sequences complementary to the bound mature miRNA/siRNA strand, inhibiting translation or cleaving the mRNA molecule, depending on imperfect or perfect complementarity, respectively. Identified miRNA encode imperfect complementarity to their target mRNAs, and therefore preferentially suppress translation as opposed to mRNA degradation (Ha, Wightman, and Ruvkun 1996; Olsen and Ambros 1999; Sijen et al. 2001; Bernstein et al. 2001; Paddison et al. 2002; Haley and Zamore 2004). Understanding the endogenous gene silencing mechanism has permitted researchers to harness the potential of this regulatory mechanism for genetic manipulation studies, with generation of short-interfering RNA (siRNA, mimicking Dicer products) and short hairpin RNA (shRNA, mimic pre-miRNA) permitting gene-specific regulation.

1.6.2.2 Short Interfering RNA (siRNA)

The method of short-interfering RNA (siRNA) dependent RNAi (Figure 1.7, step 6) relies upon the introduction of double-stranded 21 nucleotide RNA molecules with 2 nucleotides unpaired at the 3' ends and 5' phosphates (Elbashir et al. 2001). siRNAs are generated to be perfectly complementary to the mRNA target of interest. Engineered siRNA-induced gene silencing does not require Dicer for processing of the double stranded RNA to mature siRNA, but still relies upon Argonaute proteins and the active

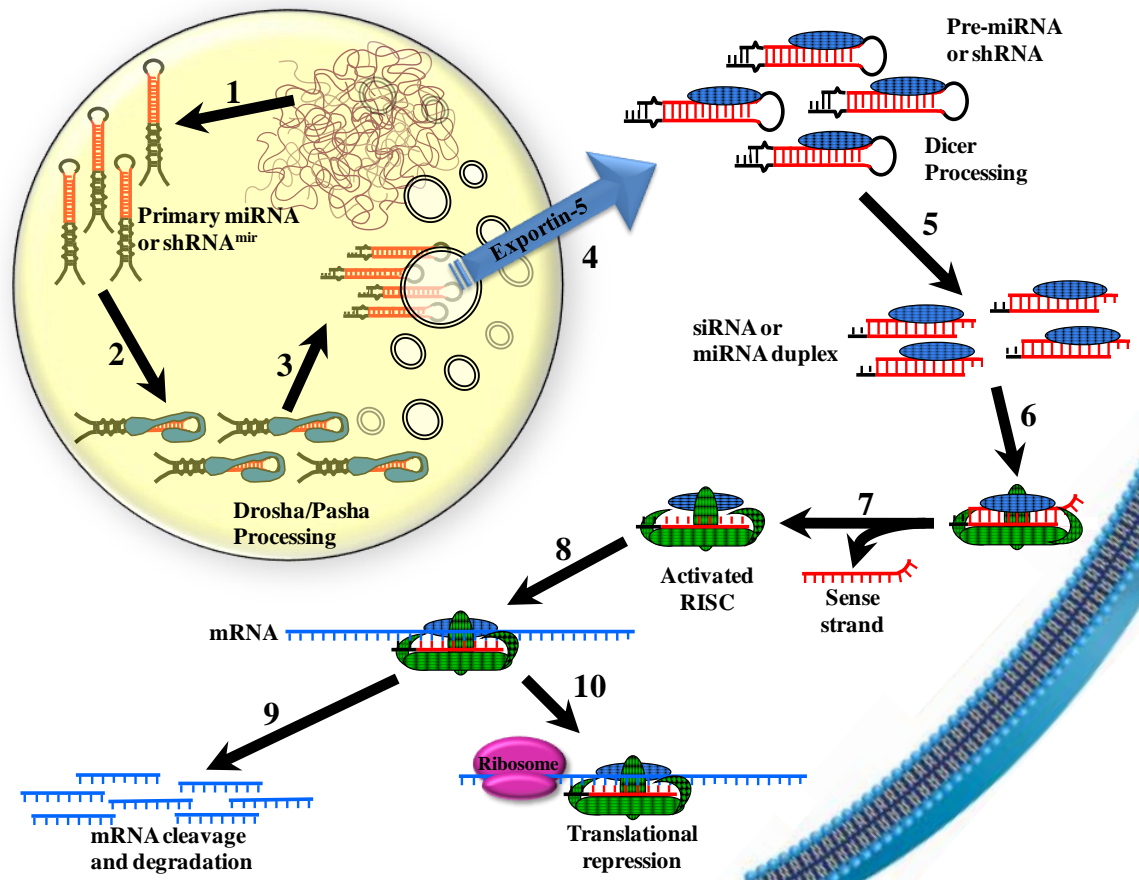


Figure 1.7: RNAi Molecule Expression and Processing

(1) The primary shRNA is transcribed by endogenous RNA polymerases (pol II or pol III depending on the promoter sequence) then (2) processed by the Drosha/Pasha microprocessor complex to (3) pre-mi/shRNA. These pre-mi/shRNA molecules are (4) exported from the nucleus to the cytoplasm by Exportin-5 (Lund et al. 2004) and (5) processed to siRNA-like (siRNA) molecules by the RNase III enzyme, Dicer. (6) siRNA are recognized and bound by the RNA induced silencing complex (RISC), (7) the sense strand is removed and the RISC complex is activated by the mature miRNA/siRNA molecules. (8) The RISC complex scans mRNA for complementary sequence and (9) catalyzes cleavage of perfectly complementary mRNA or (10) represses translation of imperfectly bound transcript by blocking ribosomal processing.

RISC complex for recognition of target mRNA species and degradation, which is termed gene knockdown (Elbashir et al. 2001; Donze and Picard 2002; Hannon 2002).

Introduction of siRNA molecules into cells may be accomplished by one of two methods. The first is transfection of synthesized siRNA directly. Though siRNA molecules are potent gene silencers, their effect is transient and only detectable for ~48 hours depending on the cell type, prohibiting long term genetic studies (McManus et al. 2002). The second method is transfection or transduction of an expression vector into which both strands of the siRNA coding sequence has been cloned. Long acting or stably expressed siRNA-like molecules which are processed through the endogenous gene silencing pathway overcomes the hurdle of transient functionality (McManus et al. 2002).

1.6.2.3 Short Hairpin RNA (shRNA)

This alternate form of manipulating the endogenous gene silencing pathway more closely mimics miRNA molecules, with the incorporation of a loop sequence of varying length (4-15 nucleotides) joining two complementary target recognition strands (siRNA-like, ~19-29 nucleotides), termed short hairpin RNA (shRNA) due to their predicted stem-loop secondary structure (Figure 1.7, step 5). The 3' end of the antisense strand terminates in a 2 uracil overhang or mismatch bulge, which appears important for recognition and processing. These shRNA molecules are likely processed by Dicer to siRNA molecules through removal of the loop sequence, and the endogenous degradative RNAi pathway is utilized, although gene knockdown is less effective than with siRNA molecules (Paddison et al. 2002; McManus et al. 2002; Brummelkamp, Bernards, and Agami 2002). The most effective shRNA molecules encode perfectly complementary

19-29 nucleotide stems with no mismatches to their intended mRNA. Stable expression of effective shRNA molecules may be accomplished by cloning the coding sequence into an expression vector, with shRNA transcription driven by a RNA polymerase III promoter (commonly H1 or U6) and terminating with a 4-5 thymidine (uridines in transcript) stretch (Paddison et al. 2002; McManus et al. 2002; Brummelkamp, Bernards, and Agami 2002; Yu, DeRuiter, and Turner 2002; Paul et al. 2002). Use of RNA polymerase III promoters permits synthesis of short RNA species with a well defined transcription start and termination site. Expression of these shRNA from an expression vector with a selectable marker provides a means of long term, stable expression for extended analysis (Brummelkamp, Bernards, and Agami 2002; Yu, DeRuiter, and Turner 2002).

1.7 Short Hairpin RNA (shRNA) Library Evolution

The potential power of shRNA molecules for studying genetic disorders rapidly led to the creation of various vector-encoded shRNA libraries targeting tens-of-thousands of genes, with usually 3 or more shRNA per gene, leading to hundreds-of-thousands of shRNAs. These first generation shRNA libraries expressed a 19-29 nucleotide siRNA with a 4-15 nucleotide loop sequence. The vector backbone encoded a selectable antibiotic resistance marker, a U6 or H1 promoter to drive transcription of the shRNA, and signal sequences for packaging the shRNA expression cassette into retroviral or lentiviral transducing particles (Paddison et al. 2004; Berns et al. 2004; Westbrook et al. 2005; Huang, Wang, and Lu 2008). These packaged shRNA expression cassettes could be efficiently transduced into a variety of cell types. The use of long terminal repeat

(LTR)-directed recombination into the host genome provided a means of stable integration and shRNA expression (Silva et al. 2005; Chang, Elledge, and Hannon 2006).

As the mechanism of gene silencing was studied and better understood, second-generation shRNA libraries were constructed. The most notable and largest second-generation shRNA library was encoded within the pSM2 retroviral vector backbone. The major improvement was the inclusion of approximately 125 nucleotides derived from the endogenous primary miRNA-30 (miR30) flanking the 5' and 3' ends of the shRNA, as well as the loop sequence. Inclusion of these miR30 sequences encompassing the shRNA (shRNA^{mir}) (Figure 1.7, step 1) significantly enhanced recognition and processing by the Drosha/Pasha microprocessor complex and Dicer to miRNA/siRNA-like duplex molecules, and ultimately improved knockdown efficiency (Silva et al. 2005; Chang, Elledge, and Hannon 2006; Hinton et al. 2008).

Due to inefficiencies of retroviral packaging and poor transduction efficiencies of certain cell types (e.g. neuronal), the pSM2-encoded shRNA^{mir} sequences have been subcloned into two alternative vectors, pGIPZ and pTRIPZ. Both pGIPZ and pTRIPZ are lentiviral vectors that result in much higher packaging and transduction efficiencies, even of non-replicating neuronal cells. pGIPZ co-expresses an enhanced green fluorescent protein (EGFP) along with the shRNA^{mir} from an RNA polymerase II cytomegalovirus (CMV) promoter to drive high expression levels of mRNA transcripts. Inclusion of EGFP permits tracking of transduction efficiency and confirmation of active transcription. The pTRIPZ vector encodes the shRNA^{mir} cassette downstream of a tetracycline-inducible promoter (TRE), which drives co-expression of turbo red fluorescent protein (tRFP) and the shRNA^{mir}. The tRFP permits visual confirmation of

transduction and expression efficiencies, while the TRE promoter provides a means of regulating when shRNA^{mir} are transcribed (Ansaloni et al. 2010). First and second-generation shRNA libraries have been used to study a variety of cellular phenomenon including cell adhesion, regulation of telomerase activity, and to identify mediators of cancerous cell growth (Westbrook et al. 2005; Huang, Wang, and Lu 2008; Coussens et al. 2010).

1.8 Short Hairpin RNA (shRNA) Library Screening Considerations

Cell culture models present a means by which relevant experiments can be carried out in a cost-effective and scalable manner. Transformed cell lines can be especially useful for screening libraries as these cells are capable of continuously dividing, thereby offering a means to expand clonal populations that carry a marker of resistance, such as a particular shRNA. This provides a way of testing the efficacy of large numbers of potential therapeutics or RNAi molecules against a particular disease.

All large-scale high-throughput techniques pose the problem of identifying which results represent targets of interest for further study. shRNA libraries consisting of hundreds-of-thousands of shRNA molecules targeting tens-of-thousands of genes are no exception. Various methodologies are employed to identify the shRNA eliciting a desirable phenotype from these library screens: (i) extract genomic DNA from clonal cell populations of interest, PCR amplify and sequence the stably integrated shRNA, and use the online NCBI database to determine the complementary mRNA targeted by the identified shRNA (Berns et al. 2004; Huang, Wang, and Lu 2008); (ii) certain shRNA libraries encode a shRNA-specific genetic “bar-code”, which can be PCR-amplified from

pools of clones of interest and relative proportions analyzed by microarray hybridization (Paddison et al. 2004; Berns et al. 2004; Westbrook et al. 2005; Moffat et al. 2006); (iii) the latest means of determining shRNA targeting genes of interest also utilizes the genetic “bar-code”, but employs deep-sequencing techniques to analyze relative copy numbers of each shRNA “bar-code” from complex pools (Bassik et al. 2009).

1.9 Methods for Validating shRNA Library-Identified Positives

Upon identification of shRNA targeting genes of interest, validation studies must be undertaken to confirm the involvement of a particular gene product in the pathway of interest. There is no absolute experimental way of confirming such genetic importance next to knockout or regulated gene expression in animal models, but various methods have been employed prior to moving into experimental animal models. Repetition of the gene knockdown experiment with individual shRNAs identified from the library screen provides the first line of supporting evidence for the importance the identified gene product(s) play in the pathway of interest. The next experimental evidence comes from alternate shRNAs targeting the same genes, preferably expressed from an alternate vector backbone, arguing against off-target (non-specific) effects (Jackson et al. 2003; Falschlehner et al. 2010; Mohr, Bakal, and Perrimon 2010). Further validation that the shRNA is targeting the gene of interest is via quantitative real-time PCR (qPCR) analysis of mRNA expression levels or immunoblotting for protein level determination. Other means of confirming importance of identified gene targets include, but are not limited to: (i) test effect of mRNA-encoded protein overexpression; (ii) compare effect of target gene knockdown in related affected species cell type; and (iii) analyze expression levels

of mRNA and protein by qPCR and immunoblotting techniques in tissue from rodent models (Mohr, Bakal, and Perrimon 2010).

1.10 Objectives

This doctoral research project had 5 primary objectives:

1. Develop a cell culture model of prion-mediated neurotoxicity, using the PrP¹⁰⁶⁻¹²⁶ peptide to mimic PrP^{res} toxicity.
2. Using the model from objective 1, screen a library of shRNA^{mir} targeting all known open reading frames of the human genome to identify genes essential to prion-mediated neurotoxicity.
3. Correlate candidate genes identified from objective 2 with prion disease by examining the relative mRNA expression level in brains from a mouse model.
4. Validate protection conferred upon human neuroblastoma cells against prion-mediated neurotoxicity through use of alternative shRNA^{mir} targeting genes of interest from the library screen in objective 2.
5. Validate that shRNA^{mir} expression does reduce mRNA and protein levels of the targeted gene.

1.11 Hypothesis

The neurotoxicity associated with rogue PrP^{res} requires the expression of one or more alternative host-encoded proteins.

2. Materials and Methods

2.1 Cell Culture

2.1.1 Maintenance of HEK-293-based Packaging Cells

The human embryonic kidney (HEK)-derived cell lines, GP2-293 and 293T/17 were purchased from Clontech as a component of the Pantropic Retroviral Expression System (Cat.#631512, Clontech, Mountain View, CA) or the American Type Culture Collection (ATCC CRL-11268, Burlington, ON), respectively. Both cell lines were maintained in Dulbecco's Modified Eagle's media (DMEM) (ATCC #30-2002, Burlington, ON) + 10% heat inactivated fetal bovine serum (HI-FBS, Invitrogen #12484-028, Burlington, ON) + 1% antibiotic/antimycotic (Ab/Am, Invitrogen #15240-062, Burlington, ON) (HI-DMEM10). Cells were passaged upon reaching 80% confluency to ensure healthy and active growth as well as prevent over-growth of the culture. When passaging, cells were rinsed with 1X phosphate buffered saline (PBS, Invitrogen #10010-023, Burlington, ON), exposed to 0.25% Trypsin (Invitrogen, #15050-065, Burlington, ON) for 3 minutes at room temperature or until cells started to slough off the surface, and then resuspended in HI-DMEM10. Cells were plated at 5×10^6 per T150 cell culture treated flask (Corning Life Sciences, distributed by VWR International, West Chester, PA), and a complete media change was performed 24 hours post-plating. Once a week, during passaging of either cell line, the cells were gently passed through a 40 μ m cell strainer (BD Biosciences #352340, Mississauga, ON) to minimize cell clumps which significantly reduce transfection efficiency.

2.1.2 Maintenance of Mouse Fibroblast NIH/3T3 Cells

The mouse fibroblast cell line, NIH/3T3, was purchased from ATCC (CRL-1658, Burlington, ON) and maintained in HI-DMEM10. Cells were passaged 2-3 times per week (upon reaching 80% confluency) as stated above. Cells were maintained in T100 low profile CellBIND[®] coated flasks (Corning Life Sciences, distributed by VWR, West Chester, PA). As with HEK-based cell lines, NIH/3T3 cells were strained through a 40µm cell strainer (BD Biosciences #352340, Mississauga, ON) every third passaging to minimize cell clumps.

2.1.3 Maintenance of Human Neuroblastoma SK-N-FI Cells

The human neuroblastoma cell line, SK-N-FI, was purchased from ATCC (CRL-2142, Burlington, ON) and maintained in DMEM + 10% filter sterile FBS (FS-FBS) + 1 X non-essential amino acids (NEAA, Invitrogen #11140-050, Burlington, ON) + 1% Ab/Am (SK-FS-DMEM10). Cells were passaged upon reaching 80% confluency as stated above. As with the HEK-based cell lines, SK-N-FI cells were strained through a 40µm cell strainer to minimize clumps, however, for these cells straining was performed with each passage. Cells were plated at 7.5×10^6 cells per T150 flask.

2.1.4 Freezing Down Cells

To prepare frozen stock cultures of all cell lines, 2 days prior to freezing, cells were passaged into a T150 flask to ensure a large number of cells were available. The day of freezing, cells were rinsed with room temperature PBS, incubated with 2mL of warm 0.25% Trypsin for 3 minutes or until cells started to lift off the plate, followed by a

gentle knocking of the side of the flask. Cells were resuspended in 13mL growth media and transferred to a 15mL polystyrene Falcon tube. The cells were spun for 5 minutes at 1000 rpm in a Beckman Allegra® 6KR Kneewell™ centrifuge (Beckman Coulter Canada Inc., 366830, Mississauga, ON), and the media was decanted from the cell pellet. The pellet was resuspended in 7.5mL growth media, 6mL FS-FBS and 1.5mL dimethyl sulfoxide (DMSO, Sigma-Aldrich, #D1435-1L, Oakville, ON) which had been sterile filtered through a 0.2µm cellulose acetate syringe filter (SFCA, VWR International, Cat.#28145-477, Mississauga, ON). To each 2mL labelled cryovial, 1mL (~1.5 X 10⁶ cells) of resuspended cells was added, the tubes were placed in a cryocontainer, and transferred to a -80°C freezer. The next day, the tubes were transferred to a liquid nitrogen storage tank.

2.1.5 SK-N-FI Cell Viability Assay Using AlamarBlue

To determine the relative number of SK-N-FI cells surviving challenge with the PrP scrambled (PrP^{Scram}) or PrP¹⁰⁶⁻¹²⁶ neurotoxic peptide, the non-cytotoxic dye AlamarBlue (Invitrogen, DAL1100, Burlington, ON) was utilized. To calculate the number of surviving cells, standard curves were generated by plating 0, 50, 100, 500, 1000, 5000, 10 000, 50 000, 100 000, or 500 000 SK-N-FI cells per well into 6-well plates in SK-FS-DMEM10, with a full 6-well plate of the respective cell number (i.e. 6 technical replicates). Twenty-four hours post plating, growth media was removed and 2mL of AlamarBlue, diluted 10-fold in SK-FS-DMEM10, was added. Five different time points were chosen to measure the absorbance, which were 5, 24, 48, 72, and 96-hours post AlamarBlue application. At the appropriate time, 100µL was removed from each

well and transferred to a 96-well flat bottom clear plate (Nunc, ThermoScientific, Rochester, NY). Absorbance was measured at 570nm and 600nm using a SpectraMax Plus spectrophotometer (Molecular Devices, Silicon Valley, CA) to determine the relative amount of reduced AlamarBlue. The percent reduction was calculated using the formula:

$$\frac{(\epsilon_{\text{OX}})\lambda_2 A\lambda_1 - (\epsilon_{\text{OX}})\lambda_1 A\lambda_2 \text{ of test well}}{(\epsilon_{\text{RED}})\lambda_1 A^\circ\lambda_2 - (\epsilon_{\text{RED}})\lambda_2 A^\circ\lambda_1 \text{ of control well}} \times 100$$

λ_1 = absorbance at 570nm

λ_2 = absorbance at 600nm

$(\epsilon_{\text{OX}}\lambda_2) = 117,216$

$(\epsilon_{\text{OX}}\lambda_1) = 80,586$

$(\epsilon_{\text{RED}}\lambda_1) = 155,677$

$(\epsilon_{\text{RED}}\lambda_2) = 14,652$

$A\lambda$ = Absorbance reading of test well

$A^\circ\lambda$ = Absorbance of negative control well (media + AlamarBlue only)

To generate standard curves, the percent AlamarBlue reduced was plotted against the known number of SK-N-FI cells, and the equation for a 4-parameter best-fit curve was calculated by the SOFTmax PRO version 2.6.1 software (Molecular Devices, Silicon Valley, CA).

2.2 PrP¹⁰⁶⁻¹²⁶ Mediated Neurotoxicity

SK-N-FI cells were passaged and strained through a 40 μ M cell strainer, then 40,000 cells were added to each well in a 6-well plate in 2mL DMEM + 5% HI-FBS (Gibco, Invitrogen, Burlington, ON, Lot# 358343) + 1 X NEAA + 1% Ab/Am (SK-HI-DMEM5) (Day 0). Twenty-four hours post-plating, the media was changed to 2mL DMEM + 1% HI-FBS (Gibco, Invitrogen, Lot# 358343) + 1 X NEAA (SK-HI-DMEM1) (Day 1). Twenty-four hours later, PrP scrambled (PrP^{Scram}) or PrP¹⁰⁶⁻¹²⁶ peptide (PolyPeptide, Strasbourg, France) was resuspended in 400 μ L SK-HI-DMEM5 (3.8%) and added to 10.06mL SK-HI-DMEM1 (96.2%) per milligram peptide, for a final concentration of 50 μ M. Two millilitres of resuspended peptide was added to each well gently (Day 2). This was repeated every 48 hours for a total of 5 treatments (on Days 4, 6, 8, and 10), rotating the plate 90° for each removal of media and application of fresh peptide. Forty-eight hours following the fifth treatment, 2mL of 400 μ L SK-HI-DMEM5 per 10.06mL SK-HI-DMEM1 was added to each well (Day 12). Forty-eight hours later (Day 14), 2mL SK-HI-DMEM5 was added to each well. Finally, on Days 16 and 19 media was changed to SK-FS-DMEM10 (Figure 2.1).

To determine the relative number of viable SK-N-FI cells following peptide treatment, AlamarBlue diluted 10-fold in SK-FS-DMEM10 was applied to each well of cells at the appropriate time (Day 22). The percent reduction was measured at 5, 24, or 48 hours post application and calculated as outlined above (section 2.1.5). Using the percent AlamarBlue reduced, the number of viable cells was back calculated based upon the time-point appropriate standard curve. The number of surviving SK-N-FI cells challenged with PrP^{Scram} was averaged and the individual number of cells for each

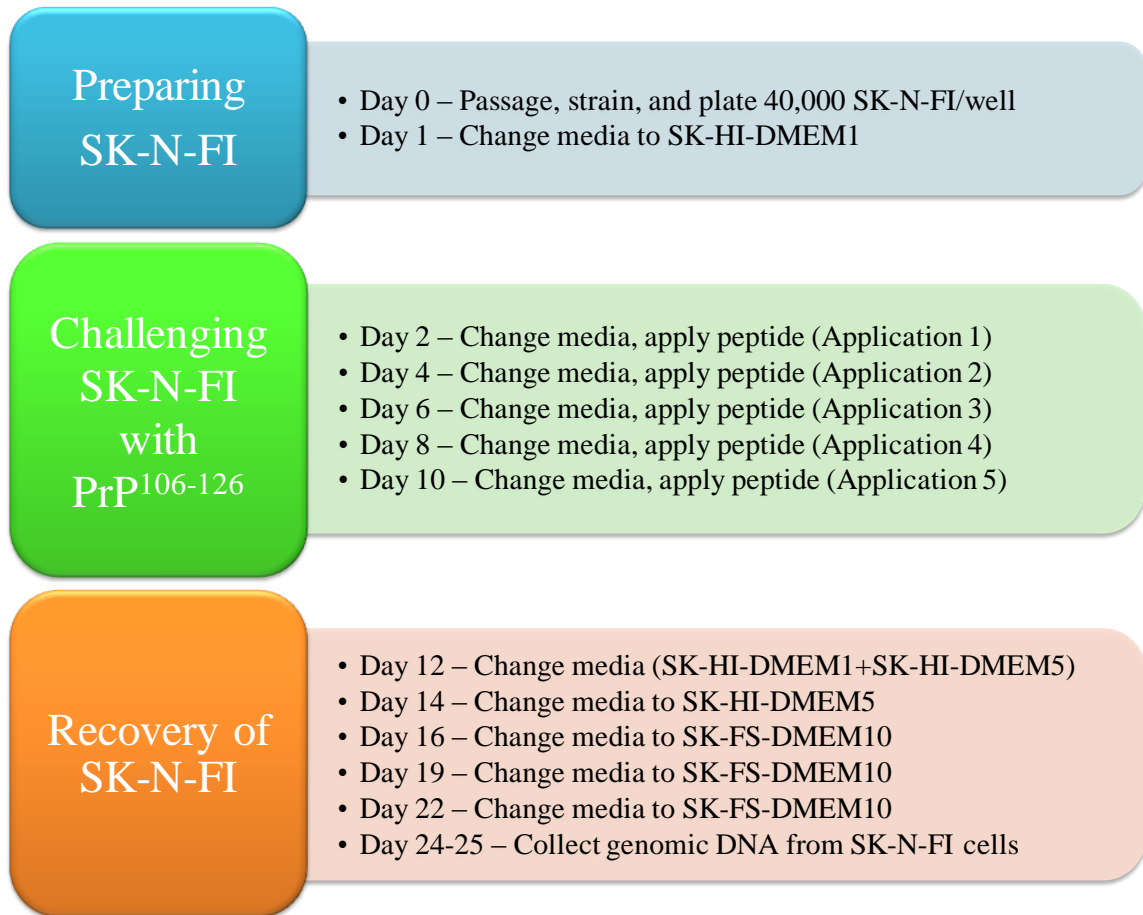


Figure 2.1: SK-N-FI Challenge Schedule with the PrP¹⁰⁶⁻¹²⁶ Peptide

Summary of the PrP¹⁰⁶⁻¹²⁶ peptide application schedule found to elicit the highest neurotoxic effects on human SK-N-FI cells. The challenge of the SK-N-FI cells with PrP¹⁰⁶⁻¹²⁶ is separated into 3 distinct phases; preparation, challenge, and recovery. The preparation phase includes passaging SK-N-FI cells, straining them through a 40µm cell strainer, and plating 40,000 cells per well of a 6-well plate in SK-HI-DMEM5. The challenge phase encompasses repeated application of the PrP¹⁰⁶⁻¹²⁶ peptide every 48 hours in 96.2% SK-HI-DMEM1 + 3.8% SK-HI-DMEM5. The recovery phase allows cells to re-grow following peptide challenge to permit a reasonable number of cells from which either DNA can be isolated or cell number can be determined using AlamarBlue.

PrP^{Scram} or PrP¹⁰⁶⁻¹²⁶ challenged test well was normalized to this average. The ratio of viable cells challenged with PrP¹⁰⁶⁻¹²⁶ was calculated relative to the survival rate of cells challenged with PrP^{Scram}.

2.3 Preparation and Retroviral Packaging of the pSM2+shRNA^{mir} Library

2.3.1 Replication and Amplification of the Human shRNA^{mir} Library

The human pSM2-based retroviral Expression Arrest™ microRNA-adapted shRNA (shRNA^{mir}) library was purchased from OpenBiosystems (Huntsville, AL) as bacterial glycerol stocks (Figure 2.2). The entire library consisted of approximately 70,000 individual pSM2+shRNA^{mir} constructs. Upon arrival at the National Microbiology Laboratory in Winnipeg (NML), the library was replicated and amplified. Of the glycerol bacterial stock, 3µL was inoculated into 100µL 2X LB (low salt) broth (Peptone = 20g/L, Yeast extract = 10g/L, NaCl = 5g/L) + 25µg/mL chloramphenicol (LB^{Chlor}) (Sigma-Aldrich, Oakville, ON) + 8% glycerol in multiple 96-well flat bottom plates (VWR International, 353070, Mississauga, ON). To a 2.2mL deep-well culture block (Millipore, Nepean, ON) containing 1mL of 2X LB^{Chlor} (low salt), 3µL of the original bacterial stock was inoculated. This was performed using a Biomek® FX Laboratory Automation Workstation (Beckman Coulter Inc., Mississauga, ON) with a 96-channel head attachment. Flat bottom plates, barcoded for later reference, were sealed with aluminum sealing foil (Beckman-Coulter, 538619, Mississauga, ON) and incubated at 37°C overnight without shaking. The next day, these plates were transferred to -80°C.

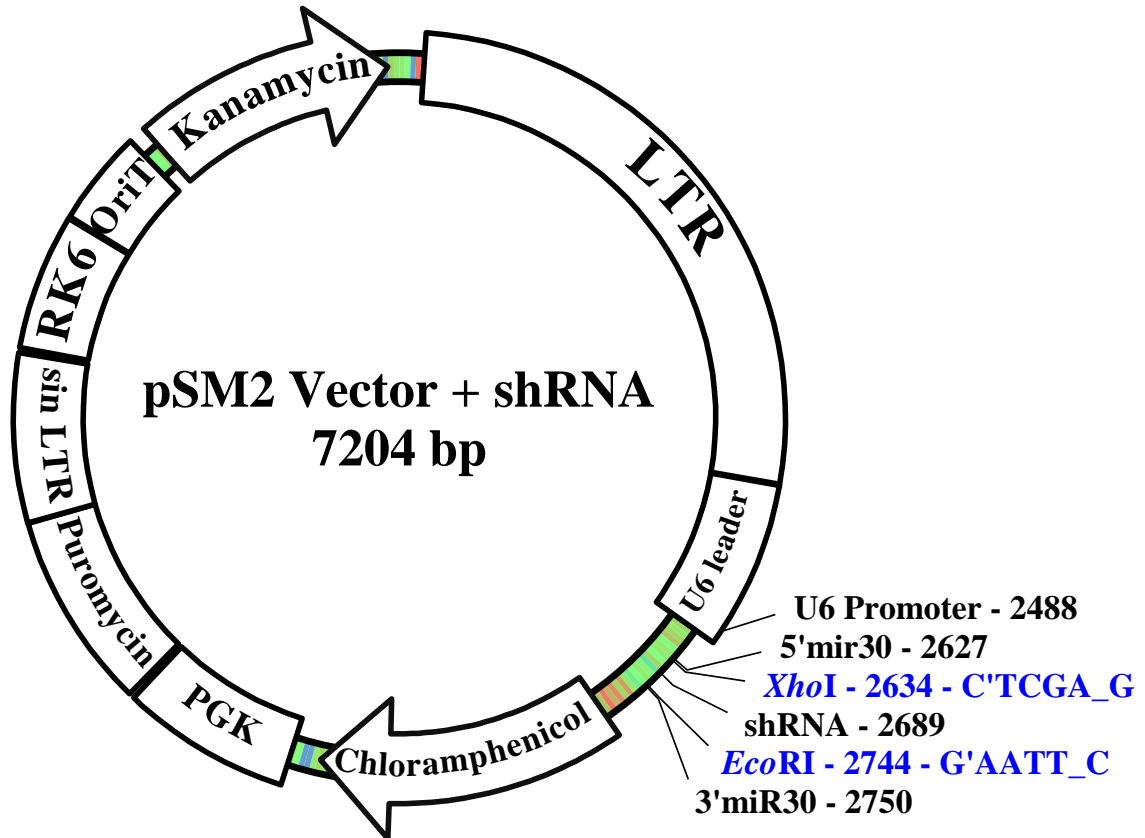


Figure 2.2: Features of the pSM2 shRNA^{mir} Retrovector.

Representation of the pSM2 retrovector from OpenBiosystems, which encodes for the miRNA30 adapted shRNA human library. The shRNA is encompassed by human miRNA30 5' and 3' sequences (shRNA^{mir}). Expression of the shRNA^{mir} is driven by a RNA pol III U6 promoter, with a psi⁺ packaging signal encoded within the U6 leader sequence. The entire shRNA^{mir} expression cassette is encompassed by long terminal repeats (LTRs), one of which is self-inactivating. Kanamycin and chloramphenicol, are bacterial antibiotic resistance markers. PGK is the phosphoglycerate kinase promoter which drives expression of the puromycin resistance marker. RK6 γ is a conditional origin of replication that requires expression of Pir1. The OriT sequence is necessary for host to recipient plasmid transfer. Plasmid representation generated using pDRAW32.

The deep-well culture blocks were sealed with Air-Pore tape (Qiagen, Mississauga, ON) and incubated at 37°C overnight with shaking at 250rpm.

2.3.2 Human pSM2+shRNA^{mir} Plasmid Isolation, Quantification and Pooling

Following overnight incubation of bacterial cultures, the deep-well culture plates were spun down at 3000rpm for 5 minutes in an Eppendorf 5804R centrifuge (Fisher Scientific, Nepean, ON) and the supernatant was discarded. Plasmid was extracted from pelleted *E. coli* cells using the Biomek FX according to the Montage Plasmid Miniprep HTS 96 protocol (Millipore, Nepean, ON). The eluted plasmid was aliquoted into replicate 96-well plates, barcoded, and stored at -80°C.

Concentrations of purified plasmids were determined according to the Quant-iT™ PicoGreen® assay (Invitrogen, Molecular Probes, Burlington, ON) on a Biomek FX with an attached DTX 880 Micro Plate Reader (Beckman Coulter Inc., Mississauga, ON). Of the eluted plasmid, 2µL was added to 100µL PicoGreen working solution + 98µL TE buffer, for a final volume of 200µL. Using an excitation wavelength of 480nm and an emission wavelength of 520nm, fluorescence readings were compared to a standard curve to back calculate plasmid concentration.

Of the total volume, 200ng of each plasmid was pooled together, with a given pool composed of 10 X 96-well plates of plasmids (960 different plasmids per pool, 73 different pools). The pools were aliquoted into 1mL volumes and stored at -80°C. Replication, amplification, purification, quantification, and pooling of the

pSM2+shRNA^{mir} library plasmids were performed by the Genomics Core Facility at the NML.

2.3.3 Removal of Endo Toxins from pSM2+shRNA^{mir} Pools

Previously generated pSM2+shRNA^{mir} pools were re-purified according to the Qiagen Mini Plasmid Kit (Cat.#12125, Mississauga, ON), modified to clean previously extracted plasmid and result in EndoFree plasmid of a higher concentration. To do this, ~1mL (equivalent amount of buffer to plasmid) 1.5M NaCl and 100mM MOPS, pH7.0 was added to each tube of pooled shRNA^{mir} plasmids (~2mL total) followed by addition of 200µL ER buffer and incubated on ice for 30 minutes. The Qiagen TIP-20s were activated by applying 1mL Buffer QBT, followed by addition of the resuspended plasmid pools. The TIP-20 columns were washed twice with 2mL EndoFree QC Buffer and the plasmid was eluted using 800µL EndoFree QN buffer. To the eluate, 560µL isopropanol was added, mixed, and then centrifuged at 16,200xg for 30 minutes at room temperature. The supernatant was removed and 500µL EndoFree 70% ethanol was applied to each pellet, vortexed gently to loosen pellet, and re-spun for 10 minutes at 16,200xg. The supernatant was pipetted off and tubes were spun briefly to bring down any remaining liquid, which was removed. Pellets were air dried for 5 minutes, then 100µL EndoFree TE buffer was added and the tubes were incubated at 4°C overnight. The next day, tubes were vortexed on a VWR VortexGenie II on setting 4 for 30 seconds, spun at 16,200xg for 30 seconds, and the supernatant was transferred to a Nuclease-Free tube. This EndoFree plasmid was stored at -20°C.

2.3.4 Packaging of pSM2+shRNA^{mir} Library Pools

The GP2-293 cell line was used to package the pSM2 retrovector-based shRNA^{mir}-expressing vectors (Figure 2.2) into non-replicative retroviral particles (Figure 2.3). GP2-293 cells were passaged the day of transfection, plating 7.8×10^6 cells/10cm dish in DMEM + 10% FS-FBS + 1% Ab/Am + 25% preconditioned media (sterile filtered through a 0.45 μ m cellulose acetate syringe filter (SFCA)), in a final volume of 11mL. Dishes were incubated for 6 hours, media was removed and replaced with 7mL media DMEM + 10% FS-FBS + 1% Ab/Am (FS-DMEM10). Two hours later, the cells were co-transfected with 1.3 μ g of each pVSV-G (Figure 2.4) (Clontech, Mountain View, CA) and pSM2+shRNA^{mir} using Effectene (Qiagen, Mississauga, ON). The DNA was resuspended in a final volume of 800 μ L EC buffer in 15mL polystyrene Falcon tubes, and Enhancer was added at a 5:1 ratio. This mixture was vortexed at setting 4 on a VWR VortexGenieII for 10 seconds and incubated at room temperature for 10 minutes. Effectene was then added at a 6:1 ratio, vortexed as above and incubated at room temperature for 10 minutes. Media was removed, and the transfection complex was resuspended in 3.2mL FS-DMEM10 by pipetting up and down 3 times. The solution was gently applied to the cells. The dishes were incubated for 4 hours, followed by removal of the transfection complex and addition of 10mL fresh FS-DMEM10. Approximately 12 hours later, media was removed and replaced with 8mL FS-DMEM10. Twenty-four hours later, media was changed as above.

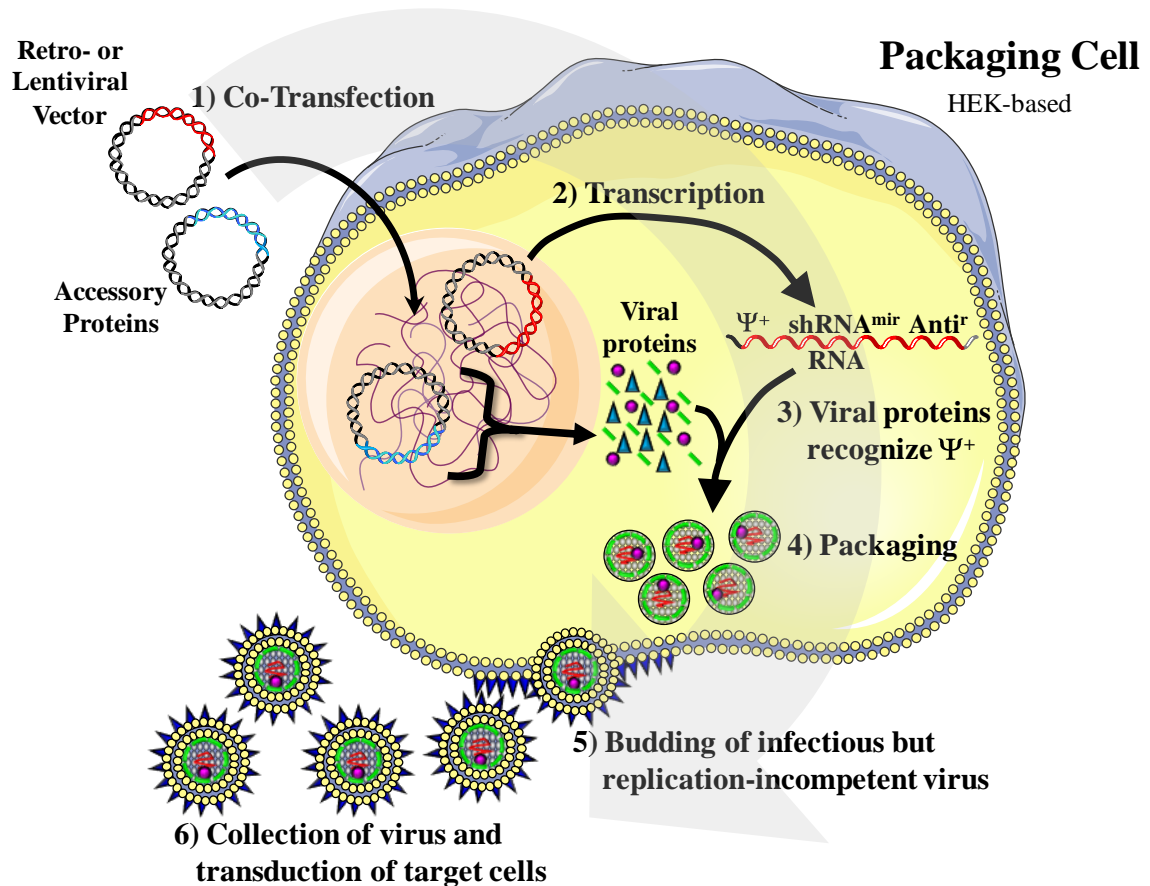


Figure 2.3: Retro- or Lentiviral production by co-transfection of HEK-based cells

HEK-based packaging cells were co-transfected with the pSM2+shRNA^{mir} retrovector and pVSV-G, or the pGIPZ+shRNA^{mir} lentiviral vector, pMD2.G, and psPAX2. pVSV-G, pMD2.G, and psPAX2 encode accessory proteins for efficient viral vector packaging and transduction. The accessory proteins accumulate within the cytoplasm, while the retro- or lentiviral vector-encoded expression cassette is transcribed as a single RNA transcript. The viral accessory proteins associate with the RNA transcript and form non-enveloped viral particles within the cytoplasm. These particles migrate to the cell membrane where VSV-G envelope proteins aggregate and bud from the cell membrane, gaining an envelope. Budding viral particles are replication-incompetent due to the separation of accessory proteins and the viral transcript.

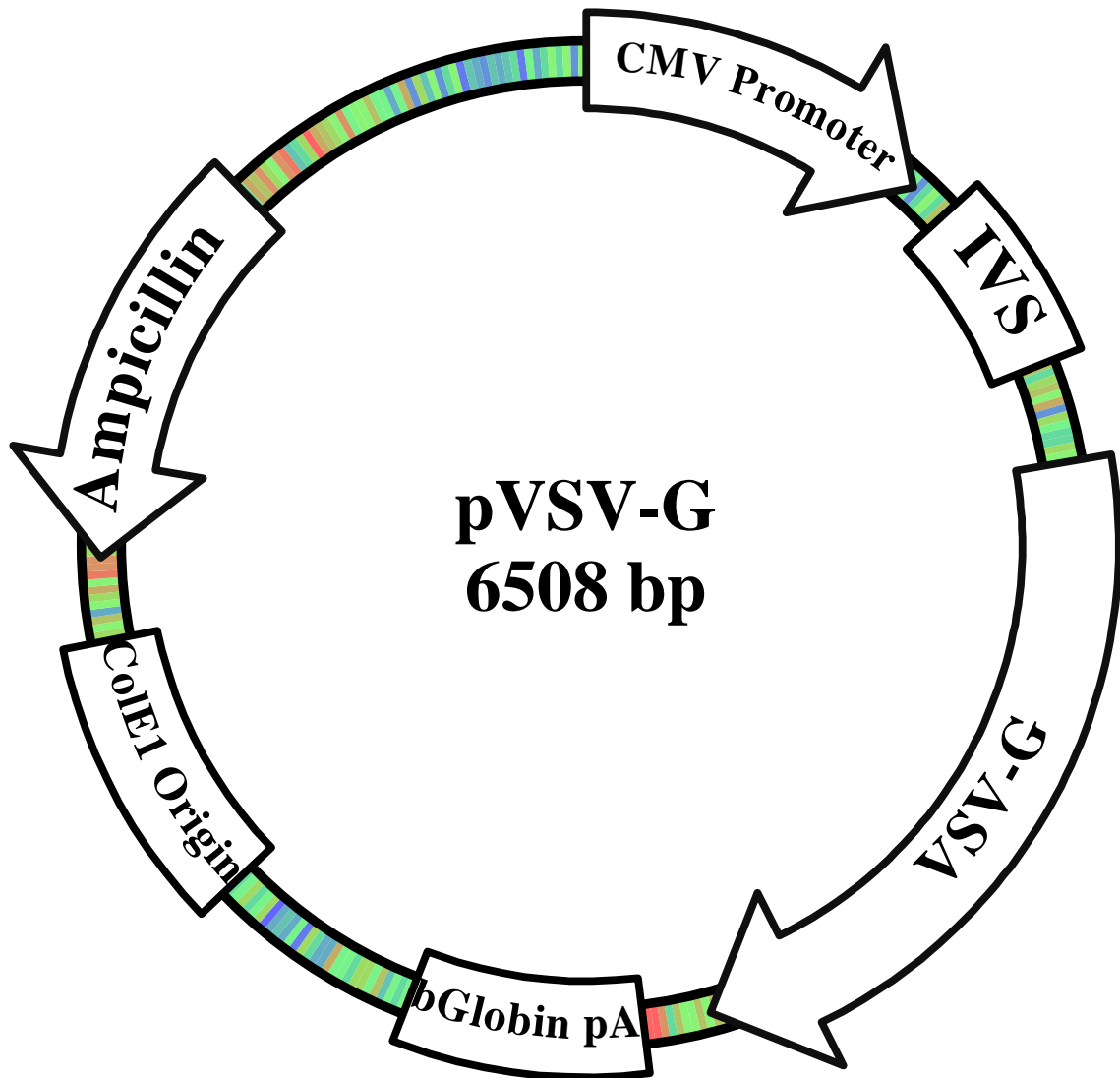


Figure 2.4: Features of the pVSV-G Expression Vector

Key features of the pVSV-G expression vector from Clontech are shown. The ColE1 origin drives plasmid replication, while the ampicillin resistance marker permits selection in bacterial cells. Expression of the VSV-G protein is driven by a CMV promoter for high level expression. The IVS is a synthetic intron derived from the rabbit β -globin gene that stabilizes the mRNA. Inclusion of the rabbit β -Globin polyadenylation (bGlobin pA) signal ensures efficient mRNA termination and translation. Plasmid representation generated using pDRAW32.

2.3.5 Retroviral Titre Determination

The day prior to retroviral titre determination, SK-N-FI cells were passed through a 40 μ M cell strainer, then 500,000 cells were plated per well in a 6-well tissue-culture treated dish (Corning Life Sciences, VWR International, West Chester, PA). Cells were incubated at 37°C with 5% CO₂ overnight. Twenty-four hours later, 500 μ L of DMEM + 2% FS-FBS + 1 X NEAA + 1% Ab/Am (SK-FS-DMEM2) containing 5 μ g/mL polybrene was added to each well of the 6-well dish. Retroviral supernatant was collected in a syringe and filtered through a 0.45 μ m SFCA filter. A 10-fold serial dilution of clarified retroviral supernatant was prepared by diluting 100 μ L into 900 μ L SK-FS-DMEM2 media + 5 μ g/mL polybrene. To the first well, 500 μ L of undiluted filtered retroviral supernatant was added, with each subsequent well having 500 μ L diluted retroviral supernatant added, and the final well having just media. The plates were gently rocked back and forth to ensure even distribution, spun at 2500rpm (123xg) for 2 hours at room temperature in a Beckman Allegra 6KR, and then returned to the incubator for 4 hours. Following this incubation, 100 μ L FS-FBS was added to each well, plates were rocked to mix, and returned to the incubator. The media was removed 24 hours post-transduction and replaced with 2mL SK-FS-DMEM10.

Forty-eight hours post transduction, the media was removed and replaced with SK-FS-DMEM10 + 2 μ g/mL puromycin. Selective media was replaced every 2 days until all control cells were killed. Viral titre was determined by counting the number of colonies in the well that contained individual cell colonies, multiplying by 2 or 20 (if diluted to account for the initial 100 μ L retroviral supernatant), and the dilution factor to

determine the number of infectious units per millilitre. The average retroviral titre as determined on SK-N-FI cells was ~15,000 transducing units/mL (TU/mL).

2.4 pSM2+shRNA^{mir} Library Screening

2.4.1 SK-N-FI Cell Transduction with pSM2 Retrovirus

Concurrent with retroviral titre determination, SK-N-FI cells were transduced with the packaged pSM2+shRNA^{mir} library pools. The day prior to transduction, SK-N-FI cells were strained through a 40 μ M cell strainer, and 500,000 cells were plated per well of a 6-well tissue-culture treated dish in SK-FS-DMEM10 and incubated overnight. Twenty hours post-plating, 1mL SFCA filtered retroviral supernatant was added to each well to give a multiplicity of infection (MOI) of ~0.03 (as titred on SK-N-FI cells) for pSM2+shRNA^{mir} library screening, with polybrene added to a final concentration of 5 μ g/mL. The plates were gently rocked back and forth, spun at 2500rpm (123xg) for 2 hours at room temperature in a Beckman Allegra 6KR. The plates were returned to the incubator for 4 hours. Following this incubation, 100 μ L FS-FBS was added to each well. The plates were rocked gently to mix, and returned to the incubator. Twenty four hours post-transduction, media was removed and replaced with 2mL SK-FS-DMEM10. Media was changed every 48 hours until cells achieved ~80% confluence.

2.4.2 PrP¹⁰⁶⁻¹²⁶ Mediated Neurotoxicity

Following transduction and growth to 80% confluence, SK-N-FI cells were passaged and strained through a 40 μ M cell strainer, then 40,000 cells were added to each

well in a 6-well plate in 2mL DMEM + 5% HI-FBS (Gibco, Invitrogen, Burlington, ON, Lot# 358343) + 1 X NEAA + 1% Ab/Am (SK-HI-DMEM5) (Day 0). Twenty-four hours post-plating, the media was changed to 2mL DMEM + 1% HI-FBS (Gibco, Invitrogen, Lot# 358343) + 1 X NEAA (SK-HI-DMEM1) (Day 1). SK-N-FI cells were then exposed to PrP¹⁰⁶⁻¹²⁶ neurotoxic peptide as outlined above (section 2.2).

2.4.3 Identification of Protective shRNA^{mir}

To identify shRNA^{mir} sequences stably encoded within the genome of PrP¹⁰⁶⁻¹²⁶ resistant SK-N-FI cells, genomic DNA was extracted, shRNA^{mir} sequences were PCR amplified and cloned, and then integrated amplicons were sequenced (Figure 2.5).

2.4.3.1 Extraction of Genomic DNA from PrP¹⁰⁶⁻¹²⁶ Resistant SK-N-FI Cells

Following selection for SK-N-FI cells carrying a shRNA^{mir} conferring resistance to challenge with the PrP¹⁰⁶⁻¹²⁶ peptide, genomic DNA (gDNA) was collected according to the DNeasy Mini Kit (Qiagen, Mississauga, ON) on day 24 or 25. Briefly, 6-well plates of SK-N-FI cells were placed on ice for 5 minutes, rinsed gently with ice-cold PBS, then 200µL ice-cold trypsin was added to each well and incubated for 3 minutes at room temperature. Cells were collected using a rubber cell scraper and the supernatant from all wells of a 6-well plate representing 1 pool was transferred to a single 1.5mL Eppendorf tube, which was spun at 1,000xg for 5 minutes. Supernatant was removed, and the cells were resuspended in 200µL ice-cold PBS. To each tube, 20µL Proteinase K and 200µL buffer AL was added, followed by incubation at 56°C for 10 minutes. Following this incubation, 200µL anhydrous ethanol was added, mixed by pipetting up

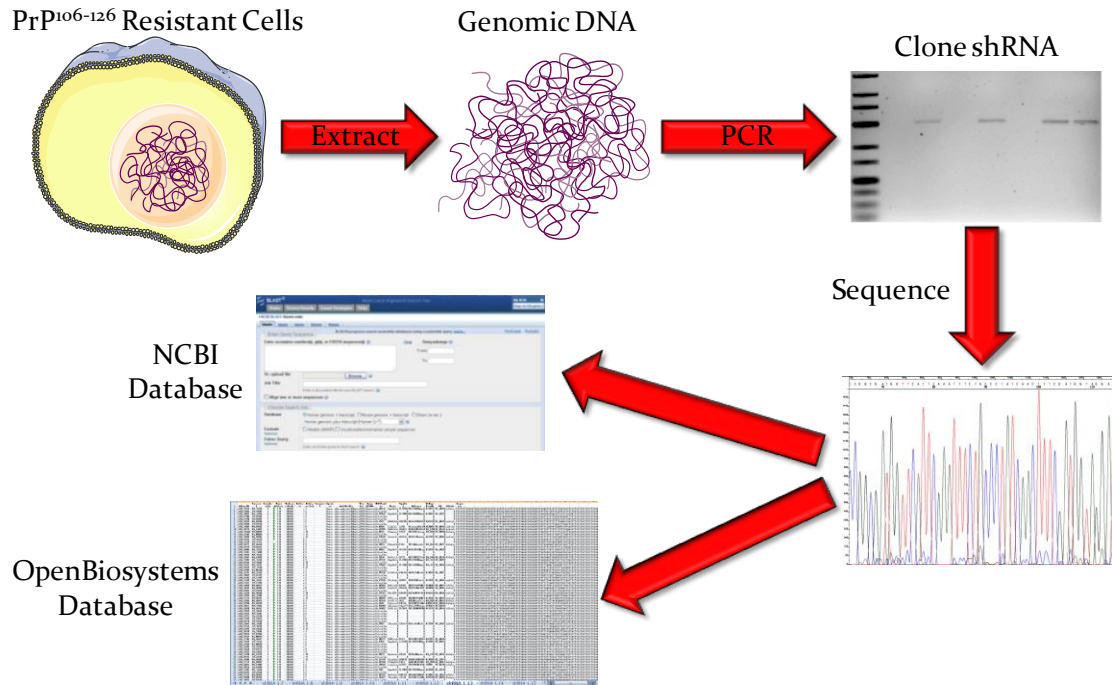


Figure 2.5: Overview of Identifying Protective shRNA^{mir} Sequences

Stably integrated and protective shRNA^{mir} sequences were identified and their corresponding gene targets confirmed using the OpenBiosystems and online NCBI databases. Genomic DNA was extracted from PrP¹⁰⁶⁻¹²⁶ resistant SK-N-FI cells, the encoded shRNA^{mir} sequence amplified using primers encompassing the recognition stem sequences and common to all pSM2-encoded shRNA^{mir}. These amplicons were separated on a 2% agarose gel, purified, cloned into the pCR2.1 vector, transformed into TOP10 *E. coli*, and 24 random colonies representing each shRNA^{mir} pool were transferred to LB^{cb} growth media. Sequencing of the cloned shRNA^{mir} sequences was performed by the Genomics Core Facility at the NML in Winnipeg. The complementary mRNA sequence was identified by scanning of the included OpenBiosystems database, as well as the online NCBI database.

and down 3 times, and then the lysate was applied to a DNeasy Mini spin column and centrifuged at 6,000xg for 1 minute. The column was transferred to a new collection tube, 500µL Buffer AW1 was applied, and centrifuged as above. The column was again transferred to a new collection tube, 500µL Buffer AW2 was applied, and centrifuged at 20,000xg for 3 minutes to dry the DNeasy Mini spin column membrane. The column was transferred to a Nuclease-Free 1.5mL Eppendorf tube, 200µL Buffer AE was applied and incubated at room temperature for 2 minutes, then spun at 16,200xg for 1.5 minutes. The concentration was determined on a NanoDrop and adjusted to 50ng/µL in Buffer AE. The gDNA was stored at -20°C.

2.4.3.2 Amplification of shRNA^{mir} Conferring Resistance

Genomic DNA extracted from PrP¹⁰⁶⁻¹²⁶ resistant SK-N-FI cells was digested with BamHI restriction enzyme (New England Biolabs (NEB), Pickering, ON) to enhance PCR efficiency. This was accomplished by adding 500ng of gDNA, 4µL 10X NEB3 buffer, 0.4µL bovine serum albumin (BSA), 0.4µL BamHI (8 units) (NEB), and adjusted to a final volume of 40µL with Nuclease-Free water in a thin-walled PCR tube. The reaction was incubated at 37°C for 1 hour, then 80°C for 20 minutes to inactivate the enzyme. The digested gDNA was used as template for PCR amplification of the stably integrated shRNA^{mir} retroviral sequence. To a thin-walled PCR tube, 19.625µL Nuclease-Free water, 2.5µL 10X PCR Buffer + 1.5mM Mg²⁺ (Roche, Mississauga, ON), 0.375µL 10mM dNTP mix (Invitrogen, Burlington, ON), 0.25µL (12.5ng) pSM2c2514F (AGTCGACTAGGGATAACAG), 0.25µL (12.5ng) pSM2c2714R (TCAAAGAGATAGCAAGGTA), 0.25µL Taq (Roche, Mississauga, ON), and 2µL

(25ng) BamHI digested gDNA was added. The cycling conditions were 95°C for 5 minutes, then 40 cycles of 95°C X 30 seconds, 55°C for 30 seconds, 72°C for 30 seconds, followed by 72°C for 10 minutes and cooling to 4°C. PCR was carried out on a PTC-200 ThermoCycler (MJ Research, Waltham, MA).

2.4.3.3 Cloning of shRNA^{mir} Conferring Resistance

Amplicons were separated on a 2% agarose gel run at 80 volts for 90 minutes in TAE buffer. The amplicons were visualized using a UV box, and the appropriate bands were cut out of the gel using a razor blade. DNA was extracted from the gel slice according to the QIAEXII Gel Extraction Kit protocol (Qiagen, Mississauga, ON), eluted in 16µL EB buffer, and the concentration was determined on a NanoDrop.

Gel purified amplicons were ligated into the pCR2.1 vector backbone (Invitrogen, Burlington, ON) at a 3:1 insert to vector ratio. To a thin-walled PCR tube, 1µL (25ng) pCR2.1, 1µL 10X T4 DNA Ligase Buffer, 0.5µL T4 DNA Ligase, and 5.77ng amplicon were added, with the final volume adjusted to 10µL with Nuclease-Free water. This ligation reaction was incubated at 14°C overnight (~16 hours). Of the ligation reaction, 2µL was transformed into 25µL chemically competent TOP10 *E. coli* according to the protocol (Invitrogen, Burlington, ON). Briefly, 25µL TOP10 *E. coli* were transferred to an ice-cold 1.5mL Eppendorf tube, 2µL of the overnight ligation product was added, the tube was tapped gently to mix, and incubated on ice for 10 minutes. The tube was plunged into a 42°C water bath for 30 seconds, returned to ice for 2 minutes, and then resuspended in 250µL S.O.C. media and incubated at 37°C for 1 hour with horizontal

shaking at 225rpm. Of this, 50 μ L was plated onto an LB + 200 μ g/mL carbenicillin (LB^{cb}) plate and incubated overnight at 30°C.

The following day, 24 individual colonies were picked from each LB^{cb} plate (each plate representing 1 shRNA^{mir} pool of 960 different constructs) and individually transferred to a 2.2mL 96-well deep well culture block (Millipore, Nepean, ON). Each well contained 1.8mL of LB broth Lennox (Tryptone = 10g/L, Yeast Extract = 5g/L, NaCl = 5g/L) + 200 μ g/mL carbenicillin (LB^{cb}). The culture blocks were incubated at 37°C with horizontal shaking at 225rpm overnight. Each 96-well deep well culture block was used to grow 4 different shRNA^{mir} pools.

2.4.3.4 Sequencing of shRNA^{mir} Conferring Resistance

Plasmid was extracted from overnight cultures according to the Wizard SV 96 Plasmid DNA Purification System protocol (Promega, distributed by Fisher, Nepean, ON). The culture block was centrifuged at 1500xg for 15 minutes, supernatant was poured off and bacterial pellets were resuspended in 250 μ L Cell Resuspension Solution by vortexing at setting 4 on a VortexGenieII for 5 minutes at room temperature. To this, 250 μ L Cell Lysis Solution was added and vortexed as above for 1 minute. Then, 350 μ L Neutralization Solution was added to each well, vortexed as above for 1 minute, and the lysates were applied to a Lysate Clearing Plate stacked on top of a Binding Plate, all on a Vac-Man 96 Vacuum Manifold (Promega, distributed by Fisher, Nepean, ON). A vacuum was applied until all sample passed through the Clearing Plate, then the clearing plate was removed, 500 μ L Neutralization Solution was added to each well of the Binding Plate, and again a vacuum was applied for 1 minute. The bound plasmid was washed 2

times with 1mL Wash Solution (630mL 95% Ethanol + 370mL Wash Buffer), with a vacuum applied for 1 minute or 10 minutes, respectively. During the second wash, the Binding Plate was periodically removed from the vacuum manifold and tapped onto KimWipes to remove excess Wash Solution. The Binding Plate was placed atop a 96-well thin-walled V-bottom PCR plate, 60 μ L Nuclease-Free water was added to each well, the plate was incubated for 2 minutes at room temperature, and then spun at 3000rpm in a Legend RT benchtop centrifuge (Sorvall, ThermoScientific, Huntsville, AL) for 1.5 minutes. The PCR plate was sealed with plate sealer foil (MJS BioLynx Inc., Brockville, ON) and sent for sequencing to the Genomics Core Facility at the NML using the M13(-20) Forward (GTAAAACGACGGCCAGT) and M13 Reverse (CAGGAAACAGCTATGAC) primers. All shRNA^{mir} sequences were recorded and tabulated, but only those that appeared 3 or more times were considered to be of interest.

Statistically, the probability of a particular shRNA^{mir} appearing 3 or more times is $24/960^3 = 0.0000027\%$ (24 colonies picked per pool, 960 different shRNA^{mir} per pool, a given sequence appearing at least 3 times). The shRNA^{mir} sequences appearing ≥ 3 times were compared to the OpenBiosystems pSM2+shRNA^{mir} human library database to determine the targeted gene. Results were confirmed using the BLAST program on the NCBI website (<http://blast.ncbi.nlm.nih.gov/Blast.cgi>).

2.5 Preliminary Validation of the First 30 shRNA^{mir} Identified

2.5.1 Purification of Endotoxin Free Plasmid from Individual Bacterial Clones

For preliminary confirmation of PrP¹⁰⁶⁻¹²⁶ resistance conferred upon SK-N-FI cells by shRNA^{mir} identified from the library screen, PirPlus⁺ *E. coli* carrying the identified pSM2+shRNA^{mir} were selected from a replicate plate of the original glycerol bacterial stocks of the OpenBiosystems library. These clones were grown in 25mL LB broth + 25µg/mL chloramphenicol (LB^{chlor}) and incubated at 37°C overnight with shaking at 225rpm. Plasmid was extracted according to the Qiagen Plasmid Mini Kit protocol, with the use of EndoFree buffers and the addition of buffer ER at a 1 in 10 ratio (90µL) to the lysate after clearing of the cellular debris by centrifugation. The tubes were incubated on ice for 30 minutes and then the protocol was continued without further modifications upon loading onto the activated TIP-20. Following precipitation of the plasmid DNA in ethanol, the pellet was resuspended in 200µL EndoFree TE buffer and stored at 4°C overnight. The next day, the tubes were vortexed on a VWR VortexGenie II on setting 4 for 30 seconds, spun at 16,200xg for 30 seconds, and the supernatant was transferred to a Nuclease-Free tube. This EndoFree plasmid was stored at -20°C.

2.5.2 Retroviral Packaging, Titration, and Transduction

The individual pSM2+shRNA^{mir} vectors, as well as pSM2+shRNA^{mir} targeting the cell cycle regulator Eg5 (Ambion recommended control), were packaged into retroviral particles using GP2-293 and titred on SK-N-FI cells as described above (sections 2.3.4 & 2.3.5). Transduction of SK-N-FI cells was also performed as stated above with the exception that retroviral particles were transduced at an MOI of 0.06. Following a 4 hour incubation, 100µL FS-FBS was added to each well and incubated for

a further 24 hours. Media was changed to SK-FS-DMEM10, and replaced every 48 hours until cells achieved ~80% confluency.

2.5.3 Confirming pSM2+shRNA^{mir} Confer Resistance Against PrP¹⁰⁶⁻¹²⁶ Peptide

SK-N-FI cells transduced with the first 30 individual pSM2+shRNA^{mir} molecules identified from the library screen, and packaged into retroviral particles, were selected for resistance against the PrP¹⁰⁶⁻¹²⁶ neurotoxic peptide as stated above (section 2.4.2). SK-N-FI cells were exposed to a total of 5 applications of 50µM PrP¹⁰⁶⁻¹²⁶ diluted in 400µL SK-HI-DMEM5 + 10.06mL SK-HI-DMEM1 per milligram peptide, replaced every 48 hours. Forty eight hours following the 5th application of PrP¹⁰⁶⁻¹²⁶, media was changed to 400µL SK-HI-DMEM5 per 10.06mL SK-HI-DMEM1 and cells were incubated for 48 hours. Media was changed to SK-HI-DMEM5 for 48 hours, and then changed to SK-FS-DMEM10, which was replaced every 3 days until individual cell colonies were visible.

2.5.4 Individual pSM2+shRNA^{mir} Conferred Cellular Resistance

Cell viability was measured using AlamarBlue as described above. Percent reduction of the AlamarBlue reagent was compared back to previously generated standard curves and used to quantitate cell number. The relative cell survival was determined by comparing the number of surviving cells transduced with an identified pSM2+shRNA^{mir} to that of SK-N-FI cells transduced with pSM2+shRNA^{mir} targeting Eg5.

2.6 Confirming Protection of 2 Identified shRNA^{mir} Using Lentiviral Vectors

2.6.1 Replication and Isolation of Lentiviral Vectors

Individual *E. coli* glycerol stock clones carrying a lentiviral vector backbone with an shRNA^{mir} targeting the genes of interest, carried in the pGIPZ+shRNA^{mir} vector backbone (Figure 2.6), were purchased from OpenBiosystems (ThermoFisher Scientific, Huntsville, AL). Individual clones were grown in 25mL LB^{cb} overnight at 30°C with shaking at 225rpm. Plasmid was extracted according to the Qiagen Plasmid Mini Kit protocol as described above.

2.6.2 Replication and Purification of the Lentiviral Packaging Vectors

The psPAX2 vector backbone encoding lentiviral packaging proteins (Gag, Pol, RRE, Tat, and Rev) (Figure 2.7) and the pMD2.G vector backbone (encoding the VSV-G membrane protein) (Figure 2.8) were generous gifts from the laboratory of Dr. Chris Anderson at the St. Boniface Research Center in Winnipeg, Manitoba, originally purchased from Addgene (plasmid 12260 and 12259, respectively, Cambridge, MA). Plasmids were transformed into electrocompetent TOP10 *E. coli* cells (Invitrogen, Burlington, ON) by electroporation using a Bio-Rad GenePulser® II electroporator (Mississauga, ON) at 1.2kV, 25µF, and 200Ω. Cells were grown on LB^{cb} agar plates overnight at 30°C. An individual colony was grown in 25mL LB^{cb} broth at 30°C overnight with shaking at 225rpm. Plasmid was extracted according to the Qiagen Plasmid Mini Kit protocol as described above.

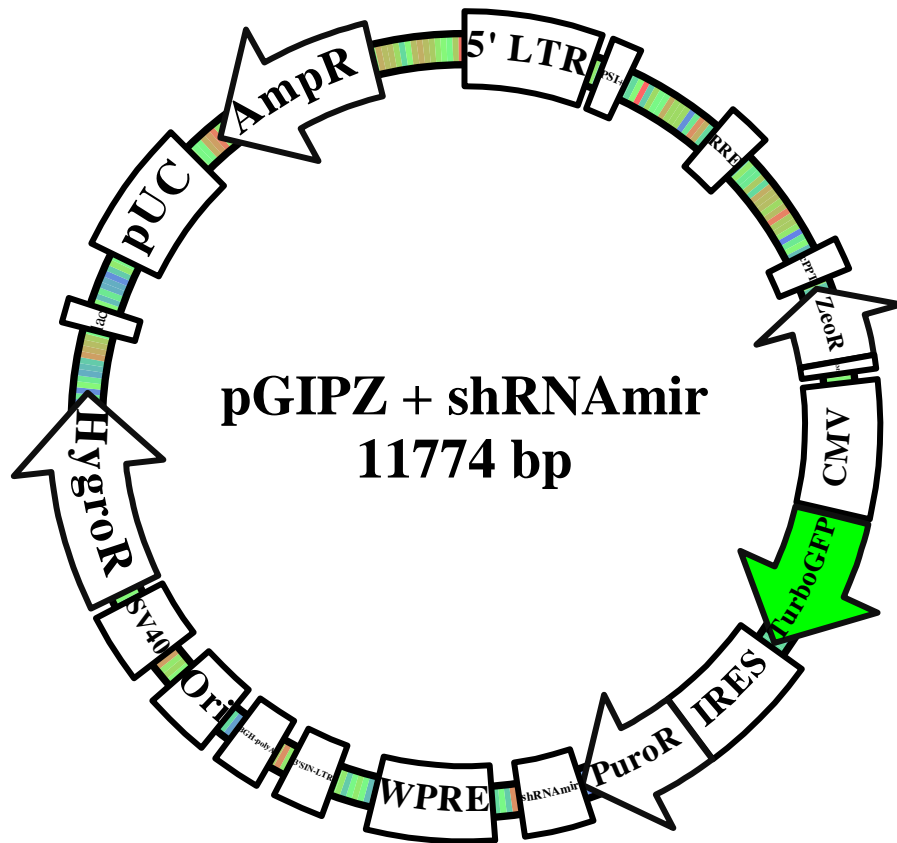


Figure 2.6: Features of the pGIPZ+shRNA^{mir} Expression Vector

The pGIPZ+shRNA^{mir} lentiviral expression vector from OpenBiosystems. Ampicillin is a bacterial selection marker, and the pUC origin drives replication in bacteria. Hygromycin is both a bacterial and eukaryotic selection marker. Puromycin and zeocin are eukaryotic selection markers. The shRNA^{mir} expression cassette lies between LTRs, one of which is self-inactivating. Tat protein interacts with LTRs to direct integration via Pol. A CMV promoter drives transcription of an mRNA encoding the tGFP and puromycin markers, as well as the shRNA^{mir}. The psi⁺ signal permits efficient packaging of viral RNA into lentiviral particles. The RRE element directs transport of viral mRNA to the cytoplasm. The cPPT sequence aids in translocation of the viral pre-integration complex into the nucleus. The woodchuck hepatitis virus post-transcriptional regulatory element (WPRE) enhances mRNA stability and translation.

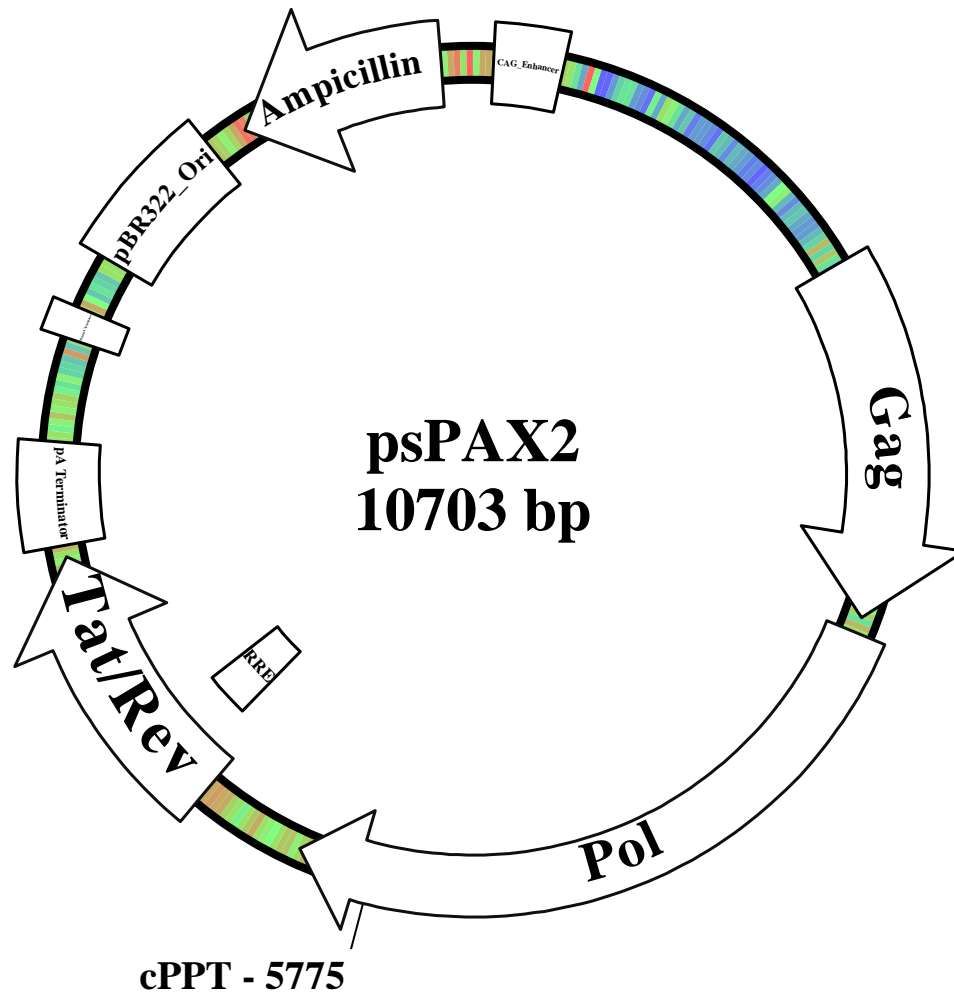


Figure 2.7: Features of the psPAX2 Lentiviral Packaging Vector

Diagrammatic representation of the psPAX2 lentiviral packaging vector from Addgene. Ampicillin is a bacterial antibiotic selection marker, and the pBR322 is a bacterial origin of replication. The CAG promoter efficiently drives expression of the packaging proteins. The Gag protein composes the viral capsid. The Pol protein converts viral RNA to dsDNA. The Tat protein is a transactivator that drives high levels of transcription and binds to LTRs to direct integration of the viral genome via Pol. The Rev protein binds the RRE regulatory element and shuttles viral mRNA from the nucleus to the cytoplasm for efficient protein production. The central polypurine tract (cPPT) sequence aids in translocation of the viral pre-integration complex into the nucleus.

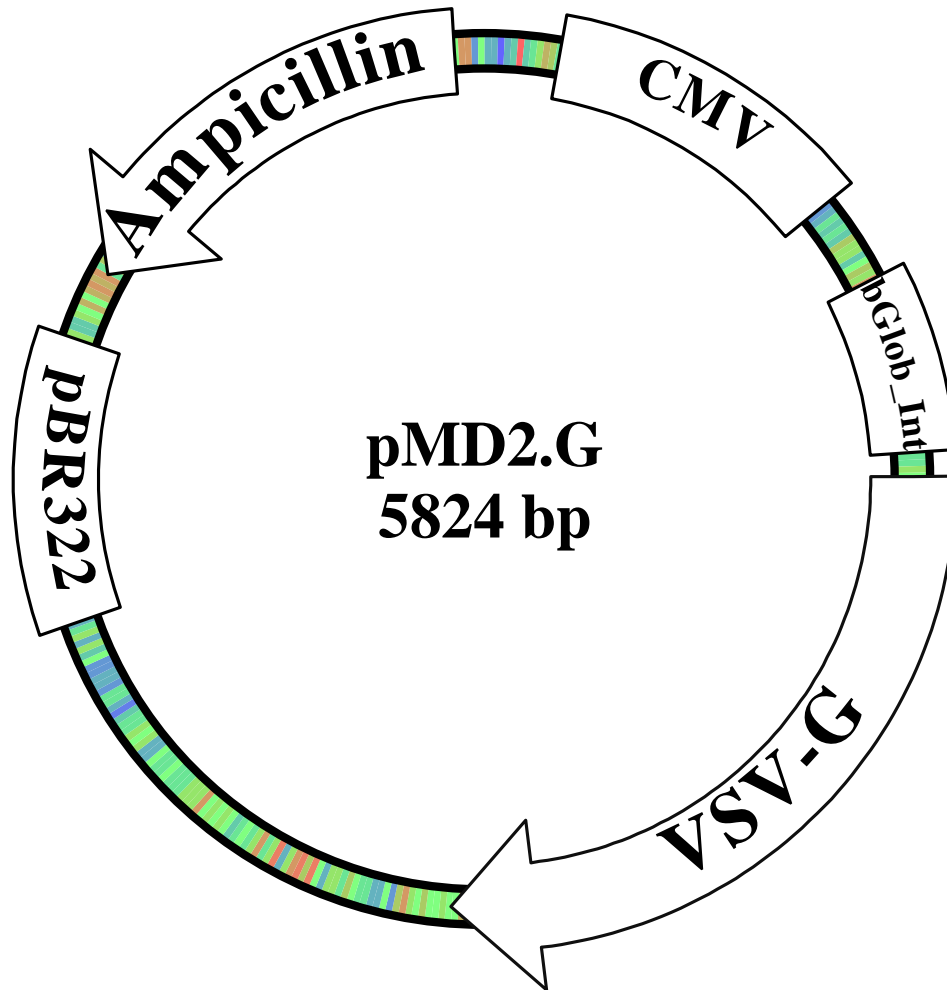


Figure 2.8: Features of the pMD2.G VSV-G Expression Vector

Key features of the pMD2.G VSV-G expression vector from Addgene. Ampicillin is a bacterial antibiotic selection marker, and the pBR322 is a bacterial origin of replication. The viral CMV promoter drives high levels of transcription of the VSV-G. Inclusion of the β -globin intron enhances transcription and mRNA stability.

2.6.3 Packaging of Lentiviral Vectors

The HEK-based 293T/17 cell line was used to package the pGIPZ+shRNA^{mir} expression vectors (including a Non-Silencing shRNA^{mir} control construct) into replication deficient lentiviral particles (Figure 2.3). 293T/17 cells were passaged, strained through a 40µm cell strainer, and plated at 3×10^6 cells per 6cm tissue culture treated dish (Nunc, ThermoScientific, Rochester, NY) in a final volume of 6mL HI-DMEM10 the day prior to transfection. Twenty-four hours later, cells were co-transfected with 250ng, 750ng, and 1µg of pMD2.G, psPAX2, and pGIPZ+shRNA^{mir} vector respectively, using Effectene (Qiagen, Mississauga, ON).

The DNA was resuspended in a final volume of 305µL EC buffer in 15mL polystyrene Falcon tubes, and Enhancer was added at a 4:1 ratio (8µL). This mixture was vortexed at setting 4 on a VWR VortexGenieII for 10 seconds and incubated at room temperature for 10 minutes. Effectene was added at a 5:1 ratio (10µL), vortexed as above, and incubated at room temperature for 10 minutes. Media was removed from the 6cm dishes, the transfection complex was resuspended in 1.2mL FS-DMEM10, and gently applied evenly over the cells. The dishes were incubated overnight. Twenty four hours post-transfection, the complex was removed and replaced with 2.5mL FS-DMEM10 and incubated overnight. Approximately 48 hours post-transfection, media was collected using a sterile syringe, filtered through a 0.45µm SFCA filter, and aliquoted in 1mL volumes into Nuclease-Free 1.5mL tubes (Applied Biosystems, Streetsville, ON). Lentiviral particles were snap-frozen in an isopropanol dry ice bath, and stored at -80°C.

2.6.4 Lentiviral Titre Determination

The day prior to titre determination, NIH/3T3 cells were strained through a 40 μ M cell strainer, then 40,000 cells were plated per well of a 12-well tissue-culture treated dish (Corning Life Sciences, VWR International, West Chester, PA) in a final volume of 1mL. This was incubated at 37°C with 5% CO₂ overnight. Twenty-four hours later, 10 μ L of filtered lentiviral supernatant was added to 990 μ L (10^{-2} dilution) DMEM + 2% FS-FBS + 1% Ab/Am (FS-DMEM2) containing 5 μ g/mL polybrene. This 10^{-2} diluted lentiviral supernatant was further serially diluted 10-fold down to 10^{-6} by adding 60 μ L to 540 μ L DMEM + 2% FS-FBS + 1% Ab/Am (FS-DMEM2) containing 5 μ g/mL polybrene. Of the diluted supernatant ($10^{-3} \rightarrow 10^{-6}$), 500 μ L of each dilution was added per well. The plates were gently rocked back and forth to mix, and returned to the incubator for 24 hours. Following this incubation, the media was removed and replaced with 750 μ L FS-DMEM10 + 2.25 μ g/mL puromycin.

Selective media was replaced every 2 days until all control cells were killed. The number of transducing units per millilitre (TU/mL) was determined by counting the number of colonies in the well that contained individual cell colonies, multiplying by the dilution factor (typically 10,000) and 200 (to account for 10 μ L of original supernatant used for the dilution series and 500 μ L being added to each well).

2.6.5 SK-N-FI Cell Transduction with Lentivirus

The day prior to transduction, SK-N-FI cells were strained through a 40 μ m cell strainer, and then 2.5×10^6 cells were plated per 6cm tissue-culture treated dish (Corning

Life Sciences, VWR International, West Chester, PA) in SK-FS-DMEM10 and incubated overnight. Twenty hours post-plating, the appropriate volume of SFCA filtered lentiviral supernatant was added to each well to give a multiplicity of infection (MOI) of 10, with SK-FS-DMEM2 added to a final volume of 1.5mL + 5µg/mL polybrene. The dishes were gently rocked back and forth to ensure even distribution and returned to the incubator. Twenty four hours post-transduction, media was removed and replaced with 4mL SK-FS-DMEM10. Media was changed every 48 hours until cells achieved ~80% confluency.

2.6.5.1 Confirmation of Identified shRNA^{mir} for Conferring PrP¹⁰⁶⁻¹²⁶ Resistance

SK-N-FI cells transduced with lentiviral particles carrying pGIPZ+shRNA^{mir} molecules were selected for resistance against the PrP¹⁰⁶⁻¹²⁶ neurotoxic peptide relative to PrP^{Scram} peptide as stated above (section 2.2), with the exception that the concentration of peptide applied was 20µM. Briefly, SK-N-FI cells were exposed to a total of 5 applications, replenished every 48 hours, of 20µM PrP¹⁰⁶⁻¹²⁶ or PrP^{Scram} diluted in 1mL (3.8%) SK-HI-DMEM5 + 25.15mL (96.2%) SK-HI-DMEM1. Forty eight hours following the 5th application of PrP¹⁰⁶⁻¹²⁶ or PrP^{Scram}, media was changed to 1mL SK-HI-DMEM5 per 25.15mL SK-HI-DMEM1 and cells were incubated for 48 hours. Media was then changed to SK-HI-DMEM5 for 48 hours, and then replaced with regular growth media (SK-FS-DMEM10), which was replenished every 3 days until individual cell colonies were visible.

Cell viability was measured using AlamarBlue as described above. Percent reduction of the AlamarBlue reagent was compared back to previously generated

standard curves and used to quantitate cell number. The relative cell survival was determined by comparing the number of surviving cells transduced with a particular pGIPZ+shRNA^{mir} molecule exposed to PrP¹⁰⁶⁻¹²⁶ to the number of surviving cells exposed to PrP^{Scram}. This ratio was then divided by the ratio of surviving SK-N-FI cells transduced with the pGIPZ+Non-Silencing control vector.

2.6.5.2 Collection of RNA and protein from SK-N-FI Cells

Excess transduced SK-N-FI cells were plated in T25 tissue culture-treated flasks (Corning Life Sciences, VWR International, West Chester, PA) and selected for stable transductants using 2.25µg/mL puromycin. RNA and protein was isolated according to the Ambion PARIS kit protocol (Applied Biosystems, Streetsville, ON). Briefly, SK-N-FI cells were incubated on ice for 5 minutes, rinsed with ice-cold PBS, and lysed using 500µL Cell Disruption Buffer. SK-N-FI cell lysate was collected using a rubber cell scraper and transferred to a 1.5mL ice-cold Nuclease-Free tube. Lysate was passed through a 20G needle 10 times gently. Of the total lysate, 200µL was transferred to a Nuclease-Free tube containing 200µL 2X Lysis/Binding Solution (RNA extraction), while the remaining supernatant was stored on ice (Protein extraction).

RNA Extraction – total RNA was isolated from the SK-N-FI cell lysate according to the Qiagen RNeasy Mini kit protocol (Mississauga, ON). RNA was recovered from the column by applying 30µL nuclease-free water directly to the RNeasy Mini column filter and incubating for 2 minutes at room temperature. The tube was spun at 16,200xg for 1.5 minutes to elute the RNA. The concentration of RNA was determined on a NanoDrop and the eluted RNA was stored at -80°C.

Protein Extraction – the remaining SK-N-FI cell lysate was used for protein isolation according to the Amersham 2D Clean Up kit (Oakville, ON). Following the final wash, the pellet was air-dried and resuspended in rehydration buffer (0.03 M Tris-HCl, 8 M Urea, 2 M Thiourea, 2% Chaps, pH 8.5) overnight at 4°C. The resuspended protein was centrifuged at 10,000xg for 10 minutes and the supernatant was transferred to a Nuclease-Free tube. The concentration of protein was determined according to the Amersham 2D Quant Kit protocol (Oakville, ON) and stored at -80°C.

2.6.5.3 Generation of cDNA from SK-N-FI RNA

Contaminating DNA was eliminated from RNA extracted from SK-N-FI cell lysate according to the TURBO DNA-*free*[™] protocol (Applied Biosystems, Streetsville, ON). To 4µg total RNA, 1µL (0.1 volumes) 10X TURBO DNase Buffer and 1µL TURBO DNase were added, and the volume was adjusted to 10µL using Nuclease-Free water. This was incubated at 37°C for 30 minutes, followed by addition of 1µL DNase Inactivation Reagent and incubation at room temperature for 5 minutes. Tubes were spun at 10,000xg for 1.5 minutes and RNA-containing supernatant was transferred to a Nuclease-Free microcentrifuge tube. The entire 10µL of recovered TURBO DNase treated RNA was reverse transcribed to cDNA according to the Invitrogen SuperScript[™] III RNase H⁻ Reverse Transcriptase protocol (SSIII, Burlington, ON).

Briefly, total RNA was resuspended in Nuclease-Free water to a final volume of 11µL. To this, 1µL 10mM dNTPs (Invitrogen, Burlington, ON) and 1µL oligo(dT)₂₀ (50µM) primer (Invitrogen, Burlington, ON) was added and heated to 65°C for 5 minutes, then transferred immediately to ice for 1 minute. The tubes were briefly spun

and 4µL 5X First-Strand Buffer, 1µL 0.1M DTT, 1µL RNaseOUT™ Recombinant RNase Inhibitor (Invitrogen, Burlington, ON), and 1µL SuperScript™ III RT was added to each tube. Tubes were mixed gently by pipetting up and down 3 times, incubated at 50°C for 1 hour in a pre-heated ThermoCycler with a heated lid (MJ Research, Waltham, MA), followed by heating to 70°C for 15 minutes to inactivate the enzyme. Tubes were cooled to 37°C, 1µL RNase H (Invitrogen, Burlington, ON) was added to each tube and incubated for 20 minutes. Reactions were cleaned up according to the Qiagen PCR Purification kit protocol (Mississauga, ON). The cDNA was eluted by applying 20µL Nuclease-Free water to the column, letting sit at room temperature for 2 minutes, and spinning at 16,200xg for 1.5 minutes.

2.6.5.4 Quantification of *abcb4*, *ube2cbp*, and *prnp* from SK-N-FI cDNA

The concentration of cDNA was determined on a NanoDrop and adjusted to 10ng/µL using Nuclease-Free water. Primers specific to human *abcb4*, *ube2cbp*, *prnp*, and *gapdh* were found on the Universal ProbeLibrary website (Roche, <http://www.roche-applied-science.com/sis/rtpcr/upl/ezhome.html>) or designed using Primer-BLAST (NCBI, <http://www.ncbi.nlm.nih.gov/tools/primer-blast/>), with primer pairs spanning an exon-exon junction where possible (Table 2.1). De-salted primers were ordered from the Genomics DNA Core Facility (National Microbiology Laboratory, Winnipeg, Canada) and the concentrations were adjusted to 50ng/µL in Nuclease-Free water. To each well of a 96-well white PCR plate (Roche, Laval, QC), 6µL Nuclease-Free water, 1µL of each primer, 10µL 2X LightCycler 480 SYBR Green Master Mix (Roche, Laval, QC), and 2µL cDNA (20ng) was added. Cycling parameters for the LightCycler® 480 were as

Table 2.1: Primer Pairs for qPCR Analysis of SK-N-FI *abcb4*, *ube2cbp*, and *prnp*

Primers were designed to target the human *abcb4*, *ube2cbp*, and *prnp* genes, the first 2 of which were identified from the pSM2+shRNA^{mir} library screen, while *prnp* was used as a control. Real-time quantitative PCR (qPCR) was performed on a Roche LightCycler® 480 system using the LightCycler® 480 SYBR Green I Master mix (Roche Applied Science, Laval, QC). Listed below are the human genes, primer pairs, expected size, annealing temperature, extension times, and the number of cycles. Samples were initially denatured at 95°C for 5 minutes, followed by 40 or 45 cycles of 95°C for 5 seconds, annealing of primer pairs at 60 or 63°C, and primer extension at 72°C. Human *gapdh* was used as the housekeeping gene to normalize the relative mRNA expression. Amplification was followed by melt curve analysis for confirmation of single product specificity.

Genbank Accession Number (Human)	Gene	Primer Pairs (5'--->3')	Size (bp)	Anneal °C	Extension 72°C (sec)	Cycles
NM_000443.3	<i>abcb4</i>	TGCGCTTCAGAGATGTTATTCT TGCAGACAGCTTAGCTTTAGCAT	110	60	7	45
NM_198920.1	<i>ube2cbp</i>	GCCGTGTGAATTCCTTTCAG TGTGCTCCTGCTTGAGAGC	96	60	7	45
NM_000311.3	<i>prnp</i>	TGGCGGCTACATGCTGGGAAGTG TTAACGTCGGTCTCGGTGAAGT	237	63	11	45
NM_002046.3	<i>gapdh</i>	TTCGACAGTCAGCCGCATCTTCTT CAGGCGCCCAATACGACCAAATC	110	60	8	40

follows: 95°C for 5 minutes, followed by 40 (*gapdh*) or 45 cycles of 95°C for 5 seconds, 60 (*gapdh*, *abcb4*, or *ube2cbp*) or 63°C (*prnp*) for 5 seconds, and 72°C for 7-11 seconds (Table 2.1), followed by melt curve analysis. The relative expression level of the gene of interest was determined using plasmid-based calibrators and normalized to the housekeeping gene *gapdh* as calculated by the Roche LightCycler® 480 software (Stobart et al. 2007; Stobart et al. 2009).

The average relative expression level for the gene of interest was determined for the control samples (pGIPZ+Non-Silencing shRNA^{mir}), and then individual relative expression levels were normalized to this average for each time point respectively. These normalized ratios were averaged, and the gene expression levels of SK-N-FI cells transduced with pGIPZ+shRNA^{mir} targeting *abcb4* or *ube2cbp*, as well as *prnp*, were compared to the control samples. Statistically significant differences in expression levels between control and gene of interest targeted shRNA^{mir}-expressing vectors were determined using a Students' two-tail t-test assuming equal variance.

2.6.5.5 Quantification of Ube2cbp Protein from SK-N-FI Cells

Of the total protein, 25µg was boiled at 99°C for 5 minutes in diluted 4X XT loading buffer (Bio-Rad, Hercules, CA) + 10% SDS + 4% βME, and loaded onto a 12% Bis-Tris Criterion pre-cast SDS-PAGE gel (Bio-Rad, Hercules, CA). Gels were run at 200V for 1 hour in 1X MOPS XT running buffer (Bio-Rad, Hercules, CA). Protein was transferred to a nitrocellulose membrane using the iBlot system (Invitrogen, Burlington, ON) and blocked in TBST + 5% bovine serum albumin (BSA, Sigma, Oakville, ON) with rocking at room temperature for 1 hour. Primary antibody (rabbit-α-Ube2cbp

(Pacific Immunology, Ramona, CA) or mouse- α -Tubulin (Sigma, T9026, Oakville, ON)) was diluted 1:2000 in TBST + 1% BSA and incubated overnight at 4°C with rocking. Note that the membrane was stripped using Restore Western Blot Stripping Buffer (ThermoScientific, Rockford, IL) and re-blocked between primary antibodies.

The membrane was washed 3 times with TBST for 5 minutes each wash. Secondary antibody (goat- α -rabbit-HRP or goat- α -mouse-HRP, DakCytomation, P0448 or P0447 respectively, Denmark) was diluted 1:2000 in TBST + 1% BSA, and the membrane was incubated at room temperature for 1 hour with rocking. The membrane was washed 3 times in TBST, rinsed 3 times for 30 seconds each rinse in TBS, and excess TBS was blotted off. To the membrane, 1mL SuperSignal West Pico Chemiluminescent reagent (ThermoScientific, Rockford, IL) was added and incubated for 2 minutes. The membrane was imaged on a VersaDoc Gel Imaging system and the relative amount of Ube2cbp was normalized to α -tubulin expression as measured using Quantity One software (Bio-Rad, Hercules, CA).

2.7 Validating Identified shRNA^{mir} in a Mouse Model of Prion Disease

2.7.1 Collection of RNA from Mouse Brains

Brains were removed from control and Scrapie ME7 infected mice at days 28, 60, 70, 90, 100, 110, 120, 130 days post inoculation (dpi) and terminal (~ 145 dpi) by the veterinary technicians at the National Microbiology Laboratory (NML, Winnipeg, MB). Brains collected from each animal were individually stored in RNAlater (Applied Biosystems, Streetsville, ON) in 15mL polypropylene Falcon tubes at -80°C. RNA was

extracted from brains according to the Ambion PARIS kit protocol (Applied Biosystems, Streetsville, ON). Briefly, samples were thawed at room temperature, and then immediately put on ice. Brains were transferred to cooled M-tubes (Miltenyi Biotec, Auburn, CA) containing 3mL ice-cold cell disruption buffer + protease inhibitors, homogenized using a gentleMACS™ Dissociator (Miltenyi Biotec, Auburn, CA) for 45 seconds, and returned to ice for 8 minutes. Samples were spun at 5,000xg for 8 minutes at 4°C, then 1mL supernatant was transferred to a 15mL polypropylene Falcon tube containing 2X Lysis/Binding Solution. RNA was purified according to the Ambion PARIS kit protocol.

Briefly, at room temperature, 1mL anhydrous ethanol (Sigma, Oakville, ON) was added to the tube containing 1mL supernatant and 1mL Lysis/Binding Solution, mixed by pipetting, and then the lysate/ethanol mixture was applied to a supplied filter cartridge. The samples were spun at 16,000xg for 30 seconds at room temperature, the column was washed with 700µL Wash Solution 1, centrifuged as above, and followed by two washes with 500µL Wash Solution 2/3. The flow-through was poured off and the filter cartridge was re-spun at 16,000xg for 1 minute to remove excess liquid. The filter cartridge was transferred to a new collection tube. To the filter cartridge, 50µL pre-heated (55°C) nuclease-free water was applied directly to the filter and incubated for 2 minutes. The tube was spun at 16,000xg for 30 seconds to elute the RNA. This was repeated with another 50µL of water, the concentration was determined using a NanoDrop, and the eluted RNA was stored at -80°C.

2.7.2 Generation of cDNA from RNA Collected from Mice

Contaminating DNA was eliminated from RNA extracted from mouse tissue using the TURBO DNA-*free*[™] kit (Applied Biosystems, Streetsville, ON). To the total 100µL of RNA extracted above, 10µL (0.1 volumes) 10X TURBO DNase Buffer and 1µL TURBO DNase were added and mixed gently. This mixture was incubated at 37°C for 30 minutes, followed by addition of 11µL DNase Inactivation Reagent and incubation at room temperature for 5 minutes. Tubes were spun at 10,000xg for 1.5 minutes and the RNA-containing supernatant was transferred to a Nuclease-Free microcentrifuge tube.

Of the total RNA collected from the brains and treated with TURBO DNase, 2µg was reverse transcribed to cDNA according to the manufacturer's protocol for SuperScript[™] III RNase H⁻ Reverse Transcriptase (SSIII, Invitrogen, Burlington, ON) as described above. Reactions were cleaned up by applying the total volume to a Microcon column (Millipore, Billerica, MA), and spinning at 16,200xg for 2 minutes. The cDNA was eluted by applying 20µL Nuclease-Free water, letting sit at room temperature for 2 minutes, and spinning at 16,200xg for 1.5 minutes. The concentration of cDNA was determined on a NanoDrop and stored at -80°C.

2.7.3 Quantification of Library Identified Gene Targets from Mouse Brain cDNA

The concentration of the generated cDNA was adjusted to 2.5ng/µL. Samples were aliquoted into replicate skirted 96-well plates (Corning Life Sciences, VWR International, West Chester, PA), covered with sealing foil, and stored at -20°C. Primers specific to the mouse equivalents of 49 of the library identified gene targets of interest were found on the Universal ProbeLibrary website (Roche, <http://www.roche-applied->

science.com/sis/rtpcr/upl/ezhome.html) or designed using Primer-BLAST (NCBI, <http://www.ncbi.nlm.nih.gov/tools/primer-blast/>), with primer pairs spanning an exon-exon junction where possible (Table 2.2). De-salted primers were ordered from the Genomics DNA Core Facility (National Microbiology Laboratory, Winnipeg, Canada) and the concentration was adjusted to 50ng/μL in Nuclease-Free water (Applied Biosystems, Streetsville, ON). To each well of a 96-well white PCR plate (Roche, Laval, QC), 4μL Nuclease-Free water, 1μL of each primer, 10μL 2X LightCycler 480 SYBR Green Master Mix (Roche, Laval, QC), and 4μL cDNA (10ng) was added. Cycling parameters for the LightCycler® 480 were as follows: 95°C for 5 minutes, followed by 40-60 cycles of 95°C for 5 seconds, 60°C for 5 seconds, 72°C for 10 seconds, followed by melt curve analysis. The relative expression level of the gene of interest was normalized to the housekeeping gene *gapdh* as calculated by the Roche LightCycler® 480 software (Roche, Laval, QC). The average relative expression level for the gene of interest was determined for the control samples for each time point, and then individual relative expression levels were normalized to this average for each time point respectively. Normalized ratios were averaged, and the gene expression levels of infected samples were compared to the control samples. Outliers, as determined by the Grubbs' test with the significance level set at 0.05 (GraphPad QuickCalcs, <http://www.graphpad.com/quickcalcs/Grubbs1.cfm>), were removed from all calculations. Statistically significant differences in expression level between control and infected samples were determined using a Students' two-tail t-test assuming equal variance.

Table 2.2: Primer Pairs for qPCR Analysis of pSM2+shRNA^{mir} Library Identified Gene Targets

Primers were designed to target the mouse genes corresponding to those identified by the human pSM2+shRNA^{mir} library screen. The primers listed below target those genes that are confirmed as protein coding and which produced a single amplicon, as confirmed by melt curve analysis and agarose gel analysis.

Genbank Accession Number (Mouse)	Gene	shRNA ^{mir} Library Accession #	Primer Pairs (5'--->3')	Size (bp)	Extension 72°C (sec)	Cycles
NM_008830.2	Abcb4	SH2422h1	GAAGGGATCTACTTCAGACTCGTT TCAACTTCAAATTCTTCTGACAGG	74	6	50
NM_175324.2	Acad11	SH2559a11	GGTGGCTATATAGTTAACGGCAAG CGATTTTGCACTTGGGATTC	67	6	50
NM_021604.2	Agri	SH2276e9	GGCTGTGAAGCAGATCCCACAACA CCTCTGGACATGTGAGAGTTGGGC	124	6	50
NM_028665.4	Ankrd42	SH2605g8	TCAAGGAAACGCTGCAGAA GACTCACACGAGTCATCTTCCA	67	6	50
NM_007478.3	Arf3	SH2524a1	GAAACTCGGGGAGATTGTCA GTCCAGACTGTGAAGCTGAT	91	6	50

NM_022979.4	Arl6ip6	SH2360g5	TGCATGCAGAAAACCTTGAAAA GATATTATCAGCAGAGACCAGAAGC	76	6	50
NM_009465.3	Axl	SH2323h1	GAGATTCATACATCGGGACCTG CACACACGGACATGTTCTCA	65	6	50
XM_985544.1	C10orf71	SH2600d7	GGAAGGCCCGTGAAATCT GCTGTCATCACTGCCCATC	74	6	50
NM_28399.1	Ccnt2	SH2399g9	GCGGATGAAGAGCTGTCG GCAGTGTTTATTGTAAGCTGAGAGA	95	6	50
NM_001004357.2	Cntnap2	SH2401h6	GTGAAGGAGTACTTTTGCATGGT CCAAGCTGGTTGCTTCCTA	109	6	50
NM_031251.4	Ctns	SH2515f7	AGCCTGGGAAGCTGTCAGT GAGAAAAGGGTCAAATAAGCAG	76	6	50
NM_133969.2	Cyp4v2	SH2149g11	CGTTTTTGTACAAGTTCCTACAGC CCATTTGCTCCCCGTA CTT	68	6	50
NM_153065.3	Ddx27	SH2484g1	AGTTCTGCAGCATCACTACCTG AGAGCGGCTTCCTGAGACTT	67	6	50

NM_007834	Dscr3	SH2516g7	TCCCCAGACTGTTACCTGT AGGACCACCACATTGACCTC	76	6	50
NM_007891.4	E2f1	SH2329c12	TGCCAAGAAGTCCAAGAATCA CTTCAAGCCGCTTACCAATC	74	6	50
NM_010134.3	En2	SH2564d4	GACCGGCCTTCTTCAGGT CCTGTTGGTCTGAAACTCAGC	132	6	50
NM_025964.3	Fam119a	SH2137d6	AGGGCTGGTGGGCATAGT GCTACTTTCCGATCCGTGATA	66	6	50
NM_022721.3	Fzd5	SH2469f6	CAGCAGGATCCTCCGAGA CAGCACTCAGTCCACACCA	84	6	50
NM_001038655.4	Gng7	SH2286d7	GGAAGGGGGCTCAGACAG GGTCCAATAGAAAGGCTTCAC	93	6	50
NM_008916.2	Inpp5k	SH2488a3	GCTGTGGGAGAAAGATCAGC GTGACGGTCAAACCTGTAGGTG	109	6	50
NM_001164598.1	Irf2bp2	SH2422c11	GCCAACGGGTCTAAAGCAG GACTTCCCCTCCGGTTCT	72	6	50

NM_010716.2	Lig3	SH2489d6	CAGAAAGGCTCCACAGGAGA ATTCAAGTTGTAAACACTCTTGATGAC	96	6	50
NM_177664.5	Lppr4	SH2117b6	GCTGGACCTGCAATTACGAT GCTCCGTTTCTTCTTTTGGGA	74	6	50
NM_026272.3	Narf	SH2592c7	TGTGAAAGACATTGCTGTGGAT TCCATCATGACGCTGGAC	70	6	50
NM_001122952.1	Nfia	SH2355c2	CCAGAACTTGGTGGATGGA GAACCATGTGTAGGCGAAGG	83	6	50
NM_008713.4	Nos3	SH2387h7	CCAGTGCCCTGCTTCATC GCAGGGCAAGTTAGGATCAG	66	6	50
NM_145562.2	Parm1	SH2633c1	GTTTGGAGGTGCAGCATAACC TAGTCATGGTCGTCCAGCAG	69	6	50
NM_011058.2	Pdgfra	SH2334c4	GTCGTTGACCTGCAGTGGA CCAGCATGGTGATACCTTTGT	61	6	50
NM_021311.3	Piwil1	SH2028b11	GTGGCTGCAATGAATACATGCCCA AACCTGGCATTGACACGCTTCTTC	184	6	50

NM_011126.3	Plunc	SH2452e5	ATCCCAGGAAGGAAGGCTAT CAAGAGGCAGGAGACTGAGC	67	6	50
NM_011133.2	Pole2	SH2469e12	GGTGGCGCCAAATCGCGAAC CTCCTGAGCAGCAAGCCCCG	88	6	50
NM_008972.2	Ptma	SH2463d11	AGTGGATAACCAGCTCCGAGA TTCTCATTTTGAGCGTTCC	115	6	50
NM_011217.2	Ptprr	SH2470e9	TGTCTGCCCTTCTCCCTTC TCCAGCGTAAGAGATACATTGG	78	6	50
NM_011220.2	Pts	SH2418a1	TGAATTTGACCGACCTCAAAG CCAGGTCCAGGTTCTTG TG	75	6	50
NM_011279.2	Rnf7	SH2614c3	GAAGTGGAACGCGGTAGC ACATCGAAGGCAGGCATC	94	6	50
NM_011018.2	Sqstm1	SH2626e8	GAAGCTGCCCTATACCCACA TGGGAGAGGGACTCAATCAG	65	6	50
NM_145838.1	St8sia6	SH2141b10	TCCCCATTCGAGAGAACATT CACACTGGTTATAGGGATAGTCCA	75	6	50

NM_019666.2	Syncrip	SH2611b1	GGGGACCAAAGTAGCAGACTC TGTAGCCTGTTCTTTCCAAAAGT	77	6	50
NM_025935.2	Tbc1d7	SH2559c8	GGGAAGCTACCTCGAAGTCC GATGGCAAGAAAGACTTCATCC	63	6	50
NM_009906.5	Tpp1	SH2531h10	TCGGATCCTAGCTCTCCTCA GTCAGGGGTGATGGTTGAA	80	6	50
NM_153417.1	Trpm6	SH2552g6	GAGGAGGAATTCGCTGTCCG CCCTTCGATCCAGGATTCT	72	6	50
NM_145367.3	Txndc5	SH2394a10	CGACGTGTGCTCTGCCCAGG GGTGGTTCGCTTCCGGCTC	171	6	50
NM_027394.2	Ube2cbp	SH2090a9	GATGGTTTACATCTGCGCTTG AAGCTTTGATTAAACTGAAATCG	74	6	50
NM_139297.5	Ugp2	SH2182h1	CAGAGACCTCCAGAAGATTCG GTTCAACACAGAAGATATGTTATCAGG	84	6	50
NM_009474.5	Uox	SH2205g6	CGTGCAGAAGACCCTCTATGA GGCTGATTTCCATGTCCTTCTATCT	77	6	50

NM_013703.2	Vldlr	SH2563e2	GAGCCCCTGAAGGAATGC CCTATAACTAGGTCTTTGCAGATATGG	83	6	50
NM_177184.3	Vps13c	SH2444f5	AAGGAGTGTGCAGTTGCTCTT GTCGATGGATGCTGGAATCT	72	6	50
NM_001014981.1	Wdr7	SH2638c1	TCTGCCTCTCCTGCTTTACCT AGTGCATGGCGGCTAACT	70	6	50
NM_173761.3	Ythd1	SH2474b7	ATTATGAGAAGCGCCAGGAG TTGTTTCGATTCTGTCTTTCCTT	61	6	50
NM_008084.2	Gapdh		CACGGCAAATTCAACGGCACAGT TGGGGGCATCGGCAGAAGG	232	10	45

3. Results

3.1 Assay Development

Dozens of conditions and numerous cell lines have been tested for susceptibility to PrP^{res} or its mimic PrP¹⁰⁶⁻¹²⁶ peptide-induced neurotoxicity, with variable rates of success. Published literature reports background survival rates of 40-50% or more for neuroblastoma cells challenged with the PrP¹⁰⁶⁻¹²⁶ peptide (White et al. 2001; O'Donovan, Tobin, and Cotter 2001; Thellung et al. 2002; Corsaro et al. 2003; Dupiereux et al. 2005; Carimalo et al. 2005; Bergstrom et al. 2005; Ning et al. 2005a; Fioriti et al. 2005a; Fioriti et al. 2005b; Dupiereux et al. 2006; Ferreiro et al. 2006; Pan et al. 2010). This significant degree of induced neurotoxicity has greatly advanced the understanding of prion diseases at the molecular level, however, it is insufficient to permit screening of large scale libraries.

Currently, no cell culture model mimicking prion neurotoxicity has been published which outlines conditions sufficient to reduce the false positive rate to a level permissive for screening a large scale shRNA library. The lack of such an assay has prevented the identification of genes essential to prion-mediated neurotoxicity. For this thesis, a plethora of conditions were tested to minimize the background survival rate of human SK-N-FI neuroblastoma cells. SK-N-FI cells were chosen for their relatively stable chromosome complement (2N +/- 1), and their innate slow growing nature combined with the fact they invariably divide. Presented here are results showing that low passage number, low-confluency human SK-N-FI neuroblastoma cells exposed to multiple applications of PrP¹⁰⁶⁻¹²⁶ peptide in serum-reduced media display a background survival rate of <1.5%.

3.1.1 Culture Conditions to Minimize Background

It was desired to minimize the background survival rate of human neuroblastoma SK-N-FI cells, simultaneously balancing that necessity with identification of conditions that were not so toxic that cells were rapidly obliterated. The variables studied were peptide concentration and multiple exposures, plating density, and media serum concentration. In the experiments described below, the estimated viability of SK-N-FI cells exposed to the PrP¹⁰⁶⁻¹²⁶ peptide is relative to PrP^{Scram} peptide exposed cells under the same set of conditions.

3.1.1.1 Influence of Peptide Concentration and Exposures

Cell survival rates of $\geq 40\%$ have been reported when cells are plated at $>100,000$ cells/well of a 6-well plate and exposed to a single or multiple exposures of PrP¹⁰⁶⁻¹²⁶ peptide (Cronier, Laude, and Peyrin 2004; Bergstrom et al. 2005; Ning et al. 2005a; Fioriti et al. 2005a; Ferreira et al. 2006). Based on these results, a constant 100,000 SK-N-FI cells plated per well of a 6-well plate (9.4cm^2) and exposed to multiple replenishments of peptide diluted in SK-FS-DMEM10 growth media was selected for initial experimentation. The concentration of peptide was adjusted to 20, 40, 80, 160, or $320\mu\text{M}$ and replaced every 48 hours 1, 2, 3, or 4 times in total. SK-N-FI cells exposed to 4 applications of $40\mu\text{M}$ peptide demonstrated an estimated survival rate of 65% (Table 3.1). The peptide concentration was maintained at $40\mu\text{M}$ for further analysis, with variations in number of cells plated and serum concentrations.

Table 3.1: Peptide Concentration and Number of Applications Compared

The influence of PrP¹⁰⁶⁻¹²⁶ neurotoxic peptide concentration and number of applications on SK-N-FI cell susceptibility was examined. SK-N-FI were plated at a constant 100,000 cells/well in a 6-well plate. Peptide was resuspended to the appropriate concentration in SK-FS-DMEM10 growth media and freshly diluted peptide was replaced every 48 hours 1, 2, 3, or 4 times. Cell viability was subjectively determined for SK-N-FI cells exposed to PrP¹⁰⁶⁻¹²⁶ relative to PrP^{Scram} peptide on a light microscope 48 hours post peptide application. Repeated application of peptide concentrations $\geq 80\mu\text{M}$ resulted in generally unhealthy looking cells. A total of 4 applications of $40\mu\text{M}$ peptide was selected for further analysis (highlight in yellow).

		Peptide Concentration				
		20 μM	40 μM	80 μM	160 μM	320 μM
Number of Applications	1	100%	100%	95%	90%	80%
	2	95%	90%	70%	60%	50% ^a
	3	90%	75%	60% ^a	40% ^a	20% ^a
	4	80%	65%	50% ^a	15% ^a	<1% ^a

^aCells did not appear healthy when viewed on a light microscope.

3.1.1.2 Influence of Cell Plating Density and Serum Concentration

Using 4 exposures of 40 μ M freshly diluted peptide replaced every 48 hours, the number of SK-N-FI cells plated was varied from 0.2-1 X 10⁵ cells/well of a 6-well plate, in increments of 2 X 10⁴ cells/well. The concentration of either filter sterilized (FS) or heat inactivated (HI) fetal bovine serum (FBS) in the growth media in which peptide was resuspended was adjusted to 0.1%, 0.5%, 1%, 2%, 5%, or 10% (Figure 3.1). Cell viability was subjectively determined 48 hours post each peptide application. At a plating density of 40,000 SK-N-FI cells per well of a 6-well plate exposed to 4 applications of 40 μ M peptide diluted in DMEM + 1% HI-FBS +1X NEAA (SK-HI-DMEM1), cell viability was estimated to be <10%, but greater than 5% (Table 3.2).

3.1.2 Optimized Prion Neurotoxicity Assay Conditions

SK-N-FI cells plated at 40,000 cells/well of a 6-well plate and repeatedly exposed to peptide diluted in DMEM + 1% HI-FBS + 1X NEAA was selected for further fine tuning, with 4 or 5 exposures of 40 or 50 μ M peptide compared. SK-N-FI cell viability was objectively determined using AlamarBlue (Figure 3.2). Those exposed to 4 applications of 40 or 50 μ M peptide demonstrated a background survival rate of 9.42% or 3.11% relative to PrP^{Scram} exposed cultures, respectively. Those exposed to 5 applications of 40 or 50 μ M peptide demonstrated a background survival rate of 7.51% or 1.41% respectively. Due to significantly slower rates of SK-N-FI cell growth under these conditions, peptide was resuspended in 400 μ L of DMEM + 5% HI-FBS + 1X NEAA + 1% Ab/Am (SK-HI-DMEM5, representing 3.8% of the final volume) per milligram of peptide.

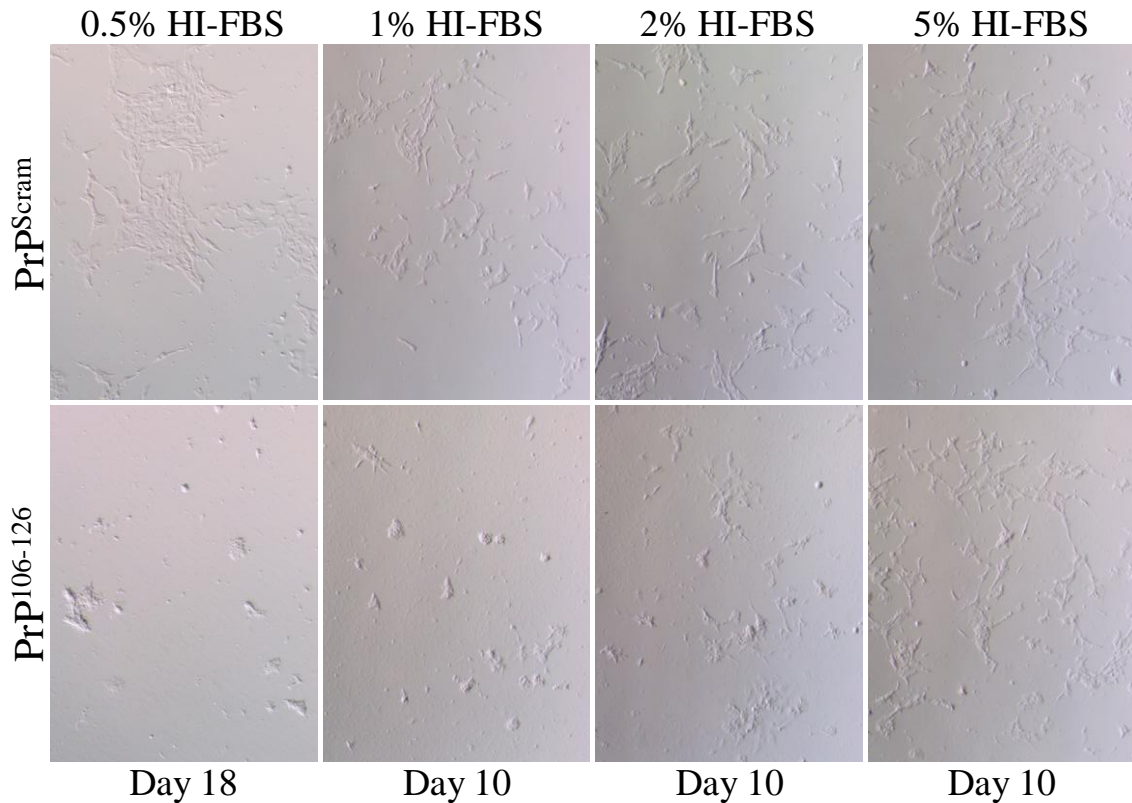


Figure 3.1: Effect of FBS Concentration on SK-N-FI Susceptibility to Peptide

Comparing the susceptibility of SK-N-FI cells challenged with PrP¹⁰⁶⁻¹²⁶ peptide resuspended in growth media supplemented with varying concentrations of HI-FBS. SK-N-FI cells plated at 100,000 cells/well in a 6-well plate were challenged with 4 applications of either PrP¹⁰⁶⁻¹²⁶ or PrP^{Scram} peptide resuspended to a final concentration of 40 μ M in DMEM + HI-FBS + 1% Ab/Am. To determine the appropriate concentration of FBS to supplement media with during selection for peptide resistant SK-N-FI cells, the final concentration was adjusted to 0.5%, 1%, 2%, or 5%. The peptide was resuspended in the respective media and applied to cells. Peptide was replaced every 2 days for a total of 4 applications. The day listed along the bottom indicated time post initial peptide application. Cells challenged with peptide in media containing 0.5% FBS required 8 extra days to re-populate such that cells were readily apparent.

Table 3.2: Cell Number and Serum Concentrations Compared to Cell Viability

The influence of cell confluency and serum concentration on SK-N-FI cells susceptibility to prion neurotoxicity was examined. SK-N-FI cells were exposed to 4 applications of 40µM peptide diluted in DMEM + 1X NEAA +1% Ab/Am + varying concentrations of filtered bovine serum (sterilized by filtration or heat inactivation). Cell viability was subjectively determined for SK-N-FI cells exposed to PrP¹⁰⁶⁻¹²⁶ relative to PrP^{Scram} peptide on a light microscope 48 hours post peptide application. A total of 40,000 SK-N-FI cells plated per well of a 6-well plate and exposed to multiple applications of peptide diluted in DMEM + 1X NEAA + 1% Ab/Am + 1% HI-FBS was selected for further refinement (highlighted in yellow).

		Cell Number				
		20,000 ^b	40,000	60,000	80,000	100,000
FS-FBS Concentration	0.1%	<1% ^a	<1% ^a	<1% ^a	<2% ^a	<2% ^a
	0.5%	<2% ^a	<5% ^a	<5% ^a	<10%	10%
	1%	<10%	10%	15%	20%	30%
	2%	15%	20%	30%	40%	45%
	5%	25%	35%	40%	50%	55%
	10%	40%	45%	55%	60%	65%
HI-FBS Concentration	0.1%	<1% ^a	<1% ^a	<1% ^a	<1% ^a	<1% ^a
	0.5%	<1% ^a	<2% ^a	<5% ^a	<5% ^a	5%
	1%	<5%	<10%	10%	15%	20%
	2%	15%	20%	20%	30%	35%
	5%	20%	30%	40%	45%	50%
	10%	30%	40%	45%	50%	55%

^aCells did not appear healthy when viewed on a light microscope.

^bToo few cells for accurate and consistent cell plating or viability measurement.

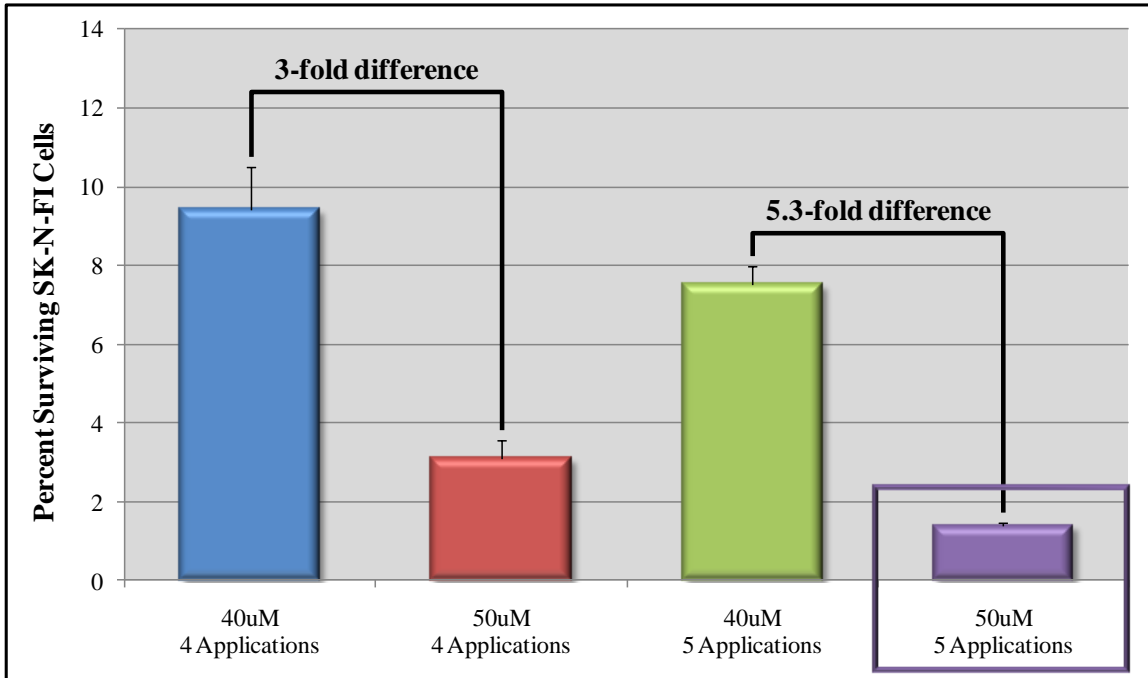


Figure 3.2: Fine Tuning of Peptide Application Conditions

The neurotoxicity associated with 4 or 5 applications of 40 μ M or 50 μ M PrP¹⁰⁶⁻¹²⁶ was compared. Peptide was resuspended in SK-HI-DMEM5 (representing 3.8% of the final volume) and adjusted to 40 μ M or 50 μ M in SK-HI-DMEM1. Resuspended peptide was applied to 40,000 SK-N-FI cells plated in 6-well tissue culture plates. Peptide was replenished every 48 hours, for a total of 4 or 5 applications, and surviving SK-N-FI cells were quantified using AlamarBlue. The conditions selected for further experimentation were 5 applications of 50 μ M peptide (1.41% \pm 0.04% survival) (purple bar and box). Error bars represent the standard deviation of the percent surviving cells in 6 independently treated wells.

It was determined that the optimal conditions representing the first cell culture model effectively mimicking acute prion neurotoxicity consisted of SK-N-FI cells plated at 40,000 cells/well of a 6-well plate in SK-HI-DMEM5. Twenty four hours later, media was replaced with 2mL SK-HI-DMEM1. Another 24 hours later, peptide was resuspended in 400 μ L SK-HI-DMEM5 and diluted to 50 μ M in 10.06mL SK-HI-DMEM1 per milligram. Of this peptide suspension, 2mL was added to each well. Peptide was replenished every 48 hours for a total of 5 applications (Figure 2.1). On day 22, AlamarBlue reagent was diluted 10-fold in SK-FS-DMEM10 growth media, and the percent reduction was measured at 5 hours, 24 hours, and 48 hours post AlamarBlue application. The relative cell number was calculated using previously generated standard curves as stated in the Materials and Methods section.

3.1.2.1 Validation of Optimized Prion Neurotoxicity Assay

To validate this model, a total of 5 independent tests were performed as per the procedure stated above. Cell viability was measured using AlamarBlue, and the results averaged. Each toxicity test consisted of 40,000 SK-N-FI cells per well of a 6-well plate challenged with 50 μ M freshly diluted PrP¹⁰⁶⁻¹²⁶ neurotoxic peptide or PrP^{Scram} peptide, which was replaced at 48 hour intervals for a total of 5 applications. All wells of a 6-well plate were used for each toxicity test. From 5 individual month long tests set up over the course of a year using SK-N-FI cells ranging in passage number from 6-9 (i.e. 5 “biological replicates” with 6 technical replicates each time), the average background survival rate of SK-N-FI cells challenged with PrP¹⁰⁶⁻¹²⁶ was calculated to be 1.46% relative to SK-N-FI challenged with PrP^{Scram} (Figure 3.3). This calculated background

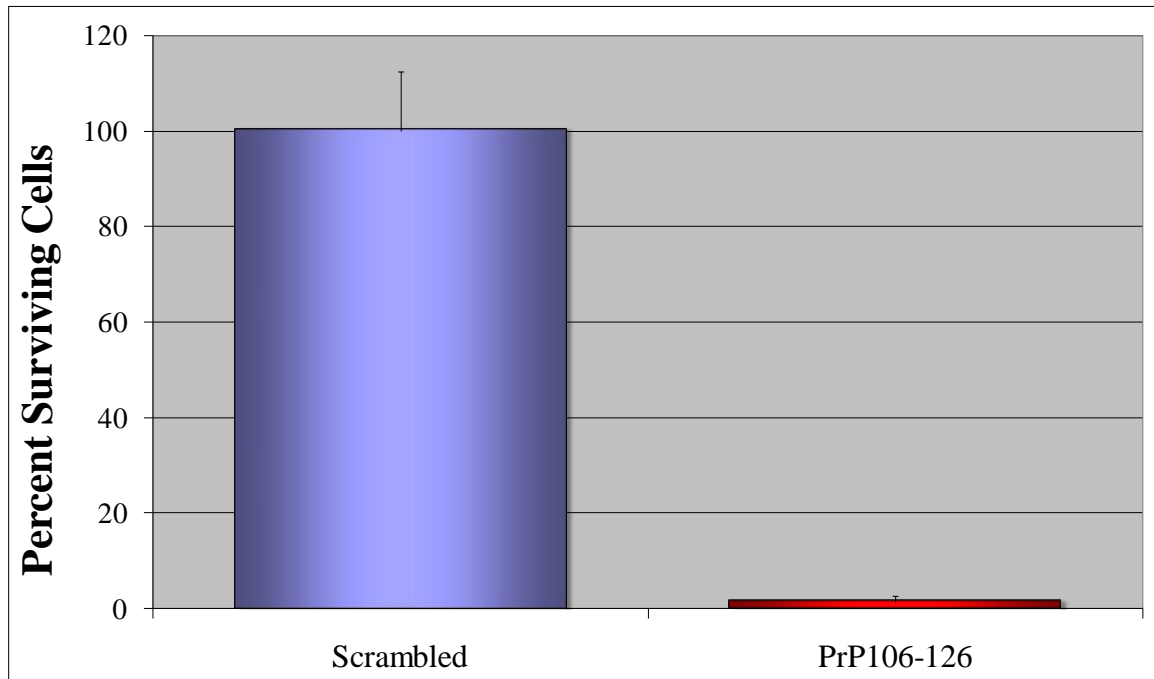


Figure 3.3: SK-N-FI Neurotoxicity Associated with 50 μ M PrP¹⁰⁶⁻¹²⁶ Challenge

Relative to application of the scrambled peptide, background survival of SK-N-FI cells challenged with 5 applications of 50 μ M PrP¹⁰⁶⁻¹²⁶ neurotoxic peptide was 1.46% as determined using AlamarBlue for 5 separate experiments. Using a Student's two-tail t-test assuming equal variance, the associated p-value was 5.38×10^{-22} , indicating a statistically significant difference in cell survival between scrambled and PrP¹⁰⁶⁻¹²⁶ treated SK-N-FI cells. This background survival rate is sufficiently low enough to permit screening of a shRNA^{mir} library while minimizing the false positive rate. Error bars represent the standard deviation of the calculated percent surviving cells.

survival rate is sufficiently low enough to permit screening of the human pSM2+shRNA^{mir} retroviral library.

3.1.3 Visualization of PrP¹⁰⁶⁻¹²⁶ Aggregation

Under the conditions listed in the Materials and Methods section, aggregates of PrP¹⁰⁶⁻¹²⁶ were clearly visible when diluted to 20 μ M or 50 μ M, and viewed at 4X magnification on a light microscope (representative images shown in Figure 3.4). Aggregates appeared as amorphous structures either suspended in the media or associated with SK-N-FI cells. Similar aggregates were not observed for equally diluted PrP^{Scram}. This demonstrates that under the conditions used for peptide challenge, PrP¹⁰⁶⁻¹²⁶ retains its aggregative properties.

3.2 Library Screen

3.2.1 Transfection Efficiency of GP2-293 and Retroviral Titre

Expression of the VSV-G protein causes cell membrane fusion, leading to syncytia formation (large, multinucleated cells) (Roberts, Kipperman, and Compans 1999). The characteristically large, multinucleated cells can be visualized by a number of techniques including light microscopy and addition of Trypan blue (a nuclear dye). These simple visualization strategies confirmed expression of functionally active VSV-G protein in transfected GP2-293 cells (Figure 3.5 A&B).

Alternatively, transfection efficiency can be estimated by using a similar sized vector that expresses a genetic marker which can be visualized directly, such as the

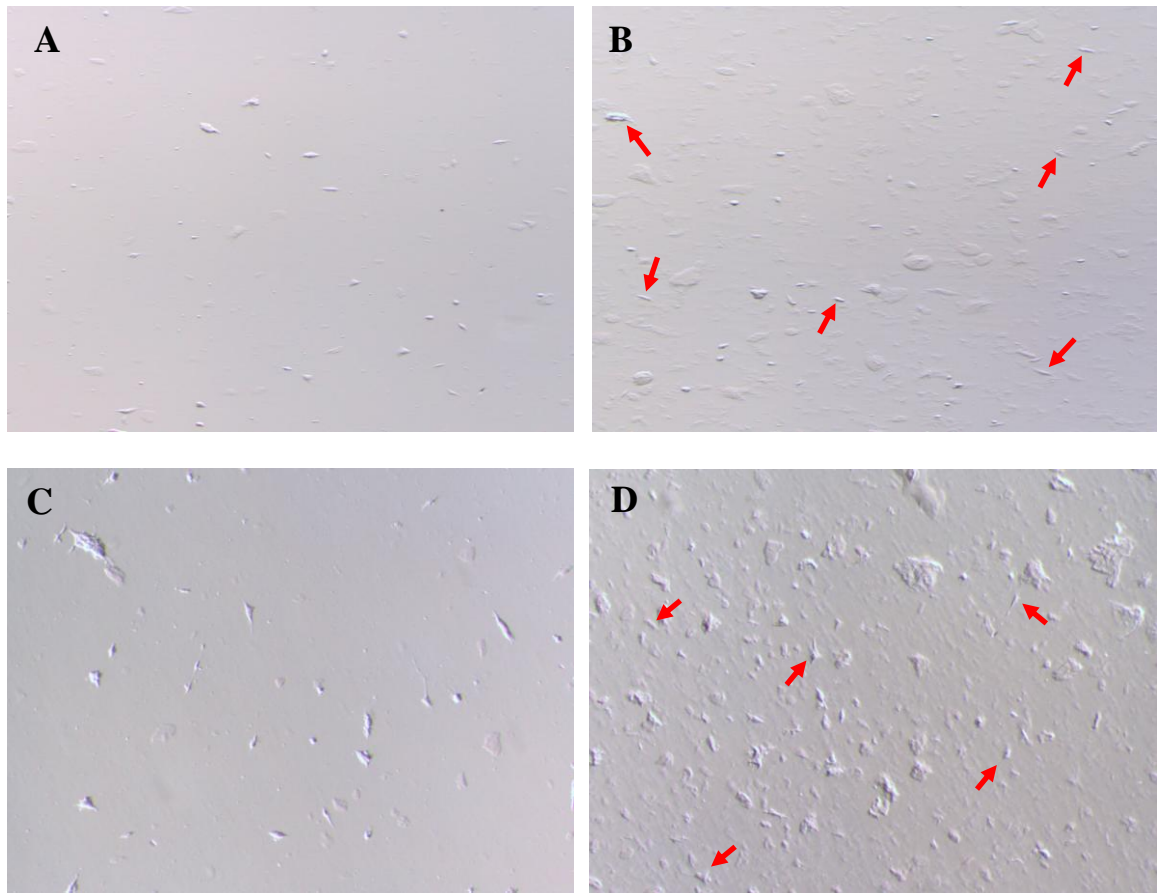


Figure 3.4: Visualization of PrP¹⁰⁶⁻¹²⁶ Peptide Aggregation

PrP¹⁰⁶⁻¹²⁶ peptide displays aggregative properties under physiological conditions. To confirm this, both PrP^{Scram} (Panel A, C) and PrP¹⁰⁶⁻¹²⁶ (Panel B, D) were diluted in DMEM + 5% HI-FBS + 1X NEAA + 1% Ab/Am (representing 3.8% of final volume) and DMEM + 1% HI-FBS + 1X NEAA (representing 96.2% of final volume) per milligram peptide (as outlined in the Materials and Methods section). Of this, 2mL was applied to 40,000 SK-N-FI cells 48 hours post plating. Panels A and B show peptide diluted to 20 μ M, while panels C and D show peptide diluted to 50 μ M. Red arrows in Panels B and D indicate SK-N-FI cells. PrP¹⁰⁶⁻¹²⁶ aggregates appear as amorphous aggregates suspended in the media or associated with cells. Minimal aggregates are visible in Panels A and C, which has been reported in the literature (Jobling et al. 1999).

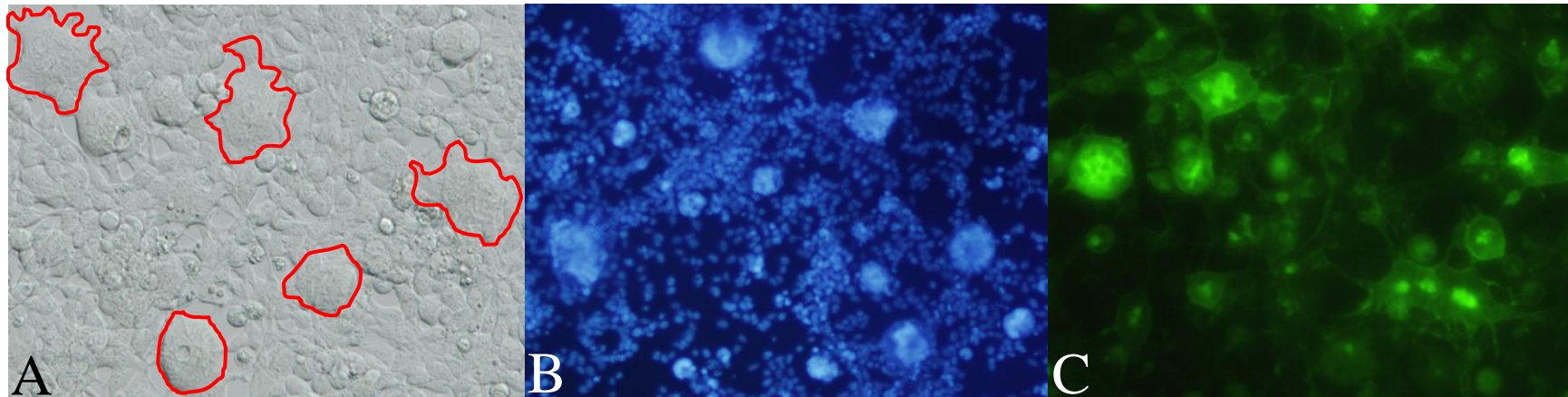


Figure 3.5: Monitoring efficiency of GP2-293 transduction

Efficient transfection of GP2-293 cells was confirmed by examining cells for syncytia formation and EGFP expression 48 hours post-transfection. A) Bright-field microscopy was used initially to confirm expression of functional VSV-G protein, which was readily apparent as seen from the large, multinucleated cells, examples of which are outlined in red. B) GP2-293 cells grown on collagen coated coverslips and transfected with pVSV-G and pSM2 + shRNA^{mir} library pool were stained with DAPI, a nuclear stain, and observed on a light microscope. The multinucleated cells were distinguishable by their large aggregates of nuclei stained blue. C) To visually estimate the efficiency of transfection, the retroviral vector pLNCX2 expressing EGFP was transfected into GP2-293 cells as per the shRNA^{mir} library pools protocol, and EGFP expression was examined on a fluorescent microscope. The estimated transfection efficiency was greater than 80%. Note that the magnification in panels A & B was 20X, and in panel C it was 40X.

enhanced green fluorescent protein (EGFP). Co-transfection of GP2-293 cells with pVSV-G and the retroviral vector pLNCX2 expressing EGFP as stated for the pSM2 + shRNA^{mir} library pools demonstrated a transfection efficiency of >80% (Figure 3.5 C).

When packaged retroviral particles were collected and titred on SK-N-FI cells, the calculated titre was ~15,000 transducing units per millilitre (TU/mL). Poor retroviral transduction efficiency of non-dividing or long doubling time cell lines, such as most neuron-derived cell types, has been previously reported (Miller, Adam, and Miller 1990). The multiplicity of infection (MOI) for the retroviral-based pSM2 + shRNA^{mir} library was 0.03. This low rate of transduction has the benefit of significantly minimizing the probability of multiple pSM2+shRNA^{mir} retrovectors transducing a single cell.

3.2.2 Overview of Identifying Protective pSM2+shRNA^{mir} Sequences

To screen the pSM2+shRNA^{mir} library and identify gene targets essential to PrP¹⁰⁶⁻¹²⁶ neurotoxicity, pools of 960 pSM2+shRNA^{mir} retrovectors were packaged into replication-deficient retroviral particles as described in the Materials and Methods section. Individual pools of 960 pSM2+shRNA^{mir} molecules were transduced onto SK-N-FI cells at an MOI of 0.03, challenged with 5 applications of 50µM PrP¹⁰⁶⁻¹²⁶, and stably integrated shRNA^{mir} were cloned and sequenced from surviving SK-N-FI cells (Figure 3.6).

Of the 73 pSM2+shRNA^{mir} pools (representing ~70,000 targets) in the library, 56 were screened (~54,000 targets), and 544 potentially protective shRNA^{mir} were identified. For results described below, 80 gene targets were considered to be of interest, and two (*abcb4* and *ube2cbp*) were selected for validation studies (Figure 3.7).

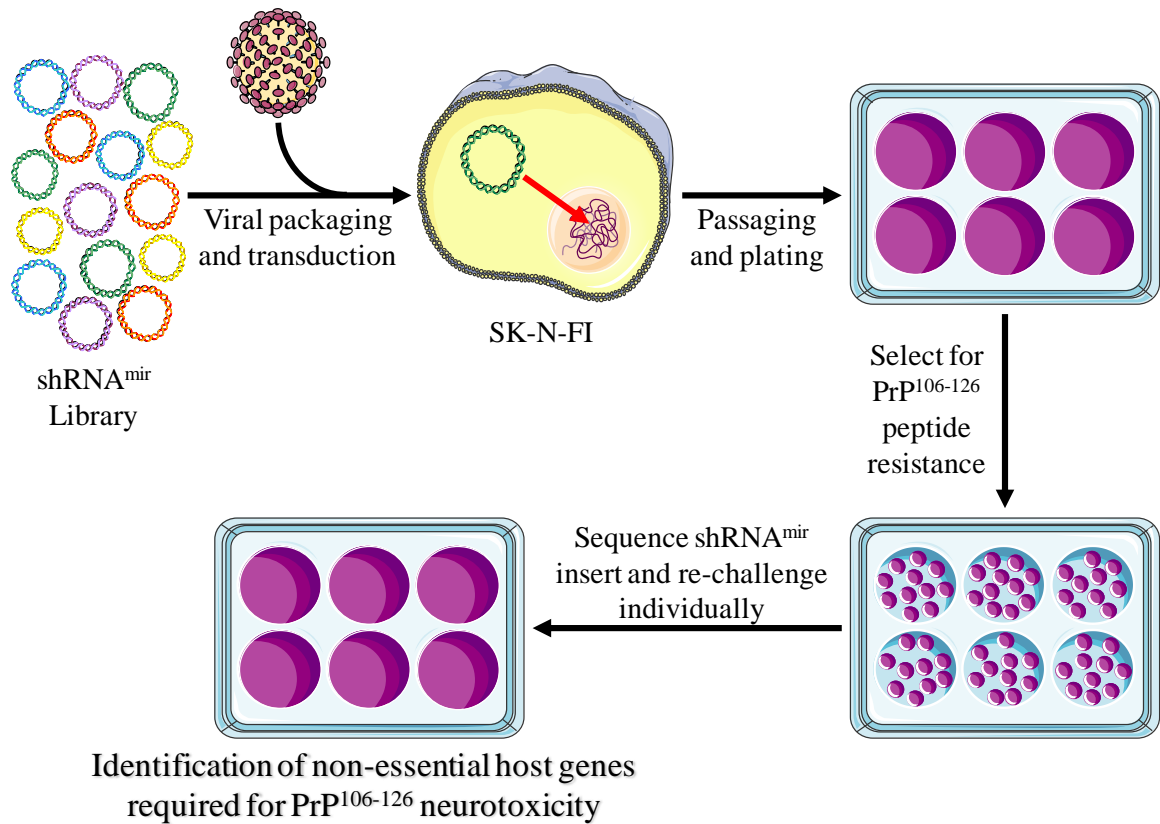


Figure 3.6: Strategy for Selecting PrP¹⁰⁶⁻¹²⁶ Resistant Clones

The shRNA^{mir} vectors are packaged into retro- or lentiviral particles by co-transfection of the appropriate host cell type using Effectene. Viral particles were titred on SK-N-FI cells and the appropriate volume of clarified viral supernatant was added to SK-N-FI neuroblastoma cells. Once SK-N-FI cells achieved ~80% confluency, they were passaged, strained, and plated into 6-well tissue culture treated dishes. Forty-eight hours post plating, cells were challenged with PrP¹⁰⁶⁻¹²⁶ neurotoxic or PrP^{Scram} control peptide for a total of 5 times, with fresh peptide added every 48 hours. Following the final challenge and media changes, gDNA was collected for shRNA^{mir} sequence analysis or cell viability was measured using AlamarBlue. The numbers of viable cells in PrP¹⁰⁶⁻¹²⁶ challenged wells were determined relative to the cell number in the respective scrambled peptide challenged wells.

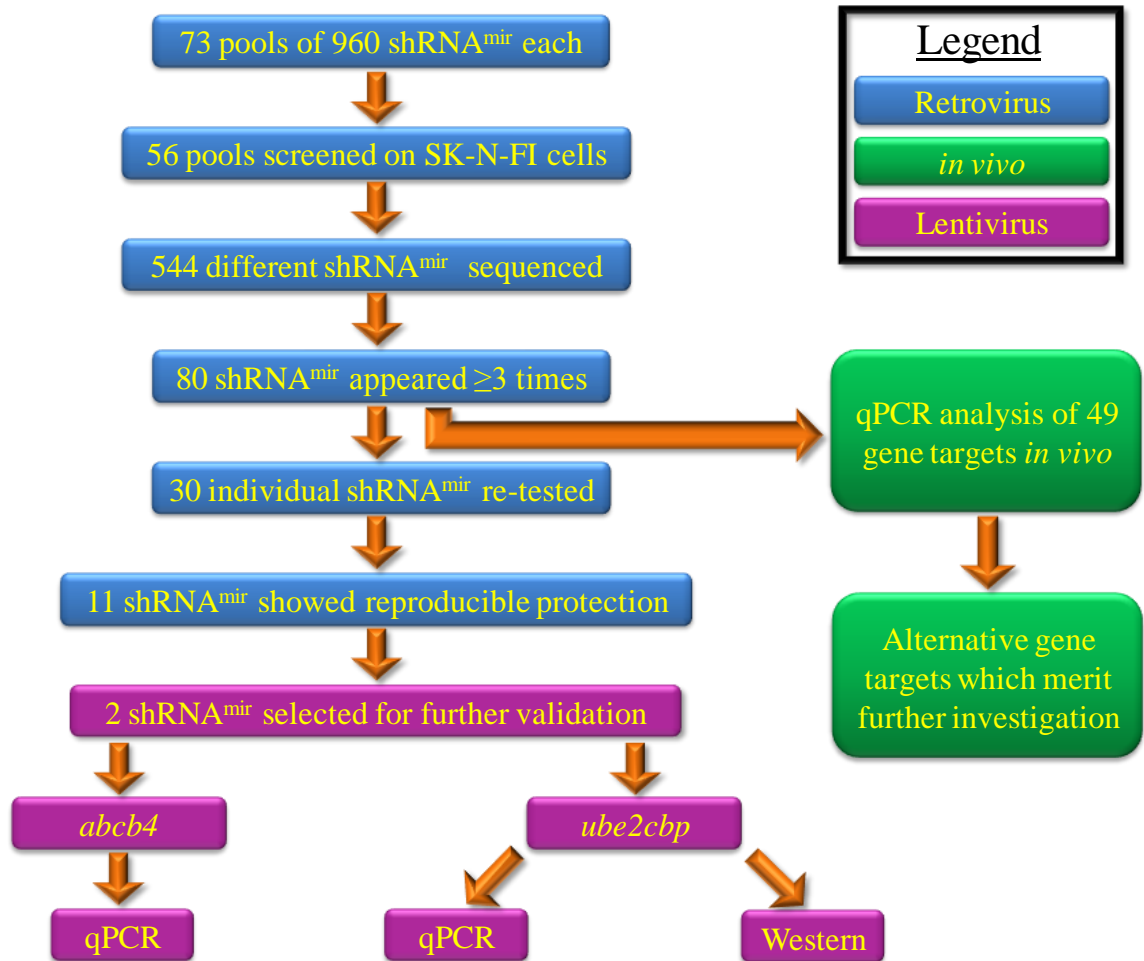


Figure 3.7: Flow Chart of Library Screening Steps and *in vitro* Validation

Overview of the completed library screening and validation of *abcb4* and *ube2cbp* *in vitro*. Initial library screening and individual re-testing was completed using SK-N-FI cells transduced at an MOI of 0.03 or 0.06, respectively, with retroviral particles (Blue) carrying pSM2+shRNA^{mir} constructs, and exposed to 5 applications of 50µM peptide. Further *in vitro* validation for gene knockdown protection was performed using lentiviral constructs (Purple) transduced into SK-N-FI cells at an MOI of 10, and exposed to 5 applications of 20µM peptide. qPCR analysis and, in the case of Ube2cbp, Western blotting was used to validate *abcb4* and *ube2cbp* knockdown mediated by pGIPZ+shRNA^{mir}.

3.2.3 Stably Integrated shRNA^{mir} Sequences from PrP¹⁰⁶⁻¹²⁶ Resistant SK-N-FI

SK-N-FI cells transduced with the pSM2+shRNA^{mir} retroviral library and surviving challenge with the PrP¹⁰⁶⁻¹²⁶ neurotoxic peptide were harvested from cell culture wells. Each well had multiple surviving colonies, each which expressed a shRNA^{mir} potentially targeting a gene involved in prion neurotoxicity. To enable identification of these protective shRNA^{mir} sequences from each library pool, isolated genomic DNA was amplified using primers targeting the common library arm sequences encompassing the shRNA^{mir} to create a pool of amplicons of interest. To ensure single, full-length amplicons were cloned for sequencing, all shRNA^{mir} amplicons were run on a 2% agarose gel, cut out, and purified. A typical gel is shown in Figure 3.8. Amplicons were cloned and transformation of TOP10 *E. coli* led to hundreds of colonies per 100mm agar plate. Each plate represented 1 pool consisting of ~960 different pSM2+shRNA^{mir}, from which 24 random colonies were picked for sequencing by the Genomics DNA Core Facility at the NML.

The sequences were aligned based upon the shRNA^{mir} pool from which they were derived, and then by sequence of the recognition arms. The sequences were compared to those of the OpenBiosystems pSM2+shRNA^{mir} human library database, as well as to the NCBI BLAST database, for identification and confirmation of gene target. All shRNA^{mir} sequences were recorded and tabularized, but only those that appeared 3 or more times were considered to be of interest, resulting in 80 gene targets of interest (Table 3.3). Of these 80 gene targets, 57 were confirmed to target transcripts within the NCBI GenBank database, and grouped according to their functional classification (Figure 3.9). Overall,

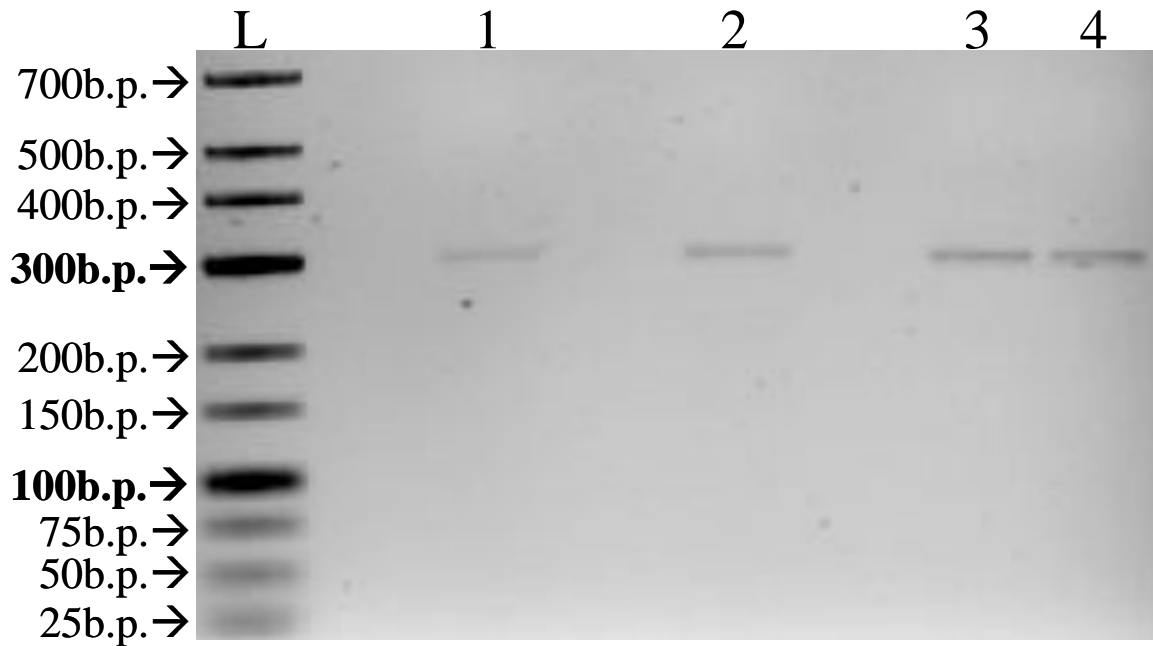


Figure 3.8: Representative gel image of shRNA^{mir} amplicons

Shown here are typical shRNA^{mir} amplicons as amplified from SK-N-FI extracted gDNA and run on a 2% agarose gel. L = Low Range DNA Ladder from Fermentas, Lane 1 = pool 28, Lane 2 = pool 29, Lane 3 = pool 30, and Lane 4 = pool 31. All lanes show individual bands of approximately 300b.p. The amplicons were cut out of the gel, purified, and ligated into the pCR2.1 Cloning Vector (Invitrogen). Ligated vectors were transformed into TOP10 *E. coli* by electroporation, grown on selective media, and 24 random colonies from each plate were selected. Vectors were extracted from bacterial cultures and sent for sequencing. Those shRNA^{mir} sequences appearing 3 or more times were considered significant and further analyzed.

Table 3.3: Identification of shRNA^{mir} gene targets from surviving SK-N-FI cells

Listed below are the 80 sequences of shRNA^{mir} conferring resistance upon SK-N-FI cells challenged with PrP¹⁰⁶⁻¹²⁶ peptide. The number of times a given shRNA^{mir} was identified is listed, along with the OpenBiosystems shRNA^{mir} library plate position, the identifier number, the GenBank accession number for the targeted human gene, and the gene name.

Sequence of Recognition Arm	Times Observed	Plate Position	shRNA ^{mir} Identifier	GenBank Accession Number	Identification of shRNA ^{mir} Gene Target
CGCTCTGGAGTGCCTATTTATT	3	SH2418a1	v2HS_92336	NM_000317.2	6-pyruvoyltetrahydropterin synthase (PTS)
AGCTGGCTTCTTGTAAGTGTAT	4	SH2298b2	v2HS_59455	NM_001005279.1	77b.p. 5' of Olfactory Receptor, Family 6, Subfamily K, Member 2 (OR6K2)
AGCTCAGTTACATTCCTTGAAT	5	SH2559a11	v2HS_118053	NM_032169.4	Acyl-Coenzyme A Dehydrogenase Family, Member 11 (ACAD11)
CGGAGGTTCTATTTCAATTTAAA	4	SH2524a1	v2HS_132686	NM_001659.2	ADP-ribosylation factor 3 (ARF3)
AAGCATCACTGTCTACTCAGAA	3	SH2360g5	v2HS_51133	NM_152522.4	ADP-ribosylation-like factor 6 interacting protein 6 (ARL6IP6)
AGCCAATACTGTGACTTCCAAA	3	SH2276e9	v2HS_46351	NM_198576.2	Agrin (AGRN)
ATGCTTTGAATGGAATCCATAT	3	SH2605g8	v2HS_213085	NM_182603.2	Ankyrin repeat domain 42 (ANKRD42)
CCCAGACAGCATCAAAGGGAAT	4	SH2422h1	v2HS_230814	NM_000443.3 NM_018849.2 NM_018850.2	ATP-binding cassette, sub-family B (MDR/TAP), member 4 (ABCB4)
CTCCAAGATTCTAGATGATTTA	3	SH2323h1	v2HS_201787	NM_021913.3 NM_001699.4	AXL receptor tyrosine kinase (AXL)

ACGCTTTAATCAAGTTCCTATT	5	SH2481h12	v2HS_177134	NR_026887.1	CCAAT/enhancer binding protein (C/EBP), alpha (CEBPA) in library Does not match mRNA target
AGCACATGCTGTTTACGATTAA	3	SH2600d7	v2HS_249936	NM_001135196.1	Chromosome 10 Open Reading Frame 71 (C10ORF71)
CCCATGAGGAAGTATAAATTAA	4	SH2613g3	v2HS_253787	NR_026866.1	Chromosome 3 open reading frame 49 (C3ORF49)
CACCCTTTAGTAAAGACATTAA	3	SH2349f9	v2HS_205313	NR_026784.1	Chromosome 6 Open Reading Frame 164 (C6ORF164), non-coding RNA
CGCATAGCAATTGGTCATTATT	4	SH2460f7	v2HS_180404	NM_001169154.1 NM_173494.1	Chromosome X Open Reading Frame 41 (CXORF41), not in Mouse
CGGAAGCAAAGTTCAAGCGATA	6	SH2483f7	v2HS_220510	NM_017812.2	Coiled-Coil-Helix-Coiled-Coil-Helix Domain Containing 3 (CHCHD3)
CGGTTATACTTGAAACCATAAT	3	SH2399g9	v2HS_226051	NM_001241.2 NM_058241.1	Cyclin T2 (CCNT2)
AGCAGTCACGCTGGTCAAGTAT	6	SH2515f7	v2HS_62136	NM_004937.2 NM_001031681.2	Cystinosis, nephropathic (CTNS)
AGGCCAATGAAATGAACGCCAA	6	SH2149g11	v2HS_120367	NM_207352.3	Cytochrome P450, Family 4, Subfamily V, Polypeptide 2 (CYP4V2)
ACCTAATACCATCAAACATTAT	3	SH2484g1	v2HS_174369	NM_017895.7	DEAD (Asp-Glu-Ala-Asp) box polypeptide 27 (DDX27)
ACCTGATTTAGGCACTGCTTTA	5	SH2516g7	v2HS_70981	NM_006052.1	Down syndrome critical region gene 3 (DSCR3)
AGGTGATTTATTTATTGGGAAA	3	SH2329c12	v2HS_43498	NM_005225.2	E2F transcription factor 1 (E2F1)
AGCGCTAAACAATGCAATAATT	3	SH2564d4	v2HS_226681	NM_001427.3	Engrailed homeobox 2 (EN2)
CCCTGATACTTGGTGCTGATAT	3	SH2137d6	v2HS_18784	NM_145280.4 NM_001127395.1	Family With Sequence Similarity 119, Member A (FAM119A)
ACCAGCTCACGTGTATTCTATT	6	SH2469f6	v2HS_172398	NM_003468.3	Frizzled Homolog 5 (Drosophila) (FZD5)

CGCTGTTACCATTACACAATAAA	5	SH2377f6	v2HS_114282	NM_002091.3 NM_001012513.1 NM_001012512.1	Gastrin Releasing Peptide (GRP)
CGGACAAGAAACCTTGTATTAT	3	SH2286d7	v2HS_49493	NM_0052847.2	Guanine Nucleotide Binding Protein (G protein), Gamma 7 (GNG7)
ACGCAAGCCTGTGTATGAAGAA	4	SH2488a3	v2HS_134877	NM_016532.3 NM_130776.2 NM_001135642.1	Inositol Polyphosphate-5-phosphatase K (INPP5K)
AGCCCTTCGAGAGCAAGTTTAA	5	SH2422c11	v2HS_232930	NM_182972.2 NM_001077397.1	Interferon regulatory factor 2 binding protein 2 (IRF2BP2)
CGCGTTCTTTCTGGCATTGGAA	3	SH2183b9	v2HS_81862	XM_304002	Intestinal N-acetylglucosamine-6-O-sulfotransferase (CHST5) and Corneal N-acetylglucosamine-6-O-sulfotransferase (CHST6) Does not match mRNA target
AGGCCAAACTTCTCCAATCTAA	3	SH2293d10	v2HS_57424	AB067525.2 NG_016137.1	KIAA1938/Synaptic Ras GTPase Activating Protein 1 Homolog (rat) (SYNGAP1) Does not match mRNA target
CCCGGATCATGTTCTCAGAAAT	9	SH2489d6	v2HS_202321	NM_013975.3 NM_002311.4	Ligase III, DNA, ATP-dependent (LIG3)
CCCTCACCCAGTGGAAGAATAA	4	SH2117b6	v2HS_23842	NM_014839.4	Lipid phosphate phosphatase-related protein type-4 (LPPR4)
CGCACACTCAGTGAAATAATTA	3	SH2592a8	v2HS_243536	NM_033281.5	Mitochondrial ribosomal protein (MRPS36)
AGCTGCAAGGATTCAGCATTAT	4	SH2387h7	v2HS_111653	NM_000603.4	Nitric oxide synthase 3 (endothelial cell) (NOS3)
ATCTCCTGGGAACATTCTAGAA	6	SH2361d5	v2HS_84717	XM_290759	No Messenger Targets In NCBI Database
CGCCATAACTCTAGAAATGGAG	5	SH2431e6	v2HS_237292	XM_293324	No Messenger Targets In NCBI Database

ACAGCATTCTGACAACATATAA	8	SH2593b12	v2HS_31304	XM_295410	No Messenger Targets In NCBI Database
CCGTAACCTTCTGAGTGTTAAT	3	SH2121d4	v2HS_26228	XM_295513	No Messenger Targets In NCBI Database
ACAGAGCTGTGTGCTCTCGTTA	3	SH2125f4	v2HS_26195	XM_295517	No Messenger Targets In NCBI Database
CCCACGGATGTTCTGATAAAT	3	SH2289g2	v2HS_51225	XM_295768	No Messenger Targets In NCBI Database
AACGTTACAGCCACATGGAAA	3	SH2126f12	v2HS_39490	XM_295929	No Messenger Targets In NCBI Database
AACGTTCACTGTCATTGTGTAT	3	SH2276c4	v2HS_52327	XM_296375	No Messenger Targets In NCBI Database
CGGCAATACTCCATAAAGCTA	3	SH2588g7	v2HS_243616	XM_296524	No Messenger Targets In NCBI Database
AAGGCTTTCTGGTATTCTAAAT	4	SH2592d5	v2HS_34162	XM_296653	No Messenger Targets In NCBI Database
AACATCTATGATGAAAGCTCTT	3	SH2516h9	v2HS_53517	XM_296958	No Messenger Targets In NCBI Database
CGGAAAGAAGCAGATGCTCTAA	3	SH2635a8	v2HS_259242	XM_298506	No Messenger Targets In NCBI Database
CGGAATATTTGTGTATAAACTT	4	SH2397e7	v2HS_226977	XM_299718	No Messenger Targets In NCBI Database
CCCAGAAATATCGAGAGAGGAA	3	SH2455h11	v2HS_187265	XM_300109	No Messenger Targets In NCBI Database
CGGGCTCCAAGCTGTTAAATAT	4	SH2446a3	v2HS_232597	XM_303640	No Messenger Targets In NCBI Database
ATGCCAAGAAGTATTAGACTAA	3	SH2396a3	v2HS_228050	XM_304488 Does Not Align With HTR3A	No Messenger Targets In NCBI Database
AGCATTTATGCATATTTGCCAA	10	SH2393h2	v2HS_128557	XM_305025	Not In NCBI Database, Interferon- induced protein with tetratricopeptide repeats 1 (IFIT1) in library
AAGAACTTGTGCCGTTGTGAAT	4	SH2437h11	v2HS_147734	XM_305315	No Messenger Targets In NCBI Database
ATGATCTGTTCTACATATTTAAA	4	SH2179a2	v2HS_84703	XM_373858 Hypothetical LOC388667	No Messenger Targets In NCBI Database
AGCACTTGCCTTTAAACTATGT	5	SH2355c2	v2HS_216840	NM_001145511.1 NM_001145512.1 NM_005595.4 NM_001134673.3	Nuclear Factor I/A (NFIA)

AGGCTCTTTGGTGAAGGATTAT	4	SH2592c7	v2HS_246092	NM_012336.3 NM_001083608.1 NM_001038618.2 NM_031968.2	Nuclear prelamin A recognition factor (NARF)
AGCTCATATATTATAGGCTCAA	4	SH2377f12	v2HS_120828	NG_004212.3	Olfactory Receptor, Family 5, Subfamily AK, Member 3 Pseudogene on Chromosome 11, (OR5AK3P)
ACCTCACAGGGATCTTGAATAA	4	SH2452e5	v2HS_135116	NM_130852.2 NM_016583.3	Palate, Lung and Nasal Epithelium Associated (PLUNC)
CGGACAAATACGATGCTATTAA	4	SH2028b11	v2HS_202153	NM_004764.4 NM_001190971.1	Piwi-Like 1 (Drosophila) (PIWIL1)
CGGCATCACAATGCTGGAAGAA	3	SH2334c4	v2HS_58980	NM_006206.4	Platelet-derived growth factor receptor, alpha polypeptide (PDGFRA)
CCCTAATAGGCAGTTCCGTAAT	4	SH2287d11	v2HS_41734	NM_138295.2	Polycystic Kidney Disease 1 Like 1 (PKD1L1)
CGGGCATACTATGGAAATATTA	3	SH2469e12	v2HS_170217	NM_002692.2	Polymerase (DNA directed), epsilon 2 (p59 subunit) (POLE2)
CGGAAATTACATTAAGTATTAA	3	SH2633c1	v2HS_257070	NM_015393.3	Prostate Androgen-Regulated Mucin-Like Protein 1 (PARM1)
ACGGTATTCATTTATAAGCATT	3	SH2470e9	v2HS_222349	NM_002849.2	Protein tyrosine phosphatase, receptor type, R (PTPRR)
CGGTTTGTATGAGATGGTAAA	3	SH2463d11	v2HS_169446	NM_001099285.1 NM_002823.4	Prothymosin, alpha (PTMA)
ACCAGTGAACAGGGTAAATAAA	5	SH2614c3	v2HS_251415	NM_014245.3 NM_183237.1	Ring finger protein 7 (RNF7)
ACGAATCTACATTAAGAGAAA	7	SH2626e8	v2HS_47987	NM_003900.4 NM_001142298.1 NM_001142299.1	Sequestosome 1 (SQSTM1)
CCGGGTACCTCTTTCAAAGTAT	3	SH2141b10	v2HS_104617	NM_001004470.1	ST8 Alpha-N-Acetyl-Neuraminidase Alpha-2,8-Sialyltransferase 6 (ST8SIA6)

CGGGCTCTATTCCTAAGAGTAA	3	SH2611b1	v2HS_214749	NM_006372.3	Synaptotagmin binding, cytoplasmic RNA interacting protein (SYNCRIP)
ACCAGATGATGAAGTGTTTCTT	3	SH2559c8	v2HS_116090	NM_016495.3 NM_001143966.1 NM_001143965.1 NM_001143964.1	TBC1 domain family, member 7 (TBC1D7)
CCGGAATATCTGCAGCAAGTAT	3	SH2394a10	v2HS_227893	NM_030810.2 NM_001145549.1	Thioredoxin domain containing 5 (endoplasmic reticulum) (TXNDC5)
CGCCAAGTCTGCCAGAATTTAA	5	SH2552g6	v2HS_155076	NM_017662.4	Transient receptor potential cation channel, subfamily M, member 6 (TRPM6)
CGGAACCTTTCCTCATCACAAA	3	SH2531h10	v2HS_92761	NM_000391.3	Tripeptidyl peptidase I (TPP1)
CGCTGCTGTTGATATTGTCAAAA	4	SH2090a9	v2HS_139486	NM_198920.1	Ubiquitin-conjugating enzyme E2C binding protein (UBE2CBP)
CCCACAGCATCATCACATGAAT	3	SH2182h1	v2HS_84686	NM_001001521.1 NM_006759.3	UDP-glucose pyrophosphorylase 2 (UGP2)
CGCTCAAGTCTACATGGAAGAA	3	SH2205g6	v2HS_180941	XM_088849 NR_003927.1	Urate Oxidase, pseudogene (UOX), non-coding RNA in humans, functional in mice
CGGTGCCTGTTGTGGAAATTTAA	6	SH2444f5	v2HS_139564	NM_017684.3 NM_001018088.1 NM_018080.2 NM_020821.1	Vacuolar Protein Sorting 13 Homolog C (<i>S. cerevisiae</i>) (VPS13C)
GGAATTACACTTGACCTTATA	3	SH2563e2	v2HS_218476	NM_003383.3 NM_001018056.1	Very Low Density Lipoprotein Receptor (VLDLR)
CGCCATTGACCCTATTAGAATA	3	SH2638c1	v2HS_257675	NM_015285.2 NM_052834.2	WD repeat domain 7 (WDR7)
AGCAGAAATTGTGTTCTTAAAT	3	SH2474b7	v2HS_173850	NM_017798.3	YTH domain family, member 1 (YTHDF1)

CGCCAATATGGTCTTGTA ACTT	3	SH2398f11	v2HS_121787	XM_209557 BC084565.1	Zinc finger protein 717 (ZNF717)
-------------------------	---	-----------	-------------	-------------------------	----------------------------------

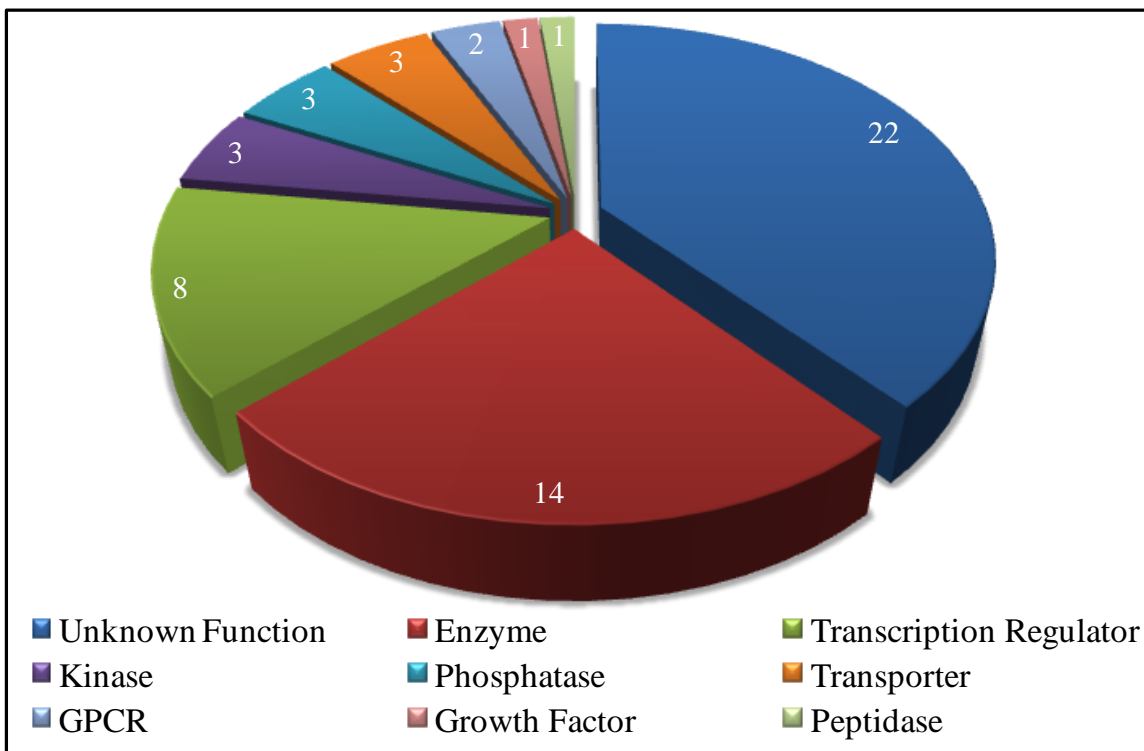


Figure 3.9: Associated Function of Library Identified Gene Targets

The associated overall function of 57 gene targets identified from the library screen. Of the 80 pSM2+shRNA^{mir} sequences identified from the library screen, 57 targeted confirmed transcripts as listed in the NCBI GenBank database. The pie chart above shows the overall classification of protein function associated with the identified gene targets, as denoted within the Ingenuity Pathway Analysis (IPA) program database. The largest group encoded proteins with an unknown function, followed by the broad grouping of enzyme function, and then transcription regulation (22, 14, and 8, respectively). The number of encoded proteins within a given functional classification is shown on the associated pie slice.

the majority of candidate genes identified had a currently unrecognized function, with the top three functions being enzyme, transcription regulator, and kinase. This highlights the variability of functions associated with proteins potentially mediating prion neurotoxicity, alluding to a complex signalling pathway underlying the observed neurotoxicity.

3.2.4 Predicted Association of pSM2+shRNA^{mir} Library Identified Positives

The 57 gene targets of interest identified and confirmed to encode validated transcripts were analyzed using the Ingenuity Pathway Analysis (IPA) program to identify common pathways and protein-protein associations. The IPA database included protein network association and subcellular localization information for 46. The gene target encoded proteins were analyzed in various ways to assess their potential interactome, and identify common proteins upstream of those identified from the library screen. Analyses included all 46 proteins recognized within the IPA database and limited the total number of proteins to 140 per network. Analyses of both direct and indirect protein associations or only direct associations were performed.

3.2.4.1 Analysis of Direct and Indirect Associations between Library Identified Proteins of Interest

The initial analysis, which included both direct and indirect associations between library identified gene targets, generated a network consisting of 45 of the 46 identified gene encoded proteins. The network associated p-value was 1×10^{-102} indicating that the probability of these gene targets associating into the predicted network by random chance is highly unlikely. The predicted network consisted of two central mediators, NF κ B and

β -estradiol, as well as three regulatory miRNA (miR-195, miR-202, and miR-let7e) (see Figure 3.11 and Discussion section 4.2.3.1).

3.2.4.2 Analysis of Direct Associations between Library Identified Proteins of Interest

A more stringent analysis maintained the maximum number of proteins per network at 140, but limited the protein associations to direct interactions only. The prominent network generated under these conditions included 40 of the 46 proteins, with an associated p-value of 1×10^{-87} (Figure 3.12). The highly statistically significant p-value associated with this network emphasizes that their association is not by random chance. Interestingly, this association network identified the Huntington protein (Htt) as directly interacting with 5 and indirectly through 1 intermediate with 11 of the 40 library identified gene encoded proteins. This suggests that there may be underlying neurotoxic pathways common to these proteinaceous neurodegenerative disorders.

This network association analysis also identified 3 miRNA sequences (miR-let7E, miR-195, and miR-202) as mediating the expression of 2, 2, or 3 identified gene targets, respectively. The biological diseases and disorders category associated with the 46 library identified gene target encoded proteins, in which at least 3 of the identified proteins are known to play a role, are listed in Table 3.4.

3.2.5 Verification of Pooled Library Identified Gene Targets *in vivo*

One method of verifying the relevance of gene targets identified from a library screen of pooled shRNA^{mir} to disease is to look at the relative expression levels of the

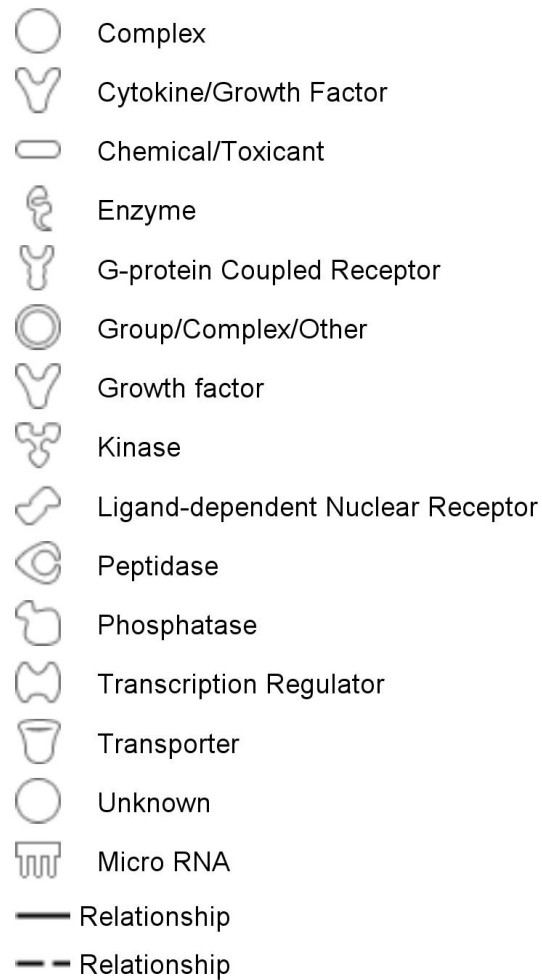


Figure 3.10: Legend of Associated Protein Function for IPA Generated Networks

The legend corresponds to IPA generated predicted network association analyses, where the various shapes are representative of a particular protein function, and line patterning is indicative of the inter-protein association.

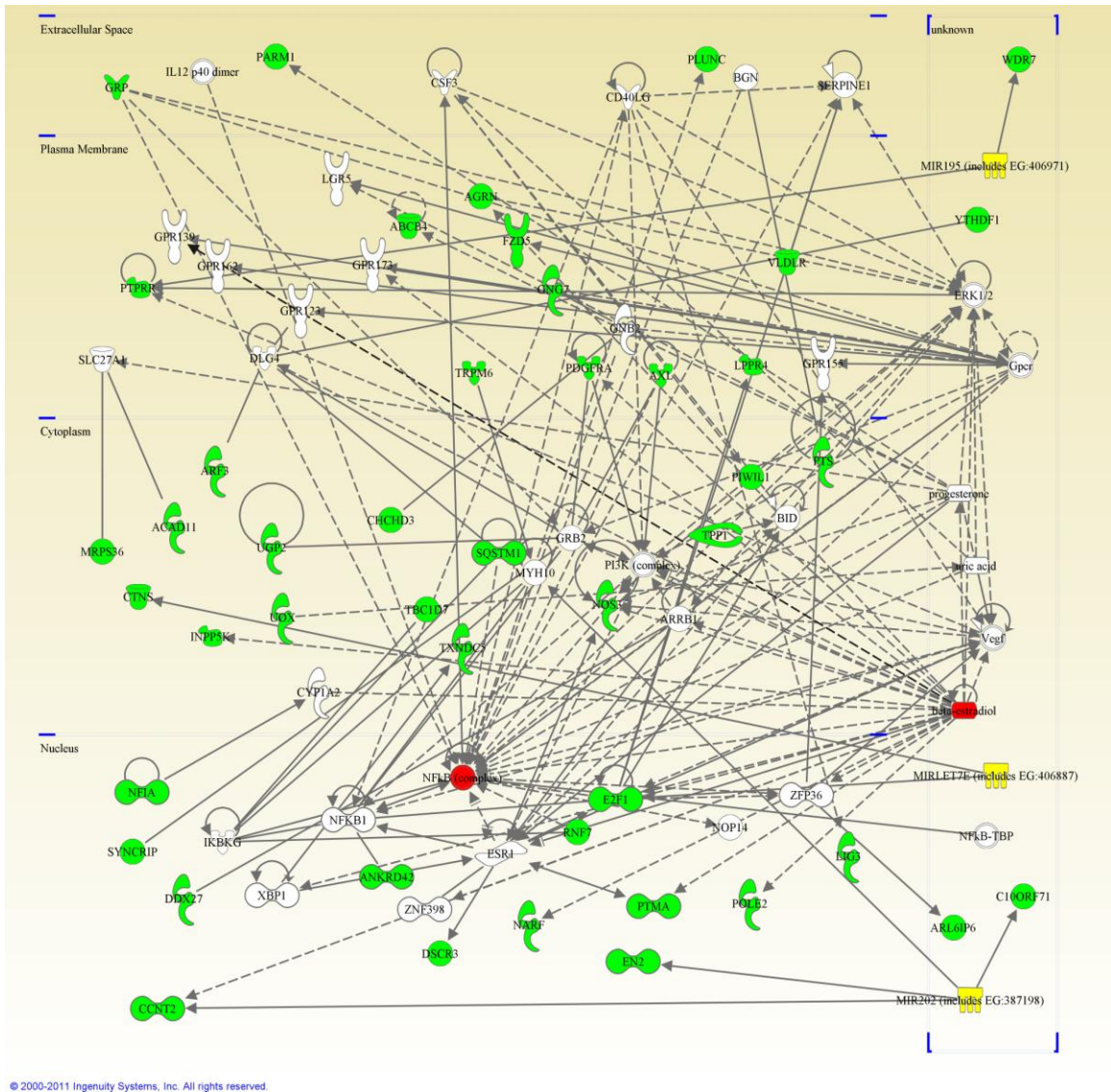


Figure 3.11: Direct and Indirect Network Associations between Library Positives

Analysis of the 46 library identified gene target encoded proteins for which the IPA database contains information associate in the represented manner. Allowing for a maximum of 140 molecules per network, and including both direct and indirect associations, 45 of the 46 encoded proteins associate into 1 network, with a $p\text{-value} = 1 \times 10^{-102}$. Both NF κ B and β -estradiol (highlighted in red) can be seen to act as central players in the association network predicted by the IPA software, which have previously been implicated in prion disease. See Figure 3.10 for legend.

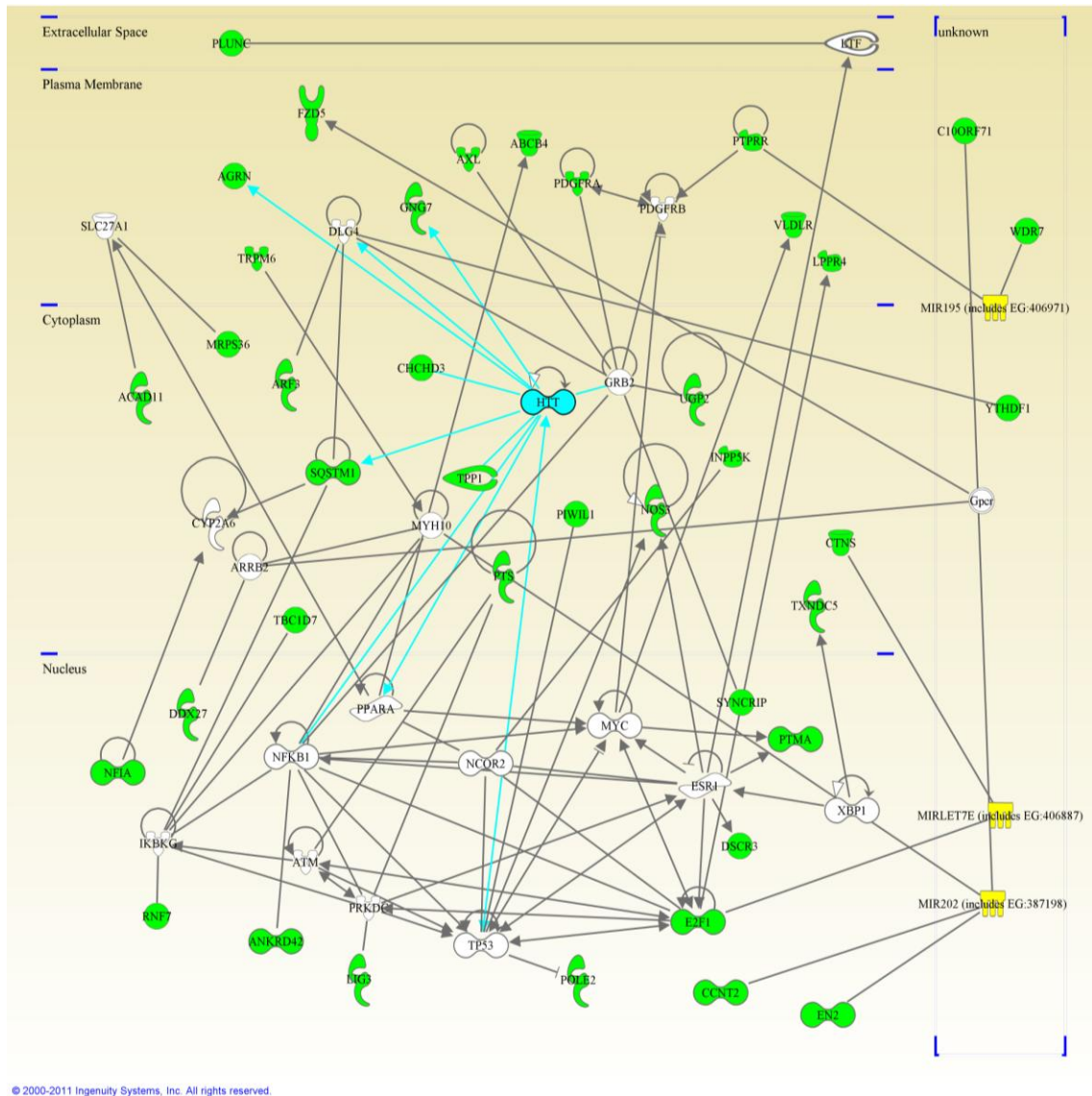


Figure 3.12: Direct Network Association Analysis of Library Positives

Validated gene targets identified from the pSM2+shRNA^{mir} library screen were analyzed using the IPA software. Forty six of the 57 gene targets analyzed were placed in known protein association networks. In this analysis, only direct protein associations were considered. Under these settings, 40 of the 46 gene targets grouped into 1 association network. Gene targets identified are green, miRNAs are yellow, and the Huntingtin protein is light blue. The p-value for the 40 molecules associating into 1 network is 1×10^{-87} . See Figure 3.10 for legend.

Table 3.4: Biological Disorders Associated with Identified Gene Targets

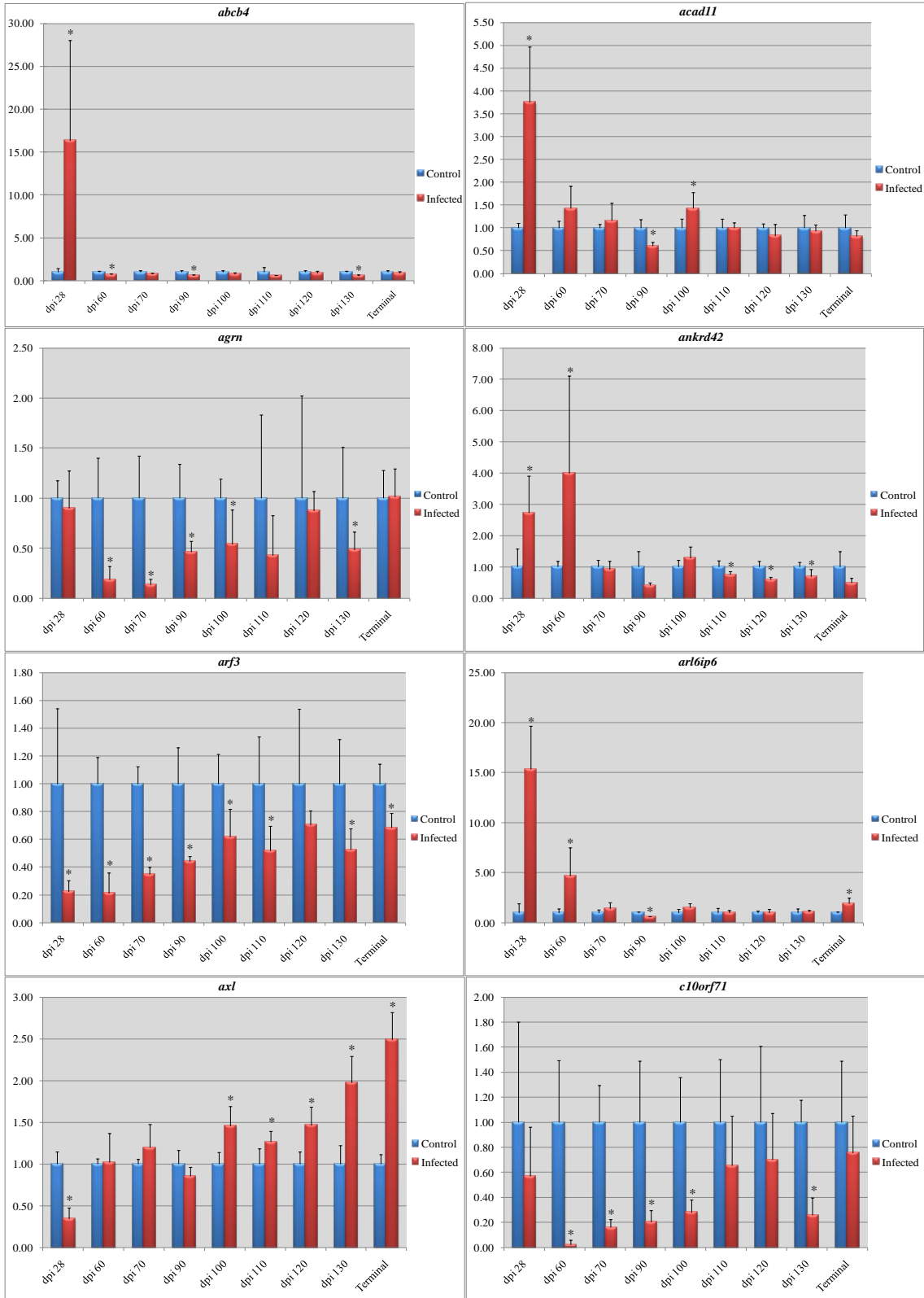
Analysis of the biological diseases and disorders associated with the 46 library identified gene targets encoding proteins which are functionally described within the IPA database. Of the 57 library identified gene targets, information for 46 was available in the IPA database, which analyzed these proteins for their previously described involvement in biological disturbances. Only those biological disorders for which at least 3 identified targets are known to participate in are tabulated. The number of identified targets associated with a particular disorder is listed along with the IPA calculated p-value. As seen from the table below, the list of described disorders is comprehensive.

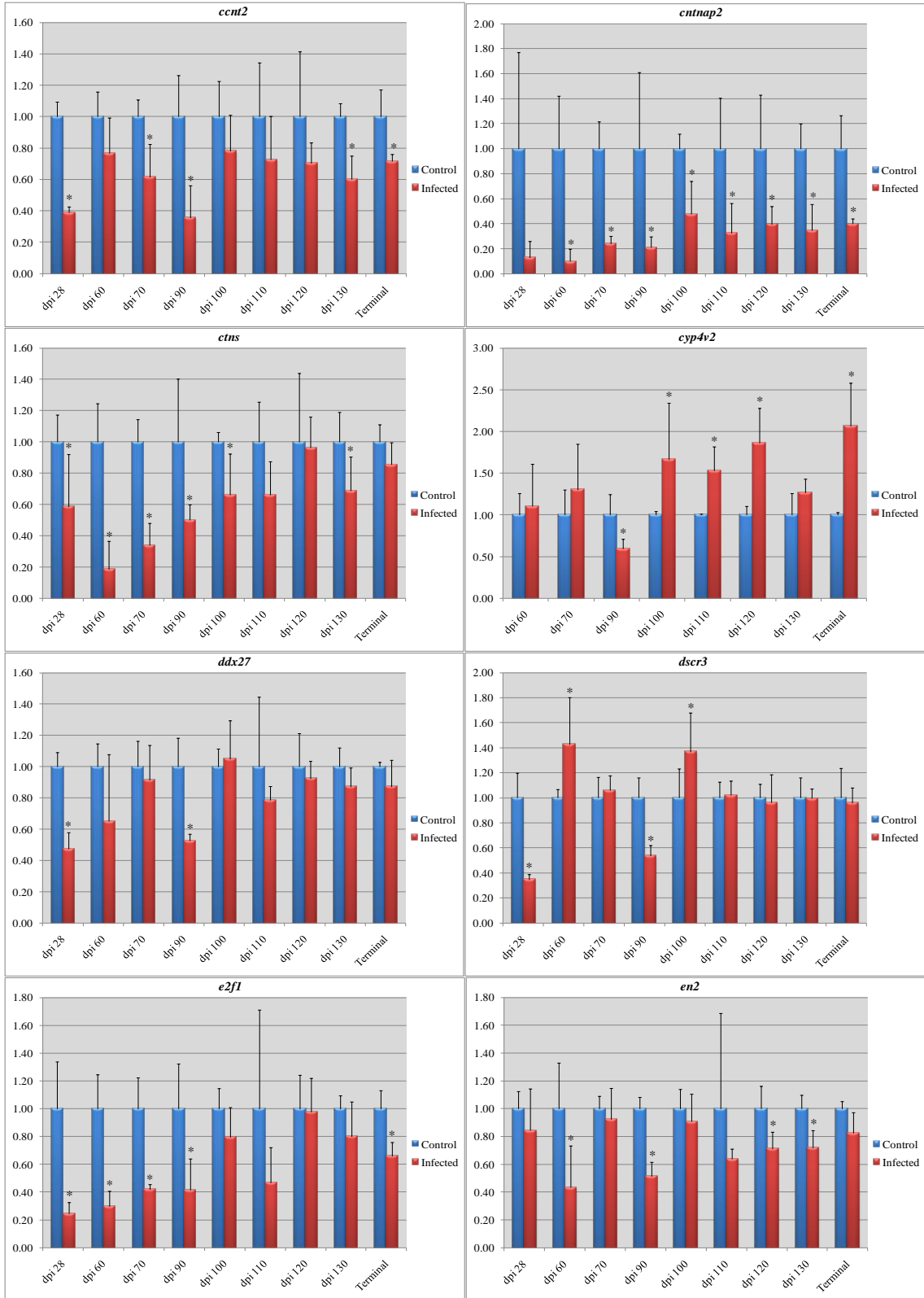
Category	p-value	Number of Molecules
Genetic Disorder	1.14E-02	28
Neurological Disease	1.43E-02	19
Metabolic Disease	1.51E-03	17
Immunological Disease	2.31E-03	16
Inflammatory Disease	1.25E-02	16
Skeletal and Muscular Disorders	2.36E-02	15
Cellular Growth and Proliferation	1.87E-03	13
Endocrine System Disorders	2.23E-02	13
Psychological Disorders	1.54E-02	10
Cell Death	3.57E-02	9
Organismal Development	3.03E-02	7
Tissue Development	1.22E-02	7
Small Molecule Biochemistry	6.77E-03	6
Molecular Transport	6.77E-03	6
Organ Development	2.68E-02	6
Lipid Metabolism	6.77E-03	6
Cancer	1.48E-02	5
Renal and Urological Disease	1.38E-02	5
Gastrointestinal Disease	2.08E-02	5
Respiratory Disease	1.48E-02	5
Carbohydrate Metabolism	1.84E-03	5
Cardiovascular Disease	1.43E-03	5

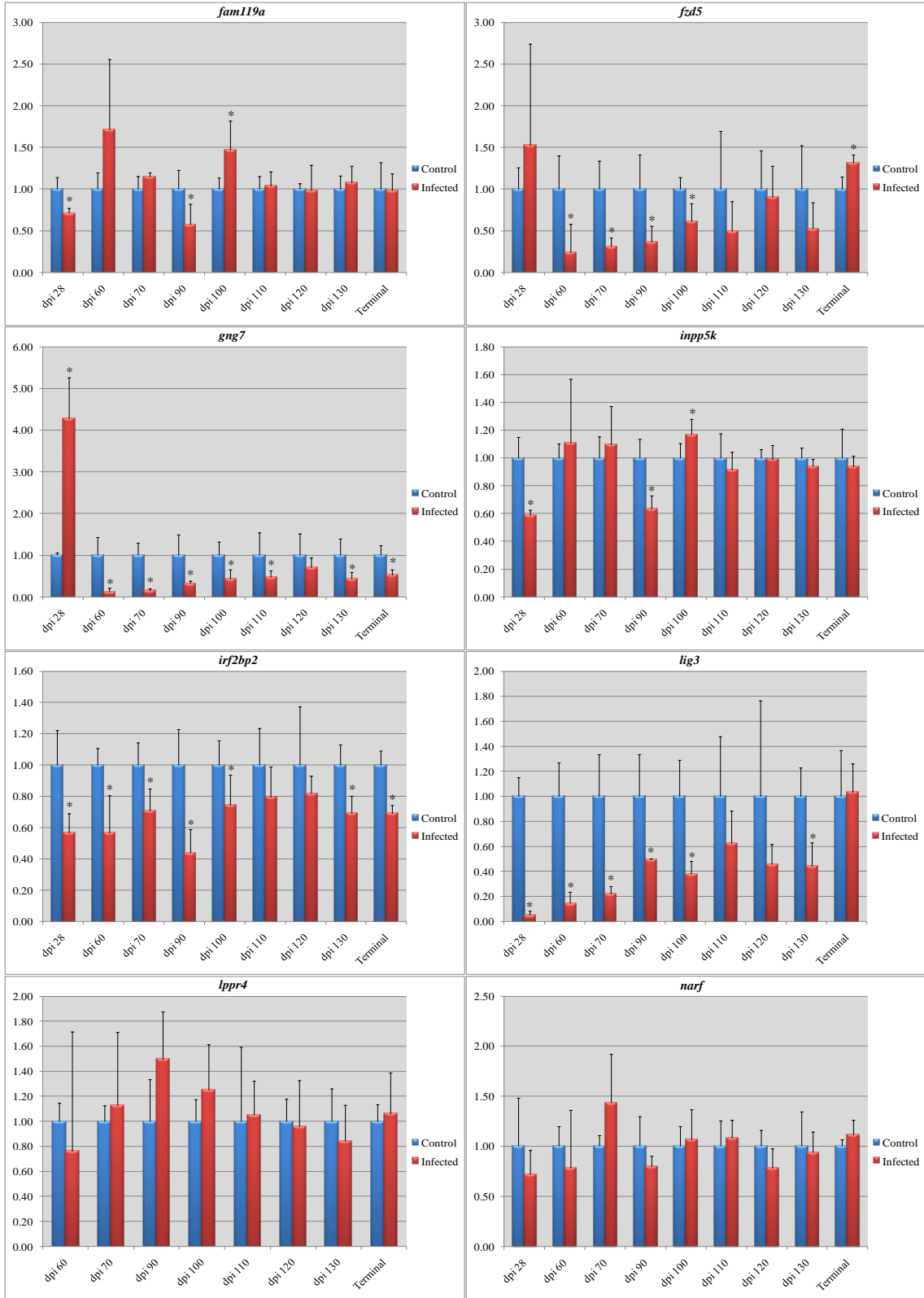
Cellular Development	1.50E-02	4
Nervous System Development and Function	7.87E-03	4
Cardiovascular System Development and Function	9.79E-04	4
Hepatic System Disease	2.11E-02	4
Organismal Injury and Abnormalities	1.55E-02	4
Cell Cycle	2.43E-02	4
Organismal Survival	3.27E-02	4
Cell-To-Cell Signaling and Interaction	2.58E-02	3
Reproductive System Development and Function	2.40E-02	3
Connective Tissue Development and Function	2.11E-02	3
DNA Replication, Recombination, and Repair	1.34E-02	3
Skeletal and Muscular System Development and Function	3.92E-03	3
Developmental Disorder	1.38E-02	3
Cellular Movement	1.47E-02	3
Inflammatory Response	1.80E-02	3
Amino Acid Metabolism	3.67E-03	3

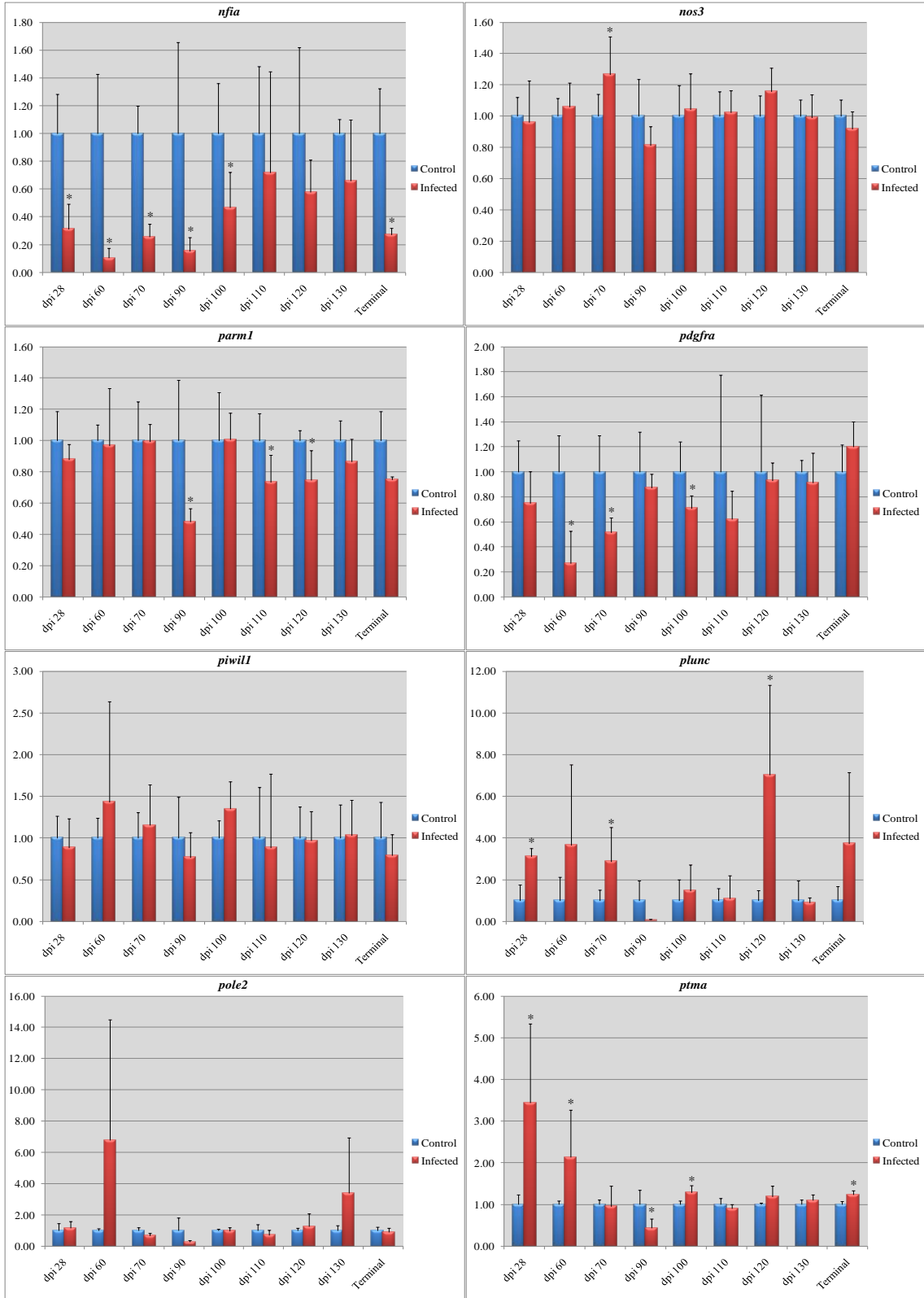
corresponding gene targets in animal models (Mohr, Bakal, and Perrimon 2010). To provide *in vivo* supportive evidence of the relevance of library identified gene targets to prion disease, qPCR analysis of 49 of the 57 confirmed gene transcripts identified for which gene-specific primers could be generated was performed on a LightCycler® 480 real-time PCR instrument (Roche Diagnostics, Laval, QC). These *in vivo* experiments were carried out concurrently with *in vitro* validation of gene targets. The *in vivo* experiments included C57BL/6 mice which had been intracranially (i.c.) inoculated with brain homogenate from either control or scrapie ME7 infected mice. RNA extraction from brains and reverse transcription to cDNA was carried out as described in the Materials and Methods section. Analysis of mRNA expression levels was carried out at 9 time points post i.c. inoculation (dpi 28, 60, 70, 90, 100, 120, 130, and terminal (~dpi 145)). Analysis was carried out on 6 control and 6 infected mice for each time point, with the exception of terminal, where there were only 4 control and 4 infected samples available. Primers used and qPCR analysis results are presented in Table 2.2 and Figure 3.13 respectively.

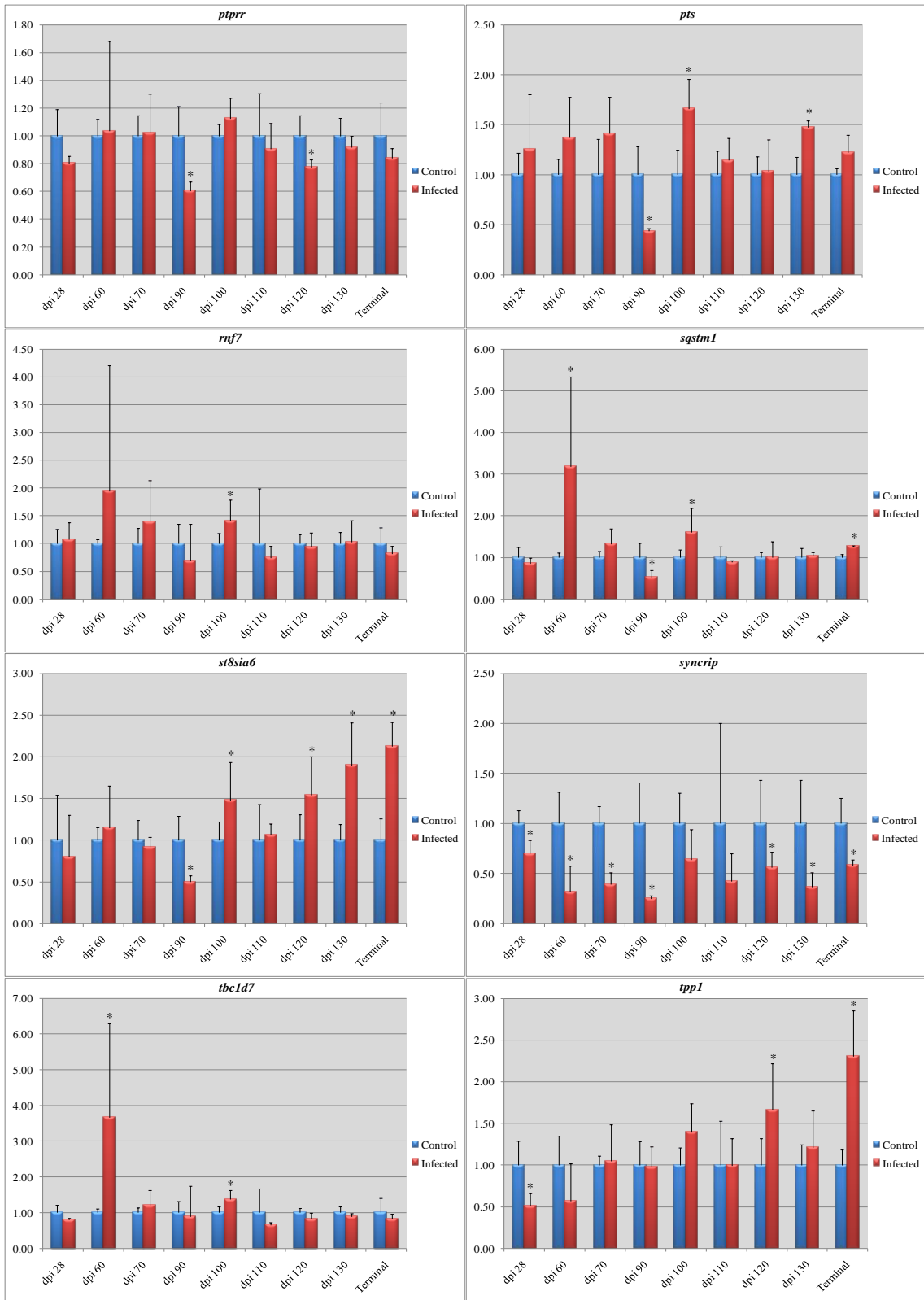
The relative expression level was unique for each library identified gene target at a particular time point, but 4 distinct patterns were observed which were broken down to: genes induced early, genes induced late, genes reduced early, and genes not differentially expressed. Expression levels of *abcb4*, *ankrd42*, *arl6ip6*, *gng7*, *plunc*, *ptma*, *trpm6*, and *ugp2* were all significantly upregulated in prion infected brains as early as 28dpi. The gene targets *axl*, *st8sia6*, and *tpp1*, were significantly upregulated in prion infected mice relative to controls late in the disease course. Gene targets *agn*, *arf3*, *c10orf71*, *cntnap2*, *ctns*, *e2f1*, *fzd5*, *irf2bp2*, *lig3*, *nfia*, *pdgfra*, *syncrip*, *trpm6* (significantly increased at

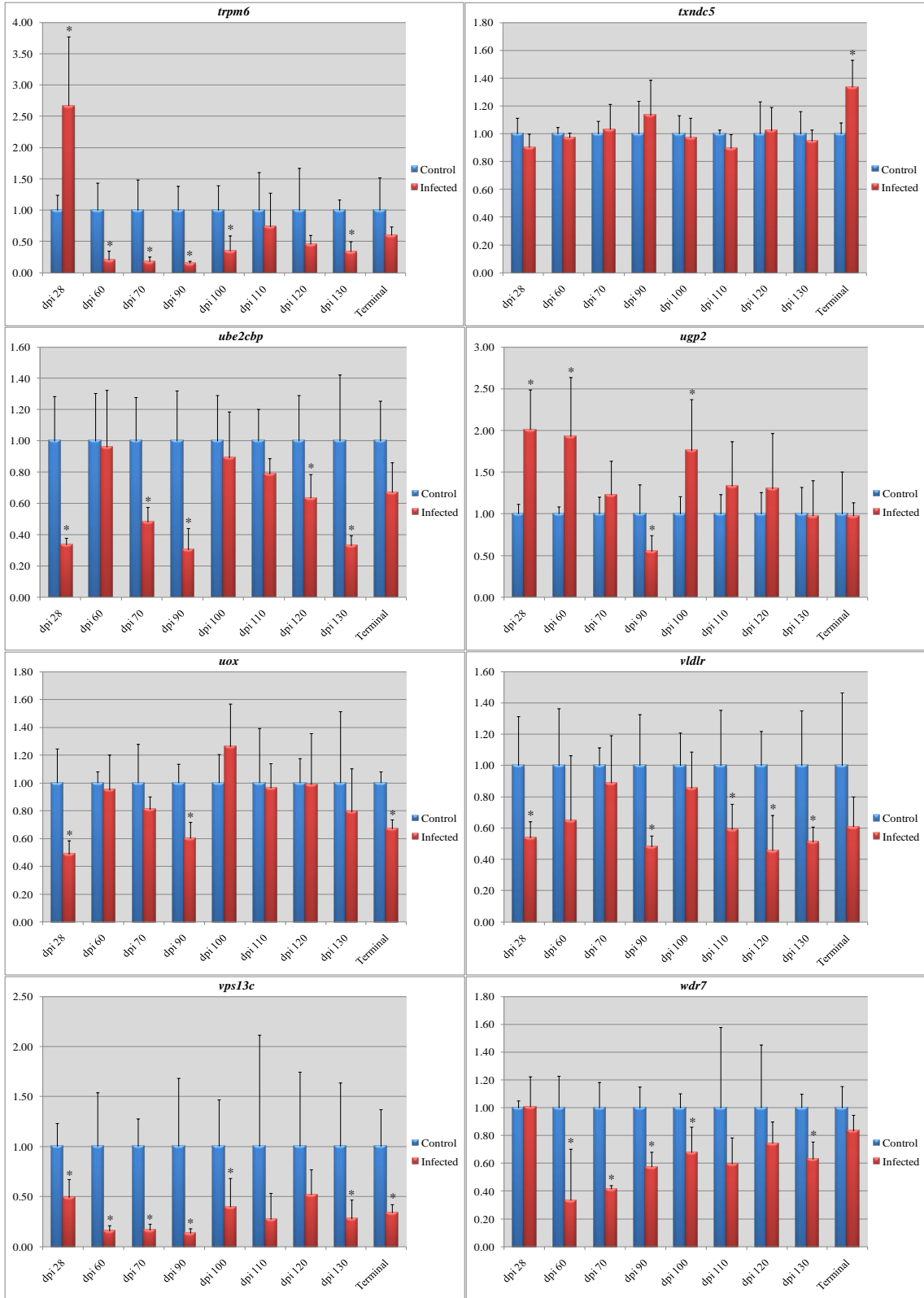












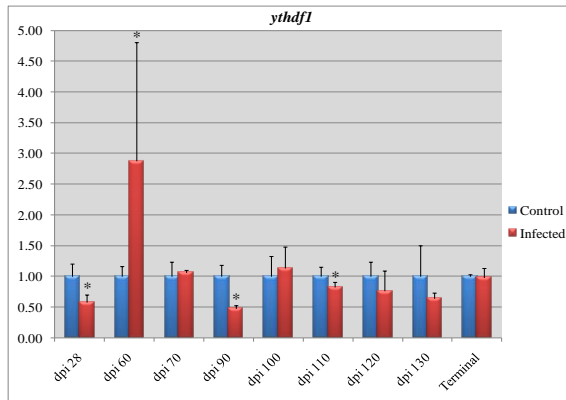


Figure 3.13: qPCR Analysis of Library Identified Gene Targets in Mouse Brain

Shown above are the real-time qPCR analyses of the 49 gene targets identified from the pSM2+shRNA^{mir} library screen for which gene-specific primers could be identified. Relative expression levels were determined for mRNA extracted from whole brain of C57BL/6 mice inoculated via the i.c. route with control or scrapie ME7 infected brain homogenate. Samples were collected at the 9 time points post inoculation indicated in each graph (dpi 28-terminal), with 6 control and 6 infected mice at each time point, except for terminal where only 4 of each were available. Relative mRNA expression levels were measured on the Roche LightCycler[®] 480 system and normalized to the housekeeping gene, *gapdh*. The normalized expression level for a given gene in control samples was averaged, and individual normalized ratios for either control or infected samples were divided by this average. In all graphs above, blue bars indicate control and red bars indicate infected samples. Significantly differentially expressed mRNA in infected samples relative to control samples at a given time point is denoted by an asterisk. The relative abundance is displayed along the Y-axis, and the days post intracranial inoculation is displayed along the X-axis.

28dpi, then significantly declined by dpi 60), *ube2cbp*, *vps13c*, and *wdr7* all demonstrated a significant reduction in prion infected brains early in disease course. The remaining library identified gene targets *ccnt2*, *ddx27*, *dscr3*, *en2*, *fam119a*, *inpp5k*, *lppr4*, *narf*, *nos3*, *parm1*, *piwil1*, *pole2*, *ptpr*, *pts*, *rnf7*, *sqstm1*, *tbc1d7*, *txndc5*, *uox*, and *ythdf1* showed no general pattern of differential expression between infected and control animals, although significant differences were observed for some at individual time points. Overall, the differential expression observed supports the suggestion that the gene targets identified by the *in vitro* prion neurotoxicity assay described in this thesis are influenced by prion disease as observed using an *in vivo* model. This fact strongly supports not only the validity of the library-identified candidate genes, but also the relevance of the candidates to prion disease.

3.3 Verifying Pooled pSM2+shRNA^{mir} Library Identified Gene Targets *in vitro*

Recognized methods employed for verifying the relevance of gene targets pulled out of the pooled shRNA library screen include:

- i) test individual shRNA species targeting an identified gene target;
- ii) use an alternate shRNA expression system;
- iii) confirm knockdown of target mRNA and/or protein levels in the presence of a shRNA; or
- iv) correlating identified gene targets to related disorders (Mohr, Bakal, and Perrimon 2010).

3.3.1 Analyzing Resistance Conferred by Identified pSM2-shRNA^{mir}

The pSM2+shRNA^{mir} retrovectors targeting the first 30 identified gene targets that were sequenced from 3 or more bacterial colonies following the library screen were re-analyzed individually. The time required to perform these confirmatory assays permitted continued library screening and *in vivo* qPCR analyses to proceed concurrently. Individual pSM2+shRNA^{mir} retrovectors were packaged into retroviral particles as described in the Materials and Methods section. SK-N-FI cells were transduced with individual pSM2-carrying retroviral particles at an MOI of 0.06 as determined by titring on SK-N-FI cells. Plating and screening of transduced SK-N-FI cells for resistance to challenge with 50 μ M PrP¹⁰⁶⁻¹²⁶ neurotoxic peptide was carried out as described in the Materials and Methods section. The protection conferred upon host cells transduced with a particular shRNA^{mir} was compared to that of SK-N-FI cells transduced with pSM2 expressing a shRNA^{mir} targeting Eg5 (the Ambion recommended control gene target for knockdown experiments). Compared to Eg5-targeted shRNA^{mir} transduced SK-N-FI cells, those transduced with shRNA^{mir} targeting the following 11 genes were re-confirmed as conferring resistance against PrP¹⁰⁶⁻¹²⁶ induced neurotoxicity: *abcb4*, *acad11*, *ccnt2*, *irf2bp2*, *or6k2*, *rnf7*, *syncrip*, *txndc5*, *ube2cbp*, XM_290759, and XM_296653 (Figure 3.14).

Based upon the protection observed from this preliminary confirmatory assay, the inclusion of the gene target in the NCBI database, and the ability to identify gene specific primers spanning an exon-exon junction in both human and mouse, *abcb4* and *ube2cbp* gene targets were the focus of all further experiments (Figure 3.15). In addition, the only

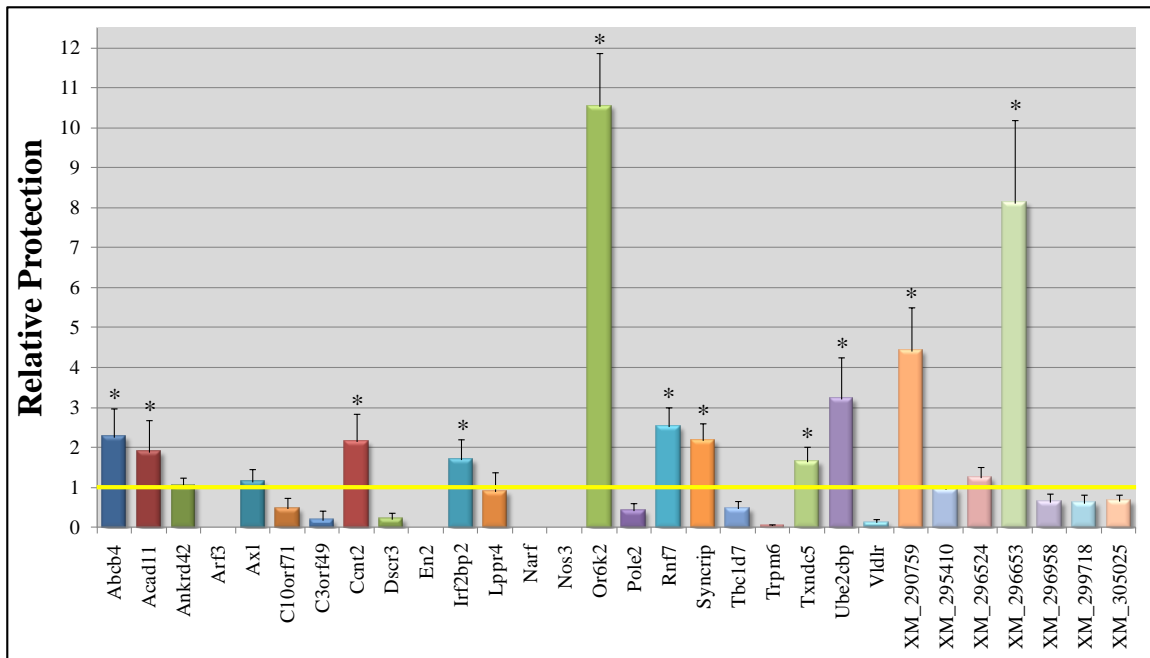


Figure 3.14: Percent Protection Conferred by Individual pSM2-based shRNA^{mir}

The protection conferred upon SK-N-FI cells transduced individually with the first 30 shRNA^{mir} identified 3 times from the library screen against PrP¹⁰⁶⁻¹²⁶ cytotoxicity was re-analyzed. The level of background control survival (i.e. those cells transduced with an Eg5 targeted shRNA^{mir}) was set at 1 (yellow line). Of the 30 shRNA^{mir} tested, those targeting *abcb4*, *acad11*, *ccnt2*, *irf2bp2*, *or6k2*, *rnf7*, *syncrip*, *txndc5*, *ube2cbp*, XM_290759, and XM_296653 genes were confirmed as protective by this screen. The number of surviving cells transduced with *arf3*, *en2*, *narf*, and *nos3* targeting shRNA was below detectable limits. Considering the number of times each was pulled out of the library, whether the targeted transcript is validated in GenBank, the relative protection conferred, and the ability to identify gene specific primers where at least one spanned an exon-exon junction, *abcb4* and *ube2cbp* were selected for further investigation, with *prnp* as a positive control. An asterisk indicates significant protection. Relative protection is presented as a fold change.

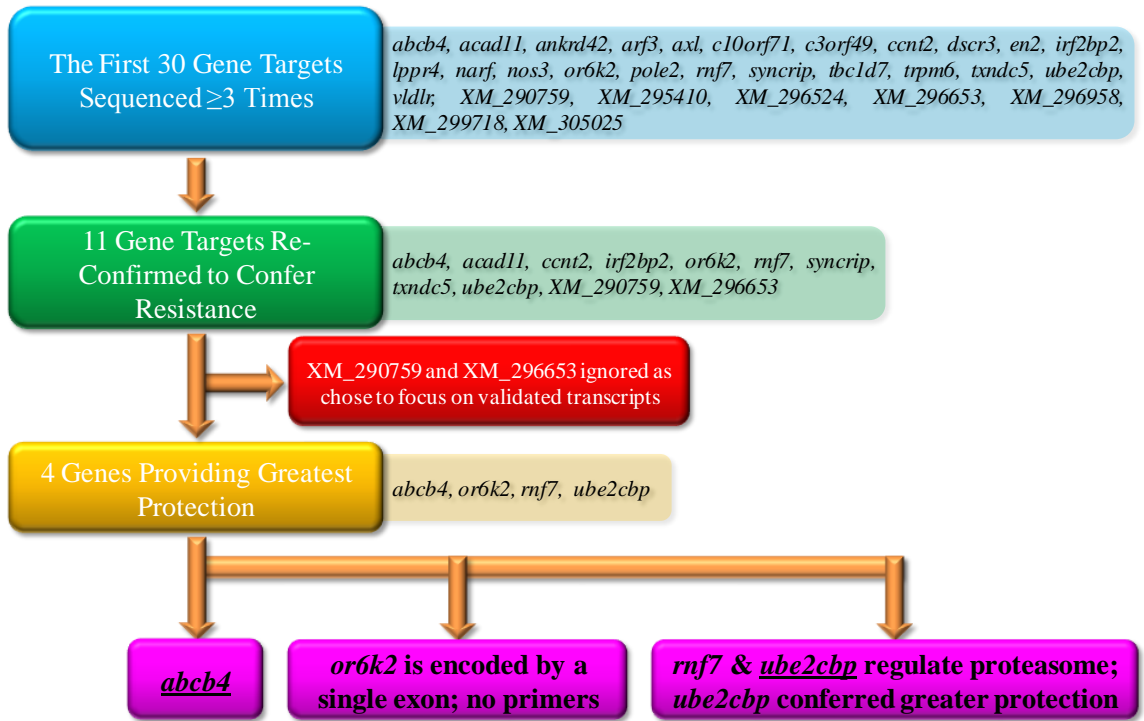


Figure 3.15: Criteria for Selecting *abcb4* and *ube2cbp* for Further Analysis

Upon completion of screening 56 pools, each consisting of 960 pSM2+shRNA^{mir} retrovectors, a total of 80 shRNA^{mir} sequences were identified 3 times from a random colony picking strategy. Of these 80, the first 30 were re-confirmed for their ability to reduce susceptibility of human SK-N-FI cells to the neurotoxic PrP¹⁰⁶⁻¹²⁶ peptide. Transduction of SK-N-FI cells with individual pSM2+shRNA^{mir} of interest, followed by selection for resistance to the PrP¹⁰⁶⁻¹²⁶ peptide, re-confirmed 11 pSM2+shRNA^{mir}. Of these, 2 targeted non-validated transcripts and were excluded from further analysis. The four shRNA^{mir} conferring the greatest protection targeted human *abcb4*, *or6k2*, *rnf7*, and *ube2cbp*. The olfactory receptor gene family consists of thousands of highly related sequences and primers specific to *or6k2* could not be identified. Both *rnf7* and *ube2cbp* participate in ubiquitination of proteins, with *ube2cbp* conferring greater protection. For these reasons *abcb4* and *ube2cbp* were selected for validation studies.

host gene demonstrated to influence prion disease, *prnp*, was included as a control gene target.

3.3.2 Validation of *abcb4* and *ube2cbp* Knockdown Conferring Protection *in vitro*

The *abcb4* and *ube2cbp* results were confirmed *in vitro* using alternate shRNA^{mir} constructs targeting the same transcripts encoded within lentiviral vector backbones. Using these lentiviral constructs to confirm protection has multiple benefits including: 1) higher titres; 2) higher transduction efficiency due to their ability to infect non-dividing cells; and 3) controlling for possible off-target effects by providing an alternate shRNA model to knockdown the same gene.

Confirmation of *abcb4* and *ube2cbp* transcript knockdown conferring significant protection against prion-mediated neurotoxicity was performed using pGIPZ+shRNA^{mir}-expressing lentiviral constructs. The SK-N-FI cells were transduced at an MOI of 10 with the lentiviral particles carrying pGIPZ-based shRNA^{mir} constructs (see Table 3.5). Both *abcb4* and *ube2cbp* were targeted by 3 pGIPZ+shRNA^{mir} constructs (*prnp* by 2 constructs), however, the vendor only guarantees that 1 of 3 will reduce mRNA expression levels by at least 70% relative to the pGIPZ+Non-Silencing control (OpenBiosystems 2011). Using these lentiviral constructs, the protection conferred upon SK-N-FI cells was calculated relative to SK-N-FI cells transduced with the pGIPZ+Non-Silencing control vector. To provide a more accurate calculation of protection, the number of surviving SK-N-FI cells challenged with PrP¹⁰⁶⁻¹²⁶ was compared to those challenged with an equal concentration of PrP^{Scram} peptide. In this confirmatory experiment, cells were challenged with 20µM peptide diluted and replenished as stated

Table 3.5: Gene Targets, Vectors Backbones, and shRNA Tested for Protection

Based upon gene targets identified from the library screen and re-tested using individual shRNA^{mir} retroviral constructs, lentiviral vector-based pGIPZ+shRNA^{mir} targeting *abcb4*, *ube2cbp*, and *prnp* were purchased with at least 1 representing the same shRNA^{mir} sequence identified from the library screen. Vectors were purified from bacterial stocks according to the Qiagen Plasmid Mini kit, packaged into lentiviral particles and titered as outlined in the Materials and Methods section. Lentiviral particles were transduced onto SK-N-FI cells at an MOI = 10 and challenged with 20 μ M PrP¹⁰⁶⁻¹²⁶ neurotoxic peptide. Listed below are the shRNA used to confirm results, and which antisense sequences provided reproducible protection. The expected proportion of shRNA^{mir} capable of reducing mRNA expression level by at least 70% is 1 out of 3 (OpenBiosystems 2011).

Gene Target	Vector Backbone	Oligo ID	Mature shRNA Antisense Sequence 5' \rightarrow 3'	Confers Protection
<i>abcb4</i>	pGIPZ	93064	ATATCAAAGATCACATATG	No
		93067	ATAGCAATAGGGTAACTG	Yes
		230814	TTCCCTTTGATGCTGTCTG	No
<i>ube2cbp</i>	pGIPZ	139483	TTCATCTGGAGTGAAGATG	No
		139486	TTGACAATATCAACAGCAG	Yes
		273404	TATTCCTAGGATTTACAG	No
<i>prnp</i>	pGIPZ	92301	TACATGAAACGATTCAGTG	Yes
		232888	TAGTTTAAAGAAAGGAATG	No

previously (peptide was resuspended in 1mL SK-DMEM5 + 25.15mL SK-DMEM1 per milligram, and replenished every 48 hours for a total of 5 applications). The background survival rate of SK-N-FI cells challenged with 20 μ M PrP¹⁰⁶⁻¹²⁶ relative to PrP^{Scram} peptide was 8.04%. The observed background survival rate is sufficiently low enough for the protective effect of knocking down the gene targets of interest to be observed. Comparing the number of surviving cells challenged with PrP¹⁰⁶⁻¹²⁶ to those challenged with the PrP^{Scram} peptide, and taking into account the background survival rate of SK-N-FI cells transduced with the pGIPZ+Non-Silencing control vector, the degree of protection was calculated.

3.3.3 Protection Conferred by pGIPZ+shRNA^{mir} Mediated Gene Knockdown

It was observed that of the multiple pGIPZ+shRNA^{mir} vectors targeting *abcb4*, *prnp*, or *ube2cbp* tested, only one targeting a particular transcript conferred a significant level of protection (Table 3.5). Of the 3 pGIPZ+shRNA^{mir} lentiviral vectors targeting *abcb4* (93064, 93067, and 230814), only 93067 conferred protection. The number of surviving SK-N-FI transduced with 93064 or 230814 was below the detectable limits of AlamarBlue. The relative protection conferred by pGIPZ+shRNA^{mir} 93067-mediated *abcb4* knockdown was 3.75-fold compared to SK-N-FI cells transduced with the pGIPZ+Non-Silencing shRNA^{mir} control (Table 3.5 and Figure 3.16). Of the 3 pGIPZ+shRNA^{mir} lentiviral vectors targeting *ube2cbp* (139483, 139486, or 273404), only 139486 conferred protection. The number of surviving SK-N-FI transduced with 139483 or 273404 was below the detectable limits of AlamarBlue. The relative protection conferred by pGIPZ+shRNA^{mir} 139486-mediated knockdown of *ube2cbp* was

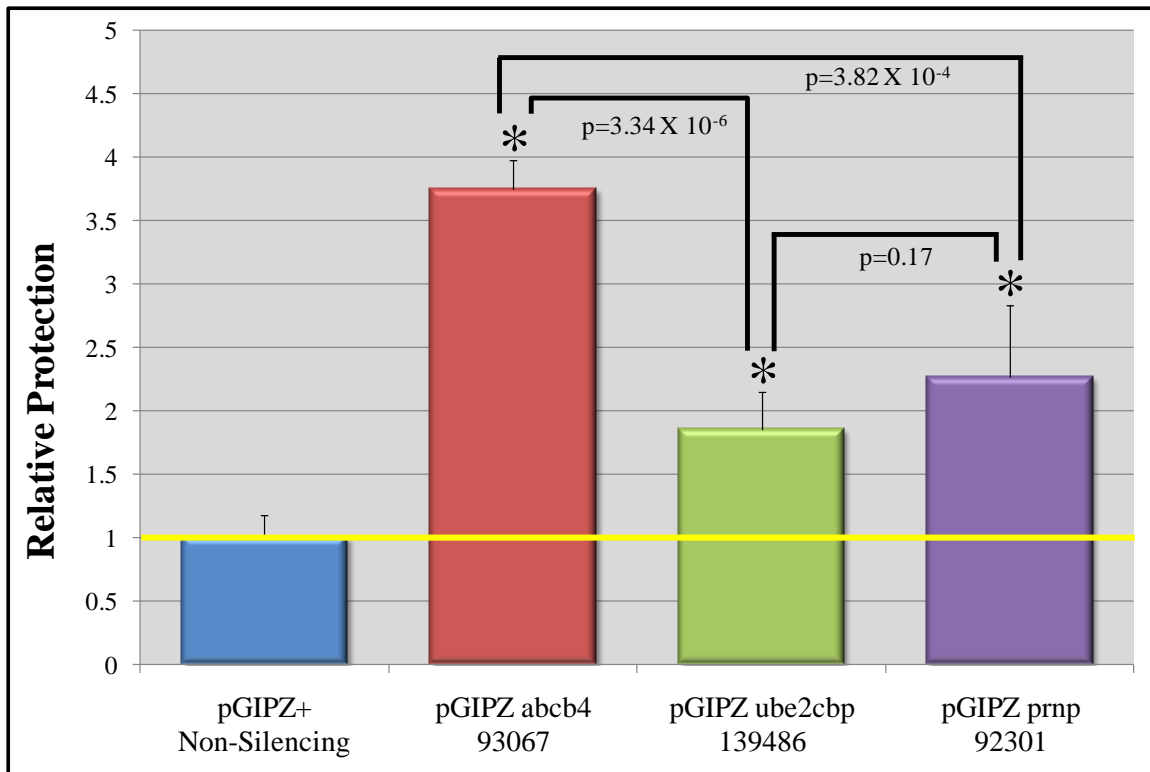


Figure 3.16: Relative Protection Conferred upon SK-N-FI Cells Expressing pGIPZ-based shRNA^{mir}

Knockdown of *abcb4* and *ube2cbp* using lentiviral pGIPZ-based shRNA^{mir} targeting these genes, as well as *prnp* for control, confers protection upon the host SK-N-FI cells against PrP¹⁰⁶⁻¹²⁶ neurotoxicity. Cells were challenged, as outlined in the Materials and Methods section, with 20 μ M PrP¹⁰⁶⁻¹²⁶ or PrP^{Scram} peptides. One of the three pGIPZ-based shRNA^{mir} targeting either *abcb4* or *ube2cbp* conferred significant protection against PrP¹⁰⁶⁻¹²⁶ neurotoxicity, while one of the two targeting *prnp* provided significant protection. The relative protection shown is relative to PrP^{Scram} exposed cultures, and compared to cells transduced with the pGIPZ+Non-Silencing shRNA^{mir} control (set to 1, yellow line). An asterisk indicates significant protection relative to control. Error bars represent the standard deviation of relative protection.

1.84-fold compared to SK-N-FI cells transduced with the pGIPZ+Non-Silencing shRNA^{mir} control (Table 3.5 and Figure 3.16). Both pGIPZ+shRNA^{mir} constructs targeting *prnp* (92301 and 232888) had sufficient SK-N-FI cell survival to quantitate cell number using AlamarBlue. Those transduced with pGIPZ+92301 showed a relative protection of 2.26-fold compared to controls (Table 3.5 and Figure 3.16). In contrast, those transduced with pGIPZ+232888 showed a 0.46-fold protection rate compared to controls (data not shown), indicating that 232888 actually increased the sensitivity of SK-N-FI cells to challenge with the PrP¹⁰⁶⁻¹²⁶ neurotoxic peptide.

3.3.4 Confirming *abcb4*, *ube2cbp*, and *prnp* Targeted shRNA Functionality

Synthetic shRNA constructs are expected to reduce the detectable mRNA expression levels due to their perfect complementarities, which should be reflected in the protein expression levels. Given this, quantitative real-time PCR (qPCR) and Western blotting analyses were employed to determine the functional activity of a given shRNA.

3.3.4.1 Analysis of *abcb4*, *ube2cbp*, and *prnp* mRNA Knockdown Efficiency

Primers specific to human *abcb4*, *ube2cbp*, and *prnp* mRNA were used to quantitate the relative expression levels of each gene. Analysis was carried out in 96-well format plates on a LightCycler® 480 instrument (Roche Diagnostics, Laval, QC). Relative expression levels of *abcb4*, *ube2cbp*, and *prnp* were normalized to *gapdh* expression (loading control), and compared to the corresponding gene expression level in SK-N-FI cells transduced with the pGIPZ+Non-Silencing control, which was considered to represent a relative expression level of 1. This qPCR analysis was performed once on

SK-N-FI cells which had been maintained under 2.25µg/mL puromycin selection prior to RNA isolation.

Transduction of SK-N-FI cells with the pGIPZ+93067 (*abcb4*) shRNA^{mir} construct significantly reduced the *abcb4* mRNA expression levels to 0.31 relative to SK-N-FI cells transduced with the pGIPZ+Non-Silencing shRNA^{mir} construct. Transduction of SK-N-FI cells with the pGIPZ+139486 (*ube2cbp*) shRNA^{mir} construct significantly reduced the *ube2cbp* mRNA expression levels to 0.35 relative to SK-N-FI cells transduced with the pGIPZ+Non-Silencing shRNA^{mir} construct. Transduction of SK-N-FI cells with the pGIPZ+92301 (*prnp*) shRNA^{mir} construct significantly reduced the *prnp* mRNA expression levels to 0.23 relative to SK-N-FI cells transduced with the pGIPZ+Non-Silencing shRNA^{mir} construct (Figure 3.17). In contrast, transduction of SK-N-FI cells with pGIPZ+232888 reduced mRNA expression levels to 0.56 relative to those transduced with the pGIPZ+Non-Silencing shRNA^{mir} control vector (data not shown). From the relative mRNA expression levels, it can be seen that efficiency of knockdown varies greatly depending upon gene target and shRNA^{mir} construct used.

3.3.4.2 Analysis of *abcb4*, *ube2cbp*, and *prnp* Protein Knockdown Efficiency

The quantities of Abcb4 and PrP in human SK-N-FI cells were below the limit of detection with the various commercially available antibodies. Antibodies tested for detection of Abcb4 included sc-58221 (Santa Cruz) and PAB4698 (Abnova). Those tested for detection of PrP included 6H4 (Prionics), P0110 (Sigma-Aldrich, 8H4), MAB1562 (Millipore, 3F4), sc-15312 (Santa Cruz, FL-253), 189720 (Cayman Chemical, SAF-32), and 189755 (Cayman Chemical, SAF-61). Antibodies commercially available

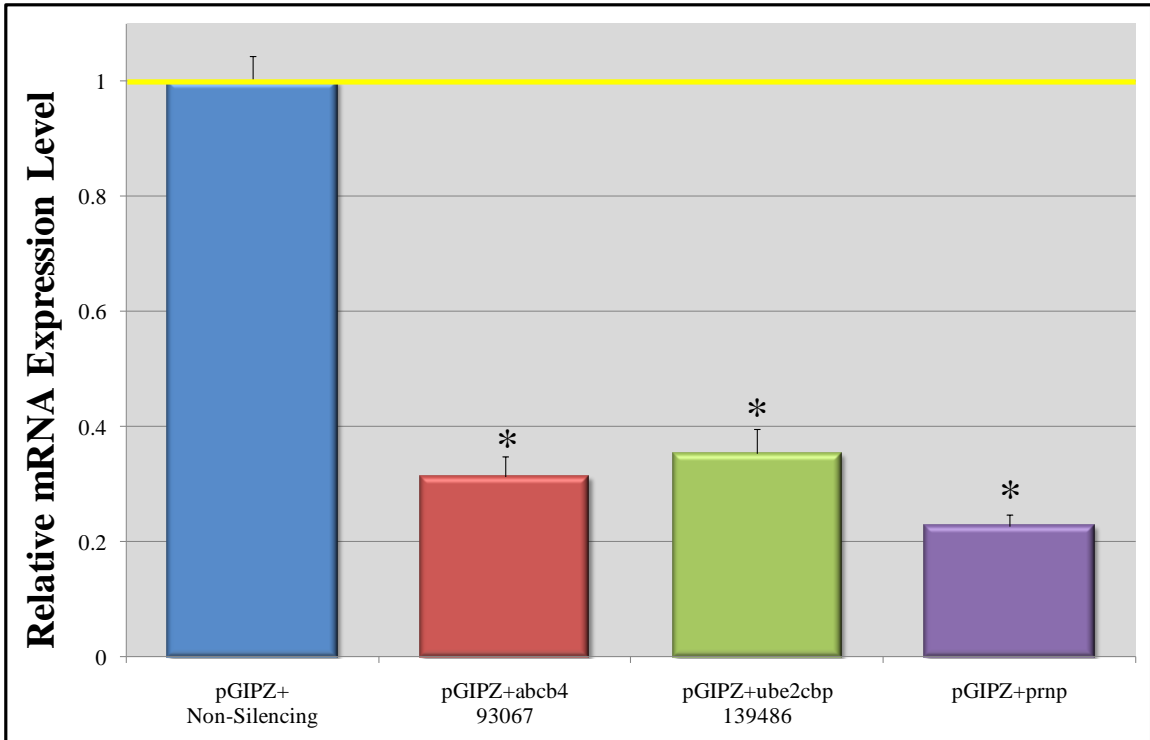


Figure 3.17: qPCR Analysis of *abcb4*, *ube2cbp*, and *prnp* Expression Levels

SK-N-FI cells transduced with lentivirus at an MOI of 10 were plated into tissue culture flasks and selected for stable shRNA^{mir} expression using puromycin. mRNA was reverse transcribed to cDNA according to the Invitrogen SSIII RNase H⁻ RT protocol. Relative mRNA expression levels of human *abcb4*, *ube2cbp*, and *prnp* were determined on a Roche LightCycler 480 Real-Time PCR system. Expression levels were normalized to the housekeeping gene *gapdh*. mRNA expression levels are presented relative to that of SK-N-FI cells stably encoding the pGIPZ+Non-Silencing shRNA^{mir} control (set to 1, blue bar graph, yellow line). An asterisk indicates a significant reduction relative to control cells.

other than those already tested or custom synthesized antibodies may be sufficiently sensitive enough to detect Abcb4 and PrP protein for future analysis.

Custom antibodies were designed against amino acid residues 118-134, 205-214, or 269-280 of human Ube2cbp (Pacific Immunology, San Diego, CA) due to the current lack of commercially available antibodies specific for human Ube2cbp. After testing all 3 antibodies by Western blot analysis, the antibody recognizing residues 269-280 was selected for further study. This antibody recognized a band of approximately the expected size (43kDa not including post-translation modifications). Two additional bands, potentially splice variants, were also observed (Figure 3.18). Using the Quantity 1 software (Bio-Rad, Hercules, CA), the density of human Ube2cbp, as well as α -tubulin, were measured. Protein abundance was normalized to α -tubulin expression, and the relative Ube2cbp expression in shRNA^{mir} knockdown SK-N-FI cells was compared to the normalized abundance in pGIPZ+Non-Silencing control cells. The upper most band (band 1, ~51kDa) and the middle band (band 2, ~40kDa) detected in SK-N-FI cells transduced with pGIPZ+139486 (*ube2cbp*) both showed a reduction in protein abundance to 0.72 or 0.80 relative to SK-N-FI cells transduced with the pGIPZ+Non-Silencing shRNA^{mir} control. The lowest band (band 3, ~27kDa) demonstrated an increase in abundance to 1.56 relative to control SK-N-FI (Figure 3.19). Pre-incubation of the Ube2cbp antibody with a 5-fold excess of blocking peptide in TBST + 5% BSA for 2 hours at room temperature completely abolished all observable banding, confirming the specificity of the antibody for the corresponding peptide sequence.

A summary of results obtained from knockdown of *abcb4* and *ube2cbp* using individual shRNA^{mir} expressing pGIPZ lentiviral vectors are presented in Table 3.6.

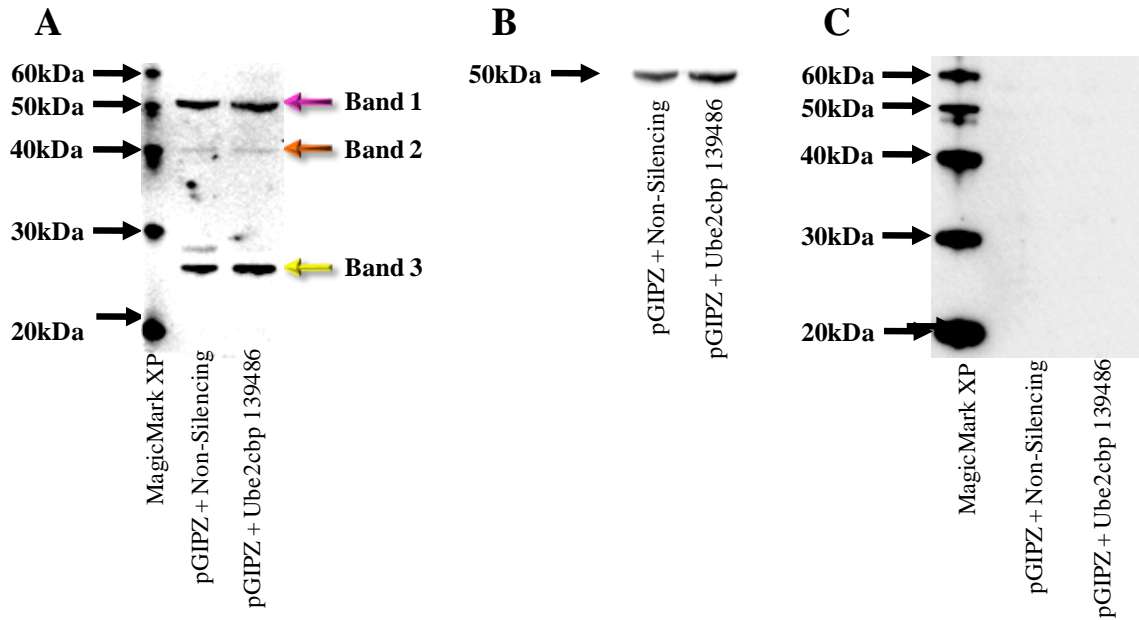


Figure 3.18: Western Blot Detection of SK-N-FI Ube2cbp Protein

Using custom antibodies raised against human Ube2cbp amino acids 269-280 in rabbits (Pacific Immunology) for Western blot analysis, Ube2cbp banding pattern and relative band intensities were visualized. SK-N-FI cells transduced with lentivirus carrying pGIPZ+shRNA^{mir} were maintained under puromycin selection. Protein was extracted and 25 μ g was loaded onto a pre-cast 12% BisTris-HCl Criterion SDS-PAGE gel. Protein was transferred to a nitrocellulose membrane using the iBlot system. (A) The banding pattern for human Ube2cbp as recognized by the custom antibody used shows 3 distinct prominent bands of ~51, 41, and 26kDa (Bands 1, 2, and 3 respectively). (B) Human α -tubulin was used as a loading control, with one prominent band at ~50kDa. (C) Specificity of the custom Ube2cbp antibody was confirmed by pre-incubating the primary antibody with a 5-fold excess of blocking peptide and using this to probe the blot. The lack of observable bands strongly supports the specificity of the antibody for the Ube2cbp peptide sequence against which it was raised.

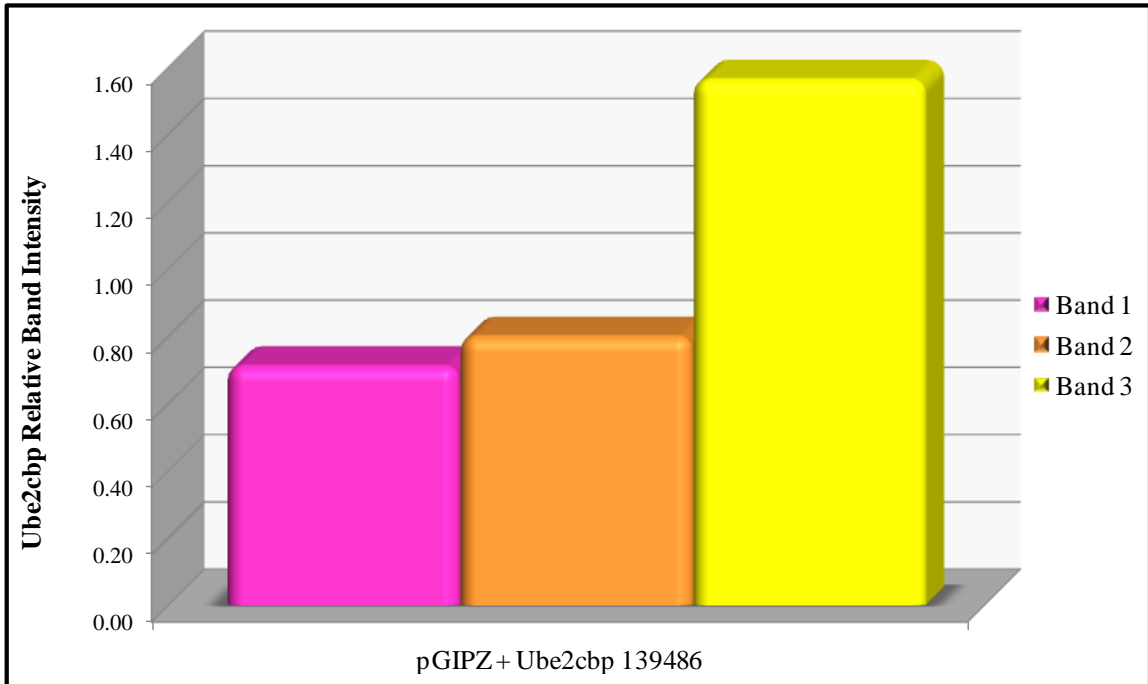


Figure 3.19: Ube2cbp Protein Knockdown Efficiency in Human SK-N-FI Cells

The relative protein knockdown efficiency of the pGIPZ+shRNA^{mir} *ube2cbp* targeting construct was determined for all 3 prominent bands visualized in SK-N-FI cells. The band intensities of control and shRNA^{mir}-expressing cells were normalized to α -tubulin. The relative Ube2cbp band intensities were calculated by dividing the normalized band intensity in pGIPZ+*ube2cbp* (139486) shRNA^{mir} expressing cells to that of SK-N-FI cells expressing pGIPZ+Non-Silencing control vector (set to 1). Relative band intensity for bands 1, 2, and 3 were calculated individually for SK-N-FI cells stably expressing *ube2cbp*-targeting shRNA^{mir}. From the graph, bands 1 and 2 appear to be reduced relative to control (0.72 and 0.80 remaining respectively). The relative intensity of band 3 was increased to 1.56 compared to the pGIPZ+Non-Silencing control.

Table 3.6: pGIPZ+shRNA^{mir} 93067 (*abcb4*) and 139486 (*ube2cbp*) Summary

Shown below is a table summarizing the results obtained from the *in vitro* analyses of pGIPZ+shRNA^{mir} 93067 (*abcb4*) and 139486 (*ube2cbp*) efficiency. This includes SK-N-FI protection against challenge with the PrP¹⁰⁶⁻¹²⁶ neurotoxic peptide, relative mRNA expression remaining, and the relative band intensity of Ube2cbp. All values are presented as percentages compared to SK-N-FI cells transduced with the pGIPZ+Non-Silencing shRNA^{mir} lentiviral vector construct.

		pGIPZ+shRNA ^{mir}	
	<i>abcb4</i>	3.75	Relative Protection
	<i>ube2cbp</i>	1.85	
	<i>abcb4</i>	0.31	Relative mRNA
	<i>ube2cbp</i>	0.35	
<i>ube2cbp</i>	band 1	0.72	Relative Protein
	band 2	0.80	
	band 3	1.57	

4. Discussion

4.1 Genes Known to Mediate Prion Disease

Directed mutational studies in which the prion protein coding gene has been deleted or knocked down demonstrates that expression of PrP is essential to prion propagation and pathogenesis *in vivo* (Bueler et al. 1993; Prusiner et al. 1993; Sailer et al. 1994; Fischer et al. 1996). However, it has also been demonstrated that PrP expression is non-essential for oligomeric β -sheet rich PrP neurotoxicity (Simoneau et al. 2007), suggesting that oligomers of β -sheet rich prion protein are capable of directly inducing neurotoxicity through stimulation of unidentified molecular pathways.

Due to the lack of a published cell culture model of prion neurotoxicity, current studies to identify genes essential to prion disease rely on hypotheses based on suspected prion protein (PrP) functions and associations. In addition, the absence of a cell culture model has meant that testing potential genetic factors underlying prion disease has relied on the generation of transgenic animals and this has significantly limited the number of potential candidates that have been examined.

To address the potential involvement of non-PrP proteins in prion disease, one group focused on 20 proteins known to co-localize with PrP, which exhibit elevated expression levels during prion pathogenesis, influence PrP activity, or have been previously demonstrated to participate in Alzheimer's disease. Through deletion or overexpression of the 20 proteins of interest, it was observed that only 3 (*app*^{0/0}, *illr1*^{0/0}, and overexpression of *sod1*) conferred moderate prolongation of disease incubation (13-19%) in transgenic mice inoculated with infectious brain homogenate. The authors concluded that many genes previously postulated to potentially be involved in prion pathogenesis showed no discernible protection *in vivo*, and that elucidation of the

complex molecular network underlying prion disease would provide options for treating these fatal neurodegenerative disorders (Tamguney et al. 2008).

The study outlined above involved thousands of mice, and required up to 300 days, with only 20 different genes studied for their potential role in prion disease, emphasizing the necessity of a cell culture model able to mimic prion neurotoxicity. A cell culture model would permit affordable and rapid focused studies on proteins of interest, or permit large scale screening assays to identify novel molecular mechanisms involved in prion neurotoxicity.

4.2 Development of the Novel Prion Neurotoxicity Assay Utilized to Screen an shRNA^{mir} Library

Commercially available short hairpin RNA (shRNA) libraries have opened the field of RNAi research, permitting large-scale screens for gene targets previously unidentified as mediators contributing to a particular phenotype or cellular behaviour. Assay systems in which an easily distinguishable characteristic can be observed (e.g. cell migration, apoptosis, cell-surface attachment) or for which a highly effective model already exists with discernible results (e.g. viral-induced cell death), applying a library screen to study the underlying mechanisms is readily feasible.

One example of this is the study of molecular factors influencing cell adhesion. Constitutive expression of Abl kinase causes cells to detach from the growth surface, presenting a readily identifiable phenotype. A group interested in identifying proteins involved in cell adhesion took advantage of this phenotype to screen a GeneNet™ shRNA library. Through multiple rounds of selection for cells that remained bound to

the surface of a culture dish, cells in which genes essential to cell detachment had been knocked down were enriched. Amplification of encoded shRNA and microarray hybridization permitted identification and quantification of cellular encoded shRNAs. Using bioinformatic analysis techniques of the enriched shRNAs, including predicted gene association network analysis, the authors identified gene targets encoding proteins potentially involved in cell adhesion. Of these, Il6st, which had been previously shown to mediate cell adhesion in cardiomyocytes, was validated for its role in Abl kinase-mediated cell detachment (Huang, Wang, and Lu 2008).

Other examples in which large-scale screens have been implemented to study the underlying mechanisms of a particular phenotype include: the identification of genes involved in cancer (Berns et al. 2004; Westbrook et al. 2005; Gazin et al. 2007; Luo et al. 2008; Gobeil et al. 2008; Luo et al. 2009; Mullenders et al. 2009), telomerase activity (Coussens et al. 2010), apoptosis (Kimura et al. 2008; Tsujii et al. 2010), oxidative stress response (Nagaoka-Yasuda et al. 2007), and host-pathogen interactions (Yeung et al. 2009).

A major impediment to screening for genes essential to prion neurotoxicity has been the lack of a sufficiently neurotoxic cell culture model to permit implementation of a large-scale RNAi screen for identification of genes involved in prion-mediated neurodegeneration. Published studies state background survival rates of human neuroblastoma cell lines challenged with concentrations of PrP¹⁰⁶⁻¹²⁶ as high as 200 μ M range from 40-80% relative to controls (White et al. 2001; O'Donovan, Tobin, and Cotter 2001; Thellung et al. 2002; Corsaro et al. 2003; Dupiereux et al. 2005; Carimalo et al. 2005; Bergstrom et al. 2005; Ning et al. 2005a; Fioriti et al. 2005a; Fioriti et al. 2005b;

Dupiereux et al. 2006; Ferreira et al. 2006; Pan et al. 2010). These studies highlight that human cell lines exhibit significant susceptibility to prion neurotoxicity, but the degree of cell death is insufficient for large-scale screening or validation of individual proteins of interest.

The influence of growth rate on susceptibility has been hypothesized to explain the insensitivity of the rapidly dividing mouse neuroblastoma N2a cell line towards prion brain homogenate or the PrP¹⁰⁶⁻¹²⁶ peptide. It is proposed that rapidly dividing cells do not accumulate neurotoxic prion protein species to concentrations sufficient for inducing cell death (Hetz et al. 2003). Therefore, primary neuronal cultures which do not divide may be more sensitive to PrP¹⁰⁶⁻¹²⁶-induced neurotoxicity than cell lines, however, cell lines offer two distinct advantages: (i) consistent neuronal cell population with no contaminating astrocytes, microglia, or oligodendrocytes; and (ii) unlike primary neurons, neuroblastoma cells continuously divide, permitting expansion of resistant cells into colonies for easy analysis. Taking advantage of cell line attributes, this hypothesis implied that culture conditions minimizing neuroblastoma growth should enhance susceptibility to prion neurotoxicity, and therefore, conditions that influence growth rate were manipulated using the human neuroblastoma SK-N-FI cell line. Due to the lack of a cell viability assay during the early trial experiments, SK-N-FI viability was subjectively estimated for those exposed to PrP¹⁰⁶⁻¹²⁶ relative to PrP^{Scram} peptide. It was considered necessary that the background survival rate be as low as possible to limit the number of false positives.

4.2.1 Manipulation of Culture Conditions to Optimize SK-N-FI Susceptibility to PrP¹⁰⁶⁻¹²⁶-Induced Neurotoxicity

Published literature described the plating of cell numbers ranging from 0.18-4.2 x 10⁶ cells, with 80μM peptide as a commonly applied concentration (Cronier, Laude, and Peyrin 2004; Bergstrom et al. 2005; Ning et al. 2005a; Fioriti et al. 2005a; Ferreiro et al. 2006). With the exception of one publication examined, a single application of peptide was studied. The one publication testing the efficacy of multiple peptide exposures demonstrated an increasing degree of cell toxicity with an increasing number of exposures (Ning et al. 2005a). We tested a range of peptide concentrations, and although higher concentrations of peptide were more neurotoxic (Table 3.1), 40μM was selected for further analysis because a balance between survival and toxicity was deemed important for identification of protective shRNA^{mir}. High background would mask false positives, but too rapid an onset of toxicity would completely abolish the ability to pull out any protective shRNA^{mir} sequences.

Beyond peptide variabilities, sensitivity should also be influenced by growth rate. Both cell density and serum are known modulators of cell growth rate. Through plating tumorigenic epithelial cells at various initial seeding densities, it has been observed that not only did cells plated at higher seeding densities achieve maximal confluency more rapidly, but that these higher densities also influenced the final cell confluency (Hosick 1974). The growth rate of cells is also known to be influenced by both the serum concentration (Bai et al. 2003) and serum preparation (HyClone Labs 1996), which is attributed to the effect of the chosen method on growth factors in the serum. The two methods of serum preparation compared were filter sterilization (FS-FBS) or heat

inactivation (HI-FBS) followed by filter sterilization of fetal bovine serum. Prion peptides were resuspended in media where the composition of FBS was altered, which demonstrated a significant impact on SK-N-FI susceptibility (Table 3.2). PrP¹⁰⁶⁻¹²⁶ or PrP^{Scram} resuspended in media containing 0.5%, 1%, 2%, or 5% HI-FBS were viewed on a light microscope and representative images were taken (Figure 3.1). Serum concentrations $\leq 0.5\%$ were too low to support healthy maintenance of SK-N-FI cells over extended periods, while concentrations $\geq 5\%$ supported healthy growth of the cells, but also significantly enhanced resistance to challenge with the peptide.

From all the conditions tested and utilizing AlamarBlue to quantify cell number, the background survival rate under the ideal conditions was calculated to be 1.46% (Figure 3.3). As the transduction efficiency of the human pSM2+shRNA^{mir} retroviral library was only 3%, a background survival rate of $< 1.5\%$ was sufficiently low enough to permit identification of true positives. Validation studies evolved to utilization of pGIPZ+shRNA^{mir} lentiviral vectors, which offered significantly improved transduction efficiency estimated at 80%. Enhanced transduction of SK-N-FI cells permitted a higher background survival rate to be acceptable. To address this, the concentration of peptide was reduced to 20 μ M, which resulted in a background survival rate of 8.04%.

Our results demonstrated that serum concentration appeared to have the largest impact on the sensitivity of SK-N-FI cells to challenge with the PrP¹⁰⁶⁻¹²⁶ peptide mimicking infectious prion protein. The observation that low plating confluency, method of serum preparation, and serum concentration significantly impacted sensitivity to PrP¹⁰⁶⁻¹²⁶ induced neurotoxicity supports the hypothesis that growth rate is an important regulator of neuronal susceptibility.

4.2.2 Gene Targets Identified from Screening the pSM2+shRNA^{mir} Human Library Utilizing the Novel Prion Neurotoxicity Assay

Identification of culture conditions under which the background survival rate of the human neuroblastoma SK-N-FI cell line was 1.46% permitted screening of the OpenBiosystems pSM2+shRNA^{mir} retroviral library targeting all known open reading frames in the human genome. Completion of screening ~54,000 pSM2+shRNA^{mir} expression vectors identified a total of 544 constructs, of which 80 were sequenced ≥ 3 times and considered to be of interest (Table 3.3). Upon identification of 30 gene targets of interest, validation studies ensued (section 4.4) while library screening continued.

4.2.3 Predicted Network Association of Candidate Genes Identified

Of the total 544 shRNA^{mir} sequenced from surviving SK-N-FI cells, the Ingenuity Pathway Analysis (IPA) software had network association information for 217 (Figure 4.1, Figure 4.2, Figure 4.3, and Figure 4.4). These four major pathways highlight a direct association between candidate gene targets identified, lending support to the validity of those gene targets identified, as well as emphasizing the complex molecular mechanisms potentially underlying prion-mediated neurotoxicity.

Of these, 80 were observed ≥ 3 times from a random colony picking strategy, 21 of which targeted genes currently unconfirmed to encode a protein, and 2 which were predicted to target genomic regions. Of the 57 library identified shRNA^{mir} targeting confirmed transcripts, 46 encoded proteins with function and protein associations described within the IPA database (Figure 3.9). The range of functions associated with

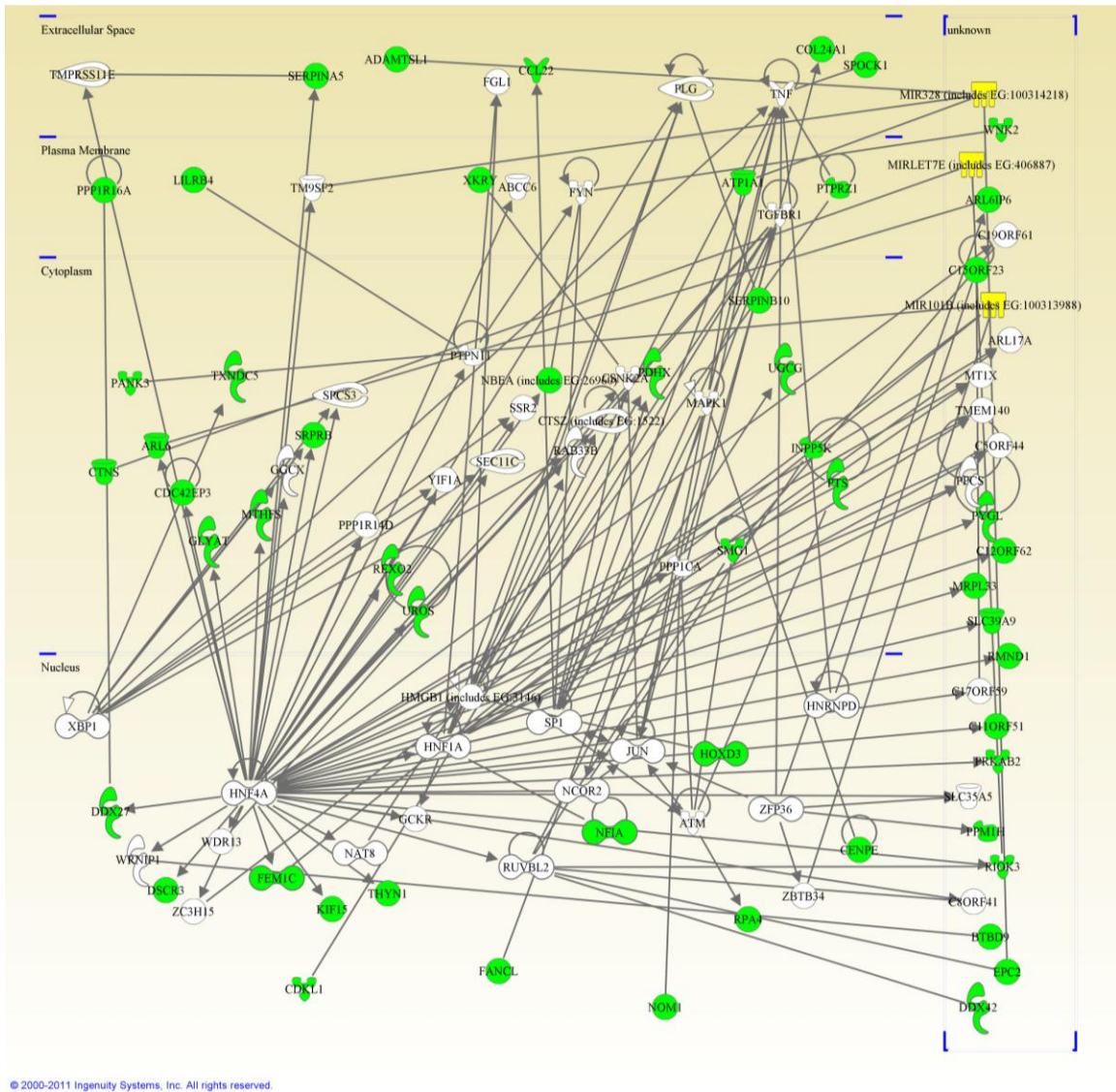


Figure 4.2: Analysis of all shRNA^{mir} Gene Targets Identified, Network 2

Direct network analysis of all gene targets identified from the pSM2+shRNA^{mir} library screen, network 2. Of the 544 gene targets identified, the IPA database contained information for 247. Shown above is network 2, which included 54 focus molecules with an associated p-value of 1×10^{-72} . The associated biological functions are gene expression, DNA replication, recombination and repair, and energy production. Library identified gene targets are highlighted in green, miRNA in yellow. See Figure 3.10 for legend.

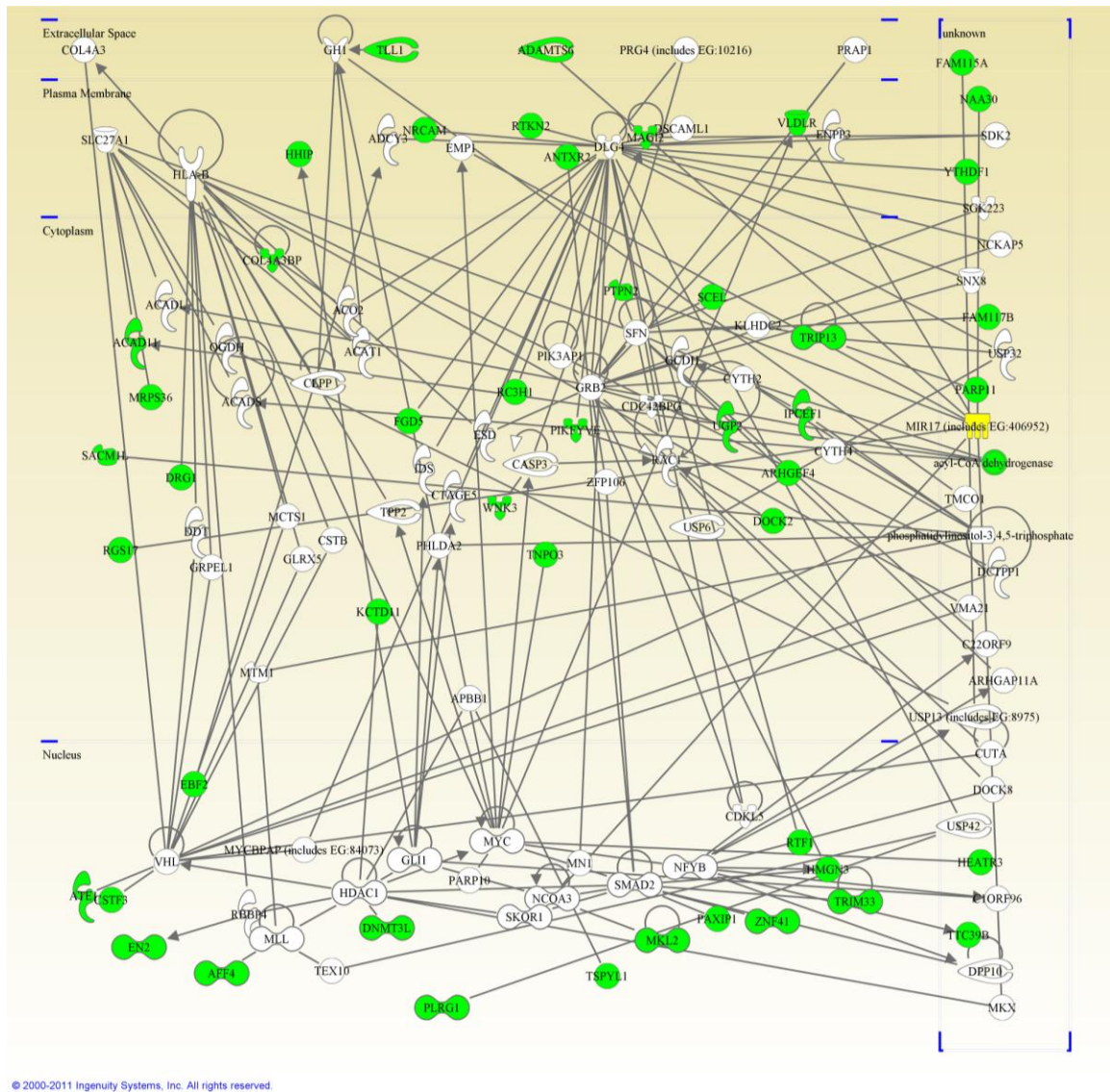


Figure 4.3: Analysis of all shRNA^{mir} Gene Targets Identified, Network 3

Direct network analysis of all gene targets identified from the pSM2+shRNA^{mir} library screen, network 3. Of the 544 gene targets identified, the IPA database contained information for 247. Shown above is network 3, which included 49 focus molecules with an associated p-value of 1×10^{-64} . The associated biological functions are cellular growth and proliferation, tissue morphology, and gene expression. Library identified gene targets are highlighted in green, miRNA in yellow. See Figure 3.10 for legend.

the library-identified candidate genes further confirms the diverse molecular mechanisms potentially mediating prion-mediated neurotoxicity.

4.2.3.1 Predicted Indirect Network Association of Library Identified Positives

Analysis of direct and indirect associations between all 46 library identified gene targets for which information was described within the IPA database revealed a network which included 45 of the 46 molecules. The network associated p-value was 1×10^{-102} indicating that the association of the identified gene targets into this network by random chance is statistically insignificant (Figure 3.11). Of the central regulators of this network association, nuclear factor kappa B (NF κ B) and β -estradiol were of particular interest as both have been previously reported to influence prion disease (Kim et al. 1999; Bacot et al. 2003; Waschbisch et al. 2006; Bai et al. 2008; Loeuillet et al. 2010). The central role these key regulators have in the identified network provide strong support for the prion neurotoxicity assay described in this thesis as effectively mimicking the *in vivo* disease mechanism.

4.2.3.2 Predicted Direct Network Association of Library Identified Positives

Analysis of the association networks between all 46 library identified gene target encoded proteins described within the IPA database, permitting a maximum of 140 molecules per network and only considering direct associations, identified 40 as intermediates of a single network (Figure 3.12). The analysis revealed the top three biological functions associated with these 46 proteins are (i) genetic disorder, (ii) neurological disease, and (iii) metabolic disease (28, 19, or 17 proteins, respectively)

(Table 3.4). The 3 top biological functions associated with the identified proteins have been previously attributed to prion diseases. In reference to the first associated attribute, it has been well established that prion diseases can be genetically transmitted and that susceptibility is influenced by genetic mutations (Hamir et al. 2009; Hiraga, Kobayashi, and Kitamoto 2009; Lukic et al. 2010; Alzualde et al. 2010; Béjot et al. 2010). The second associated attribute can be interpreted as either referring to the fact that in prion disease, the central nervous system is the predominant site affected, or that those afflicted with a prion disorder present with neurological disturbances. Immunohistological examination of brain tissue from prion affected individuals display extensive neurodegeneration. Those suffering from a prion disease often initially present with symptoms of neurological dysfunction including behavioural and memory disturbances (Gajdusek and Zigas 1959; Forloni et al. 1993; Jeffrey et al. 1995; Fatzer et al. 1996). The third associated attribute is disruption of normal metabolic processing in prion infected hosts. Abnormal metabolic processing has been previously identified in those suffering from a prion disorder, the importance of which is currently not recognized. For example, reduced N-acetylaspartate (the precursor to the neurotransmitter N-acetylaspartylglutamate and a mediator of neuronal mitochondrial energy metabolism) and increased myo-inositol (influences behaviour) are observed in advanced prion disease (Forloni et al. 1993; Booth et al. 2004; Vidal et al. 2006; Simon et al. 2008), but whether this is a cause or effect of prion pathogenesis is not known.

The fact that these 3 functions have been previously implicated in prion disease and are the top biological functions associated with the genes identified from the library screen provides supporting evidence for the relevance of the gene targets identified using

the prion neurotoxicity assay described in this thesis. These characteristics are also observed in related proteinaceous neurological disorders including Alzheimer's and Huntington's diseases (Ferreira et al. 2010; Rosenstock, Duarte, and Rego 2010).

4.2.3.3 Association of Library Identified Gene Targets with Htt-Interacting Proteins

A subset of library-identified gene targets potentially mediating prion neurotoxicity were found to associate with Huntington (Htt)-interacting proteins. The Htt protein is the causative agent of Huntington's disease, which, similar to prion disease, is a proteinaceous neurological disorder that is invariably fatal (Rubinsztein and Carmichael 2003; Nakamura and Aminoff 2007; Ramaswamy, Shannon, and Kordower 2007; Walker 2007). Five library identified gene targets associate directly with the Htt protein (Agrn, Chchd3, Gng7, Sqstm1, and Tpp1). Within the same network, 11 identified proteins associated with the Htt protein through 1 intermediate (Ankrd42, Arf3, Axl, E2f1, Nos3, Pdgfra, Pole2, Piwil1, Syncrip, Ugp2, and Ythdf1). With the associated p-value of this network being 1×10^{-87} , it is statistically unlikely that the 16 different library identified protein candidates that directly or indirectly interact with the Htt protein were sequenced from the respective pools by random chance. The close association of the above mentioned library identified gene targets with Htt interacting proteins suggests that the underlying neurotoxic mechanisms of these two proteinaceous diseases could be via common underlying modulators. It has been previously reported that overexpression of PrP^c in neuronal cells expressing the disease-associated mutant Htt protein influences Htt protein aggregation (Lee et al. 2007), lending support to the idea that a similar genetic pathway may mediate these two related proteinaceous neurodegenerative disorders.

Therefore, knockdown of specific gene targets identified may offer potential therapeutic targets for Huntington's and prion disease, or they could represent genetic factors common to proteinaceous neurodegenerative disorders.

4.2.3.4 MicroRNAs Involved in the Identified Network Association

There were 3 miRNAs identified as mediators of the direct association network determined by the IPA software for the 46 library identified positives for which information was known. These were miR-let-7E, miR-195, and miR-202. Of the limited number of studies looking at miRNAs in neurodegenerative disorders, miR-195 has been previously shown to be differentially expressed in a macaque model of prion disease using microarray technology (Montag et al. 2009). Identification of gene targets regulated by miR-195 using the described prion neurotoxicity assay adds support to its potential involvement in prion disease, and provides preliminary validation as to the involvement of these gene targets in prion-mediated neurodegeneration.

4.3 Gene Expression of Identified Gene Targets in Mouse Brain

Of the 80 identified gene targets appearing ≥ 3 times from the library screen, 57 targeted validated transcripts, with individual validation using 3 lentiviral vectors per gene being beyond the scope of this Ph.D project. To provide an alternative validation of the relevance of library identified gene targets to prion disease, qPCR analysis of the relative expression levels in brains of control and prion infected mice was performed (Mohr, Bakal, and Perrimon 2010). This technique aided in identification of which gene targets warranted further investigation in the future. Those observed to be significantly

increased or decreased in concert with disease progression in infected relative to control mouse brains were considered the most interesting. Due to discrepancies between the human and mouse genomes, as well as including the limitation that at least one primer of the set must span an exon-exon junction, gene specific primers targeting 49 of the 57 validated transcripts were designed against the mouse gene equivalents and their relative expression level was determined in mouse brain (Figure 3.7).

There was no specific trend expected for library-identified positives, but differential expression in disease relative to control samples supports their involvement in prion disease (Figure 3.13). It is important to note that the observed relative mRNA expression profiles could be cell type specific as no measures were taken to look at specific cellular subtypes, instead the whole brain was used for qPCR analysis. Future experimentation using selectivity for specific cellular populations (neurons, astrocytes, microglia, etc.) or brain regions would clarify the expression pattern of a particular gene target in a given cell type or cerebral centers. Regardless, the fact that the majority of library identified gene targets exhibit differential relative mRNA abundance between control and scrapie ME7 prion infected mouse brains highlights their involvement in prion disease neurotoxicity.

The differential abundance of the majority of gene targets between brains of control and prion infected mice suggests that their pattern of expression may be indicative of prion infection. The relative expression level was unique for each library identified gene target at a particular time point, but 4 distinct patterns were observed which were broken down to genes induced early, genes induced late, genes reduced early, and genes exhibiting no discernible pattern. Expression levels of *abcb4*, *ankrd42*,

arl6ip6, *gng7*, *plunc*, *ptma*, *trpm6*, and *ugp2* were all significantly upregulated in prion infected relative to control rodent brains as early as 28dpi, indicating these gene targets could potentially represent early genetic markers of prion affliction. Other gene targets, such as *axl*, *st8sia6*, and *tpp1*, were not significantly upregulated in prion infected mice relative to controls until late in the disease course. The expression of these gene targets may be directly influenced by accumulation of PrP^{res} aggregates, limited activity of PrP^c, or in response to significant neurodegeneration. Those gene targets identified that demonstrated a significant reduction in their relative expression level early in disease course were *agnr*, *arf3*, *c10orf71*, *cntnap2*, *ctns*, *e2f1*, *fzd5*, *irf2bp2*, *lig3*, *nfia*, *pdgfra*, *syncrip*, *trpm6* (significantly increased at 28dpi, then significantly reduced by dpi 60), *ube2cbp*, *vps13c*, and *wdr7*. The observation that the library screen identified knockdown of these transcripts as protective, and that *in vivo* their relative expression is reduced, implies that a reduction of these genes is an endogenous response to prion infection. It also suggests that there may be a threshold of remaining protein activity sufficient to support disease progression, or that interplay between a number of identified gene targets is essential to disease manifestation in a complex organ such as the brain. It may also be that the observed reduction in the relative gene expression in whole brain of infected relative to control mice is masking a neuronal-specific pattern. The remaining library identified gene targets included *ccnt2*, *ddx27*, *dscr3*, *en2*, *fam119a*, *inpp5k*, *lppr4*, *narf*, *nos3*, *parm1*, *piwill*, *pole2*, *ptpr*, *pts*, *rnf7*, *sqstm1*, *tbc1d7*, *txndc5*, *uox*, and *ythdf1* which showed a general pattern of no differential expression between infected and control, although significant differences were observed for some at various time points. These gene targets require further experimentation as significant reduction of the

associated protein may confer resistance upon neuronal cells against prion-mediated neurodegeneration. Furthermore, their potential role in disease progression may have been previously overlooked as analyses such as microarray technologies would fail to identify genes not significantly differentially expressed.

The possibility that the differentially abundant genes mentioned above could be used as biomarkers of prion infection as early as 28dpi in the case of the C57BL/6 mouse model of scrapie ME7 should not be overlooked. Therefore, examination of their involvement in prion-mediated neurodegeneration and their potential as biomarkers in other affected species, including humans, is warranted. Examination of the expression profile of the 49 gene targets listed above in alternate models of neurological disease, for example ALS, Alzheimer's, and Huntington's disease, would be particularly interesting as these may represent commonly dysregulated gene transcripts. More importantly, there may be a unique expression profile for each of these neurodegenerative disorders, presenting the possibility of a genetic screen for disease discrimination.

4.4 Validation Studies of Library Identified Gene Targets of Interest *in vitro*

Individual pSM2+shRNA^{mir} targeting the first 30 gene targets identified from the library screen were re-confirmed for their ability to confer protection upon SK-N-FI cells against prion neurotoxicity. During these confirmation studies, screening of the pSM2+shRNA^{mir} library continued, which identified a further 50 gene targets, for a total of 80 that were sequenced ≥ 3 times (Table 3.3).

4.4.1 Confirming Protection against PrP¹⁰⁶⁻¹²⁶ Induced Neurotoxicity Using a Subset of Library Identified pSM2+shRNA^{mir} Sequences

Of the 30 gene targets initially identified from the library screen, 11 showed reproducible and significant protection against challenge with the PrP¹⁰⁶⁻¹²⁶ peptide relative to SK-N-FI cells expressing a pSM2+shRNA^{mir} targeting Eg5 (Figure 3.14). These results do not exclude the other identified gene targets as conferring protection due to the unknown effects of Eg5 knockdown on PrP¹⁰⁶⁻¹²⁶ induced neurotoxicity. A comparison of the relative survival rate of a cell population transduced with a particular shRNA^{mir} challenged with PrP¹⁰⁶⁻¹²⁶ compared to PrP^{Scram} would eliminate the possible confounding influence of a control gene target on cell survival as well as remove differences due to transduction efficiency.

It is recognized that cell survival of PrP¹⁰⁶⁻¹²⁶ exposed SK-N-FI cell cultures was not compared back to that of cells challenged with PrP^{Scram}, and therefore it must be acknowledged that the protective potential of knockdown of all other identified gene targets cannot be ignored. Validation studies of library-identified gene targets using individual pGIPZ+shRNA^{mir} lentiviral vectors compared the relative cell survival of transduced SK-N-FI cells exposed to PrP¹⁰⁶⁻¹²⁶ to those exposed to the PrP^{Scram} peptide. This comparison accounts for the relative survival rate of SK-N-FI cells expressing a particular shRNA^{mir}, cellular growth rate, and initial cell number plated.

4.4.2 Limiting the Analysis to *abcb4* and *ube2cbp*

From the 11 gene targets re-confirmed to confer significant protection against prion neurotoxicity (*abcb4*, *acad11*, *ccnt2*, *irf2bp2*, *or6k2*, *rnf7*, *syncrip*, *txndc5*,

ube2cbp, XM_290759, and XM_296653), XM_290759 and XM_296653 were eliminated from further consideration as we chose to focus on only those transcripts which have been validated. The relative protection conferred by knockdown of a specific gene transcript was taken into account, with the 4 most protective being knockdown of *or6k2*, *ube2cbp*, *rnf7*, and *abcb4*, respectively. Due to technical complications identifying gene specific primers for *or6k2* due to the high degree of homology between members of this gene family, it was eliminated from further analysis. Both *rnf7* and *ube2cbp* transcripts encode proteins predicted to function as ubiquitin E3 ligases, with *ube2cbp* conferring greater protection, and therefore *rnf7* was not further analyzed. The selection criteria resulted in two gene targets selected for validation studies, which were *abcb4* and *ube2cbp* (Figure 3.15).

4.5 The ABC Transporter System

Members of the ATP-binding cassette (ABC) transporter superfamily regulate the transport of various molecules across intracellular and extracellular membranes. Of this superfamily, ATP-binding cassette, subfamily B, member 4 (Abcb4, also termed multidrug resistance p-glycoprotein 3, Mdr-3) was identified from the library screen. Abcb4 translocates phosphatidylcholine (PC) from the inner to the outer leaflet of the hepatocyte membrane to maintain homeostasis and mediates the efflux of PC into bile (Oude Elferink and Paulusma 2007; Morita et al. 2007). Although Abcb4 has been predominantly studied in the hepatic system, it is also expressed in many other cell types and tissues including the nervous system (Lukk et al. 2010). The role of nervous system-expressed Abcb4 remains elusive, and therefore it is difficult to hypothesize its potential

role in prion neurotoxicity. Its known role as a lipid translocase could influence membrane composition, including lipid raft micro-domain formation, which is known to play a role in prion disease through the concentration of PrP^C and PrP^{res} to these domains via their GPI anchor and thereby facilitating PrP^C conversion and the formation of oligomers (Gilch, Kehler, and Schatzl 2006; Bate, Tayebi, and Williams 2010). In addition, Abcb4's action as a translocase and its ability to efflux the PC lipid could mediate simultaneous efflux of infectious PrP^{res} degradation fragments to the extracellular environment. If either hypothesis were correct, a significant reduction of Abcb4 expression levels would reduce prion-mediated neurotoxicity and spread. Through limiting lipid raft micro-domain formation, the concentration of cell-surface template PrP^C molecules would be reduced, which in turn would significantly slow or even halt rogue PrP^{res} accumulation. In terms of interfering with efflux, the spread of infectious oligomers would be hampered, limiting the neurotoxicity to individual cells versus the infectivity escalating to all neighboring cells.

4.5.1 Correlation of *abcb4* Analysis and Molecular Expectations

There are 8 potential human *abcb4* mRNA transcript splice variants, with 3 predicted to encode valid representative proteins (AceView, <http://www.ncbi.nlm.nih.gov/IEB/Research/Acembly/index.html>). The 3 predicted transcript variants were all targeted by the three pGIPZ+shRNA^{mir} tested for their ability to confer protection (93064, 93067, and 230814) against PrP¹⁰⁶⁻¹²⁶ mediated neurotoxicity. Of these three shRNA^{mir} tested, only transduction of SK-N-FI cells with pGIPZ+93067 led to a sufficient number of cells for AlamarBlue quantification. This

may be due to cellular toxicity caused by shRNA^{mir} 93064 and 230814, potentially as a result of non-specific gene knockdown.

Of the 3 transcript variants targeted by the shRNA^{mir}, only 2 had recognition sites for both the forward and reverse primers used for qPCR analysis (145.5 and 140.7kDa predicted). The third transcript (135.3kDa predicted) lacked a forward primer recognition site due to alternative splicing (Figure 4.5). The qPCR analysis showed a 68.67% knockdown of *abcb4* mRNA in SK-N-FI cells transduced pGIPZ+93067, demonstrating the significant efficiency of knockdown of this shRNA^{mir} and suggesting a correlation between *Abcb4* expression and resistance to prion neurotoxicity (Figure 3.17). These results suggest that 2 of the 3 valid transcripts were quantified by qPCR analysis using the primers listed in Table 2.1, but whether one or both transcripts were significantly reduced remains undetermined. Further experimentation is required to identify which of these transcripts are significantly reduced by the pGIPZ+93067 shRNA^{mir} and which transcript(s) plays the most significant role in prion-mediated neurotoxicity.

Independent of the impact individual transcript variants have on susceptibility to PrP¹⁰⁶⁻¹²⁶ mediated neurotoxicity, it is apparent that a reduction of *abcb4* mRNA imparts significant resistance and therefore warrants further investigation as to its potential role in prion disease.

4.6 The Ubiquitin-Proteasome System (UPS)

The ubiquitin-proteasome system (UPS) regulates protein degradation by transferring ubiquitin to target proteins through a regulated cascade (Figure 4.6).

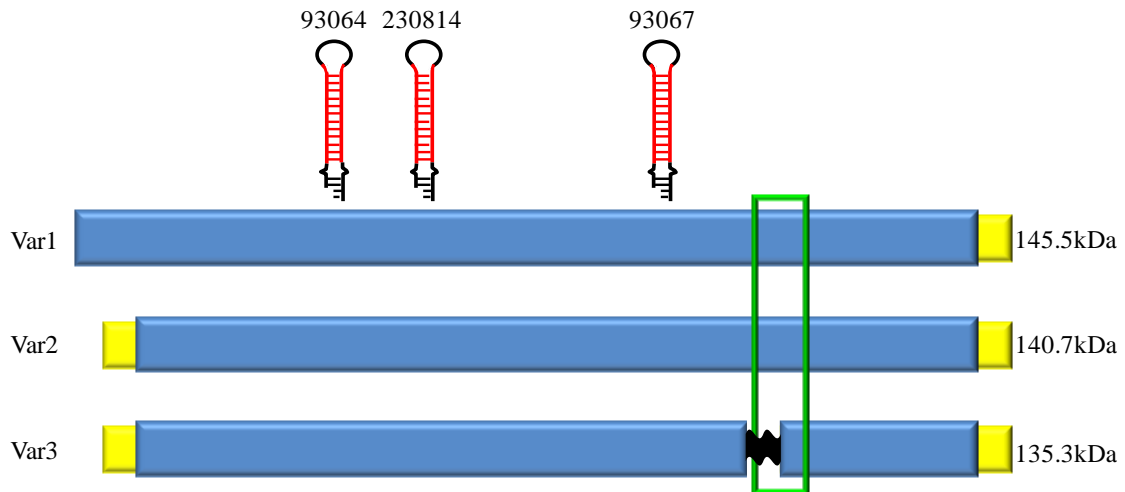


Figure 4.5: Human *abcb4* Targeting and Detection

Comparison of the human *abcb4* gene structure to that of the shRNA^{mir} and primers used to confirm results. To ensure that the results observed with the pGIPZ+shRNA^{mir} agree with the known and predicted splice variants of human *abcb4*, their targeting sequence was determined along the full length mRNA. The region of mRNA amplified by the primer pairs used was also determined to correlate expression levels with that of transcript variants targeted. Of the 3 transcript variants represented above, variant 3 lacked a binding site for the forward primer used, indicating that the relative expression levels calculated were of variants 1 and 2. Full length mRNA is shown in yellow, the open reading frame in blue. The corresponding protein sizes are listed beside the appropriate transcript. The black and red stem-loop structures indicate relative sites targeted by the shRNA^{mir} tested, with the corresponding pGIPZ accession number listed above. The green box indicates the region amplified by the PCR primers used, and the black squiggle indicates a difference in the coding region due to absence of a particular exon.

Ubiquitin is initially added to a cysteine residue of a ubiquitin-activating enzyme (E1) in an ATP-dependent reaction. There are 2 E1s known to be involved in the addition of ubiquitin to proteins, Uba1 and Uba6. Ubiquitin is then transferred to the active site of a ubiquitin-conjugating enzyme (E2), of which there are at least 30 different E2s. The E2 proteins transfer the ubiquitin protein to a ubiquitin-ligase enzyme (E3). E3 ubiquitin ligases impart specificity upon the UPS system. E3 proteins possess two important recognition domains, one for binding the E2 enzyme, and the other for interacting with proteins containing a specific amino acid sequence. There are thousands of different E3 ligases, each recognizing a unique amino acid sequence motif within both their associated E2 and target proteins (van Wijk and Timmers 2010). Highly regulated poly-ubiquitination of specific substrate proteins for degradation via the proteasome proceeds via optimized E1-E2-E3 pathways (Huang et al. 2008).

4.6.1 Involvement of the UPS in Prion Disease

Although the Ube2cbp E3 ubiquitin ligase has not been previously described as participating in prion disease, the UPS has been implicated in prion disease and related neurodegenerative disorders (Lowe et al. 1990; Leroy et al. 1998; Yedidia et al. 2001; de Pril et al. 2004; Adori et al. 2005; Kristiansen et al. 2007; Bennett et al. 2007; Saba et al. 2008; Wang et al. 2008; Cecarini et al. 2010). Drug-mediated inhibition of the proteasome sensitizes PrP^{res} exposed neuronal cells to apoptotic-mediated cell death, and leads to accumulation of cytotoxic cytoplasmic PrP^{res} aggregates (Ma, Wollmann, and Lindquist 2002; Kristiansen et al. 2005). The hypothesis that oligomeric

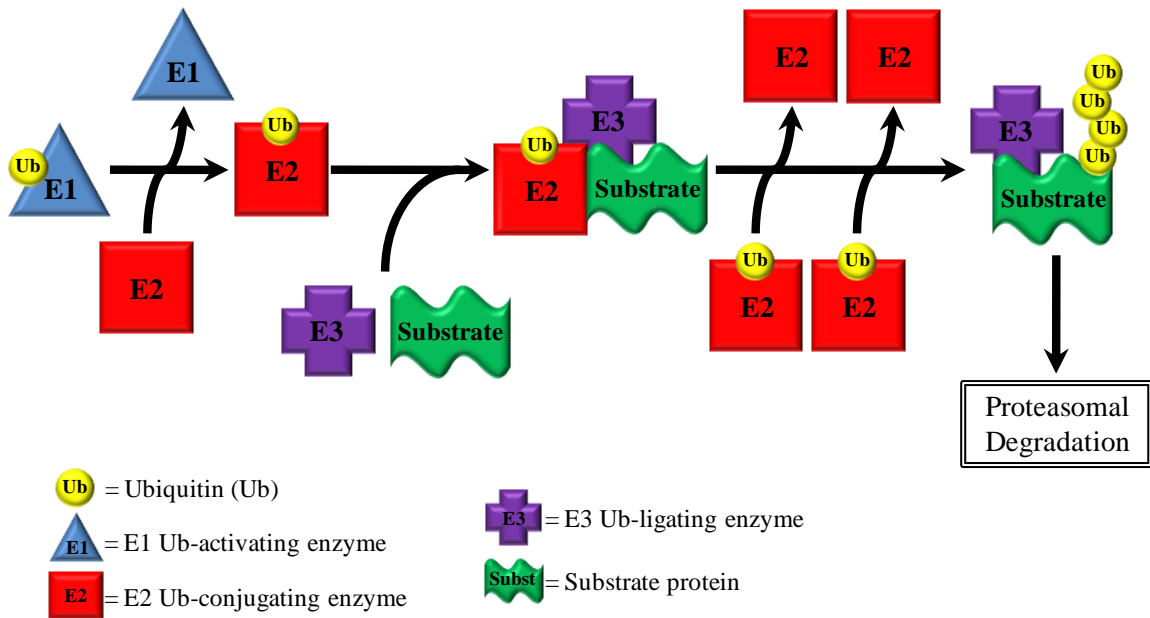


Figure 4.6: Overview of the Ubiquitination Pathway

Through a series of protein-protein interactions, ubiquitin is transferred to a specific substrate protein for targeting to the proteasome for degradation. Ubiquitin is initially bound to an E1 ubiquitin-activating enzyme via an ATP-dependent reaction. The ubiquitin is then transferred to an E2 ubiquitin-conjugating enzyme. A specific E3 ubiquitin-ligase enzyme with a recognition sequence for a particular substrate mediates the transfer of ubiquitin from the E2 enzyme to the intended substrate. Through repeated successive ubiquitin ligation reactions to the specific substrate, the intended protein becomes poly-ubiquitinated and targeted for degradation via the proteasomal system. Through this tightly regulated degradation pathway, the functionality of a specific protein is controlled. This provides a mechanism for the cell to rapidly regulate protein activity, thereby responding to a particular chemico-physical perturbation (Lehman 2009).

species of PrP^{res} represent the infectious agent is supported by the observation that oligomeric PrP^{res} inhibits the catalytic activity of the proteasome, causing accumulation of not only PrP^{res} species, but also non-functional proteins in general (Kristiansen et al. 2007).

4.6.2 Function of Ube2cbp

The function of Ube2cbp (also termed C6orf157) is currently unknown. The carboxyl terminus shows weak sequence homology to a HECT domain, an amino acid sequence found in certain E3 ubiquitin-protein ligase proteins which catalyze the addition of ubiquitin to target proteins (Kobirumaki et al. 2005; Metzger and Weissman 2010). Ube2cbp has been demonstrated to associate with and ubiquitinate Cyclin B *in vitro* via its HECT-like domain (Kobirumaki et al. 2005). Cyclin B, bound to Cdc2, is required by the anaphase-promoting complex/cyclosome (APC/C) for progression through the M-phase of the cell cycle. This suggests that Ube2cbp may play a regulatory role in the cell cycle via regulating Cyclin B activity, (Kobirumaki et al. 2005), possibly through ubiquitination and targeted proteasomal degradation. However, Cyclin B degradation is also mediated by the APC/C-Cdc20 complex (Yamamoto et al. 2005), so Ube2cbp may not represent the major regulatory factor but instead act to fine tune Cyclin B degradation.

One hypothesis as to why knockdown of Ube2cbp in SK-N-FI cells conferred protection against PrP¹⁰⁶⁻¹²⁶ mediated cell death is that Ube2cbp binds to an as yet unrecognized mediator (for example a protein protecting against excitotoxicity, or maybe even PrP itself) of prion disease. Therefore, significantly reducing expression of

Ube2cbp would limit the targeting of Protein X to the proteasome, and if indeed it does bind PrP, limit the generation of cytotoxic degradation species. Protein X could also be a naturally aggregative protein, so reducing targeting of Protein X for proteasomal degradation would prevent overloading of the proteasome system. Conversely, Ube2cbp may recognize a pro-survival protein (Protein S), and so a reduction of Ube2cbp would increase the cellular concentration of Protein S, thereby signalling cell survival and conferring protection against prion-mediated neurotoxicity. Investigation into the role Ube2cbp plays in prion-mediated neurotoxicity warrants further investigation.

4.6.2.1 Predicting Ube2cbp Protein Interactions

Using the online eukaryotic linear motif (ELM) resource for functional sites in proteins prediction software (<http://elm.eu.org/>, release current as of Dec 2010), 36 different conserved motifs were identified within Ube2cbp. Identified motifs included cyclin interaction domains, MAPK binding motifs, a 14-3-3 interaction motif (a protein consistently upregulated in CSF from CJD-affected individuals) (Chohan et al. 2010), numerous class III PDZ motifs involved in directing multisubunit protein complexes, casein kinase 1 and 2 phosphorylation motifs, GSK3 phosphorylation motifs, and 11 different motifs specifying various glycosylation modifications.

The potential interaction between the library identified Ube2cbp and a biomarker of neurodegeneration adds support for the biological relevance of the prion neurotoxicity assay described in this thesis for identifying potential gene targets of interest relevant to neurotoxicity. The presence of so many different predicted phosphorylation and

glycosylation motifs suggests that Ube2cbp activity may be tightly regulated and that multiple bands are expected upon Western blot analysis.

The predicted interaction of Ube2cbp with such a variety of protein motifs suggests that it may associate with and ubiquitinate a large number of proteins, leading to their proteasomal degradation. This leads to the hypothesis that knockdown of Ube2cbp may be protective as a result of a concomitant increase in the expression of a recognized protein. Therefore, continued study of Ube2cbp and proteins regulated by Ube2cbp is warranted.

4.6.2.2 Correlation of *ube2cbp* Analysis and Molecular Expectations

Human *ube2cbp* is predicted to produce 8 different potential protein-coding splice variants (AceView, <http://www.ncbi.nlm.nih.gov/IEB/Research/Acembly/index.html>). Of these, 2 confirmed and 1 predicted transcript encode proteins recognized by the custom antibody used targeting amino acids 269-280. Of the 3 pGIPZ+shRNA^{mir} targeting *ube2cbp* (139483, 139486, and 273404), only transduction of SK-N-FI cells with pGIPZ+139486 led to a sufficient number of cells for AlamarBlue quantification. This may be due to cellular toxicity caused by shRNA^{mir} 139483 and 273404, potentially as a result of non-specific gene knockdown.

The pGIPZ+273404 shRNA^{mir} targeted only 2 of the 3 transcripts encoding proteins recognized by the α -Ube2cbp antibody, while the other 2 shRNA^{mir} targeted all 3 transcripts (Figure 4.7). The 2 larger transcripts targeted by all 3 shRNA^{mir} possessed sequences complementary to the primer set used for qPCR analysis (43.7 and 40.3kDa predicted). The smallest predicted protein (~22.2kDa predicted) was targeted by 139483

and 139486, with 139486 targeting the non-validated 3' end (no evidence of polyadenylation). This 22.2kDa protein encoding predicted transcript was not expected to be amplified by the primer set used. The observed 64.63% knockdown of *ube2cbp* mRNA as determined by qPCR analysis is consistent with the expected results given the portion of the *ube2cbp* transcript targeted by the protective shRNA^{mir} (139486) and the primer set used (Figure 3.17).

Given the region of Ube2cbp recognized by the antibody, 3 bands of significantly different sizes, all targeted by pGIPZ+139486 shRNA^{mir}, were predicted. The expected result was that all 3 would show reduced levels or protein expression (Figure 3.18 & Figure 3.19). The unexpected result was lack of significant protein knockdown of predicted transcript variant 3 (22.2kDa). This could be due to inconsistencies between the predicted mRNA sequence and the actual sequence, or it is also possible that the antibody is detecting one of the other predicted transcript variant proteins (e.g. a 14.3kDa protein, AceView). This predicted 14.3kDa protein encoding transcript was not targeted by any of the shRNA^{mir} tested and would agree with the observed results.

Further experimentation is required to identify which of the 3 predicted *ube2cbp* variants targeted by pGIPZ+139486 shRNA^{mir} are significantly reduced and which protein-coding transcript(s) plays the most significant role in prion-mediated neurotoxicity. Independent of the impact individual variants have on susceptibility to PrP¹⁰⁶⁻¹²⁶ mediated neurotoxicity, it is apparent that a reduction of Ube2cbp, demonstrated at both the mRNA and protein level, imparts significant resistance and therefore warrants further investigation as to its potential role in prion disease. The potential of using the custom antibody for examination of Ube2cbp in brain samples from

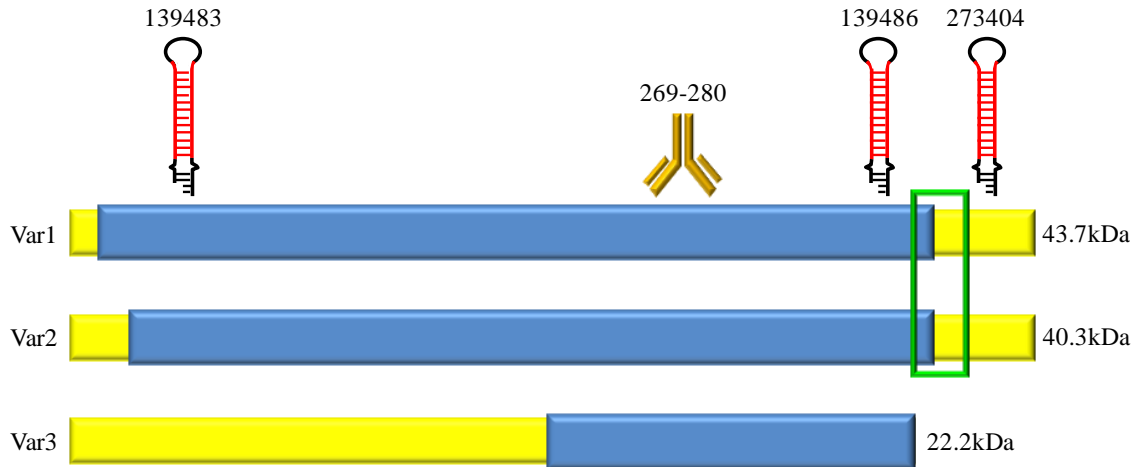


Figure 4.7: Human *ube2cbp* Targeting and Detection

Comparison of the human *ube2cbp* gene structure to that of the shRNA^{mir}, primers, and antibody used to confirm results. To ensure that the results observed with the pGIPZ+shRNA^{mir} agree with the known and predicted splice variants of human *ube2cbp*, their targeting sequence was determined along the full length mRNA. Of the 3 transcript variants represented above, variant 3 lacked a shRNA^{mir} recognition site for 273404. shRNA^{mir} 139486 recognized the very 3' end of the predicted 3rd transcript. The region of mRNA amplified by the primer pairs used was also determined to correlate expression levels with that of transcript variants targeted. The α -Ube2cbp antibody used targeting amino acids 269-280 recognized all three transcript variants depicted above and is depicted as an upside-down brown Y. Full length mRNA is shown in yellow, the open reading frame in blue. The corresponding protein sizes are listed beside the appropriate transcript. The black and red stem-loop structures indicate relative sites targeted by the shRNA^{mir} tested, with the corresponding pGIPZ accession number listed above. The green box indicates the region amplified by the PCR primers used.

prion infected mice has been demonstrated by collaborators at the St. Boniface Research Center, in that they used immunostaining to confirm cross-reactivity of this antibody with the corresponding mouse protein (Figure 4.8). Prominent expression in the cytoplasm of both astrocytes and neurons is apparent. Collaborators in Lethbridge, Alberta are currently examining the cross-reactivity potential of the Ube2cbp antibody with brain samples derived from cow, with the future goal being comparing the staining pattern between BSE infected and control samples.

4.7 Summary of Library Screening

Using the novel neurotoxicity assay described in this thesis, screening of a human shRNA^{mir} retroviral library and validation using lentiviral constructs has identified 2 previously unrecognized potential mediators of prion neurotoxicity. Further evaluation of *abcb4* and *ube2cbp*, as well as alternate gene targets identified from this screen, should be considered of particular interest in future prion research.

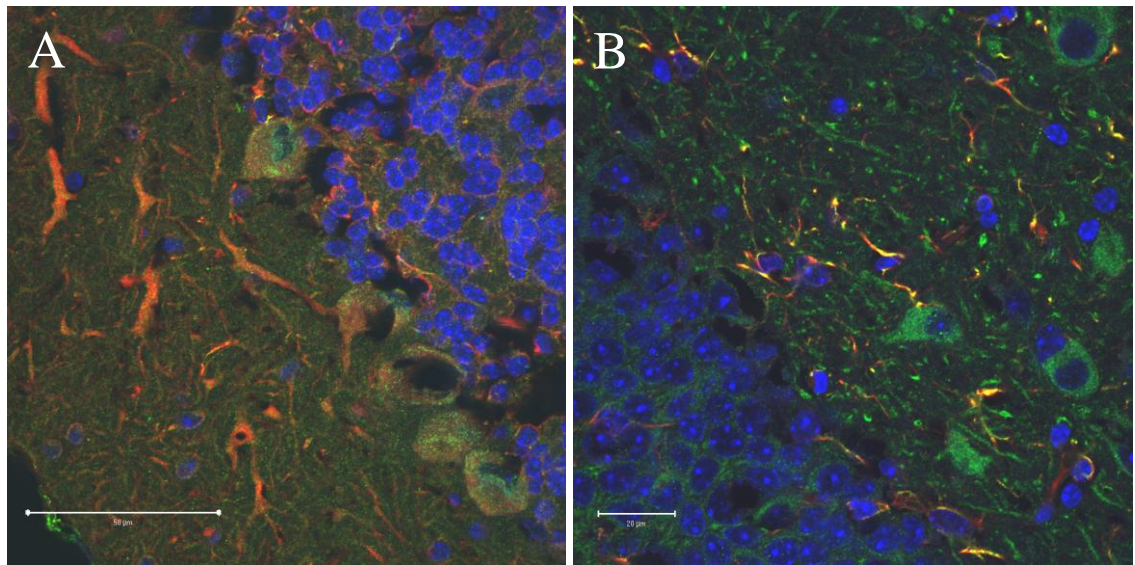


Figure 4.8: Subcellular Localization of Ube2cbp in Mouse Brain

Using the custom antibody targeting amino acid residues 269-280 of human Ube2cbp, the subcellular localization was determined. The expression pattern of Ube2cbp was analyzed in four regions of the brain (cerebellum, corpus collosum, cortex, and hippocampus) and co-localized with an astrocyte marker (GFAP) or a neuronal marker (MAP2). Two representative images are shown above. A) Cerebellum stained with Ube2cbp (Green) and MAP2 (Red). B) Hippocampus stained with Ube2cbp (Green) and GFAP (Red). Nuclei are stained blue. It can be seen clearly that Ube2cbp co-localizes within the cytoplasm of both neurons and astrocytes. This staining was generously conducted by our collaborators Jillian LeMaistre and Christopher Anderson at the St. Boniface Research Center in Winnipeg, Manitoba.

5. Conclusions

This thesis represents the first description of conditions under which human neuroblastoma cells were successfully used to model prion neurotoxicity. Summarily, these conditions consisted of plating SK-N-FI human neuroblastoma cells at 40,000 cells/well of a 6-well plate, and re-applying fresh PrP¹⁰⁶⁻¹²⁶ neurotoxic peptide every 48 hours, diluted to 50µM in SK-HI-DMEM5 (representing 3.8% of final volume) and SK-HI-DMEM1 (representing 96.2% of final volume), for a total of 5 applications. The background survival rate of SK-N-FI cells was 1.46%, which is significantly lower than any previously published results and sufficiently low enough to permit screening of a shRNA^{mir} retroviral library.

Using the novel *in vitro* prion neurotoxicity assay developed during this project, ~54,000 pSM2+shRNA^{mir} constructs were screened for their potential ability to knockdown a gene target essential to prion neurotoxicity. From this screen, 80 gene targets of interest were identified as conferring protection upon human SK-N-FI neuroblastoma cells challenged with the PrP¹⁰⁶⁻¹²⁶ peptide. Using the Ingenuity Pathway Analysis software, predicted association networks between these gene targets of interest were identified. Analysis of 49 identified gene targets encoding validated transcripts and for which gene-specific primers could be designed was carried out *in vivo*. The differential abundance of the majority observed throughout disease progression in a mouse model of prion disease supports the hypothesis that they are correlated to prion neurotoxicity, although their exact role is currently unknown.

Re-testing knockdown of 30 of these 80 gene targets confirmed that 11 confer significant protection upon human SK-N-FI neuroblastoma cells, two of which were *abcb4* and *ube2cbp*. Knockdown of *abcb4* or *ube2cbp* using lentiviral-based

pGIPZ+shRNA^{mir} expression vectors demonstrated a significant reduction at the mRNA level and further confirmed a significant degree of protection is conferred by the knockdown of the transcripts. Further analysis of the role these genes play in prion-mediated neurotoxicity is warranted.

From the work accomplished throughout this Ph.D project, it can be stated that the involvement of a subset of library identified gene targets in related neurodegenerative disorders, the differential abundance of gene targets in a mouse model of prion disease, and the reproducible protection conferred against PrP¹⁰⁶⁻¹²⁶ neurotoxicity provides strong supportive evidence for the validity of the described prion neurotoxicity cell culture assay. Reproducible protection conferred by significant knockdown of either *abcb4* or *ube2cbp* demonstrates their potential importance in mediating prion-induced neurodegeneration, and emphasizes the potential role of alternate gene targets identified from the library screen as previously unrecognized mediators of prion disease.

6. References

References

1. Adori C, Kovacs GG, Low P, Molnar K, Gorbea C, Fellingner E, Budka H, Mayer RJ, and Laszlo L (2005) The ubiquitin-proteasome system in Creutzfeldt-Jakob and Alzheimer disease: intracellular redistribution of components correlates with neuronal vulnerability. *Neurobiol.Dis.* 19 (3):427-435.
2. Aguzzi A and Calella AM (2009) Prions: protein aggregation and infectious diseases. *Physiol Rev.* 89 (4):1105-1152.
3. Aguzzi A and Polymenidou M (2004) Mammalian prion biology: one century of evolving concepts. *Cell* 116 (2):313-327.
4. Alper T, Cramp WA, Haig DA, and Clarke MC (1967) Does the agent of scrapie replicate without nucleic acid? *Nature* 214 (5090):764-766.
5. Alper T, Haig DA, and Clarke MC (1966) The exceptionally small size of the scrapie agent. *Biochem.Biophys.Res.Comm.* 22 (3):278-284.
6. Alperovitch A, Zerr I, Pocchiari M, Mitrova E, de Pedro CJ, Hegyi I, Collins S, Kretzschmar H, van Duijn C, and Will RG (1999) Codon 129 prion protein genotype and sporadic Creutzfeldt-Jakob disease. *Lancet* 353 (9165):1673-1674.
7. Alzualde A, Indakoetxea B, Ferrer I, Moreno F, Barandiaran M, Gorostidi A, Estanga A, Ruiz I, Calero M, van Leeuwen FW, Atares B, Juste R, Rodriguez-Martinez AB, and Lopez dM (2010) A novel PRNP Y218N mutation in Gerstmann-Straussler-Scheinker disease with neurofibrillary degeneration. *J.Neuropathol.Exp.Neurol.* 69 (8):789-800.
8. Anderson L, Rossi D, Linehan J, Brandner S, and Weissmann C (2004) Transgene-driven expression of the Doppel protein in Purkinje cells causes Purkinje cell degeneration and motor impairment. *Proc.Natl.Acad.Sci.U.S.A* 101 (10):3644-3649.
9. Anderson RM, Donnelly CA, Ferguson NM, Woolhouse ME, Watt CJ, Udy HJ, MaWhinney S, Dunstan SP, Southwood TR, Wilesmith JW, Ryan JB, Hoinville LJ, Hillerton JE, Austin AR, and Wells GA (1996) Transmission dynamics and epidemiology of BSE in British cattle. *Nature* 382 (6594):779-788.
10. Ansaloni S, Lelkes N, Snyder J, Epstein C, Dubey A, and Saunders AJ (2010) A streamlined sub-cloning procedure to transfer shRNA from a pSM2 vector to a pGIPZ lentiviral vector. *J.RNAi.Gene Silencing.* 6 (2):411-415.
11. Arends MJ, Morris RG, and Wyllie AH (1990) Apoptosis. The role of the endonuclease. *Am.J.Pathol.* 136 (3):593-608.

12. Bacot SM, Lenz P, Frazier-Jessen MR, and Feldman GM (2003) Activation by prion peptide PrP106-126 induces a NF-kappaB-driven proinflammatory response in human monocyte-derived dendritic cells. *J.Leukoc.Biol.* 74 (1):118-125.
13. Bai S, Goodrich D, Thron CD, Tecarro E, and Obeyesekere M (2003) Theoretical and experimental evidence for hysteresis in cell proliferation. *Cell Cycle* 2 (1):46-52.
14. Bai Y, Li Q, Yang J, Zhou X, Yin X, and Zhao D (2008) p75(NTR) activation of NF-kappaB is involved in PrP106-126-induced apoptosis in mouse neuroblastoma cells. *Neurosci.Res.* 62 (1):9-14.
15. Baringer JR, Bowman KA, and Prusiner SB (1983) Replication of the scrapie agent in hamster brain precedes neuronal vacuolation. *J.Neuropathol.Exp.Neurol.* 42 (5):539-547.
16. Basler K, Oesch B, Scott M, Westaway D, Walchli M, Groth DF, McKinley MP, Prusiner SB, and Weissmann C (1986) Scrapie and cellular PrP isoforms are encoded by the same chromosomal gene. *Cell* 46 (3):417-428.
17. Bassik MC, Lebbink RJ, Churchman LS, Ingolia NT, Patena W, LeProust EM, Schuldiner M, Weissman JS, and McManus MT (2009) Rapid creation and quantitative monitoring of high coverage shRNA libraries. *Nat.Methods* 6 (6):443-445.
18. Bate C, Tayebi M, and Williams A (2010) The glycosylphosphatidylinositol anchor is a major determinant of prion binding and replication. *Biochem.J.* 428 (1):95-101.
19. Beghi E, Gandolfo C, Ferrarese C, Rizzuto N, Poli G, Tonini MC, Vita G, Leone M, Logroscino G, Granieri E, Salemi G, Savettieri G, Frattola L, Ru G, Mancardi GL, and Messina C (2004) Bovine spongiform encephalopathy and Creutzfeldt-Jakob disease: facts and uncertainties underlying the causal link between animal and human diseases. *Neurol.Sci.* 25 (3):122-129.
20. Behrens A, Brandner S, Genoud N, and Aguzzi A (2001) Normal neurogenesis and scrapie pathogenesis in neural grafts lacking the prion protein homologue Doppel. *EMBO Rep.* 2 (4):347-352.
21. Béjot Y, Osseby GV, Caillier M, Moreau T, Laplanche JL, and Giroud M (2010) Rare E196K mutation in the PRNP gene of a patient exhibiting behavioral abnormalities. *Clin.Neurol.Neurosurg.* 112 (3):244-247.
22. Belay ED and Schonberger LB (2005) The public health impact of prion diseases. *Annu.Rev.Public Health* 26:191-212.

23. Bennett EJ, Shaler TA, Woodman B, Ryu KY, Zaitseva TS, Becker CH, Bates GP, Schulman H, and Kopito RR (2007) Global changes to the ubiquitin system in Huntington's disease. *Nature* 448 (7154):704-708.
24. Beranger F, Mange A, Solassol J, and Lehmann S (2001) Cell culture models of transmissible spongiform encephalopathies. *Biochem.Biophys.Res.Commun.* 289 (2):311-316.
25. Bergstrom AL, Chabry J, Bastholm L, and Heegaard PM (2007) Oxidation reduces the fibrillation but not the neurotoxicity of the prion peptide PrP106-126. *Biochim.Biophys.Acta* 1774 (9):1118-1127.
26. Bergstrom AL, Cordes H, Zsuzger N, Heegaard PM, Laursen H, and Chabry J (2005) Amidation and structure relaxation abolish the neurotoxicity of the prion peptide PrP106-126 in vivo and in vitro. *J.Biol.Chem.* 280 (24):23114-23121.
27. Berns K, Hijmans EM, Mullenders J, Brummelkamp TR, Velds A, Heimerikx M, Kerkhoven RM, Madiredjo M, Nijkamp W, Weigelt B, Agami R, Ge W, Cavet G, Linsley PS, Beijersbergen RL, and Bernards R (2004) A large-scale RNAi screen in human cells identifies new components of the p53 pathway. *Nature* 428 (6981):431-437.
28. Bernstein E, Caudy AA, Hammond SM, and Hannon GJ (2001) Role for a bidentate ribonuclease in the initiation step of RNA interference. *Nature* 409 (6818):363-366.
29. Bird SM (2004) Attributable testing for abnormal prion protein, database linkage, and blood-borne vCJD risks. *Lancet* 364 (9442):1362-1364.
30. Birkett CR, Hennion RM, Bembridge DA, Clarke MC, Chree A, Bruce ME, and Bostock CJ (2001) Scrapie strains maintain biological phenotypes on propagation in a cell line in culture. *EMBO J.* 20 (13):3351-3358.
31. Bizat N, Peyrin JM, Haik S, Cochois V, Beaudry P, Laplanche JL, and Neri C (2010) Neuron dysfunction is induced by prion protein with an insertional mutation via a Fyn kinase and reversed by sirtuin activation in *Caenorhabditis elegans*. *J.Neurosci.* 30 (15):5394-5403.
32. Bock LC, Griffin LC, Latham JA, Vermaas EH, and Toole JJ (1992) Selection of single-stranded DNA molecules that bind and inhibit human thrombin. *Nature* 355 (6360):564-566.
33. Bohnsack MT, Czaplinski K, and Gorlich D (2004) Exportin 5 is a RanGTP-dependent dsRNA-binding protein that mediates nuclear export of pre-miRNAs. *RNA.* 10 (2):185-191.
34. Booth S, Bowman C, Baumgartner R, Sorensen G, Robertson C, Coulthart M, Phillipson C, and Somorjai RL (2004) Identification of central nervous system

- genes involved in the host response to the scrapie agent during preclinical and clinical infection. *J.Gen.Virol.* 85 (Pt 11):3459-3471.
35. Bosque PJ and Prusiner SB (2000) Cultured cell sublimes highly susceptible to prion infection. *J.Virol.* 74 (9):4377-4386.
 36. Bounhar Y, Zhang Y, Goodyer CG, and LeBlanc A (2001) Prion protein protects human neurons against Bax-mediated apoptosis. *J.Biol.Chem.* 276 (42):39145-39149.
 37. Bourteele S, Oesterle K, Weinzierl AO, Paxian S, Riemann M, Schmid RM, and Planz O (2007) Alteration of NF-kappaB activity leads to mitochondrial apoptosis after infection with pathological prion protein. *Cell Microbiol.* 9 (9):2202-2217.
 38. Breaker RR (2004) Natural and engineered nucleic acids as tools to explore biology. *Nature* 432 (7019):838-845.
 39. Breaker RR and Joyce GF (1994) A DNA enzyme that cleaves RNA. *Chem.Biol.* 1 (4):223-229.
 40. Brown DR (2001) Copper and prion disease. *Brain Res.Bull.* 55 (2):165-173.
 41. Brown DR and Besinger A (1998) Prion protein expression and superoxide dismutase activity. *Biochem.J.* 334 (Pt 2):423-429.
 42. Brown DR, Qin K, Herms JW, Madlung A, Manson J, Strome R, Fraser PE, Kruck T, von Bohlen A, Schulz-Schaeffer W, Giese A, Westaway D, and Kretzschmar H (1997a) The cellular prion protein binds copper in vivo. *Nature* 390 (6661):684-687.
 43. Brown DR, Schmidt B, and Kretzschmar HA (1996a) A neurotoxic prion protein fragment enhances proliferation of microglia but not astrocytes in culture. *Glia* 18 (1):59-67.
 44. Brown DR, Schmidt B, and Kretzschmar HA (1996b) Role of microglia and host prion protein in neurotoxicity of a prion protein fragment. *Nature* 380 (6572):345-347.
 45. Brown DR, Schulz-Schaeffer WJ, Schmidt B, and Kretzschmar HA (1997b) Prion protein-deficient cells show altered response to oxidative stress due to decreased SOD-1 activity. *Exp.Neurol.* 146 (1):104-112.
 46. Brown DR, Wong BS, Hafiz F, Clive C, Haswell SJ, and Jones IM (1999) Normal prion protein has an activity like that of superoxide dismutase. *Biochem.J.* 344 Pt 1:1-5.

47. Brown HR, Goller NL, Rudelli RD, Merz GS, Wolfe GC, Wisniewski HM, and Robakis NK (1990) The mRNA encoding the scrapie agent protein is present in a variety of non-neuronal cells. *Acta Neuropathol.* 80 (1):1-6.
48. Bruce ME, Boyle A, Cousens S, McConnell I, Foster J, Goldmann W, and Fraser H (2002) Strain characterization of natural sheep scrapie and comparison with BSE. *J.Gen.Virol.* 83 (Pt 3):695-704.
49. Brummelkamp TR, Bernards R, and Agami R (2002) A system for stable expression of short interfering RNAs in mammalian cells. *Science* 296 (5567):550-553.
50. Budka H (2003) Neuropathology of prion diseases. *Br.Med.Bull.* 66:121-130.
51. Bueler H, Aguzzi A, Sailer A, Greiner RA, Autenried P, Aguet M, and Weissmann C (1993) Mice devoid of PrP are resistant to scrapie. *Cell* 73 (7):1339-1347.
52. Bueler H, Fischer M, Lang Y, Bluethmann H, Lipp HP, DeArmond SJ, Prusiner SB, Aguet M, and Weissmann C (1992) Normal development and behaviour of mice lacking the neuronal cell-surface PrP protein. *Nature* 356 (6370):577-582.
53. Butler DA, Scott MR, Bockman JM, Borchelt DR, Taraboulos A, Hsiao KK, Kingsbury DT, and Prusiner SB (1988) Scrapie-infected murine neuroblastoma cells produce protease-resistant prion proteins. *J.Virol.* 62 (5):1558-1564.
54. Cai X, Hagedorn CH, and Cullen BR (2004) Human microRNAs are processed from capped, polyadenylated transcripts that can also function as mRNAs. *RNA.* 10 (12):1957-1966.
55. Carimalo J, Cronier S, Petit G, Peyrin JM, Boukhtouche F, Arbez N, Lemaigre-Dubreuil Y, Brugg B, and Miquel MC (2005) Activation of the JNK-c-Jun pathway during the early phase of neuronal apoptosis induced by PrP106-126 and prion infection. *Eur.J.Neurosci.* 21 (9):2311-2319.
56. Carmell MA, Xuan Z, Zhang MQ, and Hannon GJ (2002) The Argonaute family: tentacles that reach into RNAi, developmental control, stem cell maintenance, and tumorigenesis. *Genes Dev.* 16 (21):2733-2742.
57. Caughey BW, Dong A, Bhat KS, Ernst D, Hayes SF, and Caughey WS (1991) Secondary structure analysis of the scrapie-associated protein PrP 27-30 in water by infrared spectroscopy. *Biochemistry* 30 (31):7672-7680.
58. Cecarini V, Bonfili L, Cuccioloni M, Mozzicafreddo M, Angeletti M, and Eleuteri AM (2010) The relationship between the 20S proteasomes and prion-mediated neurodegenerations: potential therapeutic opportunities. *Apoptosis.* 15 (11):1322-1335.

59. Chandler RL (1961) Encephalopathy in mice produced by inoculation with scrapie brain material. *Lancet* 1 (7191):1378-1379.
60. Chang K, Elledge SJ, and Hannon GJ (2006) Lessons from Nature: microRNA-based shRNA libraries. *Nat.Methods* 3 (9):707-714.
61. Chen S, Mange A, Dong L, Lehmann S, and Schachner M (2003) Prion protein as trans-interacting partner for neurons is involved in neurite outgrowth and neuronal survival. *Mol.Cell Neurosci.* 22 (2):227-233.
62. Chen SG, Teplow DB, Parchi P, Teller JK, Gambetti P, and Autilio-Gambetti L (1995) Truncated forms of the human prion protein in normal brain and in prion diseases. *J.Biol.Chem.* 270 (32):19173-19180.
63. Chendrimada TP, Gregory RI, Kumaraswamy E, Norman J, Cooch N, Nishikura K, and Shiekhattar R (2005) TRBP recruits the Dicer complex to Ago2 for microRNA processing and gene silencing. *Nature* 436 (7051):740-744.
64. Chesebro B, Race R, Wehrly K, Nishio J, Bloom M, Lechner D, Bergstrom S, Robbins K, Mayer L, Keith JM, and . (1985) Identification of scrapie prion protein-specific mRNA in scrapie-infected and uninfected brain. *Nature* 315 (6017):331-333.
65. Chesebro B, Trifilo M, Race R, Meade-White K, Teng C, LaCasse R, Raymond L, Favara C, Baron G, Priola S, Caughey B, Masliah E, and Oldstone M (2005) Anchorless prion protein results in infectious amyloid disease without clinical scrapie. *Science* 308 (5727):1435-1439.
66. Chiarini LB, Freitas AR, Zanata SM, Brentani RR, Martins VR, and Linden R (2002) Cellular prion protein transduces neuroprotective signals. *EMBO J.* 21 (13):3317-3326.
67. Chohan G, Pennington C, Mackenzie JM, Andrews M, Everington D, Will RG, Knight RS, and Green AJ (2010) The role of cerebrospinal fluid 14-3-3 and other proteins in the diagnosis of sporadic Creutzfeldt-Jakob disease in the UK: a 10-year review. *J.Neurol.Neurosurg.Psychiatry* 81 (11):1243-1248.
68. Christensen HM, Dikranian K, Li A, Baysac KC, Walls KC, Olney JW, Roth KA, and Harris DA (2010) A highly toxic cellular prion protein induces a novel, nonapoptotic form of neuronal death. *Am.J.Pathol.* 176 (6):2695-2706.
69. Collinge J, Palmer MS, and Dryden AJ (1991) Genetic predisposition to iatrogenic Creutzfeldt-Jakob disease. *Lancet* 337 (8755):1441-1442.
70. Collinge J, Sidle KC, Meads J, Ironside J, and Hill AF (1996) Molecular analysis of prion strain variation and the aetiology of 'new variant' CJD. *Nature* 383 (6602):685-690.

71. Collinge J, Whittington MA, Sidle KC, Smith CJ, Palmer MS, Clarke AR, and Jefferys JG (1994) Prion protein is necessary for normal synaptic function. *Nature* 370 (6487):295-297.
72. Corsaro A, Thellung S, Villa V, Principe DR, Paludi D, Arena S, Millo E, Schettini D, Damonte G, Aceto A, Schettini G, and Florio T (2003) Prion protein fragment 106-126 induces a p38 MAP kinase-dependent apoptosis in SH-SY5Y neuroblastoma cells independently from the amyloid fibril formation. *Ann.N.Y.Acad.Sci.* 1010:610-622.
73. Coussens M, Davy P, Brown L, Foster C, Andrews WH, Nagata M, and Allsopp R (2010) RNAi screen for telomerase reverse transcriptase transcriptional regulators identifies HIF1alpha as critical for telomerase function in murine embryonic stem cells. *Proc.Natl.Acad.Sci.U.S.A* 107 (31):13842-13847.
74. Croes EA, Roks G, Jansen GH, Nijssen PC, and van Duijn CM (2002) Creutzfeldt-Jakob disease 38 years after diagnostic use of human growth hormone. *J.Neurol.Neurosurg.Psychiatry* 72 (6):792-793.
75. Cronier S, Laude H, and Peyrin JM (2004) Prions can infect primary cultured neurons and astrocytes and promote neuronal cell death. *Proc.Natl.Acad.Sci.U.S.A* 101 (33):12271-12276.
76. Dassie JP, Liu XY, Thomas GS, Whitaker RM, Thiel KW, Stockdale KR, Meyerholz DK, McCaffrey AP, McNamara JO, and Giangrande PH (2009) Systemic administration of optimized aptamer-siRNA chimeras promotes regression of PSMA-expressing tumors. *Nat.Biotechnol.* 27 (9):839-849.
77. de Pril R, Fischer DF, Maat-Schieman ML, Hobo B, de Vos RA, Brunt ER, Hol EM, Roos RA, and van Leeuwen FW (2004) Accumulation of aberrant ubiquitin induces aggregate formation and cell death in polyglutamine diseases. *Hum.Mol.Genet.* 13 (16):1803-1813.
78. de Soultrait VR, Lozach PY, Altmeyer R, Tarrago-Litvak L, Litvak S, and Andreola ML (2002) DNA aptamers derived from HIV-1 RNase H inhibitors are strong anti-integrase agents. *J.Mol.Biol.* 324 (2):195-203.
79. Della-Bianca V, Rossi F, Armato U, Dal Pra I, Costantini C, Perini G, Politi V, and Della VG (2001) Neurotrophin p75 receptor is involved in neuronal damage by prion peptide-(106-126). *J.Biol.Chem.* 276 (42):38929-38933.
80. Dickinson AG, Meikle VM, and Fraser H (1968) Identification of a gene which controls the incubation period of some strains of scrapie agent in mice. *J.Comp Pathol.* 78 (3):293-299.
81. Donze O and Picard D (2002) RNA interference in mammalian cells using siRNAs synthesized with T7 RNA polymerase. *Nucleic Acids Res.* 30 (10):e46.

82. Donzé O and Picard D (2002) RNA interference in mammalian cells using siRNAs synthesized with T7 RNA polymerase. *Nucleic Acids Res.* 30 (10):e46.
83. Dorandeu A, Wingertsman L, Chretien F, Delisle MB, Vital C, Parchi P, Montagna P, Lugaresi E, Ironside JW, Budka H, Gambetti P, and Gray F (1998) Neuronal apoptosis in fatal familial insomnia. *Brain Pathol.* 8 (3):531-537.
84. Draper GJ and Parry HB (1962) Scrapie in sheep: the hereditary component in a high incidence environment. *Nature* 195:670-672.
85. Drisaldi B, Stewart RS, Adles C, Stewart LR, Quaglio E, Biasini E, Fioriti L, Chiesa R, and Harris DA (2003) Mutant PrP is delayed in its exit from the endoplasmic reticulum, but neither wild-type nor mutant PrP undergoes retrotranslocation prior to proteasomal degradation. *J.Biol.Chem.* 278 (24):21732-21743.
86. Dupiereux I, Zorzi W, Lins L, Brasseur R, Colson P, Heinen E, and Elmoualij B (2005) Interaction of the 106-126 prion peptide with lipid membranes and potential implication for neurotoxicity. *Biochem.Biophys.Res.Comm.* 331 (4):894-901.
87. Dupiereux I, Zorzi W, Rachidi W, Zorzi D, Pierard O, Lhereux B, Heinen E, and Elmoualij B (2006) Study on the toxic mechanism of prion protein peptide 106-126 in neuronal and non neuronal cells. *J.Neurosci.Res.* 84 (3):637-646.
88. Edenhofer F, Rieger R, Famulok M, Wendler W, Weiss S, and Winnacker EL (1996) Prion protein PrP_C interacts with molecular chaperones of the Hsp60 family. *J.Virol.* 70 (7):4724-4728.
89. Elbashir SM, Harborth J, Lendeckel W, Yalcin A, Weber K, and Tuschl T (2001) Duplexes of 21-nucleotide RNAs mediate RNA interference in cultured mammalian cells. *Nature* 411 (6836):494-498.
90. Ellington AD and Szostak JW (1992) Selection in vitro of single-stranded DNA molecules that fold into specific ligand-binding structures. *Nature* 355 (6363):850-852.
91. Enari M, Flechsig E, and Weissmann C (2001) Scrapie prion protein accumulation by scrapie-infected neuroblastoma cells abrogated by exposure to a prion protein antibody. *Proc.Natl.Acad.Sci.U.S.A* 98 (16):9295-9299.
92. Ettaiche M, Pichot R, Vincent JP, and Chabry J (2000) In vivo cytotoxicity of the prion protein fragment 106-126. *J.Biol.Chem.* 275 (47):36487-36490.
93. Fairbairn DW, Carnahan KG, Thwaites RN, Grigsby RV, Holyoak GR, and O'Neill KL (1994) Detection of apoptosis induced DNA cleavage in scrapie-infected sheep brain. *FEMS Microbiol.Lett.* 115 (2-3):341-346.

94. Falschlehner C, Steinbrink S, Erdmann G, and Boutros M (2010) High-throughput RNAi screening to dissect cellular pathways: a how-to guide. *Biotechnol.J.* 5 (4):368-376.
95. Fatzer R, Graber HU, Meyer RK, Cardozo C, Vandeveld M, and Zurbriggen A (1996) Neuronal degeneration in brain stem nuclei in bovine spongiform encephalopathy. *Zentralbl.Veterinarmed.A* 43 (1):23-29.
96. Feraudet C, Morel N, Simon S, Volland H, Frobert Y, Creminon C, Vilette D, Lehmann S, and Grassi J (2005) Screening of 145 anti-PrP monoclonal antibodies for their capacity to inhibit PrPSc replication in infected cells. *J.Biol.Chem.* 280 (12):11247-11258.
97. Ferreira IL, Resende R, Ferreiro E, Rego AC, and Pereira CF (2010) Multiple defects in energy metabolism in Alzheimer's disease. *Curr.Drug Targets.* 11 (10):1193-1206.
98. Ferreiro E, Resende R, Costa R, Oliveira CR, and Pereira CM (2006) An endoplasmic-reticulum-specific apoptotic pathway is involved in prion and amyloid-beta peptides neurotoxicity. *Neurobiol.Dis.* 23 (3):669-678.
99. Fioriti L, Dossena S, Stewart LR, Stewart RS, Harris DA, Forloni G, and Chiesa R (2005a) Cytosolic prion protein (PrP) is not toxic in N2a cells and primary neurons expressing pathogenic PrP mutations. *J.Biol.Chem.* 280 (12):11320-11328.
100. Fioriti L, Quaglio E, Massignan T, Colombo L, Stewart RS, Salmona M, Harris DA, Forloni G, and Chiesa R (2005b) The neurotoxicity of prion protein (PrP) peptide 106-126 is independent of the expression level of PrP and is not mediated by abnormal PrP species. *Mol.Cell Neurosci.* 28 (1):165-176.
101. Fire A, Xu S, Montgomery MK, Kostas SA, Driver SE, and Mello CC (1998) Potent and specific genetic interference by double-stranded RNA in *Caenorhabditis elegans*. *Nature* 391 (6669):806-811.
102. Fischer M, Rulicke T, Raeber A, Sailer A, Moser M, Oesch B, Brandner S, Aguzzi A, and Weissmann C (1996) Prion protein (PrP) with amino-proximal deletions restoring susceptibility of PrP knockout mice to scrapie. *EMBO J.* 15 (6):1255-1264.
103. Flechsig E, Hegyi I, Leimeroth R, Zuniga A, Rossi D, Cozzio A, Schwarz P, Rulicke T, Gotz J, Aguzzi A, and Weissmann C (2003) Expression of truncated PrP targeted to Purkinje cells of PrP knockout mice causes Purkinje cell death and ataxia. *EMBO J.* 22 (12):3095-3101.
104. Forloni G, Angeretti N, Chiesa R, Monzani E, Salmona M, Bugiani O, and Tagliavini F (1993) Neurotoxicity of a prion protein fragment. *Nature* 362 (6420):543-546.

105. Gadotti VM, Bonfield SP, and Zamponi GW (2011) Depressive-like Behaviour of Mice Lacking Cellular Prion Protein. *Behav.Brain Res.*
106. Gajdusek DC and Zigas V (1959) Kuru; clinical, pathological and epidemiological study of an acute progressive degenerative disease of the central nervous system among natives of the Eastern Highlands of New Guinea. *Am.J.Med.* 26 (3):442-469.
107. Garcao P, Oliveira CR, and Agostinho P (2006) Comparative study of microglia activation induced by amyloid-beta and prion peptides: role in neurodegeneration. *J.Neurosci.Res.* 84 (1):182-193.
108. Gasset M, Baldwin MA, Fletterick RJ, and Prusiner SB (1993) Perturbation of the secondary structure of the scrapie prion protein under conditions that alter infectivity. *Proc.Natl.Acad.Sci.U.S.A* 90 (1):1-5.
109. Gazin C, Wajapeyee N, Gobeil S, Virbasius CM, and Green MR (2007) An elaborate pathway required for Ras-mediated epigenetic silencing. *Nature* 449 (7165):1073-1077.
110. Genoud N, Behrens A, Miele G, Robay D, Heppner FL, Freigang S, and Aguzzi A (2004) Disruption of Doppel prevents neurodegeneration in mice with extensive Prnp deletions. *Proc.Natl.Acad.Sci.U.S.A* 101 (12):4198-4203.
111. Ghetti B, Dlouhy SR, Giaccone G, Bugiani O, Frangione B, Farlow MR, and Tagliavini F (1995) Gerstmann-Straussler-Scheinker disease and the Indiana kindred. *Brain Pathol.* 5 (1):61-75.
112. Giese A, Groschup MH, Hess B, and Kretzschmar HA (1995) Neuronal cell death in scrapie-infected mice is due to apoptosis. *Brain Pathol.* 5 (3):213-221.
113. Gilch S, Kehler C, and Schatzl HM (2006) The prion protein requires cholesterol for cell surface localization. *Mol.Cell Neurosci.* 31 (2):346-353.
114. Glatzel M, Stoeck K, Seeger H, Luhrs T, and Aguzzi A (2005) Human prion diseases: molecular and clinical aspects. *Arch.Neurol.* 62 (4):545-552.
115. Gobeil S, Zhu X, Doillon CJ, and Green MR (2008) A genome-wide shRNA screen identifies GAS1 as a novel melanoma metastasis suppressor gene. *Genes Dev.* 22 (21):2932-2940.
116. Goldfarb LG and Brown P (1995) The transmissible spongiform encephalopathies. *Annu.Rev.Med.* 46:57-65.
117. Gorodinsky A and Harris DA (1995) Glycolipid-anchored proteins in neuroblastoma cells form detergent-resistant complexes without caveolin. *J.Cell Biol.* 129 (3):619-627.

118. Govaerts C, Wille H, Prusiner SB, and Cohen FE (2004) Evidence for assembly of prions with left-handed beta-helices into trimers. *Proc.Natl.Acad.Sci.U.S.A* 101 (22):8342-8347.
119. Graner E, Mercadante AF, Zanata SM, Forlenza OV, Cabral AL, Veiga SS, Juliano MA, Roesler R, Walz R, Minetti A, Izquierdo I, Martins VR, and Brentani RR (2000a) Cellular prion protein binds laminin and mediates neuritogenesis. *Brain Res.Mol.Brain Res.* 76 (1):85-92.
120. Graner E, Mercadante AF, Zanata SM, Martins VR, Jay DG, and Brentani RR (2000b) Laminin-induced PC-12 cell differentiation is inhibited following laser inactivation of cellular prion protein. *FEBS Lett.* 482 (3):257-260.
121. Gray BC, Skipp P, O'Connor VM, and Perry VH (2006) Increased expression of glial fibrillary acidic protein fragments and mu-calpain activation within the hippocampus of prion-infected mice. *Biochem.Soc.Trans.* 34 (Pt 1):51-54.
122. Gray F, Chretien F, Adle-Biassette H, Dorandeu A, Ereau T, Delisle MB, Kopp N, Ironside JW, and Vital C (1999) Neuronal apoptosis in Creutzfeldt-Jakob disease. *J.Neuropathol.Exp.Neurol.* 58 (4):321-328.
123. Grenier C, Bissonnette C, Volkov L, and Roucou X (2006) Molecular morphology and toxicity of cytoplasmic prion protein aggregates in neuronal and non-neuronal cells. *J.Neurochem.* 97 (5):1456-1466.
124. Grishok A, Pasquinelli AE, Conte D, Li N, Parrish S, Ha I, Baillie DL, Fire A, Ruvkun G, and Mello CC (2001) Genes and mechanisms related to RNA interference regulate expression of the small temporal RNAs that control *C. elegans* developmental timing. *Cell* 106 (1):23-34.
125. Gu Y, Fujioka H, Mishra RS, Li R, and Singh N (2002) Prion peptide 106-126 modulates the aggregation of cellular prion protein and induces the synthesis of potentially neurotoxic transmembrane PrP. *J.Biol.Chem.* 277 (3):2275-2286.
126. Gu Y, Luo X, Basu S, Fujioka H, and Singh N (2006) Cell-specific metabolism and pathogenesis of transmembrane prion protein. *Mol.Cell Biol.* 26 (7):2697-2715.
127. Ha I, Wightman B, and Ruvkun G (1996) A bulged lin-4/lin-14 RNA duplex is sufficient for *Caenorhabditis elegans* lin-14 temporal gradient formation. *Genes Dev.* 10 (23):3041-3050.
128. Haase AD, Jaskiewicz L, Zhang H, Laine S, Sack R, Gatignol A, and Filipowicz W (2005) TRBP, a regulator of cellular PKR and HIV-1 virus expression, interacts with Dicer and functions in RNA silencing. *EMBO Rep.* 6 (10):961-967.
129. Haley B and Zamore PD (2004) Kinetic analysis of the RNAi enzyme complex. *Nat.Struct.Mol.Biol.* 11 (7):599-606.

130. Hamilton AJ and Baulcombe DC (1999) A species of small antisense RNA in posttranscriptional gene silencing in plants. *Science* 286 (5441):950-952.
131. Hamir AN, Richt JA, Kunkle RA, Greenlee JJ, Bulgin MS, Gregori L, and Rohwer RG (2009) Characterization of a US sheep scrapie isolate with short incubation time. *Vet.Pathol.* 46 (6):1205-1212.
132. Hammond SM, Bernstein E, Beach D, and Hannon GJ (2000) An RNA-directed nuclease mediates post-transcriptional gene silencing in *Drosophila* cells. *Nature* 404 (6775):293-296.
133. Hammond SM, Boettcher S, Caudy AA, Kobayashi R, and Hannon GJ (2001) Argonaute2, a link between genetic and biochemical analyses of RNAi. *Science* 293 (5532):1146-1150.
134. Hannon GJ (2002) RNA interference. *Nature* 418 (6894):244-251.
135. Harris DA (2003) Trafficking, turnover and membrane topology of PrP. *Br.Med.Bull.* 66:71-85.
136. Haseloff J and Gerlach WL (1988) Simple RNA enzymes with new and highly specific endoribonuclease activities. *Nature* 334 (6183):585-591.
137. Head MW, Ritchie D, Smith N, McLoughlin V, Nailon W, Samad S, Masson S, Bishop M, McCardle L, and Ironside JW (2004) Peripheral tissue involvement in sporadic, iatrogenic, and variant Creutzfeldt-Jakob disease: an immunohistochemical, quantitative, and biochemical study. *Am.J.Pathol.* 164 (1):143-153.
138. Hegde RS, Mastrianni JA, Scott MR, DeFea KA, Tremblay P, Torchia M, DeArmond SJ, Prusiner SB, and Lingappa VR (1998) A transmembrane form of the prion protein in neurodegenerative disease. *Science* 279 (5352):827-834.
139. Hegde RS, Tremblay P, Groth D, DeArmond SJ, Prusiner SB, and Lingappa VR (1999) Transmissible and genetic prion diseases share a common pathway of neurodegeneration. *Nature* 402 (6763):822-826.
140. Herschlag D and Cech TR (1990) Catalysis of RNA cleavage by the *Tetrahymena thermophila* ribozyme. 1. Kinetic description of the reaction of an RNA substrate complementary to the active site. *Biochemistry* 29 (44):10159-10171.
141. Hetz C, Russelakis-Carneiro M, Maundrell K, Castilla J, and Soto C (2003) Caspase-12 and endoplasmic reticulum stress mediate neurotoxicity of pathological prion protein. *EMBO J.* 22 (20):5435-5445.
142. Hill AF, Desbruslais M, Joiner S, Sidle KC, Gowland I, Collinge J, Doey LJ, and Lantos P (1997) The same prion strain causes vCJD and BSE. *Nature* 389 (6650):448-50, 526.

143. Hill AF, Joiner S, Linehan J, Desbruslais M, Lantos PL, and Collinge J (2000) Species-barrier-independent prion replication in apparently resistant species. *Proc.Natl.Acad.Sci.U.S.A* 97 (18):10248-10253.
144. Hinton TM, Wise TG, Cottee PA, and Doran TJ (2008) Native microRNA loop sequences can improve short hairpin RNA processing for virus gene silencing in animal cells. *J.RNAi.Gene Silencing*. 4 (1):295-301.
145. Hiraga C, Kobayashi A, and Kitamoto T (2009) The number of octapeptide repeat affects the expression and conversion of prion protein. *Biochem.Biophys.Res.Communic.* 382 (4):715-719.
146. Hornemann S, Korth C, Oesch B, Riek R, Wider G, Wuthrich K, and Glockshuber R (1997) Recombinant full-length murine prion protein, mPrP(23-231): purification and spectroscopic characterization. *FEBS Lett.* 413 (2):277-281.
147. Hoshi K, Yoshino H, Urata J, Nakamura Y, Yanagawa H, and Sato T (2000) Creutzfeldt-Jakob disease associated with cadaveric dura mater grafts in Japan. *Neurology* 55 (5):718-721.
148. Hosick HL (1974) A note on growth patterns of epithelial tumor cells in primary culture. *Cancer Res.* 34 (1):259-261.
149. Huang DT, Zhuang M, Ayrault O, and Schulman BA (2008) Identification of conjugation specificity determinants unmasks vestigial preference for ubiquitin within the NEDD8 E2. *Nat.Struct.Mol.Biol.* 15 (3):280-287.
150. Huang X, Wang JY, and Lu X (2008) Systems analysis of quantitative shRNA-library screens identifies regulators of cell adhesion. *BMC.Syst.Biol.* 2:49.
151. Hunter N, Foster J, Chong A, McCutcheon S, Parnham D, Eaton S, MacKenzie C, and Houston F (2002) Transmission of prion diseases by blood transfusion. *J.Gen.Virol.* 83 (Pt 11):2897-2905.
152. Hutvagner G, McLachlan J, Pasquinelli AE, Balint E, Tuschl T, and Zamore PD (2001) A cellular function for the RNA-interference enzyme Dicer in the maturation of the let-7 small temporal RNA. *Science* 293 (5531):834-838.
153. HyClone Labs (1996) Heat Inactivation: Are you wasting your time? *Art to Science* 15:1-5.
154. Ironside JW, Head MW, Bell JE, McCardle L, and Will RG (2000) Laboratory diagnosis of variant Creutzfeldt-Jakob disease. *Histopathology* 37 (1):1-9.
155. Jackson AL, Bartz SR, Schelter J, Kobayashi SV, Burchard J, Mao M, Li B, Cavet G, and Linsley PS (2003) Expression profiling reveals off-target gene regulation by RNAi. *Nat.Biotechnol.* 21 (6):635-637.

156. Jamieson E, Jeffrey M, Ironside JW, and Fraser JR (2001) Activation of Fas and caspase 3 precedes PrP accumulation in 87V scrapie. *Neuroreport* 12 (16):3567-3572.
157. Jarrett JT and Lansbury PT, Jr. (1993) Seeding "one-dimensional crystallization" of amyloid: a pathogenic mechanism in Alzheimer's disease and scrapie? *Cell* 73 (6):1055-1058.
158. Jeffrey M, Fraser JR, Halliday WG, Fowler N, Goodsir CM, and Brown DA (1995) Early unsuspected neuron and axon terminal loss in scrapie-infected mice revealed by morphometry and immunocytochemistry. *Neuropathol.Appl.Neurobiol.* 21 (1):41-49.
159. Jobling MF, Stewart LR, White AR, McLean C, Friedhuber A, Maher F, Beyreuther K, Masters CL, Barrow CJ, Collins SJ, and Cappai R (1999) The hydrophobic core sequence modulates the neurotoxic and secondary structure properties of the prion peptide 106-126. *J.Neurochem.* 73 (4):1557-1565.
160. Joshi P and Prasad VR (2002) Potent inhibition of human immunodeficiency virus type 1 replication by template analog reverse transcriptase inhibitors derived by SELEX (systematic evolution of ligands by exponential enrichment). *J.Virol.* 76 (13):6545-6557.
161. Katamine S, Nishida N, Sugimoto T, Noda T, Sakaguchi S, Shigematsu K, Kataoka Y, Nakatani A, Hasegawa S, Moriuchi R, and Miyamoto T (1998) Impaired motor coordination in mice lacking prion protein. *Cell Mol.Neurobiol.* 18 (6):731-742.
162. Kato Y, Tsunemi M, Miyagishi M, Kawasaki H, and Taira K (2004) Functional gene discovery using hybrid ribozyme libraries. *Methods Mol.Biol.* 252:245-256.
163. Kawasaki H, Kuwabara T, Miyagishi M, and Taira K (2003) Identification of functional genes by libraries of ribozymes and siRNAs. *Nucleic Acids Res.Suppl* (3):331-332.
164. Kawasaki H, Onuki R, Suyama E, and Taira K (2002a) Identification of genes that function in the TNF-alpha-mediated apoptotic pathway using randomized hybrid ribozyme libraries. *Nat.Biotechnol.* 20 (4):376-380.
165. Kawasaki H and Taira K (2001) Discovery of functional genes in the post-genome era by novel RNA-protein hybrid ribozymes. *Nucleic Acids Res.Suppl* (1):133-134.
166. Kawasaki H and Taira K (2002a) A functional gene discovery in the Fas-mediated pathway to apoptosis by analysis of transiently expressed randomized hybrid-ribozyme libraries. *Nucleic Acids Res.* 30 (16):3609-3614.

167. Kawasaki H and Taira K (2002b) Identification of genes by hybrid ribozymes that couple cleavage activity with the unwinding activity of an endogenous RNA helicase. *EMBO Rep.* 3 (5):443-450.
168. Kawasaki H, Tsunemi M, Iyo M, Oshima K, Minoshima H, Hamada A, Onuki R, Suyama E, and Taira K (2002b) A functional gene discovery in cell differentiation by hybrid ribozyme and siRNA libraries. *Nucleic Acids Res. Suppl* (2):275-276.
169. Kawasaki H, Warashina M, Kuwabara T, and Taira K (2004) Helicase-attached novel hybrid ribozymes. *Methods Mol. Biol.* 252:237-243.
170. Kennerdell JR and Carthew RW (1998) Use of dsRNA-mediated genetic interference to demonstrate that frizzled and frizzled 2 act in the wingless pathway. *Cell* 95 (7):1017-1026.
171. Ketting RF, Fischer SE, Bernstein E, Sijen T, Hannon GJ, and Plasterk RH (2001) Dicer functions in RNA interference and in synthesis of small RNA involved in developmental timing in *C. elegans*. *Genes Dev.* 15 (20):2654-2659.
172. Kim JI, Ju WK, Choi JH, Choi E, Carp RI, Wisniewski HM, and Kim YS (1999) Expression of cytokine genes and increased nuclear factor-kappa B activity in the brains of scrapie-infected mice. *Brain Res. Mol. Brain Res.* 73 (1-2):17-27.
173. Kim SJ and Hegde RS (2002) Cotranslational partitioning of nascent prion protein into multiple populations at the translocation channel. *Mol. Biol. Cell* 13 (11):3775-3786.
174. Kimura J, Nguyen ST, Liu H, Taira N, Miki Y, and Yoshida K (2008) A functional genome-wide RNAi screen identifies TAF1 as a regulator for apoptosis in response to genotoxic stress. *Nucleic Acids Res.* 36 (16):5250-5259.
175. Klamt F, Dal Pizzol F, Conte da Frota ML JR, Walz R, Andrades ME, da Silva EG, Brentani RR, Izquierdo I, and Fonseca Moreira JC (2001) Imbalance of antioxidant defense in mice lacking cellular prion protein. *Free Radic. Biol. Med.* 30 (10):1137-1144.
176. Klohn PC, Stoltze L, Flechsig E, Enari M, and Weissmann C (2003) A quantitative, highly sensitive cell-based infectivity assay for mouse scrapie prions. *Proc. Natl. Acad. Sci. U.S.A* 100 (20):11666-11671.
177. Knaus KJ, Morillas M, Swietnicki W, Malone M, Surewicz WK, and Yee VC (2001) Crystal structure of the human prion protein reveals a mechanism for oligomerization. *Nat. Struct. Biol.* 8 (9):770-774.
178. Kobirumaki F, Miyauchi Y, Fukami K, and Tanaka H (2005) A novel UbcH10-binding protein facilitates the ubiquitinylation of cyclin B in vitro. *J. Biochem.* 137 (2):133-139.

179. Korth C, Kaneko K, and Prusiner SB (2000) Expression of unglycosylated mutated prion protein facilitates PrP(Sc) formation in neuroblastoma cells infected with different prion strains. *J.Gen.Virol.* 81 (Pt 10):2555-2563.
180. Krasemann S, Neumann M, Geissen M, Bodemer W, Kaup FJ, Schulz-Schaeffer W, Morel N, Aguzzi A, and Glatzel M (2010) Preclinical deposition of pathological prion protein in muscle of experimentally infected primates. *PLoS.ONE.* 5 (11):e13906.
181. Kretzschmar HA, Prusiner SB, Stowring LE, and DeArmond SJ (1986) Scrapie prion proteins are synthesized in neurons. *Am.J.Pathol.* 122 (1):1-5.
182. Kristiansen M, Deriziotis P, Dimcheff DE, Jackson GS, Ovaa H, Naumann H, Clarke AR, van Leeuwen FW, Menendez-Benito V, Dantuma NP, Portis JL, Collinge J, and Tabrizi SJ (2007) Disease-associated prion protein oligomers inhibit the 26S proteasome. *Mol.Cell* 26 (2):175-188.
183. Kristiansen M, Messenger MJ, Klohn PC, Brandner S, Wadsworth JD, Collinge J, and Tabrizi SJ (2005) Disease-related prion protein forms aggregates in neuronal cells leading to caspase activation and apoptosis. *J.Biol.Chem.* 280 (46):38851-38861.
184. Kurschner C and Morgan JI (1995) The cellular prion protein (PrP) selectively binds to Bcl-2 in the yeast two-hybrid system. *Brain Res.Mol.Brain Res.* 30 (1):165-168.
185. Lagos-Quintana M, Rauhut R, Lendeckel W, and Tuschl T (2001) Identification of novel genes coding for small expressed RNAs. *Science* 294 (5543):853-858.
186. Lansbury PT (1994) Mechanism of scrapie replication. *Science* 265 (5178):1510.
187. Lasmezas CI, Deslys JP, Demaimay R, Adjou KT, Hauw JJ, and Dormont D (1996) Strain specific and common pathogenic events in murine models of scrapie and bovine spongiform encephalopathy. *J.Gen.Virol.* 77 (Pt 7):1601-1609.
188. Lau NC, Lim LP, Weinstein EG, and Bartel DP (2001) An abundant class of tiny RNAs with probable regulatory roles in *Caenorhabditis elegans*. *Science* 294 (5543):858-862.
189. Lee KJ, Panzera A, Rogawski D, Greene LE, and Eisenberg E (2007) Cellular prion protein (PrPC) protects neuronal cells from the effect of huntingtin aggregation. *J.Cell Sci.* 120 (Pt 15):2663-2671.
190. Lee RC and Ambros V (2001) An extensive class of small RNAs in *Caenorhabditis elegans*. *Science* 294 (5543):862-864.

191. Lee Y, Ahn C, Han J, Choi H, Kim J, Yim J, Lee J, Provost P, Radmark O, Kim S, and Kim VN (2003) The nuclear RNase III Drosha initiates microRNA processing. *Nature* 425 (6956):415-419.
192. Lee Y, Hur I, Park SY, Kim YK, Suh MR, and Kim VN (2006) The role of PACT in the RNA silencing pathway. *EMBO J.* 25 (3):522-532.
193. Lee Y, Kim M, Han J, Yeom KH, Lee S, Baek SH, and Kim VN (2004) MicroRNA genes are transcribed by RNA polymerase II. *EMBO J.* 23 (20):4051-4060.
194. Lehman NL (2009) The ubiquitin proteasome system in neuropathology. *Acta Neuropathol.* 118 (3):329-347.
195. Leroy E, Boyer R, Auburger G, Leube B, Ulm G, Mezey E, Harta G, Brownstein MJ, Jonnalagada S, Chernova T, Dehejia A, Lavedan C, Gasser T, Steinbach PJ, Wilkinson KD, and Polymeropoulos MH (1998) The ubiquitin pathway in Parkinson's disease. *Nature* 395 (6701):451-452.
196. Li A, Christensen HM, Stewart LR, Roth KA, Chiesa R, and Harris DA (2007) Neonatal lethality in transgenic mice expressing prion protein with a deletion of residues 105-125. *EMBO J.* 26 (2):548-558.
197. Lledo PM, Tremblay P, DeArmond SJ, Prusiner SB, and Nicoll RA (1996) Mice deficient for prion protein exhibit normal neuronal excitability and synaptic transmission in the hippocampus. *Proc.Natl.Acad.Sci.U.S.A* 93 (6):2403-2407.
198. Llewelyn CA, Hewitt PE, Knight RS, Amar K, Cousens S, Mackenzie J, and Will RG (2004) Possible transmission of variant Creutzfeldt-Jakob disease by blood transfusion. *Lancet* 363 (9407):417-421.
199. Locht C, Chesebro B, Race R, and Keith JM (1986) Molecular cloning and complete sequence of prion protein cDNA from mouse brain infected with the scrapie agent. *Proc.Natl.Acad.Sci.U.S.A* 83 (17):6372-6376.
200. Loeuillet C, Boelle PY, Lemaire-Vieille C, Baldazza M, Naquet P, Chambon P, Cesbron-Delauw MF, Valleron AJ, Gagnon J, and Cesbron JY (2010) Sex effect in mouse and human prion disease. *J.Infect.Dis.* 202 (4):648-654.
201. Lowe J, McDermott H, Kenward N, Landon M, Mayer RJ, Bruce M, McBride P, Somerville RA, and Hope J (1990) Ubiquitin conjugate immunoreactivity in the brains of scrapie infected mice. *J.Pathol.* 162 (1):61-66.
202. Lukic A, Beck J, Joiner S, Fearnley J, Sturman S, Brandner S, Wadsworth JD, Collinge J, and Mead S (2010) Heterozygosity at polymorphic codon 219 in variant creutzfeldt-jakob disease. *Arch.Neurol.* 67 (8):1021-1023.

203. Lukk M, Kapushesky M, Nikkila J, Parkinson H, Goncalves A, Huber W, Ukkonen E, and Brazma A (2010) A global map of human gene expression. *Nat.Biotechnol.* 28 (4):322-324.
204. Lumley JS (2008) The impact of Creutzfeldt-Jakob disease on surgical practice. *Ann.R.Coll.Surg.Engl.* 90 (2):91-94.
205. Lund E, Guttinger S, Calado A, Dahlberg JE, and Kutay U (2004) Nuclear export of microRNA precursors. *Science* 303 (5654):95-98.
206. Luo B, Cheung HW, Subramanian A, Sharifnia T, Okamoto M, Yang X, Hinkle G, Boehm JS, Beroukhim R, Weir BA, Mermel C, Barbie DA, Awad T, Zhou X, Nguyen T, Piquani B, Li C, Golub TR, Meyerson M, Hacohen N, Hahn WC, Lander ES, Sabatini DM, and Root DE (2008) Highly parallel identification of essential genes in cancer cells. *Proc.Natl.Acad.Sci.U.S.A* 105 (51):20380-20385.
207. Luo J, Emanuele MJ, Li D, Creighton CJ, Schlabach MR, Westbrook TF, Wong KK, and Elledge SJ (2009) A genome-wide RNAi screen identifies multiple synthetic lethal interactions with the Ras oncogene. *Cell* 137 (5):835-848.
208. Ma J, Wollmann R, and Lindquist S (2002) Neurotoxicity and neurodegeneration when PrP accumulates in the cytosol. *Science* 298 (5599):1781-1785.
209. Maddox RA, Belay ED, Curns AT, Zou WQ, Nowicki S, Lembach RG, Geschwind MD, Haman A, Shinozaki N, Nakamura Y, Borer MJ, and Schonberger LB (2008) Creutzfeldt-Jakob disease in recipients of corneal transplants. *Cornea* 27 (7):851-854.
210. Maiti NR and Surewicz WK (2001) The role of disulfide bridge in the folding and stability of the recombinant human prion protein. *J.Biol.Chem.* 276 (4):2427-2431.
211. Manson JC, Clarke AR, Hooper ML, Aitchison L, McConnell I, and Hope J (1994) 129/Ola mice carrying a null mutation in PrP that abolishes mRNA production are developmentally normal. *Mol.Neurobiol.* 8 (2-3):121-127.
212. Marella M and Chabry J (2004) Neurons and astrocytes respond to prion infection by inducing microglia recruitment. *J.Neurosci.* 24 (3):620-627.
213. Marsh RF and Kimberlin RH (1975) Comparison of scrapie and transmissible mink encephalopathy in hamsters. II. Clinical signs, pathology, and pathogenesis. *J.Infect.Dis.* 131 (2):104-110.
214. Martinez T and Pascual A (2007) Identification of genes differentially expressed in SH-SY5Y neuroblastoma cells exposed to the prion peptide 106-126. *Eur.J.Neurosci.* 26 (1):51-59.

215. McHattie SJ, Brown DR, and Bird MM (1999) Cellular uptake of the prion protein fragment PrP106-126 in vitro. *J.Neurocytol.* 28 (2):149-159.
216. McKinley MP, Bolton DC, and Prusiner SB (1983) A protease-resistant protein is a structural component of the scrapie prion. *Cell* 35 (1):57-62.
217. McLennan NF, Rennison KA, Bell JE, and Ironside JW (2001) In situ hybridization analysis of PrP mRNA in human CNS tissues. *Neuropathol.Appl.Neurobiol.* 27 (5):373-383.
218. McManus MT, Petersen CP, Haines BB, Chen J, and Sharp PA (2002) Gene silencing using micro-RNA designed hairpins. *RNA.* 8 (6):842-850.
219. Metzger MB and Weissman AM (2010) Working on a chain: E3s ganging up for ubiquitylation. *Nat.Cell Biol.* 12 (12):1124-1126.
220. Meyer RK, McKinley MP, Bowman KA, Braunfeld MB, Barry RA, and Prusiner SB (1986) Separation and properties of cellular and scrapie prion proteins. *Proc.Natl.Acad.Sci.U.S.A* 83 (8):2310-2314.
221. Miller DG, Adam MA, and Miller AD (1990) Gene transfer by retrovirus vectors occurs only in cells that are actively replicating at the time of infection. *Mol.Cell Biol.* 10 (8):4239-4242.
222. Minunni M, Tombelli S, Gullotto A, Luzi E, and Mascini M (2004) Development of biosensors with aptamers as bio-recognition element: the case of HIV-1 Tat protein. *Biosens.Bioelectron.* 20 (6):1149-1156.
223. Miura T, Yoda M, Takaku N, Hirose T, and Takeuchi H (2007) Clustered negative charges on the lipid membrane surface induce beta-sheet formation of prion protein fragment 106-126. *Biochemistry* 46 (41):11589-11597.
224. Moffat J, Grueneberg DA, Yang X, Kim SY, Kloepfer AM, Hinkle G, Piqani B, Eisenhaure TM, Luo B, Grenier JK, Carpenter AE, Foo SY, Stewart SA, Stockwell BR, Hacohen N, Hahn WC, Lander ES, Sabatini DM, and Root DE (2006) A lentiviral RNAi library for human and mouse genes applied to an arrayed viral high-content screen. *Cell* 124 (6):1283-1298.
225. Mohr S, Bakal C, and Perrimon N (2010) Genomic screening with RNAi: results and challenges. *Annu.Rev.Biochem.* 79:37-64.
226. Montag J, Hitt R, Opitz L, Schulz-Schaeffer WJ, Hunsmann G, and Motzkus D (2009) Upregulation of miRNA hsa-miR-342-3p in experimental and idiopathic prion disease. *Mol.Neurodegener.* 4:36.
227. Montagna P, Cortelli P, Avoni P, Tinuper P, Plazzi G, Gallassi R, Portaluppi F, Julien J, Vital C, Delisle MB, Gambetti P, and Lugaresi E (1998) Clinical features

- of fatal familial insomnia: phenotypic variability in relation to a polymorphism at codon 129 of the prion protein gene. *Brain Pathol.* 8 (3):515-520.
228. Montagna P, Gambetti P, Cortelli P, and Lugaresi E (2003) Familial and sporadic fatal insomnia. *Lancet Neurol.* 2 (3):167-176.
229. Moore RC, Lee IY, Silverman GL, Harrison PM, Strome R, Heinrich C, Karunaratne A, Pasternak SH, Chishti MA, Liang Y, Mastrangelo P, Wang K, Smit AF, Katamine S, Carlson GA, Cohen FE, Prusiner SB, Melton DW, Tremblay P, Hood LE, and Westaway D (1999) Ataxia in prion protein (PrP)-deficient mice is associated with upregulation of the novel PrP-like protein doppel. *J.Mol.Biol.* 292 (4):797-817.
230. Morita SY, Kobayashi A, Takanezawa Y, Kioka N, Handa T, Arai H, Matsuo M, and Ueda K (2007) Bile salt-dependent efflux of cellular phospholipids mediated by ATP binding cassette protein B4. *Hepatology* 46 (1):188-199.
231. Moser M, Colello RJ, Pott U, and Oesch B (1995) Developmental expression of the prion protein gene in glial cells. *Neuron* 14 (3):509-517.
232. Muchowski PJ and Wacker JL (2005) Modulation of neurodegeneration by molecular chaperones. *Nat.Rev.Neurosci.* 6 (1):11-22.
233. Muhleisen H, Gehrman J, and Meyermann R (1995) Reactive microglia in Creutzfeldt-Jakob disease. *Neuropathol.Appl.Neurobiol.* 21 (6):505-517.
234. Mullenders J, Fabius AW, Madiredjo M, Bernards R, and Beijersbergen RL (2009) A large scale shRNA barcode screen identifies the circadian clock component ARNTL as putative regulator of the p53 tumor suppressor pathway. *PLoS.ONE.* 4 (3):e4798.
235. Nagaoka-Yasuda R, Matsuo N, Perkins B, Limbaeck-Stokin K, and Mayford M (2007) An RNAi-based genetic screen for oxidative stress resistance reveals retinol saturase as a mediator of stress resistance. *Free Radic.Biol.Med.* 43 (5):781-788.
236. Nakagawa T, Zhu H, Morishima N, Li E, Xu J, Yankner BA, and Yuan J (2000) Caspase-12 mediates endoplasmic-reticulum-specific apoptosis and cytotoxicity by amyloid-beta. *Nature* 403 (6765):98-103.
237. Nakamura K and Aminoff MJ (2007) Huntington's disease: clinical characteristics, pathogenesis and therapies. *Drugs Today (Barc.)* 43 (2):97-116.
238. Ning ZY, Zhao DM, Liu HX, Yang JM, Han CX, Cui YL, Meng LP, Wu CD, Liu ML, and Zhang TX (2005a) Altered expression of the prion gene in rat astrocyte and neuron cultures treated with prion peptide 106-126. *Cell Mol.Neurobiol.* 25 (8):1171-1183.

239. Ning ZY, Zhao DM, Yang JM, Cui YL, Meng LP, Wu CD, and Liu HX (2005b) Quantification of prion gene expression in brain and peripheral organs of golden hamster by real-time RT-PCR. *Anim Biotechnol.* 16 (1):55-65.
240. Nishida N, Harris DA, Vilette D, Laude H, Frobert Y, Grassi J, Casanova D, Milhavel O, and Lehmann S (2000) Successful transmission of three mouse-adapted scrapie strains to murine neuroblastoma cell lines overexpressing wild-type mouse prion protein. *J.Virol.* 74 (1):320-325.
241. Norstrom EM and Mastrianni JA (2005) The AGAAAAGA palindrome in PrP is required to generate a productive PrP^{Sc}-PrP^C complex that leads to prion propagation. *J.Biol.Chem.* 280 (29):27236-27243.
242. Nunziante M, Gilch S, and Schatzl HM (2003) Prion diseases: from molecular biology to intervention strategies. *Chembiochem.* 4 (12):1268-1284.
243. Nykanen A, Haley B, and Zamore PD (2001) ATP requirements and small interfering RNA structure in the RNA interference pathway. *Cell* 107 (3):309-321.
244. O'Donovan CN, Tobin D, and Cotter TG (2001) Prion protein fragment PrP-(106-126) induces apoptosis via mitochondrial disruption in human neuronal SH-SY5Y cells. *J.Biol.Chem.* 276 (47):43516-43523.
245. Oesch B, Westaway D, Walchli M, McKinley MP, Kent SB, Aebersold R, Barry RA, Tempst P, Teplow DB, Hood LE, Prusiner SB, and Weissmann C (1985) A cellular gene encodes scrapie PrP 27-30 protein. *Cell* 40 (4):735-746.
246. Okouchi M, Ekshyyan O, Maracine M, and Aw TY (2007) Neuronal apoptosis in neurodegeneration. *Antioxid.Redox.Signal.* 9 (8):1059-1096.
247. Olsen PH and Ambros V (1999) The lin-4 regulatory RNA controls developmental timing in *Caenorhabditis elegans* by blocking LIN-14 protein synthesis after the initiation of translation. *Dev.Biol.* 216 (2):671-680.
248. OpenBiosystems (2011) GIPZ Lentiviral shRNAmir. *Thermo Scientific.*
249. Oude Elferink RP and Paulusma CC (2007) Function and pathophysiological importance of ABCB4 (MDR3 P-glycoprotein). *Pflugers Arch.* 453 (5):601-610.
250. Paddison PJ, Caudy AA, Bernstein E, Hannon GJ, and Conklin DS (2002) Short hairpin RNAs (shRNAs) induce sequence-specific silencing in mammalian cells. *Genes Dev.* 16 (8):948-958.
251. Paddison PJ, Silva JM, Conklin DS, Schlabach M, Li M, Aruleba S, Balija V, O'Shaughnessy A, Gnoj L, Scobie K, Chang K, Westbrook T, Cleary M, Sachidanandam R, McCombie WR, Elledge SJ, and Hannon GJ (2004) A

- resource for large-scale RNA-interference-based screens in mammals. *Nature* 428 (6981):427-431.
252. Padovani A, D'Alessandro M, Parchi P, Cortelli P, Anzola GP, Montagna P, Vignolo LA, Petraroli R, Pocchiari M, Lugaresi E, and Gambetti P (1998) Fatal familial insomnia in a new Italian kindred. *Neurology* 51 (5):1491-1494.
 253. Paitel E, Alves dC, Vilette D, Grassi J, and Checler F (2002) Overexpression of PrPc triggers caspase 3 activation: potentiation by proteasome inhibitors and blockade by anti-PrP antibodies. *J.Neurochem.* 83 (5):1208-1214.
 254. Palmer MS, Dryden AJ, Hughes JT, and Collinge J (1991) Homozygous prion protein genotype predisposes to sporadic Creutzfeldt-Jakob disease. *Nature* 352 (6333):340-342.
 255. Pan KM, Baldwin M, Nguyen J, Gasset M, Serban A, Groth D, Mehlhorn I, Huang Z, Fletterick RJ, Cohen FE, and . (1993) Conversion of alpha-helices into beta-sheets features in the formation of the scrapie prion proteins. *Proc.Natl.Acad.Sci.U.S.A* 90 (23):10962-10966.
 256. Pan YH, Wang YC, Zhang LM, and Duan SR (2010) Protective effect of edaravone against PrP106-126-induced PC12 cell death. *J.Biochem.Mol.Toxicol.* 24 (4):235-241.
 257. Parchi P, Giese A, Capellari S, Brown P, Schulz-Schaeffer W, Windl O, Zerr I, Budka H, Kopp N, Piccardo P, Poser S, Rojiani A, Streichemberger N, Julien J, Vital C, Ghetti B, Gambetti P, and Kretzschmar H (1999) Classification of sporadic Creutzfeldt-Jakob disease based on molecular and phenotypic analysis of 300 subjects. *Ann.Neurol.* 46 (2):224-233.
 258. Parry HB (1960) Scrapie: a transmissible hereditary disease of sheep. *Nature* 185:441-443.
 259. Paul CP, Good PD, Winer I, and Engelke DR (2002) Effective expression of small interfering RNA in human cells. *Nat.Biotechnol.* 20 (5):505-508.
 260. Pedro-Cuesta J, Mahillo-Fernandez I, Rabano A, Calero M, Cruz M, Siden A, Laursen H, Falkenhorst G, and Molbak K (2011) Nosocomial transmission of sporadic Creutzfeldt-Jakob disease: results from a risk-based assessment of surgical interventions. *J.Neurol.Neurosurg.Psychiatry* 82 (2):204-212.
 261. Perreault JP, Wu TF, Cousineau B, Ogilvie KK, and Cedergren R (1990) Mixed deoxyribo- and ribo-oligonucleotides with catalytic activity. *Nature* 344 (6266):565-567.
 262. Pocchiari M (1994) Prions and related neurological diseases. *Mol.Aspects Med.* 15 (3):195-291.

263. Prusiner SB (1982) Novel proteinaceous infectious particles cause scrapie. *Science* 216 (4542):136-144.
264. Prusiner SB (1998) Prions. *Proc.Natl.Acad.Sci.U.S.A* 95 (23):13363-13383.
265. Prusiner SB, Groth D, Serban A, Koehler R, Foster D, Torchia M, Burton D, Yang SL, and DeArmond SJ (1993) Ablation of the prion protein (PrP) gene in mice prevents scrapie and facilitates production of anti-PrP antibodies. *Proc.Natl.Acad.Sci.U.S.A* 90 (22):10608-10612.
266. Prusiner SB, McKinley MP, Bowman KA, Bolton DC, Bendheim PE, Groth DF, and Glenner GG (1983) Scrapie prions aggregate to form amyloid-like birefringent rods. *Cell* 35 (2 Pt 1):349-358.
267. Race RE, Fadness LH, and Chesebro B (1987) Characterization of scrapie infection in mouse neuroblastoma cells. *J.Gen.Virol.* 68 (Pt 5):1391-1399.
268. Rachidi W, Vilette D, Guiraud P, Arlotto M, Riondel J, Laude H, Lehmann S, and Favier A (2003) Expression of prion protein increases cellular copper binding and antioxidant enzyme activities but not copper delivery. *J.Biol.Chem.* 278 (11):9064-9072.
269. Ramaswamy S, Shannon KM, and Kordower JH (2007) Huntington's disease: pathological mechanisms and therapeutic strategies. *Cell Transplant.* 16 (3):301-312.
270. Rangel A, Burgaya F, Gavin R, Soriano E, Aguzzi A, and Del Rio JA (2007) Enhanced susceptibility of Prnp-deficient mice to kainate-induced seizures, neuronal apoptosis, and death: Role of AMPA/kainate receptors. *J.Neurosci.Res.* 85 (12):2741-2755.
271. Riek R, Hornemann S, Wider G, Billeter M, Glockshuber R, and Wuthrich K (1996) NMR structure of the mouse prion protein domain PrP(121-321). *Nature* 382 (6587):180-182.
272. Riek R, Hornemann S, Wider G, Glockshuber R, and Wuthrich K (1997) NMR characterization of the full-length recombinant murine prion protein, mPrP(23-231). *FEBS Lett.* 413 (2):282-288.
273. Riesner D (2003) Biochemistry and structure of PrP(C) and PrP(Sc). *Br.Med.Bull.* 66:21-33.
274. Roberts PC, Kipperman T, and Compans RW (1999) Vesicular stomatitis virus G protein acquires pH-independent fusion activity during transport in a polarized endometrial cell line. *J.Virol.* 73 (12):10447-10457.

275. Rosenstock TR, Duarte AI, and Rego AC (2010) Mitochondrial-associated metabolic changes and neurodegeneration in Huntington's disease - from clinical features to the bench. *Curr.Drug Targets*. 11 (10):1218-1236.
276. Roucou X, Gains M, and LeBlanc AC (2004) Neuroprotective functions of prion protein. *J.Neurosci.Res*. 75 (2):153-161.
277. Rubenstein R, Carp RI, and Callahan SM (1984) In vitro replication of scrapie agent in a neuronal model: infection of PC12 cells. *J.Gen.Virol*. 65 (Pt 12):2191-2198.
278. Rubinsztein DC and Carmichael J (2003) Huntington's disease: molecular basis of neurodegeneration. *Expert.Rev.Mol.Med*. 5 (20):1-21.
279. Saba R, Goodman CD, Huzarewich RL, Robertson C, and Booth SA (2008) A miRNA signature of prion induced neurodegeneration. *PLoS.ONE*. 3 (11):e3652.
280. Safar J, Roller PP, Gajdusek DC, and Gibbs CJ, Jr. (1993a) Conformational transitions, dissociation, and unfolding of scrapie amyloid (prion) protein. *J.Biol.Chem*. 268 (27):20276-20284.
281. Safar J, Roller PP, Gajdusek DC, and Gibbs CJ, Jr. (1993b) Thermal stability and conformational transitions of scrapie amyloid (prion) protein correlate with infectivity. *Protein Sci*. 2 (12):2206-2216.
282. Sailer A, Büeler H, Fischer M, Aguzzi A, and Weissmann C (1994) No propagation of prions in mice devoid of PrP. *Cell* 77 (7):967-968.
283. Sakaguchi S, Katamine S, Nishida N, Moriuchi R, Shigematsu K, Sugimoto T, Nakatani A, Kataoka Y, Houtani T, Shirabe S, Okada H, Hasegawa S, Miyamoto T, and Noda T (1996) Loss of cerebellar Purkinje cells in aged mice homozygous for a disrupted PrP gene. *Nature* 380 (6574):528-531.
284. Santoro SW and Joyce GF (1997) A general purpose RNA-cleaving DNA enzyme. *Proc.Natl.Acad.Sci.U.S.A* 94 (9):4262-4266.
285. Santoro SW and Joyce GF (1998) Mechanism and utility of an RNA-cleaving DNA enzyme. *Biochemistry* 37 (38):13330-13342.
286. Savran CA, Knudsen SM, Ellington AD, and Manalis SR (2004) Micromechanical detection of proteins using aptamer-based receptor molecules. *Anal.Chem*. 76 (11):3194-3198.
287. Schatzl HM, Laszlo L, Holtzman DM, Tatzelt J, DeArmond SJ, Weiner RI, Mobley WC, and Prusiner SB (1997) A hypothalamic neuronal cell line persistently infected with scrapie prions exhibits apoptosis. *J.Virol*. 71 (11):8821-8831.

288. Serio TR, Cashikar AG, Kowal AS, Sawicki GJ, Moslehi JJ, Serpell L, Arnsdorf MF, and Lindquist SL (2000) Nucleated conformational conversion and the replication of conformational information by a prion determinant. *Science* 289 (5483):1317-1321.
289. Shmerling D, Hegyi I, Fischer M, Blattler T, Brandner S, Gotz J, Rulicke T, Flechsig E, Cozzio A, von Mering C, Hangartner C, Aguzzi A, and Weissmann C (1998) Expression of amino-terminally truncated PrP in the mouse leading to ataxia and specific cerebellar lesions. *Cell* 93 (2):203-214.
290. Shyng SL, Heuser JE, and Harris DA (1994) A glycolipid-anchored prion protein is endocytosed via clathrin-coated pits. *J. Cell Biol.* 125 (6):1239-1250.
291. Sigurdson CJ and Miller MW (2003) Other animal prion diseases. *Br. Med. Bull.* 66:199-212.
292. Sijen T, Fleenor J, Simmer F, Thijssen KL, Parrish S, Timmons L, Plasterk RH, and Fire A (2001) On the role of RNA amplification in dsRNA-triggered gene silencing. *Cell* 107 (4):465-476.
293. Silei V, Fabrizi C, Venturini G, Salmons M, Bugiani O, Tagliavini F, and Lauro GM (1999) Activation of microglial cells by PrP and beta-amyloid fragments raises intracellular calcium through L-type voltage sensitive calcium channels. *Brain Res.* 818 (1):168-170.
294. Silva JM, Li MZ, Chang K, Ge W, Golding MC, Rickles RJ, Siolas D, Hu G, Paddison PJ, Schlabach MR, Sheth N, Bradshaw J, Burchard J, Kulkarni A, Cavet G, Sachidanandam R, McCombie WR, Cleary MA, Elledge SJ, and Hannon GJ (2005) Second-generation shRNA libraries covering the mouse and human genomes. *Nat. Genet.* 37 (11):1281-1288.
295. Silveira JR, Raymond GJ, Hughson AG, Race RE, Sim VL, Hayes SF, and Caughey B (2005) The most infectious prion protein particles. *Nature* 437 (7056):257-261.
296. Simák J, Holada K, D'Agnillo F, Janota J, and Vostal JG (2002) Cellular prion protein is expressed on endothelial cells and is released during apoptosis on membrane microparticles found in human plasma. *Transfusion* 42 (3):334-342.
297. Simon SL, Lamoureux L, Plews M, Stobart M, Lemaistre J, Ziegler U, Graham C, Czub S, Groschup M, and Knox JD (2008) The identification of disease-induced biomarkers in the urine of BSE infected cattle. *Proteome.Sci.* 6:23.
298. Simoneau S, Rezaei H, Sales N, Kaiser-Schulz G, Lefebvre-Roque M, Vidal C, Fournier JG, Comte J, Wopfner F, Grosclaude J, Schatzl H, and Lasmezas CI (2007) In vitro and in vivo neurotoxicity of prion protein oligomers. *PLoS.Pathog.* 3 (8):e125.

299. Sioud M (2004) Ribozyme- and siRNA-mediated mRNA degradation: a general introduction. *Methods Mol.Biol.* 252:1-8.
300. Solassol J, Crozet C, and Lehmann S (2003) Prion propagation in cultured cells. *Br.Med.Bull.* 66:87-97.
301. Solforosi L, Criado JR, McGavern DB, Wirz S, Sanchez-Alavez M, Sugama S, DeGiorgio LA, Volpe BT, Wiseman E, Abalos G, Masliah E, Gilden D, Oldstone MB, Conti B, and Williamson RA (2004) Cross-linking cellular prion protein triggers neuronal apoptosis in vivo. *Science* 303 (5663):1514-1516.
302. Sparkes RS, Simon M, Cohn VH, Fournier RE, Lem J, Klisak I, Heinzmann C, Blatt C, Lucero M, Mohandas T, DeArmond SJ, Westaway D, Prusiner SB, and Weiner LP (1986) Assignment of the human and mouse prion protein genes to homologous chromosomes. *Proc.Natl.Acad.Sci.U.S.A* 83 (19):7358-7362.
303. Spielhauer C and Schatzl HM (2001) PrPC directly interacts with proteins involved in signaling pathways. *J.Biol.Chem.* 276 (48):44604-44612.
304. Stahl N, Baldwin MA, Teplow DB, Hood L, Gibson BW, Burlingame AL, and Prusiner SB (1993) Structural studies of the scrapie prion protein using mass spectrometry and amino acid sequencing. *Biochemistry* 32 (8):1991-2002.
305. Steele AD, King OD, Jackson WS, Hetz CA, Borkowski AW, Thielen P, Wollmann R, and Lindquist S (2007) Diminishing apoptosis by deletion of Bax or overexpression of Bcl-2 does not protect against infectious prion toxicity in vivo. *J.Neurosci.* 27 (47):13022-13027.
306. Stewart LR, White AR, Jobling MF, Needham BE, Maher F, Thyer J, Beyreuther K, Masters CL, Collins SJ, and Cappai R (2001) Involvement of the 5-lipoxygenase pathway in the neurotoxicity of the prion peptide PrP106-126. *J.Neurosci.Res.* 65 (6):565-572.
307. Stobart MJ, Parchaliuk D, Simon SL, Lemaistre J, Lazar J, Rubenstein R, and Knox JD (2007) Differential expression of interferon responsive genes in rodent models of transmissible spongiform encephalopathy disease. *Mol.Neurodegener.* 2:5.
308. Stobart MJ, Simon SL, Plews M, Lamoureux L, and Knox JD (2009) Efficient knockdown of human prnp mRNA expression levels using hybrid hammerhead ribozymes. *J.Toxicol.EnvIRON.Health A* 72 (17):1034-1039.
309. Stockel J and Hartl FU (2001) Chaperonin-mediated de novo generation of prion protein aggregates. *J.Mol.Biol.* 313 (4):861-872.
310. Suyama E, Kawasaki H, Nakajima M, and Taira K (2003) Identification of genes involved in cell invasion by using a library of randomized hybrid ribozymes. *Proc.Natl.Acad.Sci.U.S.A* 100 (10):5616-5621.

311. Tagliavini F, Forloni G, D'Ursi P, Bugiani O, and Salmona M (2001) Studies on peptide fragments of prion proteins. *Adv. Protein Chem.* 57:171-201.
312. Tagliavini F, Prelli F, Ghiso J, Bugiani O, Serban D, Prusiner SB, Farlow MR, Ghetti B, and Frangione B (1991) Amyloid protein of Gerstmann-Straussler-Scheinker disease (Indiana kindred) is an 11 kd fragment of prion protein with an N-terminal glycine at codon 58. *EMBO J.* 10 (3):513-519.
313. Tagliavini F, Prelli F, Verga L, Giaccone G, Sarma R, Gorevic P, Ghetti B, Passerini F, Ghibaudi E, Forloni G, and . (1993) Synthetic peptides homologous to prion protein residues 106-147 form amyloid-like fibrils in vitro. *Proc. Natl. Acad. Sci. U.S.A* 90 (20):9678-9682.
314. Tamguney G, Giles K, Glidden DV, Lessard P, Wille H, Tremblay P, Groth DF, Yehiely F, Korth C, Moore RC, Tatzelt J, Rubinstein E, Boucheix C, Yang X, Stanley P, Lisanti MP, Dwek RA, Rudd PM, Moskovitz J, Epstein CJ, Cruz TD, Kuziel WA, Maeda N, Sap J, Ashe KH, Carlson GA, Tesseur I, Wyss-Coray T, Mucke L, Weisgraber KH, Mahley RW, Cohen FE, and Prusiner SB (2008) Genes contributing to prion pathogenesis. *J. Gen. Virol.* 89 (Pt 7):1777-1788.
315. Tanji K, Saeki K, Matsumoto Y, Takeda M, Hirasawa K, Doi K, Matsumoto Y, and Onodera T (1995) Analysis of PrPc mRNA by in situ hybridization in brain, placenta, uterus and testis of rats. *Intervirology* 38 (6):309-315.
316. Taraboulos A, Scott M, Semenov A, Avrahami D, Laszlo L, and Prusiner SB (1995) Cholesterol depletion and modification of COOH-terminal targeting sequence of the prion protein inhibit formation of the scrapie isoform. *J. Cell Biol.* 129 (1):121-132.
317. Telling GC, Scott M, Mastrianni J, Gabizon R, Torchia M, Cohen FE, DeArmond SJ, and Prusiner SB (1995) Prion propagation in mice expressing human and chimeric PrP transgenes implicates the interaction of cellular PrP with another protein. *Cell* 83 (1):79-90.
318. Theil D, Fatzer R, Meyer R, Schobesberger M, Zurbriggen A, and Vandeveld M (1999) Nuclear DNA fragmentation and immune reactivity in bovine spongiform encephalopathy. *J. Comp Pathol.* 121 (4):357-367.
319. Thellung S, Florio T, Villa V, Corsaro A, Arena S, Amico C, Robello M, Salmona M, Forloni G, Bugiani O, Tagliavini F, and Schettini G (2000) Apoptotic cell death and impairment of L-type voltage-sensitive calcium channel activity in rat cerebellar granule cells treated with the prion protein fragment 106-126. *Neurobiol. Dis.* 7 (4):299-309.
320. Thellung S, Villa V, Corsaro A, Arena S, Millo E, Damonte G, Benatti U, Tagliavini F, Florio T, and Schettini G (2002) p38 MAP kinase mediates the cell death induced by PrP106-126 in the SH-SY5Y neuroblastoma cells. *Neurobiol. Dis.* 9 (1):69-81.

321. Tixador P, Herzog L, Reine F, Jaumain E, Chapuis J, Le Dur A, Laude H, and Beringue V (2010) The physical relationship between infectivity and prion protein aggregates is strain-dependent. *PLoS.Pathog.* 6 (4):e1000859.
322. Tobler I, Gaus SE, Deboer T, Achermann P, Fischer M, Rulicke T, Moser M, Oesch B, McBride PA, and Manson JC (1996) Altered circadian activity rhythms and sleep in mice devoid of prion protein. *Nature* 380 (6575):639-642.
323. Tsujii H, Eguchi Y, Chenchik A, Mizutani T, Yamada K, and Tsujimoto Y (2010) Screening of cell death genes with a mammalian genome-wide RNAi library. *J.Biochem.* 148 (2):157-170.
324. Uhlenbeck OC (1987) A small catalytic oligoribonucleotide. *Nature* 328 (6131):596-600.
325. van der Kamp MW and Daggett V (2009) The consequences of pathogenic mutations to the human prion protein. *Protein Eng Des Sel* 22 (8):461-468.
326. van Wijk SJ and Timmers HT (2010) The family of ubiquitin-conjugating enzymes (E2s): deciding between life and death of proteins. *FASEB J.* 24 (4):981-993.
327. Vidal C, MERIC P, Provost F, Herzog C, Lasmezas C, Gillet B, Beloeil JC, and Dormont D (2006) Preclinical metabolic changes in mouse prion diseases detected by 1H-nuclear magnetic resonance spectroscopy. *Neuroreport* 17 (1):89-93.
328. Vilette D, Andreoletti O, Archer F, Madelaine MF, Vilotte JL, Lehmann S, and Laude H (2001) Ex vivo propagation of infectious sheep scrapie agent in heterologous epithelial cells expressing ovine prion protein. *Proc.Natl.Acad.Sci.U.S.A* 98 (7):4055-4059.
329. Vital C, Gray F, Vital A, Parchi P, Capellari S, Petersen RB, Ferrer X, Jarnier D, Julien J, and Gambetti P (1998) Prion encephalopathy with insertion of octapeptide repeats: the number of repeats determines the type of cerebellar deposits. *Neuropathol.Appl.Neurobiol.* 24 (2):125-130.
330. Wadhwa R, Ando H, Kawasaki H, Taira K, and Kaul SC (2003) Targeting mortalin using conventional and RNA-helicase-coupled hammerhead ribozymes. *EMBO Rep.* 4 (6):595-601.
331. Wadhwa R, Yaguchi T, Kaur K, Suyama E, Kawasaki H, Taira K, and Kaul SC (2004) Use of a randomized hybrid ribozyme library for identification of genes involved in muscle differentiation. *J.Biol.Chem.* 279 (49):51622-51629.
332. Wadsworth JD, Asante EA, Desbruslais M, Linehan JM, Joiner S, Gowland I, Welch J, Stone L, Lloyd SE, Hill AF, Brandner S, and Collinge J (2004) Human

- prion protein with valine 129 prevents expression of variant CJD phenotype. *Science* 306 (5702):1793-1796.
333. Walker FO (2007) Huntington's Disease. *Semin.Neurol.* 27 (2):143-150.
334. Wang F, Yin S, Wang X, Zha L, Sy MS, and Ma J (2010) Role of the highly conserved middle region of prion protein (PrP) in PrP-lipid interaction. *Biochemistry* 49 (37):8169-8176.
335. Wang J, Wang CE, Orr A, Tydlacka S, Li SH, and Li XJ (2008) Impaired ubiquitin-proteasome system activity in the synapses of Huntington's disease mice. *J.Cell Biol.* 180 (6):1177-1189.
336. Wang X, Bowers SL, Wang F, Pu XA, Nelson RJ, and Ma J (2009) Cytoplasmic prion protein induces forebrain neurotoxicity. *Biochim.Biophys.Acta* 1792 (6):555-563.
337. Wang X, Wang F, Arterburn L, Wollmann R, and Ma J (2006) The interaction between cytoplasmic prion protein and the hydrophobic lipid core of membrane correlates with neurotoxicity. *J.Biol.Chem.* 281 (19):13559-13565.
338. Waschbisch A, Fiebich BL, Akundi RS, Schmitz ML, Hoozemans JJ, Candelario-Jalil E, Virtainen N, Veerhuis R, Slawik H, Yrjanheikki J, and Hull M (2006) Interleukin-1 beta-induced expression of the prostaglandin E-receptor subtype EP3 in U373 astrocytoma cells depends on protein kinase C and nuclear factor-kappaB. *J.Neurochem.* 96 (3):680-693.
339. Weihl CC and Roos RP (1999) Creutzfeldt-Jakob disease, new variant creutzfeldt-jakob disease, and bovine spongiform encephalopathy. *Neurol.Clin.* 17 (4):835-859.
340. Westbrook TF, Martin ES, Schlabach MR, Leng Y, Liang AC, Feng B, Zhao JJ, Roberts TM, Mandel G, Hannon GJ, Depinho RA, Chin L, and Elledge SJ (2005) A genetic screen for candidate tumor suppressors identifies REST. *Cell* 121 (6):837-848.
341. White AR, Collins SJ, Maher F, Jobling MF, Stewart LR, Thyer JM, Beyreuther K, Masters CL, and Cappai R (1999) Prion protein-deficient neurons reveal lower glutathione reductase activity and increased susceptibility to hydrogen peroxide toxicity. *Am.J.Pathol.* 155 (5):1723-1730.
342. White AR, Guirguis R, Brazier MW, Jobling MF, Hill AF, Beyreuther K, Barrow CJ, Masters CL, Collins SJ, and Cappai R (2001) Sublethal concentrations of prion peptide PrP106-126 or the amyloid beta peptide of Alzheimer's disease activates expression of proapoptotic markers in primary cortical neurons. *Neurobiol.Dis.* 8 (2):299-316.

343. Will RG, Alperovitch A, Poser S, Pocchiari M, Hofman A, Mitrova E, de Silva R, D'Alessandro M, Delasnerie-Laupretre N, Zerr I, and van Duijn C (1998) Descriptive epidemiology of Creutzfeldt-Jakob disease in six European countries, 1993-1995. EU Collaborative Study Group for CJD. *Ann.Neurol.* 43 (6):763-767.
344. Will RG, Ironside JW, Zeidler M, Cousens SN, Estibeiro K, Alperovitch A, Poser S, Pocchiari M, Hofman A, and Smith PG (1996) A new variant of Creutzfeldt-Jakob disease in the UK. *Lancet* 347 (9006):921-925.
345. Will RG, Zeidler M, Stewart GE, Macleod MA, Ironside JW, Cousens SN, Mackenzie J, Estibeiro K, Green AJ, and Knight RS (2000) Diagnosis of new variant Creutzfeldt-Jakob disease. *Ann.Neurol.* 47 (5):575-582.
346. Williams AE, Lawson LJ, Perry VH, and Fraser H (1994) Characterization of the microglial response in murine scrapie. *Neuropathol.Appl.Neurobiol.* 20 (1):47-55.
347. Williams ES and Young S (1980) Chronic wasting disease of captive mule deer: a spongiform encephalopathy. *J.Wildl.Dis.* 16 (1):89-98.
348. Williams ES and Young S (1982) Spongiform encephalopathy of Rocky Mountain elk. *J.Wildl.Dis.* 18 (4):465-471.
349. Williams ES and Young S (1993) Neuropathology of chronic wasting disease of mule deer (*Odocoileus hemionus*) and elk (*Cervus elaphus nelsoni*). *Vet.Pathol.* 30 (1):36-45.
350. Yamamoto TM, Iwabuchi M, Ohsumi K, and Kishimoto T (2005) APC/C-Cdc20-mediated degradation of cyclin B participates in CSF arrest in unfertilized *Xenopus* eggs. *Dev.Biol.* 279 (2):345-355.
351. Yang JH, Usman N, Chartrand P, and Cedergren R (1992) Minimum ribonucleotide requirement for catalysis by the RNA hammerhead domain. *Biochemistry* 31 (21):5005-5009.
352. Yang L, Zhou X, Yang J, Yin X, Han L, and Zhao D (2008) Aspirin inhibits cytotoxicity of prion peptide PrP106-126 to neuronal cells associated with microglia activation in vitro. *J.Neuroimmunol.* 199 (1-2):10-17.
353. Yedidia Y, Horonchik L, Tzaban S, Yanai A, and Taraboulos A (2001) Proteasomes and ubiquitin are involved in the turnover of the wild-type prion protein. *EMBO J.* 20 (19):5383-5391.
354. Yehiely F, Bamborough P, Da Costa M, Perry BJ, Thinakaran G, Cohen FE, Carlson GA, and Prusiner SB (1997) Identification of candidate proteins binding to prion protein. *Neurobiol.Dis.* 3 (4):339-355.

355. Yeom KH, Lee Y, Han J, Suh MR, and Kim VN (2006) Characterization of DGCR8/Pasha, the essential cofactor for Drosha in primary miRNA processing. *Nucleic Acids Res.* 34 (16):4622-4629.
356. Yeung ML, Houzet L, Yedavalli VS, and Jeang KT (2009) A genome-wide short hairpin RNA screening of jurkat T-cells for human proteins contributing to productive HIV-1 replication. *J.Biol.Chem.* 284 (29):19463-19473.
357. Yi R, Qin Y, Macara IG, and Cullen BR (2003) Exportin-5 mediates the nuclear export of pre-microRNAs and short hairpin RNAs. *Genes Dev.* 17 (24):3011-3016.
358. Young K, Clark HB, Piccardo P, Dlouhy SR, and Ghetti B (1997) Gerstmann-Straussler-Scheinker disease with the PRNP P102L mutation and valine at codon 129. *Brain Res.Mol.Brain Res.* 44 (1):147-150.
359. Yu JY, DeRuiter SL, and Turner DL (2002) RNA interference by expression of short-interfering RNAs and hairpin RNAs in mammalian cells. *Proc.Natl.Acad.Sci.U.S.A* 99 (9):6047-6052.
360. Zahn R, Liu A, Luhrs T, Riek R, von Schroetter C, Lopez GF, Billeter M, Calzolari L, Wider G, and Wuthrich K (2000) NMR solution structure of the human prion protein. *Proc.Natl.Acad.Sci.U.S.A* 97 (1):145-150.
361. Zamore PD, Tuschl T, Sharp PA, and Bartel DP (2000) RNAi: double-stranded RNA directs the ATP-dependent cleavage of mRNA at 21 to 23 nucleotide intervals. *Cell* 101 (1):25-33.
362. Zeidler M, Stewart GE, Barraclough CR, Bateman DE, Bates D, Burn DJ, Colchester AC, Durward W, Fletcher NA, Hawkins SA, Mackenzie JM, and Will RG (1997) New variant Creutzfeldt-Jakob disease: neurological features and diagnostic tests. *Lancet* 350 (9082):903-907.
363. Zheng W, Wang L, Hong Y, and Sha Y (2009) PrP106-126 peptide disrupts lipid membranes: influence of C-terminal amidation. *Biochem.Biophys.Res.Commun.* 379 (2):298-303.
364. Zhou H, Zhou X, Kouadir M, Zhang Z, Yin X, Yang L, and Zhao D (2009) Induction of macrophage migration by neurotoxic prion protein fragment. *J.Neurosci.Methods* 181 (1):1-5.